CHARACTERIZATION OF DISPERSIVE AND DISTRIBUTIVE MIXING IN A CO-ROTATING TWIN-SCREW COMPOUNDING EXTRUDER

by

JOHN WILLIAM ESS

A

Thesis submitted for the degree of

Doctor of Philosophy

at the

Dept of Materials Technology

Brunel University

Uxbridge, Middlesex

May 1989

ABSTRACT

A new design of closely intermeshing co-rotating twin-screw compounding extruder, developed at Brunel University, has been utilized in the development of quantitative techniques for characterization of dispersive and distributive mixing in thermoplastics materials prepared by extrusion compounding. Image analysis procedures were used to quantify mixing of polypropylene composites containing calcium carbonate filler using reflected light microscopy on polished surfaces, and transmitted light microscopy of microtomed pigmented sections.

Stereological statistics have been applied to raw sample data; results are discussed in relation to mechanistic phenomena influencing particle agglomeration, dispersion and distribution of fillers in thermoplastics.

Dispersive or intensive mixing determined from calcium carbonate filled polypropylene specimens showed that processing parameters had no significant influence except when filler was added midway along the machine although the melting zone was highlighted as having a marked effect on the rate of filler dispersion. Premixing of filler and polymer introduced additional agglomeration into the filler. A series of model experiments were undertaken to assess the influence of specific parameters. In this context moisture content emerged as having the single most important effect on filler compaction.

Distributive or extensive mixing of carbon black pigmented specimens was very significantly affected by the presence of segmented disc elements at the end of the screws. These elements produced more than a six-fold increase in distributive mixing in the extrudate.

ACKNOWLEDGEMENTS

The author gratefully acknowledges the contributions, both financial and material, made to this project by the Polymer Engineering Directorate of the Science and Engineering Research Council, and Croxton and Garry Ltd for the supply of calcium carbonate fillers.

Appreciation to the late Mr I Boyne for his considerable efforts during the initial proving and modification trials of the TS40 twin-screw extruder development programme.

Sincere thanks to Peter Hornsby for his patience and perseverance during the later stages of this project and for his assistance and comments during the initial phase.

The technical and administrative facilities of the Dept of Materials Technology are also acknowledged, particularly those provided by Mr J Felgate, Mr K Johns and Mr L Mellett.

Assistance with the preparation, checking and collation of this report was provided by Gwen and Will.

CONTENTS

FIGURES

CHAPTER 1

INTRODUCTION

Originally, the brief for this research work entitled 'Twin-Screw Extrusion Compounding of Plastics' implied a technological study involving both material investigation and engineering development. However, as the project progressed financial constraints became more acute necessitating a concentration of resources in the area of compound analysis. As a result of this change, more emphasis was placed on investigations into a wide range of materials for inclusion in a polymer matrix.

This investigation of mixing during extrusion stems from the polymer processing industry's desire to lower materials costs while enhancing physical properties of end products. The first example of this philosophy is to be found with the thermosetting urea formaldehyde formulations which employed wood flour as a filler. More recently, fibrous fillers have found favour as means of reinforcing polymer matrices so that they can compete with metals as engineering materials. The great demands required of engineering materials has resulted in a mass of research work being undertaken to accurately specify properties and to satisfy various official agencies concerned with standards and safety.

Nevertheless, non-reinforcing (extending) fillers in polymers remain the higher volume area offering large potential cost savings with a carefully chosen polymer/filler combination. The result of incorporating extending fillers is usually some loss of physical properties, so ways have been found whereby these problems can be minimized. Two possibilities arise:- (a) the use of composite filler systems, viz. fibrous and particulate combined in the same polymer

matrix; or (*b*) the elimination of stress raisers, viz. any agglomeration of the particulate filler.

The use of composite filler systems creates additional difficulties because, in order for the fibrous element to be effective, the fibre length attrition must not be excessive while the shear stress must be sufficient to eliminate gross agglomeration. A pre-dispersed masterbatch of the particulate filler, or a higher shear first stage of a three stage extruder screw, with downstream feeding of the fibrous element will be required for this strategy to be property-efficient and then only at a significant cost penalty compared to extended systems. Composite systems do, however, prove tenable in demanding engineering situations.

Polymers employed for their aesthetic properties or in non-load bearing situations require an extending filler to provide a means of displacing expensive polymer while perhaps also pigmenting the matrix. The aesthetic nature, together with physical properties, will be undermined by agglomeration of the filler: various means exist to eliminate these agglomerates:-

(*i*) use of pre-dispersed masterbatch systems which require only blending and distribution within the polymer matrix;

(*ii*) use of shear stresses high enough to disperse all agglomerates above a size determined by the severity of specification;

(*iii*) use of screen packs to filter out the offending particles;

(*iv*) use of surface coatings, applied to the filler during its manufacture, which inhibit filler particle-particle agglomeration.

The masterbatch system of filler addition is employed, particularly for common fillers, when it is not desirable to handle the raw material or if the filler is difficult to disperse on non-specialized equipment. A prime example of this type of filler is

carbon black which presents formidable handling problems in its raw state and requires very high shear rates to achieve acceptable dispersion. A masterbatch of pre-dispersed carbon black concentrated in a matrix of the same polymer as that in the final product provides a route around these difficulties but increases raw material costs. Nevertheless, it is particularly cost-effective for low volume producers using standard formulations when compared to the capital outlay necessary for specialized dispersion equipment.

If the formulation required has unusual or confidential ingredients there are a number of options open to a Polymer Processor. Most frequently a Banbury intensive mixer is utilized to produce batches of dispersed material for subsequent processing; however, batch to batch variation and contamination can arise. More recently the twin-screw compounding extruder has been developed for directly processing 'difficult to disperse' materials without the need for pre-conditioning.

The main limitation of filtering out any agglomerates larger than a specified size is that the filter will inevitably become blocked after a period of time. The suitability of a filtering system is related to the concentration of particles to be restrained which is itself a function of the filler concentration, particle size distribution and pore size of the filter. Use of a filter is tenable when a cheap method is required and a means of changing the screen pack is possible; be it by stopping production periodically or by using automatic screen changers. However, high filler loadings preclude the use of filters as they become blocked extremely quickly and hence inhibit flow in the extruder.

Application of a coating to the filler during its manufacture enables control over the mechanisms which cause agglomeration and, in some cases, introduces a binding effect between polymer and filler.

Calcium carbonate was selected as the filler medium because it is in common use and presents many of the compounding difficulties associated with other particulate systems. In approaching these difficulties a number of extrusion and material variables were investigated. Extrusion energy management emerged early as a major controlling factor in shear input and thus inter-particle mechanisms. In order that exact control of extrusion temperatures could be achieved a water jacket cooling system was developed; this also allowed 'freezing' of material subsequent to barrel withdrawal and examination of specimens from specific screw flight locations.

Carbon black pigments possess particles up to 1000 times smaller than calcium carbonate fillers and so present different challenges. Determination of mixture quality in pigment/polymer composites is usually concerned with flow, i.e. distributive mixing; any agglomerates exceeding a few microns in size should, in most cases, relegate the compound to the scrap pile. Similar extrusion variables to those used previously were employed as a means of energy control.

Quantitative analysis of mixing emerged as the most complex problem in compound development requiring a quick and accurate analysis technique. However, as a consequence of the lack of established quantitative techniques for characterizing mixture quality, a comprehensive programme was undertaken to evaluate the most suitable techniques for quantification of dispersive and distributive mixing.[1]

The most promising method for examining calcium carbonate dispersion appears to be one of the simplest, viz. examination of polished surfaces with reflected light. For carbon black, a thin microtomed section is produced which is viewed by transmitted light microscopy.

Manual sizing of agglomerates proved totally impractical, therefore 'image analysis' was considered as an alternative. After a

period of software development this automatic system of characterization has proved to be capable of fast, accurate sizing of high contrast features exhibited by specimens viewed by the integral microscope. The calcium-carbonate-agglomeration image analysis technique was adapted to allow rapid direct assessment of striations within carbon black/polypropylene composite sections.[2]

For this work a new design of co-rotating twin-screw compounding extruder, subsequently designated the Betol BTS40, has been employed to process various types of calcium carbonate in a matrix of polypropylene homopolymer. The calcium carbonate grades selected differ in their origin and particle size distributions whilst several coated grades of the former have been studied to examine the role of surface coatings. One of the uncoated grades has been processed in nylon to assess the effects of a polar matrix. A number of model experiments have been undertaken to investigate the influence of preconditioning of the filler, viz. pressure and temperature encountered during intensive premixing, moisture content of the filler and its particle size distribution. An extensive range of processing conditions were utilized together with variations in configuration of the screw and barrel in order that the effect of applying high shear forces during processing could be studied.[3] Each composite of calcium carbonate/ polymer was frozen within the barrel of the extruder and representative sections removed for characterization.

For distributive mixing studies it was necessary to ensure that the pigment be adequately dispersed prior to distribution so a carbon black masterbatch was employed. Various processing conditions and screw/barrel configurations were used to produce an extrudate with a very low carbon black concentration that facilitated characterization of samples removed from the 'metering' section of the screws after having been frozen by crash cooling.

CHAPTER 2

LITERATURE REVIEW

2.1 TWIN-SCREW EXTRUSION

2.1.1 Background

2.1.1.1 Single-screw extrusion

The process known as 'single-screw extrusion' has been extensively investigated and its working well described.[4-7] The single-screw extruder consists of a screw rotating in a closely fitting barrel so that if the process material adheres to the screw and slips at the barrel surface, there will be no output from the extruder because the material rotates on the screw without being pushed forward. Maximum output is achieved when the material slips as freely as possible on the screw surface whilst adhering as much as possible to the wall. Under these circumstances the rotational speed of the screw is greater than that of the material which is forced along the extruder by the leading edge of the flight.

The materials employed by the Plastics Industry tend to adhere to all internal surfaces in the extruder during processing and can be introduced into the extruder in two distinct forms:- (*a*) as a molten feed requiring 'melt extrusion'; or (*b*) as solid material, viz. granules or powder, requiring 'plastifying extrusion'.

Melt extrusion usually refers to the portion of the screw channel which is completely filled with molten material but the term is also used to describe feeding already molten material into the hopper of a machine. In the latter case, some compacting must take place before the screw channel is completely filled and true melt extrusion commences. When cold polymer granules or powder are fed into an

extruder and the material melted down before being extruded through a die, the process is known as plastifying extrusion.[7]

In general, plastifying extrusion requires a single-screw machine with a well designed screw which has distinct zones capable of performing the following functions:-

(*i*) Solids transport zone. In this zone, just beneath the hopper, the solid material is conveyed in the form of granules, powder, pellets or chips. Since, for continuity reasons, the output will be the same as the input, a poor design of the solids transport zone will limit the output considerably as will an inadequate hopper design;

(*ii*) Compression and melting zone. This zone starts at the point where the first liquid forms at the barrel wall and can extend along a considerable length to the point at which all the material in the cross-section of the channel is molten;

(*iii*) Homogenization, metering and pump zone. In the first part of this zone the channel volume decreases resulting in a transitional section where the polymer is compressed to eliminate cavities. In the second part of this zone, the metering zone, the melt is transported and homogenized to produce the main pressure build-up within the processor.[8]

Apart from the functions outlined above, it is possible to improve single-screw extruder performance by adding refinements to the basic screw.[9-11] Specific improvements can be obtained in three main areas:-

(*a*) the imposition of compulsive solids pumping enables a significantly greater packing of material so that output rates are optimised. In order to achieve this extra pumping, Kosel [12] has examined a tapered feed-barrel section while Krueger [13] utilized a grooved feed-screw section;

(*b*) the introduction of a kneading action to generate extra shear which can be directed either towards improving the melting action by altering the design of the screw or to encouraging better dispersion through the use of a barrier-type mixing section;[14-17]

(*c*) an increase in homogeneity within the molten polymer can be attained by repeated sub-division of the melt within or after the metering section. Gale [18] has tackled the problem with a device which comprises of a stator bolted on the end of the extruder barrel and a rotor attached to the end of the screw. The stator and rotor both have cavities which are intended to facilitate sub-division. Other investigators have resorted to using special sections within the existing extruder barrel. [19-21]

Refinements such as these allow the single-screw extruder to undertake many tasks, viz. homogenizing freshly polymerized melt, compounding of additives and pigments, the production of film, sheeting, pipe, cable jacketing, coatings and profiles. However, problems remain when processing:- (*i*) heat sensitive polymers such as PVC or cross-linked polyethylene and shear sensitive additives such as glass fibres because of the high shear barrier and kneading sections; or (*ii*) highly mineral-filled polymers due to blocking of the screw flights particularly in the solids conveying zone. The addition of another screw within the extruder barrel was prompted because of the difficulties encountered when processing PVC and this gave rise to twin-screw extrusion technology. [22]

2.1.1.2 Twin-screw extrusion

The main difference between single- and twin-screw extruders lies in their mechanisms of transportation. The twin-screw extruder carries

the material within the screw flights either by passing it in a 'figure of eight' around the two screws or by enclosing it in a 'C-shaped' chamber of only one screw so providing a positive pump effect. The throughput of a twin-screw extruder is usually dependent on the feed rate of material entering the hopper plus screw speed as opposed to a single-screw extruder which can normally only be controlled by screw speed because of 'flood feeding' at the hopper. While single-screw extruders usually require constant cooling to remove excessive shear heat, the twin-screw extruder without mixing elements needs heating to be applied through the barrel. Back pressure from the die of twin-screw extruders has much less influence on any mixing action than with single-screw machines thus allowing much easier use of large cross-sectional area dies. Some of the advantages put forward for twin-screw extrusion of uPVC include:- (*a*) better control of temperature; (*b*) better mixing action; (*c*) better removal of entrapped air. [23,24]

However, the twin-screw extruder is not used solely for uPVC processing but also for processing other critical materials (i.e. high performance polymers and other polymer compounds tailored precisely for specific applications). In many of the applications, the high cost of the polymer and the correspondingly high selling price of the component militates against the higher capital cost of the equipment compared to a single-screw machine. General advantages cited are:- (*i*) a greater ease of feeding difficult materials without the need for forced-feed units necessary on a single-screw extruder when handling certain mixtures; (*ii*) simpler downstream feeding which reduces the high rate of wear in the feed zone; and (*iii*) a reduction in the problems of adding high loadings of materials such as glass and other fibres. Lower circumferential screw speeds in twin-screw machines are also emphasized as a major factor in wear reduction which otherwise is a

calculable overhead incurred in the running of an extruder [25]. The twin-screw extruder lends itself more easily to starve-feeding so that optimum conditions can be reached for venting without problems of material leakage. Intensification of mixing and control of shear can be effected at any section along the length of the barrel using a variety of different shearing and mixing devices whilst if required the direction of shear can also be altered so that back mixing is applied. [22]

2.1.2 Different Formats

Of the many different types of twin-screw extruder available, only some have positive conveying characteristics and the various twin-screw extruders can show considerable differences in their modes of operation. The most important variation is that between intermeshing and non-intermeshing twin-screw extruders. When screws are non-intermeshing the flights of one screw do not protrude into the channel of the other screw and so they do not form closed or semi-closed compartments depriving them of positive conveying characteristics.

The degree of intermeshing in intermeshing extruders, can range from almost fully intermeshing to almost non-intermeshing with a corresponding range in the degree of positive conveying characteristics. Nevertheless, fully intermeshing screws are a necessary but not sufficient condition for positive conveying. In some geometries, even when the screws are fully intermeshing there is very little sealing of the screw channels and back leakage into upstream channel sections will adversely affect the positive conveying behaviour. Positive conveying occurs only when the screw channels are closed off so that the material contained in the various channel sections is fully occluded. [26]

The second discriminating characteristic is the direction of rotation: there are only two possibilities, viz. either co- or counter-rotating.

2.1.3 Operating Characteristics

2.1.3.1 Counter-rotating screws

For fully intermeshing counter-rotating screws, the compaction of the material can be achieved in a number of ways:

(*i*) by continuously reducing screw pitch;

(*ii*) by stepwise variation of pitches and numbers of screw flights;

(*iii*) by continuously increasing crest widths;

(*iv*) by continuously reducing the external diameter and continuously increasing the internal diameter.

Fully intermeshing counter-rotating screws cannot establish a sharp pressure gradient across several screw flights, neither can they ensue that air from the individual chambers is expelled completely towards the hopper. Accordingly, counter-rotating screws are intentionally manufactured with large clearances which forfeits some of the advantages of the block flow principle offered by the counter-rotating system.

Counter-rotating plasticating twin-screw models have been constructed both for materials which adhere and for those which do not adhere to the walls. The so-called 'C-shaped' chamber is established and the opposing screw is represented by rollers which close the chamber on both sides. In general terms, melting follows a broadly similar pattern to single-screw extruders:-

(*a*) melt film formation on the barrel wall;

(*b*) removal of the film by the positive screw flank;

(*c*) collection of melt in front of the positive screw flank.

The opposing screw produces a turning motion in addition to the following effects, viz. a melt whirlpool forms in the wedge intake to suck in adjacent particles so softening them whilst plasticized material is drawn through the calendar gap to gather on the passive flank. This calendar effect in counter-rotating screws does not, however, always affect more than a fraction of the volume of the chamber. A wide clearance will allow a larger amount of the chamber volume to traverse the calendar gap but any shearing effect is reduced.

2.1.3.2 Co-rotating screws

For fully intermeshing co-rotating extruders the solid material is usually compacted by restriction caused by the opposing screw (say the right-hand screw). The material has to pass across the right-hand screw, the necessary pressure being created by the upstream left-hand screw. As co-rotating screws represent a system having an open channel in the longitudinal flow direction, the enclosed air can escape in the upstream direction without difficulty. In contrast to counter-rotating screws it is possible, by correct selection of pitch and rotation speed, to ensure that the axial flow zero-shearing stress point is constantly kept outside the screw channel meaning that no areas of insufficient shearing are formed within the screw channel. Floating particles of solid material can be exposed to a far higher shearing effect than is possible in counter-rotating screws; a situation that is encouraged by higher screw speeds available with the co-rotating system. In the wedge area the material is scrapped off and passed to the opposing screw with very little calendaring taking place; the material being subjected to constant shearing velocities between the flanks. [27]

The intermeshing co-rotating extruders can be further subdivided into low- and high-speed machines. The low-speed extruders have a

closely fitting flight and channel profile which affords them a high degree of positive conveyance. However, the small mechanical clearances dictate that they run at low screw speeds (generally 10-20 rpm) to avoid build up of excessive local pressures that could cause machine wear. These machines are employed primarily in profile extrusion applications. The high-speed co-rotating extruders normally have self-wiping characteristics, although this does not mean that the flights close off the opposite channels. In fact, in these designs there is considerable opportunity for the material to leak back from one screw channel into a channel of the other screw: accordingly, these machines have a low degree of positive conveyance. The openness of the channels means that material is easily transferred from one screw to another and pressure generation in the intermeshing region is less pronounced. This allows these extruders to run at high speeds (up to 500rpm). High-speed co-rotating machines are primarily used in compounding operations where use is made of the high shear rate and frequent reorientation of the material in the extruder. [28-47]

2.2 MIXING THEORY

2.2.1 Single-Screw Machines

Flow analysis methods in single-screw extruders can vary from relatively easy calculations with a number of useful simplifications to very complex computer programs containing sophisticated algorithms which acknowledge the effects of channel curvature, advanced non-Newtonian rheology and temperature-dependent material properties. Simple analyses generally assume stationary flow of incompressible, viscous Newtonian fluid between parallel plates in the pump zone and neglect temperature effects; normally plug flow is assumed in the solids conveying zone, with the plug confined between two infinite parallel plates moving relative to one another. A wide range of books are available which guide the reader from the fundamentals of extrusion through to rather more complex analyses [4,6,8,48-50]

Analyses of single-screw extrusion tend to consider either flow through the entire machine or concentrate on one portion of the process. Paton et al [51] have presented a very complete introduction to the principles and mechanics of single-screw extrusion while others have carried out holistic studies which attempt to simulate flow and processing problems. [52-59]

Klein & Klein [60,61] have examined the solids conveying zone and considered the effects of coefficient of friction (using their own design of friction tester), screw surface temperature, thermal conductivity of barrel, solids height in hopper and channel depth. Kruder and Nunn [62] have applied solids conveying theory in a practical situation when processing a variety of materials and found that a grooved barrel significantly increased output from the extruder.

Maddock [63] has conducted a number of practical experiments which were subsequently followed through theoretically by Tadmor [64],

Vermeulen et al [65], and finally Edmondson and Fenner [66] who developed a theoretical model which allowed more natural movement of the solid bed of material. Practical applications of melting theory have involved investigations of pressure development by Lindt [67] and quantification of stress at the polymer/metal interface by McClelland and Chung.[68] Recent reviews of mathematical modeling of melting have been undertaken by Elbirli et al [69-71] but these models still require a long list of basic assumptions in order to operate; the most limiting being that leakage flows must be neglected.

For the homogenizing metering zone, Squires [30] made a distinction between one-dimensional or so-called 'simplified' theory in which flight edge effects are neglected, and two-dimensional or so-called 'exact' theory when they are taken into account. He calculated the effects of relative channel depth and curvature in relation to melt-pumping rates while Maddock [72] investigated pressure development. Janssen et al [73] more recently have experimentally determined the radial and tangential temperature profiles at the tip of the metering screw.

An interesting series of papers [74-79] were presented at a symposium in the early 1950's entitled 'Theory of Extrusion'. These papers, by then employees of DuPont, afforded a generous overview of the theory of single-screw extrusion and one of their authors (McKelvey) went on to write a book [4] which is still required reading for any serious student of extrusion.

Kruder and Nunn [80] have considered the utilization of energy within the extrusion process and found that poorly designed screws can waste energy in a number of ways: (a) the screw may result in excessive overheating of the process material unless operated at a low screw speed or make the use of drastic barrel and screw cooling necessary; and (b) the screw may give rise to poor mixing/ melting which will

limit machine operation to inefficient conditions. Linked with this is the problem of screw wear [81] which can result in high machine maintenance costs as well as a loss of mixing efficiency; all of which could stem from the aforementioned poor screw design.

2.2.2 Twin-Screw Machines

2.2.2.1 Counter-rotating

The theoretical basis of counter-rotating twin-screw extruders is dealt with effectively by Janssen [8] and Rauwendaal [50]. However, their treatments of the machines are very much aimed at a mathematical understanding rather than a practical one. Frankly, these two books are of little use in practical day to day research and preference would have to be given to books such as that by Martelli [82] which attempts to explain theory in terms which have practical implications.

Janssen et al [45] developed a model for the output of the pump zone of the counter-rotating extruder which investigated the dependence of the throughput on the pressure gradient within this zone. Various leakage flows were considered but the main three such flows to have been identified occur: (a) over the screw flights; (b) between a screw flight and the base of the opposite screw; and (c) through the tetrahedral gap of the two screws. The first two leakages, which will detract from the overall throughput expected from the machine, can be calculated analytically whilst the third is quantified empirically. Janssen and Smith [83] have concluded that for good mixing and residence time distribution the calendar gap has to be relatively wide but opposing this is the necessity to maintain throughput and heat transfer. Maheshri and Wyman [84] analyzed the cross and down channel flows in the centre of an idealized leakproof intermeshing extruder. They considered the two fluid motions simultaneously and predicted a complex path over a number of channel depths.

The most investigated aspect of twin-screw machines is the fundamental difference between the machines employing counter-rotating screws and those having co-rotating screws [26,27,29,32,85].

2.2.2.2 Co-rotating

A 30mm diameter fully intermeshing co-rotating twin-screw extruder was used by Kao and Allison [86] to determine the residence time distribution (RTD) by a stimulus-response technique. They varied three processing parameters; throughput, screw speed, and barrel temperature, whilst utilizing two different screw profiles; one with four kneading elements. The throughput emerged as the most influential variable of RTD followed by screw speed; barrel temperature profile played no part in varying RTD. Secor [87] states that partially filled twin-screw extruders are used very effectively for mixing and surface renewal of high-viscosity fluids. The drive power, the heat input to the fluid and the cooling requirements are determined by the rate of energy input. A simple model for the rate of energy dissipation in twin-screw extruders predicts that the power input is proportional to the square of the screw speed. Secor found experimentally that the screw speed should be raised to the power 1.90.

Meijer and Elemans [88] agree with my earlier contention that theoretical analysis of twin-screw extruders should not emphasize the flow in complex geometries but rather should generate results that can be directly used. They developed a simple model for hot melt within a closely intermeshing co-rotating extruder and expanded it to include nonisothermal, non-Newtonian materials so that various parameters (such as specific energy and temperature rise during processing) could be related to viscosity of the melt, screw geometry and rotational speed.

2.3 COMPOUNDING

2.3.1 Definitions

In the present context, the term 'compounding' relates not to a chemical reaction between two or more constituents but to an intimate physical mixing of filler components in a polymer matrix; chemical reactions may occur with the use of filler surface coatings. A definition of the meaning of the word 'mixing' can be divided into two independent categories; they are 'dispersion' or dispersive mixing and 'distribution' or distributive mixing:

(*i*) dispersive mixing - is an operation which reduces the agglomerate size of the minor constituent (filler) to the possible limit of the ultimate particle size suitable for concurrent or future distributive mixing;

(*ii*) distributive mixing - is an operation employed to increase the randomness of the spatial distribution of one or more minor constituents in a major (polymer) matrix with no change in the ultimate particle size of the minor constituent.

[4,18,89]

Mixing is generally achieved through a combination of four mechanisms, viz. subdivision, initial wetting, dispersion and distribution. The first stage of mixing is the breakdown of the filler into small particles and these are uniformly distributed amongst and around the surface of the polymer grains or granules. Subdivision is synonymous with the preblending/premixing step [90] and with the area at the beginning of the extruder screws in compounding operations; the degree of subdivision is likely to depend on the energy of the process.

The second stage is initial wetting which is essential to every dispersion regardless of quality. As the calcium carbonate/polymer blend reaches the heated sections of the barrel, the polymer fuses into

a melt and envelops the filler particles. A minimum requirement is that filler and polymer be sufficiently well mixed and have enough affinity for each other so they will not separate when further work is applied to the system. Nevertheless, there is an appreciable time lapse before wetting is complete and during this period the filler is liable to compaction, under mechanical compression in processing and compounding equipment, which can cause reagglomeration. Surface chemistry at the filler/polymer interface is critical as it will affect rate and efficiency of wetting. However, the mutual affinity, compatibility or wettability of the two materials can be increased through a change in the surface characteristics of either or both by use of surfactants. Good mixing also depends on the rapidity of wetting so that the maximum time is available for the shearing forces to break down the filler particles to their final size.

The third stage is the dispersion of the filler. This involves further wetting, the reduction of the filler particles to the smallest size possible (under the given conditions of shear), and their intimate wetting by the polymer.

Finally, distributive mixing is needed to achieve homogeneity in the final product. Poor distribution can lead to non-uniform additive concentration even when the actual dispersion is good. For example, a polymer UV-stabilized with carbon black would degrade if the carbon black was perfectly dispersed but not evenly distributed.[28,91-103]

2.3.2 Equipment

The compounding of fillers and polymers requires equipment that must satisfy several conditions:

(*i*) steady state running;

(*ii*) reproducibility of processing;

(*iii*) ease of cleaning;

(*iv*) adaptability for new formulations.

For optimum material quality, the equipment should generate sufficiently high internal shear stresses to facilitate dispersion of additives. Additional requirements are the capacity to expose each particle to short and equal stresses whilst enabling exact temperature control to regulate and minimize heat history.[99]

Two types of compounding process arise, viz. discontinuous and continuous systems. The original discontinuous system, in most cases, refers to Banbury intensive mixers or roll mills.[104,105] Continuous compounding systems generally are more economical due to the large volume requirements for filled plastics and offer better uniformity of product with less batch to batch variation.

Compounding can adequately be provided by single-screw extruders, most of the time, due to advanced screw design techniques [106] and special devices that aid in localized and controlled introduction of shear.[107-109] A well-known example of a single-screw compounding extruder is the 'Transfermix'. This machine is a continuous, variable intensive, stepless extensive mixer consisting of a rotor turning inside a stator which act as two opposite handed screws.[110]

Alternative strategies to single-screw extrusion include the use of ram continuous extruders [111] which can be supplemented with motionless mixers to achieve improved mixing.[112]

For difficult mixing situations, twin-screw compounding systems, if properly designed, provide maximum process control particularly in relation to shear and stock temperature whilst allowing easy removal of relatively large quantities of volatiles.[97,99,113,114] Comprehensive practical tests, however, are often the only means of determining the suitability of a particular mixing machine for a specified plastics mixture: most compounding can, at present, probably be classified as an art.[28,115]

2.3.3 Applications

Compounding includes the following extrusion functions:-

(a) fusion - in order to densify a polymer into a form or shape suitable for subsequent processing;

(*b*) dispersion - of a pigment in a polymer followed by a distributive mixing operation;

(*c*) dispersion and distribution - of two different polymers to create a new 'alloy'[116,117];

(*d*) dispersion and distribution - of a high molecular weight polymer in a virgin stock to reduce the end product 'gel count';

(*e*) dispersion and distribution - of low temperature resin in a matrix of higher temperature melt in order to normalize the melt temperature;

(*f*) dispersion and distribution - of additives such as fillers, reinforcers, stabilizers, plasticizers and lubricants into a polymer matrix in order to manufacture a desired compound.[44,95,118]

Compounding equipment, by virtue of its inherent ability to shear any viscous material, has been utilized in many varied areas. White et al [119,120] have employed a single-screw extruder to successfully process highly-filled wood flour slurries whilst Janssen et al [121] have processed self-reinforcing polymers on a counter-rotating twin-screw extruder.

The use of sophisticated computer control equipment to monitor and adjust extrusion parameters is a fast developing aspect of compounding which will allow improved reaction rates to processing fluctuations. [122-125] These controls will be increasingly necessary in future to enable the processing of engineering materials for use in critical

situations where flaws in components are unacceptable (i.e. military and aviation applications).

2.3.4 Materials

Fillers used in the plastics industry can be divided into two categories; reinforcing and non-reinforcing. Glass, in chopped or roving form, is the most common type of reinforcing filler.[126-128] Other reinforcing fillers in use are cotton, kevlar and carbon fibres. In the second category are fillers such as clay, calcium carbonate, talc, woodflour and pigments. Depending on the type of filler (reinforcing or non-reinforcing) the compounding process can be drastically different.[129,130]

Compounding of non-reinforcing fillers usually involves generating high shear stresses in order to separate the agglomerates, particularly since these fillers normally have very small particle sizes. In compounding of reinforcing fillers just the opposite approach is taken: low shear compounding is used, in order not to damage the fillers, as the main consideration is to uniformly wet the filler, devolatilize and discharge.[99,131-135]

Polypropylene, the polymer matrix material utilized for this study, has a number of properties which make it increasingly popular within the plastics industry. These properties include: ease of processing; low density (approximately 0.9); reasonable temperature performance; good chemical resistance (as discovered later in Section 3.2.1.1.2) and high toughness. Disadvantages are that it exhibits low stiffness and low melt strength. These drawbacks can be alleviated by the use of a filler medium which will cause improvements in the two areas; a number of fillers (namely asbestos, glass, mica and talc) fall into this category. However, additional complications arise due to sharply increased materials cost, a reduction of impact strength and

the health problems particularly for asbestos. A readily available alternative is represented by calcium carbonate fillers.[136]

Calcium carbonate is a polar, reactive substance which is attacked by acids; is stable to about 800-900°C; and has a trigonal crystal shape which provides little reinforcing action. Calcite is the calcium carbonate bearing rock and is found in the form of limestone, marble, calc-spar and chalk. The rock is processed by one of the following methods [137,138]:

(*i*) Beneficiated and ground. This type is by far the most common form. The rock is crushed and disintegrated to pass through a 100mesh screen (<150*um*), purified by flotation to remove iron and silica, then ground, classified and dried to a median particle diameter range from 1 to 10*um*;

(*ii*) Dry processed. This is an unpurified, coarser calcium carbonate which is suited to less stringent applications such as vinyl foam carpet backing and dark floor tiles. It has a minimum particle size of 12*um* with a high proportion of large particles, variable colour and is lower in cost than the previous method;

(*iii*) Precipitated. The calcium carbonate particles resulting from chemical reconstitution have a median diameter up to 100 times smaller than the most common type. This more costly variant has a very high purity making it suitable for food and pharmaceutical packaging applications.

Calcium carbonate particulate fillers are in widespread use within the plastics industry mainly because of their low cost, lack of toxicity during processing and service, improvement of some physical properties (a notable exception being tensile strength) and pigmentation qualities.[136] It has been established previously that particle sizes as high as 40*um* diameter can improve physical properties

in polymers but that particles below 10um were more appropriate, particularly those with an average around 3um, for calcium carbonates in polypropylene.[139]

De Souza et al [140] found a variation in physical properties for 40wt% calcium carbonate/polypropylene compounds which they could only account for by reference to the form of the original polymer. Compounds utilizing powdered polypropylene resulted in tensile strengths higher than for polypropylene granules. They also cite surface treatment to the filler as a major influence on interfacial adhesion (filler/polymer). Significant efforts have been made by other workers [126,141,142-145] to establish suitable formulations for surface coatings and quantify their effects on compound properties. The much improved processability of surface treated calcium carbonates appears the generally agreed advantage of utilizing these coatings.

2.4 CHARACTERIZATION OF MIXING

2.4.1 Representative Parameters

2.4.1.1 Indirect measurement

Changes in physical properties such as tensile strength [146,147], modulus [148-150] or density [151] are frequently used to evaluate the degree of mixing. Although these methods have the virtue of being relatively quick and straightforward in application, they are not only a function of mixture quality but may vary as a result of polymer degradation within the matrix during processing.[152] Thus, these physical property changes cannot be taken as independent measures of mixture quality.

Other indirect measurement techniques evaluate changes in rheological properties [41,153-159], chemical reactions or electrical conductivity.[160-162] Whereas these parameters closely approach an independent measure of basic mixing, they cannot be said to be unrelated to additional variables (e.g. temperature, pressure, polymer degradation and contaminants) which will tend to complicate any interpretation of results.[28]

2.4.1.2 Direct measurement

Direct measurement of mixing can range from the simplest inspection by the naked eye for gross defects on a polymer surface to highly sophisticated quantitative analysis techniques which view particles and agglomerates directly on or through the specimen and produce particle size distributions, and other statistical means and variances.

In commercial practice, inspection for colour homogeneity and colour comparison for specks, streaks or spots of unmixed filler or resin is visual.[28] These inspections for quality control purposes are

regulated by set standards which attempt to make testing at different locations comparable. However, an array of test methods, with varying criteria for levels of acceptability, exist in many countries. The British Standards Institute sets an acceptability level for the mixture quality of carbon black pigments for use in polyolefin pipes and fittings through BS2782. This standard uses a light microscope at a magnification of 100x but specimen thicknesses must necessarily be very thin. A number of alternative examination methods for carbon black have been proposed [163-166] but none have become universally accepted.

The only true quantitative measure of mixing is by direct evaluation of particle size and the numerical distribution of sizes within a population of filler particles in a solid polymer; this can be achieved by using light, X-rays or electrons as the imaging source.[128,167,168]

If the specimen under examination is in the form of a thin slice, precautions must be undertaken to ensure that the observed particles are not superimposed upon one another. Goldsmith [169] has demonstrated, in a practical manner, the theoretical calculations necessary to correct for this situation.

2.4.2 Manual Methods

The manual method of microscopy is an extremely long and tedious process made more so by the need to examine a large proportion of the sample in order to reduce sampling errors.[170,171]

Before the general availability of image analyzers, it was necessary to size particles utilizing a graticule eyepiece on a light microscope. The particles were compared to each part of the eyepiece until a comparison was achieved.[172] It was necessary for the investigator to continue collecting the measurements individually until a sufficient number ensured that the statistical diameters (or

striation thickness for flow studies) were reasonably accurate.

2.4.3 Automated Methods

More automated techniques such as microscope-based image analysis have reduced the importance of these difficulties by allowing the collection of much larger quantities of data in less time with improvements in data processing.[168,173-180]

Alternatively, an image of the specimen can be transcribed into the image analyzer through the use of a graphics tablet; this technique is particularly applicable for glass fibre studies.[181,182]

CHAPTER 3

EXPERIMENTAL

3.1 TS40 TWIN-SCREW COMPOUNDING EXTRUDER

3.1.1 Background

The closely-intermeshing co-rotating twin-screw compounding extruder, utilized for all the experiments detailed in the following sections, originated as a result of a decision taken in the late 1970's by the Director of the Science and Engineering Research Council's Polymer Engineering Directorate (A.A.L.Challis). Challis considered that existing laboratory compounding extruders at that time could not satisfy the demands of processing and design created when they were used in academic research projects. Additionally, the desire to purchase British equipment for Government funded projects was being thwarted by a total lack of domestic laboratory twin-screw extruder manufacture.

Design of the new extruder was entrusted to an ex-GKN Windsor consulting engineer (I.Boyne) who guided the programme through the manufacturing stages at Gay's (Hampton) Ltd in Middlesex, England to delivery of the machine to Brunel University on 26 May 1981. The machine required extensive proving trials and, after many modifications, met with its output specifications.

Originally, the remit of my research project was to undertake engineering development of the new twin-screw machine and use this as the basis for mixing studies. However, financial restraints in the early 1980's did not allow full exploitation of potential engineering developments to be financed by the PED or Brunel's Dept of Materials Technology so marketing rights to the machine were granted to Gothwin

Engineering Ltd in West Molesey, Surrey, England. After a short period, the manufacturing and marketing rights were transferred to Betol Ltd of Luton, Beds, England who now sell the machine worldwide under the designation 'BTS40'.

3.1.2 Design

Table 3.1.1 outlines the TS40 extruder specification. The main criterion for the design was to produce an extruder which had the flexibility to be used as research equipment while exhibiting the reliability and cost-effectiveness necessary to make it commercially viable. To this end, the main features are:

(*i*) modular barrel sections, manufactured from Nitralloy (EN41) steel, which are all 4D long, reversible and interchangeable;

(*ii*) modular screw sections with trapezoid-shaped flights and channels which afford the machine strong positive conveying characteristics;

(*iii*) a horizontal barrel withdrawal facility that fully supports the barrel weight as it is removed from the screws, which remain in place.

A photograph showing the side elevation of the machine in its original form is found in Figure 3.1.1. It will be noted that the barrel shown in the photograph (17:1 L/D ratio) has 4 heated sections, one of which incorporates twin vent ports, and a water-cooled feed block with hopper; this arrangement being that used for most of the subsequent experiments, see Figure 3.1.2 for a schematic diagram of this configuration. Each barrel section is bored and treaded to fit an offset pressure transducer, and as each section is reversible there are many permutations of pressure measurement position. Unfortunately, apart from during the initial proving trials when transducers were borrowed, it was only possible to monitor pressure at the barrel head

during mixing experiments. The barrel head, manufactured from EN24 steel, industrial chrome-plated and polished to minimize potential points of material degradation, is bored and treaded at 2 points (at 90° separation) to allow the use of both a pressure transducer and a melt temperature probe.

The screw sections (Figure 3.1.3), also manufactured in Nitralloy steel, are nitride hardened, ground and polished to withstand wear during the processing of abrasive compounds. The modular screw design enables fine tuning of the screw configuration to suit the particular characteristics of the polymer or compound to be processed. The closely-intermeshing trapezoid-shaped flights and screw channels, and a strong positive conveying capability, distinguish the machine from the so-called 'self-wiping' co-rotating twin-screw extruder. Figure 3.1.4 shows the screw configuration employed for later mixing experiments, and details of the screw dimensions are found in Figure 3.1.5.

When the barrel is withdrawn from the screws it is supported on 3 hardened extending shafts sliding in linear races mounted in the machine casing below the barrel. The barrel sections are blind dowelled and connected by quick-release taper clamps so providing a fast and easy means of removing the barrel sections for investigation of mixing within the machine after shock-cooling, Figure 3.1.6.

3.1.3 Development

When the TS40 machine was first delivered to Brunel University it was of a bare specification without a feeder unit, die or transducers.

This type of co-rotating twin-screw extruder is designed to be operated in the 'metered-starved feeding mode' [55] as opposed to the flood-feeding of most single-screw machines; a separate feeder is required to dose the material into the hopper. A simple single-screw feeder unit was assessed using a number of different polymers and

filled compounds. However, this feeder seemed unable to cope satisfactorily with mineral-filled compounds because the screw became clogged with the material. An alternative design of volumetric dosing unit considered was one exhibiting co-rotating twin feeder screws; the K-Tron Soder T20. This feeder has 20mm diameter screws with 'Planetroll' micrometer-variable mechanical speed control and was found to deal effectively with heavily-filled mineral compounds to a high degree of consistency; it can be seen on top of the extruder in Figure 3.1.1.

The die utilized was one originally belonging to a larger twin-screw extruder used for research work within the Dept of Materials Technology. A new adaptor plate had to be machined to enable this die to fit the barrel head of the TS40 extruder. The mode of output for initial trials was in the form of strands which were water-cooled and granulated. Later experiments concerned with mixing of calcium carbonate compounds made use of an alternative gate profile producing an extrudate strip of 75mm x 3mm which was collected unsized after water bath cooling.

As mentioned above, transducers were only used all along the machine during the initial proving trials after which a single transducer was placed at the barrel head with a melt temperature probe. Pressure and output results from the initial proving trials, together with the temperature profiles used, are detailed in Table 3.1.2.

However, a number of problems that arose during the course of these initial proving trials made it necessary to modify the machine. Firstly, minor changes were necessary to the internal design of the twin vent port inserts where they met the process material at the screws. Their initial design resulted in process material being partially diverted into the vents and extruded with the effect that throughputs had to be limited.

Secondly, twin-screw extruders differ from single-screw machines in that the latter generate high levels of shear-heat and require not only barrel cooling but also screw cooling while the former usually have to be heated through the barrel continuously. However, it was found that the level of temperature in zones 2 and 4 (corresponding to the melting and metering sections of the screws) was much higher than the set value (up to 30°C in some cases). In order to rectify this situation, new heater bands were installed which featured integral cooling channels. A water supply was connected to zones 2 & 4 and regulated by solenoid values directly linked to the barrel temperature controllers. Cooling was also added to zones 1 & 3, at a later date, so that shock-cooling experiments could be undertaken.

Thirdly, it was necessary to machine 0.005inch from the inside of the feed block and 0.005inch from the diameter of the feed screws because of problems encountered when processing mineral-filled compounds. These problems involved serious fluctuations in motor current demand and excruciatingly loud screeching noises emanating from the feed block.

As a consequence of these three modifications, there was a 45% increase in output of 40wt% calcium carbonate/ polypropylene compound from the 13.7kg/hr at a screw speed of 120rpm (quoted in Table 3.1.2) to 19.8kg/hr.

Other modifications included:

(a) the provision of a hydraulic pump assembly to assist in the withdrawal of the barrel after shock-cooling of compound within the machine;

(*b*) the machining of the root of the screw shaft and spacer rings to enable the discs to be split so that 2 pairs could be positioned at the end of the second stage of the screws as mixing elements while the other 2 pairs remained as melting

elements;

(*c*) the purchase of a Simon Varifeeder for use when dosing granules or during experiments involving the separate feeding of polymer and filler.

Further details of the TS40 extruder have been published elsewhere.[183] In previous work, the machine has found application in the preparation of heavily filled polymer compounds for specific end use requirements including flame-retardant and smoke-suppressing thermoplastics formulations [184] and biomedical implant materials intended for bone replacement. [185]

The Betol BTS40 machine, now available, standardizes on the 5 barrel (21:1 L/D ratio) configuration, see Figure 3.1.2, which has provision for downstream feeding and venting at two positions along the barrel. As a further development, the 4 section (17:1 L/D ratio) configuration barrel is now being used for the Brunel 'Osciblend' in-line direct blending and injection moulding machine. [186]

Table 3.1.1 TS40 co-rotating twin-screw compounding extruder specification

Screw Diameter	40mm
Distance between screw shafts	35mm
Flight depth	5mm
Direction of screw rotation	Co-rotating
Flight pitch (17:1 L/D)	Feed 24mm Compression 16 & 12mm Melting - 4 or 2 adjustable elements on each screw Devolatilization 24mm Metering 8, 12 or 16mm Mixing - zero or 2 adjustable elements on each screw
Flight pitch (21:1 L/D)	Feed 24mm Compression 16 & 12mm Melting - 4 adjustable elements on each screw Feed or Devolatilization 24mm Compression 12mm Devolatilization 24mm Compression 16mm Mixing - 2 adjustable elements on each screw Metering 12mm
Screw speed	10 to 200rpm
Drive	5.5kW dc motor with a base speed of 1500rpm; 13:1 reduction gearbox; 1:1.73 torque splitting gearbox
Output	Up to 30kg/hour depending on raw materials and die configuration

Screw length/ diameter ratios (L/D) are from front of feed port

Table 3.1.2 Processing conditions and results for the initial proving trials

	Extrusion material				
	1	2	3	4	5
Temperature Profile (°C)					
Zone 1 (Set/Indicated)	185/189	195/198	190/196	195/199	195/230
Zone 2	200/204	210/204	195/200	210/212	210/236
Zone 3	215/220	220/220	200/204	225/228	225/240
Zone 4	225/239	225/230	205/224	230/249	230/245
Zone 5	225/229	225/225	210/214	235/238	235/239
Maximum Output (kg/hour)					
30rpm	3.1				
60rpm	7.1	9.3	6.6	7.7	5.2
90rpm	10.5				
100rpm	12.2				
120rpm	14.7	16.9	11.2	13.7	9.8
150rpm	17.4				
180rpm	23.1	21.0	14.5	19.2	13.6

	Polypropylene powder (ICI-GW522M)		
Pressure (MPa)	60rpm	120rpm	180rpm
End of Zone 1	0	0	0
End of Zone 2	0.3	0.6	0.8
End of Zone 4	2.1	3.6	3.9
Barrel Head	0.8	1.2	1.2

1 = polypropylene powder (ICI-GW522M); 2 = Polystyrene granules (BP-KLP C2 Crystal; 3 = HD Polyethylene (BP-Rigidex 509201); 4 = 40wt% calcium carbonate in PP; 5 = 60wt% calcium carbonate in PP.

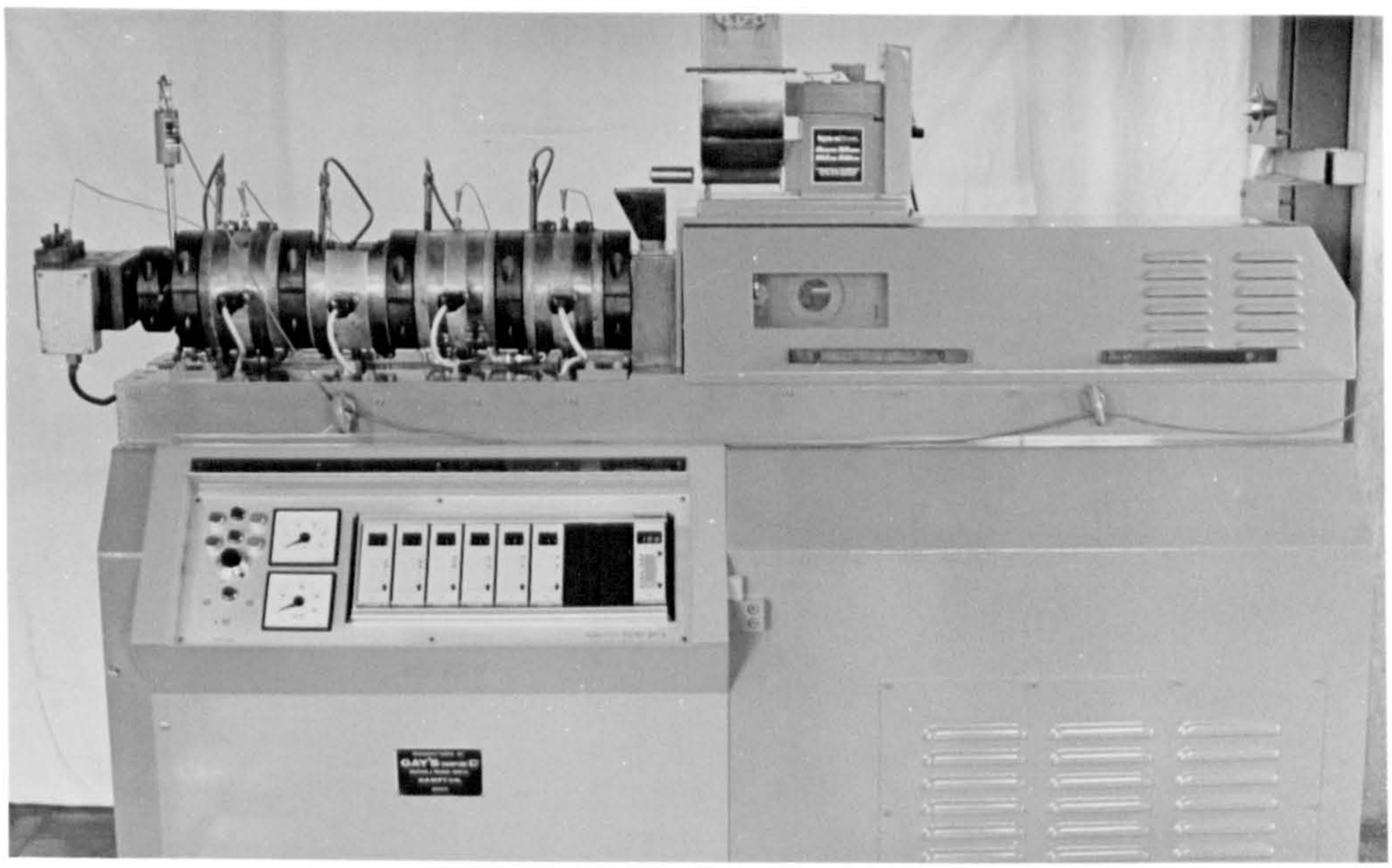

Fig.3.1.1 Side elevation of the TS40 twin-screw compounding extruder

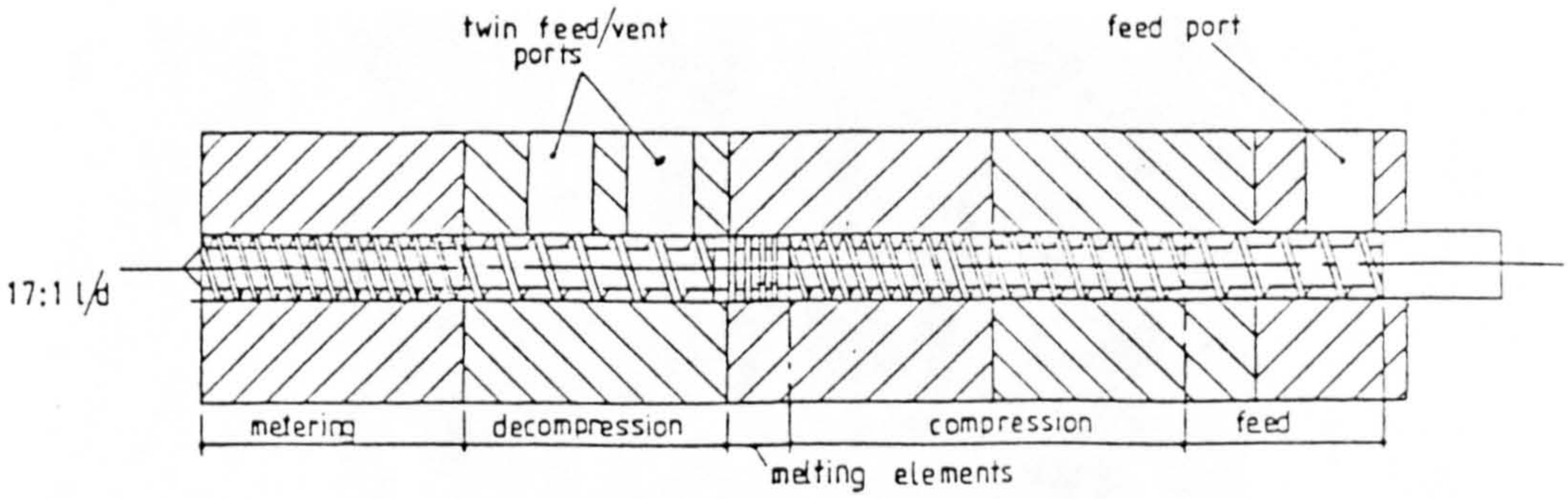

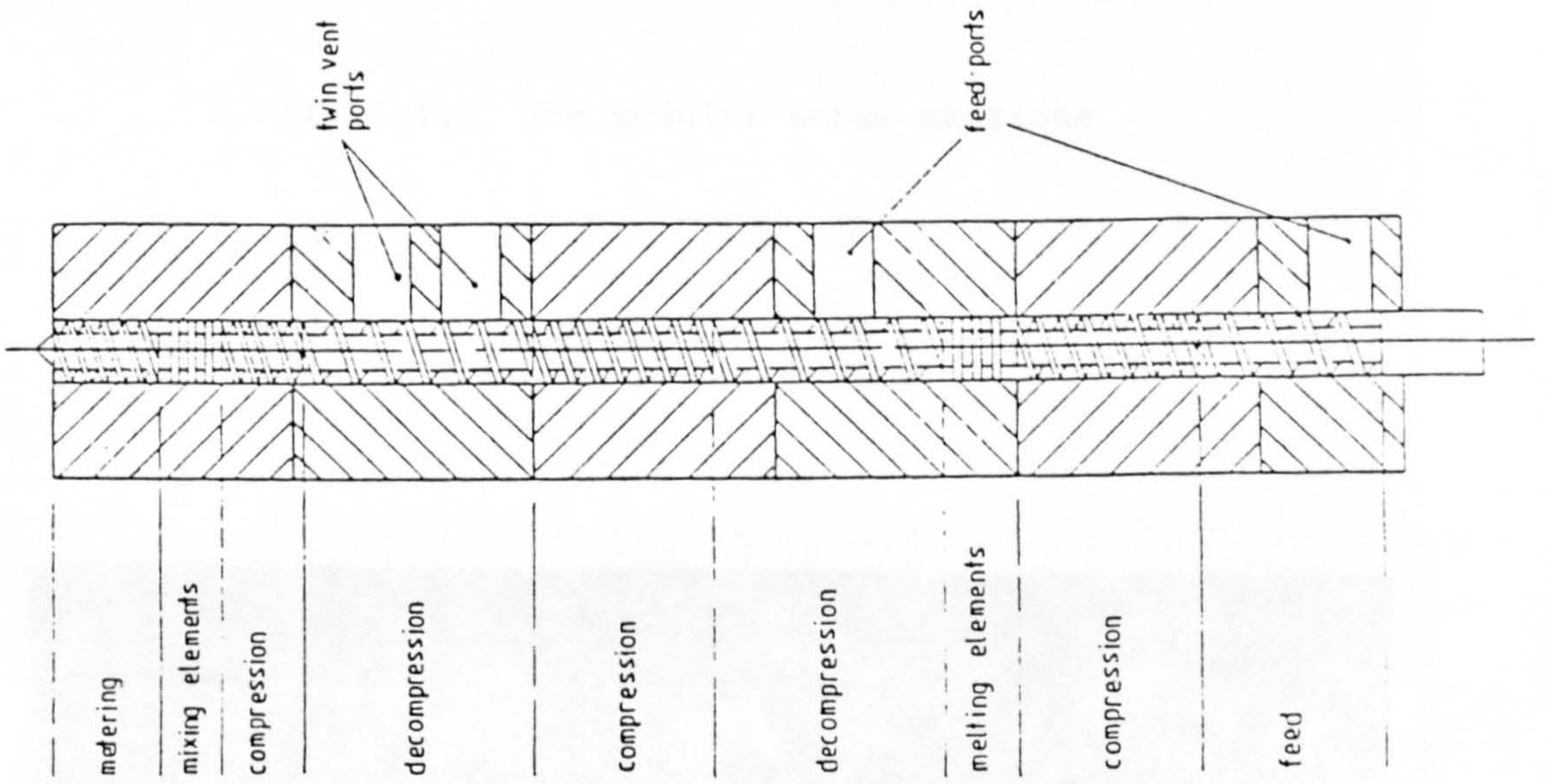

Fig. 3.1.2 Schematic diagram showing standard - 4 barrel - and extended - 5 barrel - configurations (only one screw shown for each configuration)

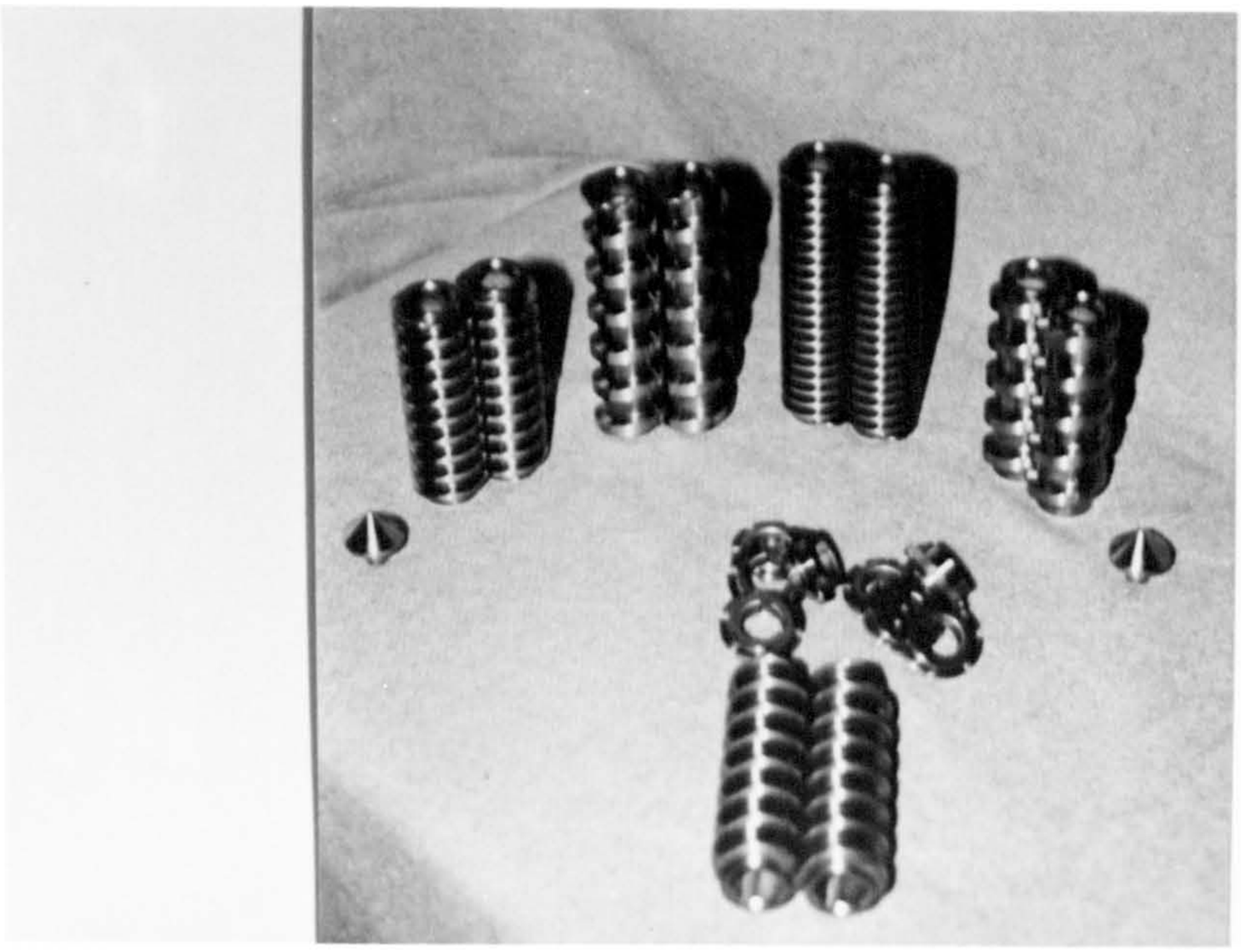

Fig.3.1.3 The modular screw sections

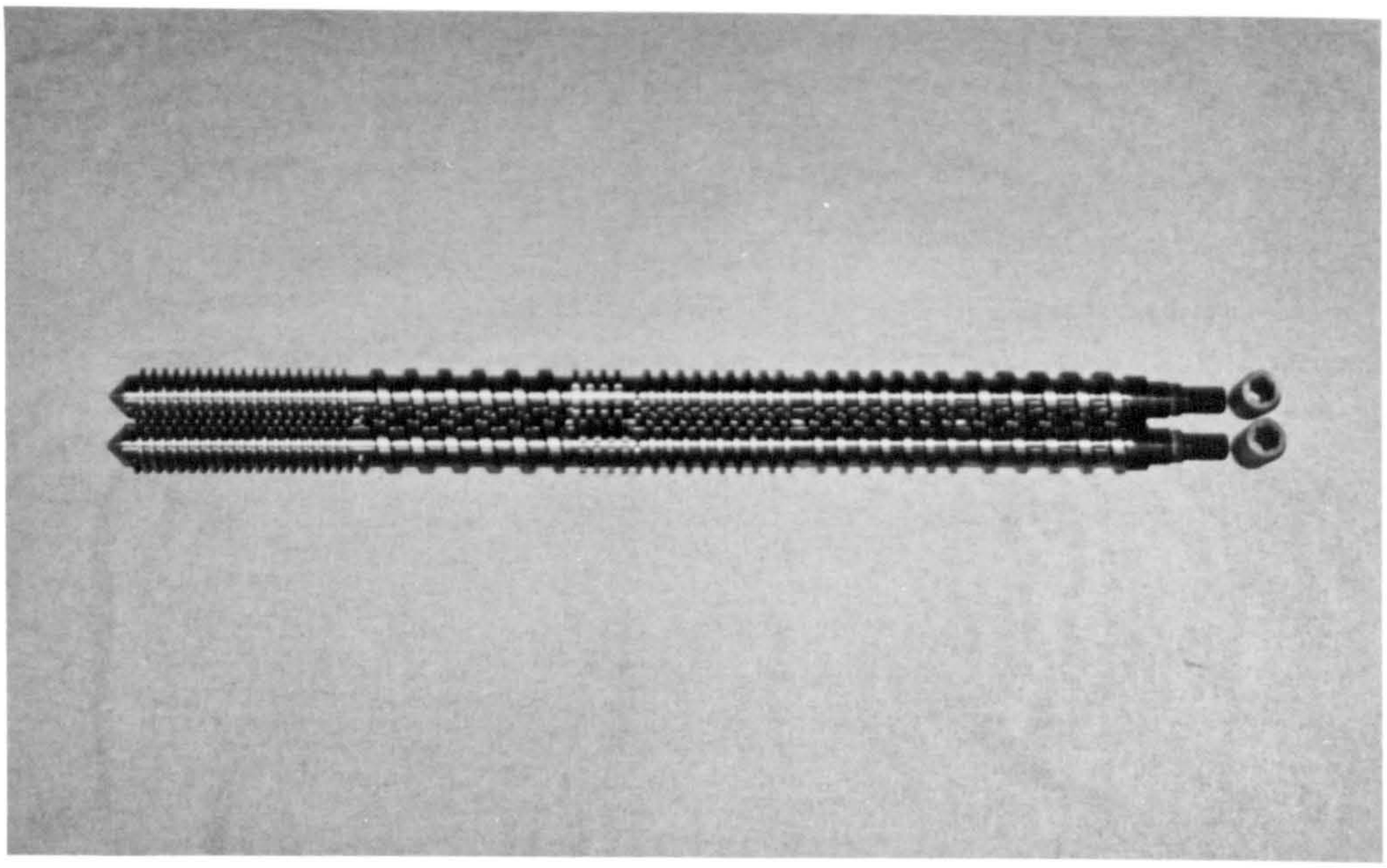

Fig.3.1.4 Screw configuration used in mixing experiments

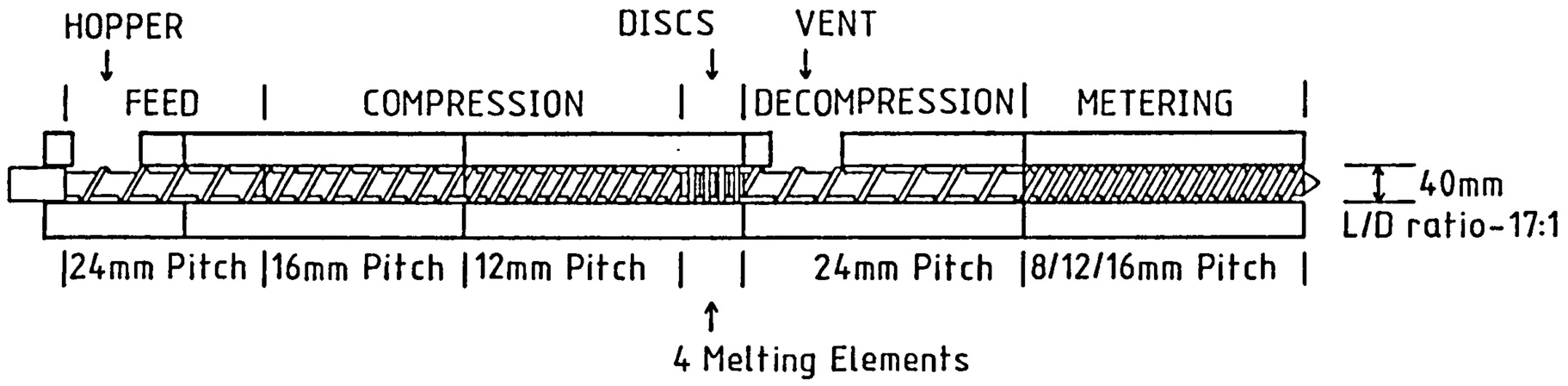

Fig. 3.1.5 Dimensions of screw configurations used in mixing experiments

Fig.3.1.6 Barrel withdrawn to the left leaving screws encased in solidified material (Feed enters at right hand side of screws)

3.2 DEVELOPMENT OF CHARACTERIZATION TECHNIQUES

The complete characterization of mixing within any composite presents formidable difficulties which are synonymous with counting and recording, one by one, the size of each brick in a large building, viz. the task is possible but very inefficient both in terms of time and effort spent. In a situation such as this the usual course is to adopt any number of mathematical 'short-cuts', collectively known as statistics, which allow global rules to be applied to the problem.

For the large building it may be assumed that the investigator does not wish to demolish the structure brick by brick merely to examine each in turn. In this case the number of bricks may be determined by first calculating the average quantity per unit area (allowing for windows and doors) and then applying the measured surface area to establish the total number of equivalent bricks. Advantages of this procedure are that only the height and width of each wall need be measured and automatic allowances are made for cut bricks at corners and around openings. The physical characteristics of the bricks may be assessed by removing a small number (not from the bottom!) as a sample for analysis. The analysis may show that all the bricks are the same size but it is unlikely; more probably there is a distribution of heights, widths and lengths about mean values. Further small samples of bricks are analyzed until accumulative mean values remain within defined limits after each sample. It is now possible to state firmly that a given percentage of the bricks are within a certain range; the width of the range will depend on the quality of the bricks analyzed.

The aforementioned characterization illustrates how the simplest of statistical assumptions and manipulations can greatly assist in the analysis of a composite structure when tolerances from absolute values are specified. Microstructural characterization of filled

thermoplastics compounds presents one with similar analysis problems to those found when examining the building except that the former exists as a randomly orientated solid rather than a structured shell. It follows that microstructural analysis of a matrix containing particles may be based either on assessing the mean number of filler particles per unit volume or on particle size distributions and mean particle sizes.

The calculation of the number of filler particles per unit volume would only be relevant if filler concentration variations (distribution) throughout the solid were of interest in which case the standard deviation would be employed. Additionally, an analysis investigating the filler particle frequency may be postulated as a measure of dispersion but both are flawed because as the particles reduce in size the probability of sizes below the examination-method resolution limit increases. Thus, the total number of particles present would, at some point, peak and then appear to decrease as dispersion progresses.

In the present context of extrusion compounding, the spatial distribution of particles is subservient in the presence of filler agglomerates because any spatial inhomogeneity can, if necessary, be eliminated during subsequent forming operations but only after the required dispersion level has been achieved. Therefore, particle size distribution analyses were conducted on solid samples selected from predetermined positions both within and outside the extruder so that valid comparisons were possible between different processing and material variables. However, initially it was necessary to consider many different methods for characterising mixture quality in order to identify the most suitable for this application because of a lack of established quantitative techniques. The following sections detail the procedures investigated which are reviewed in work already published by

the author and co-workers.[1] Since image analysis has figured prominently as the quantifying tool, its mechanisms both physical and statistical are explored in some detail.

3.2.1 Sample Preparation

In this section, experiments were undertaken to determine the most appropriate preparation technique for transforming calcium carbonate/ polypropylene compound samples into a form suitable for subsequent examination by microscopy or X-ray characterization procedures. Methods considered included isolating the particles from the matrix, forming thin films and careful preparation of solid surfaces.

3.2.1.1 Isolation of the filler

At first acquaintance, the problem of sample preparation methodology appeared to necessitate the removal of the polymer matrix, by one means or another, so that the filler particles were exposed for subsequent analysis. The isolation of the filler particles would thence enable analysis by any number of particle sizing techniques, viz. sedimentation, microscopy, sieving or electrolytic resistivity; accordingly, the following techniques were investigated.

3.2.1.1.1 Ashing of the compound

The burning off of the polymer matrix was initially utilized to determine the actual filler concentration in given samples taken after processing. A sample of approximately 10g of the compound was weighed accurately into an alumina crucible of a suitable size and approximately 4g of the corresponding raw calcium carbonate powder was also weighed into a crucible. The crucibles were placed in an electric furnace for the ashing procedure but it was necessary to exert caution over the level of temperatures used in order to avoid decomposition of

the calcium carbonate constituent. After some experimentation, the furnace was operated at 250°C for the first hour to allow the most volatile portions of the polymer to dissipate without eruption of the compound from the crucible. The remainder of the matrix was removed at a temperature of 550°C (well below the decompostion temperature range for calcite, 725-850°C [187] over a period of four hours and, after cooling overnight, the crucibles were removed and weighed accurately. Nevertheless, even during this minimal heating cycle the raw calcium carbonate powder was found to have lost about 1wt%; a second phase temperature of less than 550°C left a carbon residue from the polymer matrix. The remaining calcium carbonate material had the appearance of being compacted and would not flow so negating any attempts at analysis.

As an alternative to the bulk ashing of compound, a thin film was pressed from the sample and then ashed between glass microscope slides in the furnace using the same temperature regime as above. However, the resulting ashed material was too dense to be examined by transmitted light microscopy, Figure 3.2.1, while under reflected light the material exhibited no surface characteristics of interest. A further attempt at refinement involved the ashing of a microtomed section but the resulting specimen presented the same examination problems as before, Figure 3.2.2.

3.2.1.1.2 Dissolution of polymer matrix

In order that the calcium carbonate filler particles would not compact, dissolution of the polymer matrix in solvent was considered. A problem immediately encountered was that polypropylene is a very solvent-resistant polymer and so a variety of organic solvent systems were employed:-

(*i*) toluene;

(*ii*) o-xylene;

(*iii*) n-heptane;

(*iv*) diethyl ether/ n-hexane/ n-heptane; and

(*v*) diethyl ether/ n-heptane/ methylcyclohexane.

Samples of the compound were refluxed with each solvent system for several hours in a Soxhlet extractor but it appeared that only o-xylene had any effect on the polypropylene matrix and then only with several fresh charges of solvent. Nevertheless, even this solvent was not able to fully remove the matrix material so making very difficult the casting of the powder filler for examination. Subsequent microscopic analysis showed partial binding of the filler particles effectively preventing subsequent analysis of agglomerate structures, Figure 3.2.3.

3.2.1.2 Thin film formation

Accepting that isolation of the calcium carbonate filler from a polypropylene matrix had proved unsatisfactory, the possibility of forming a film thin enough for transmission light microscopy was considered. The most simple method available was that of hot pressing.

3.2.1.2.1 Pressing and bubble formation

A sample of the compound was placed between polished steel plates, heated to approximately 200°C and pressed at 4.3MPa to produce a free-flow film. However, the film was found to be too thick for filler particle agglomeration assessment. A range of higher pressing temperatures were investigated in order that greater flow of the compound might be encouraged; the only effect observed was an excess scorching of the polymer matrix.

The production of very thin films has been achieved by using a free blowing technique utilized during previous studies concerned with pigment dispersion [188] and as a quality control technique.[189] In

this case a thin film, produced as detailed above, was clamped around its periphery onto a simple design of free-blowing apparatus, Figure 3.2.4. The apparatus, with the film attached, was heated from above for a sufficient time to soften the compound so enabling a dome to be blown by air pressure from below. After much trial and error, it was possible to produce very thin sections within the film dome which permitted examination by transmitted light microscopy. The calcium carbonate filler particles could be identified within the polymer matrix although it transpired that few filler agglomerates were present. The problem was that the larger agglomerates remained at the periphery of any blown section; the blown section being composed mainly of polymer film. These domes also made the acquisition of a flat distortion-free sample difficult because of their tight curvature, Figure 3.2.5. Additionally, the pressed film tended to exhibit flaws, such as small voids, which repeatedly prevented the formation of a large dome.

3.2.1.2.2 Thin film extrusion

In place of film blowing, a low-intensity short L/D ratio single-screw extruder was used in order to increase the inter-particle distance in the matrix. The compound was mixed with unfilled polypropylene so that the ultimate filler concentration in the mixture was 10wt%. This mixture was then fed to the low-intensity extruder of a laboratory film casting line, Figure 3.2.6 and the extruded tape drawn down by approximately 3:1 so as to further increase particle spacing. The resulting tape, Figure 3.2.7, was found to contain large clumps (1-3mm diameter) with very few other particles present, signifying that the level of distributive mixing imparted by the extruder was not sufficient. The use of an extruder exhibiting a higher level of mixing intensity was rejected on the grounds that its

dispersive mixing contribution would complicate any subsequent analysis.

3.2.1.2.3 Microtomy

At this stage, a new direction was adopted in respect of producing a thin film for analysis by transmitted light microscopy; instead of fabricating a thin film, one would be sliced from the original solid. The technique for achieving this slicing, known as 'microtomy', is an established means of producing thin sections of polymeric materials for microstructural analysis. The *modus operandi* of this technique is very much akin to that of the butchers' bacon slicer. However, it is possible under favourable conditions to produce slithers of material as thin as 5um using a steel-bladed sledge microtome.

Particular problems arose, however, when trying to section polypropylene compounds containing high loadings of the calcium carbonate filler. The major drawback was that on cutting through the material there was a tendency for poorly bonded filler particles to be pulled from the thin specimen. Furthermore, filler particles displaced in this manner also . severely damaged the surface remaining on the original solid sample causing a drawn, wave-like deformation. Freezing of the solid sample down to -20°C (below the glass transition temperature of the polypropylene matrix) with carbon dioxide gas resulted in some reduction in the surface damage, Figure 3.2.8. Nevertheless, the steel bladed RAPRA-designed cryomicrotome, Figure 3.2.9, could not completely prevent filler particle egression from the microtomed surfaces. Additionally, examination of the microtomed sections by transmitted light microscopy revealed a further complexity, viz. some of the remaining filler particles were found to overlap making quantitative image analysis very difficult.

3.2.1.3 Polished solid surfaces

A readily available method which allows the observation of particles without overlapping effects is the metallurgical technique of surface polishing. This technique facilitates a flattening of the surface of the compound to such an extent that filler particles are contrasted against the almost mirror-finish of the polymer matrix so enabling resolution by reflected light microscopy.

In order to accommodate subsequent polishing and analysis procedures, a representative sample was removed from the whole and flash moulded, on a hydraulic compression press, at 4.3MPa to form a 3mm thick disc of 25mm diameter.[190] After encapsulation in polyester resin to form a polishing block, excess resin was removed on a mechanical sanding belt until the composite became exposed. The block was ground by hand on progressively finer emery paper down to 600 grade so that each grinding step removed the damage which resulted from the previous grade.[191] Polishing was achieved by using diamond pastes graded at 6 and 3um while final polishing to 1um was performed using a mechanical block rotator mounted above the rotary polishing mats to give standardized conditions, Figure 3.2.10. This mechanical rotator enables concurrent omni-directional polishing of six blocks while a fixed number of weights above each block provide a constant inertia.

In an attempt to further refine the technique, some initial samples were etched with dilute nitric acid to dissolve the calcium carbonate particles at the surface. However, although etching resulted in a very slight improvement in contrast between the matrix and the pits left by the calcium carbonate, the outcome did not justify the extra procedural effort involved.

3.2.2 Sample Examination

3.2.2.1 Light microscopy

The use of transmitted light microscopy as an analytical tool is obviously limited to the examination of thin films or a layer of particles. In both these cases, the possibility of particles overlapping to some extent arises; a loose layer of particles could nevertheless be further spread out within the field of view. However, as already mentioned, it has proved impossible to separate the calcium carbonate particles from the polypropylene matrix efficiently enough to form a free-flowing powder.

For examination of the compound polished to a 1um finish, a reflected light microscope was found to provide clear images of the surface containing calcium carbonate agglomerates over a range of magnifications; in this case from 60 to 160 times at the eyepiece. A magnification of 400 times was available but its usefulness limited at this level because the 1um polishing lines were visible; it would require an additional time-consuming 0.25um polishing stage in order to examine 5-7.5um diameter particles. Measurement of sub-5um particles involves an unacceptable increase in errors due to blurring of particle edges as a result of diffraction effects.[161]

3.2.2.2 Scanning electron microscopy

Scanning electron microscopy finds its greatest use in areas of study requiring surface magnifications in the high hundreds and low thousands. This type of electron microscope can also operate within the same range as a reflected light microscope giving an image with enhanced contrast and definition, although the polished compound blocks first require modification. The resin of the mounting block must be machined down to enable it access to the specimen chamber of the microscope. In order to produce an electron charge large enough to

generate images, a conducting medium of either gold or carbon is splutter-coated onto the compound surface in a vacuum deposition apparatus. However, once inside the microscope the specimen surface is subjected to a bombardment by high-speed electrons which, because of the thermoplastic nature of the matrix, can alter inherent surface characteristics after long exposure. Consequently, when the extra cost and effort demanded by this technique are taken into account, it does not appear to offer any significant advantages over reflected light microscopy.

The only exception is when it is necessary to confirm the elemental nature of a surface characteristic. The enabling technique is known as 'electron probe microanalysis' and involves a computer comparison of the X-ray radiation given out from the specimen, when bombarded by electrons, with a database of elemental wavelengths. This energy dispersive spectrum analysis allows one not only to identify a particular element, in this case calcium within the filler, but also to build up an X-ray dot-image of calcium ions detected on the sample surface, Figure 3.2.11. Therefore, it is possible to confirm the presence of calcium carbonate agglomerates observed by light microscopy when the composition of such structures may be in doubt.

3.2.2.3 Contact microradiography

In principle, this technique is similar to transmitted light microscopy in that it requires a specimen thin enough to allow the passage of radiation. The radiation in this case is not light but soft X-rays (i.e. between 1-15nm) and detection of the image is by means of a high-resolution emulsion placed beneath the sample. Identification of particles depends on a differential between the absorption coefficients of the filler and the matrix thereby causing variations in emulsion exposure. Previously, this technique has been used

successfully in studies into short-glass fibre orientation in thermoplastics.[192]

Initially, a thin film specimen was clamped to the emulsion plate under a glass sheet, placed in a shielded bag and exposed to X-rays using a simple X-ray source. However, not only were the resulting images very faint but on closer examination it was found that interference images from the shielding material were overlaid on the sample image. As an alternative method, a microtomed section of compound was placed in contact with a glass plate coated with a fine-grained X-ray sensitive emulsion and the whole installed in an electron microscope under vacuum. The X-rays, generated from a cobalt foil bombarded by electrons, were then directed onto the sample for a controlled time. The exposed plate was subsequently developed into a micronegative and viewed through a transmitted light microscope, Figure 3.2.12. The resulting image presented no apparent advantages over the direct transmitted light microscopic examination of thin sections of material.

3.2.2.4 Acoustic microscopy

Acoustic microscopy offers an intriguing method of imaging the structure of compounds composed of mineral fillers in polymers.[193] Normally, this technique is utilized in much the same way as the light microscope either in a transmitted or reflected mode depending on sample thickness. The sample is immersed in a water bath so that an acoustic beam can be focussed on the sample through a spherical sapphire/water interface and detected below for the transmitted mode or above for the reflected mode. The sound received by the detector is analyzed in respect to beam deflection, absorption and scattering which are related to the density and elasticity of materials within the sample. The beam source/detector is mechanically moved across and

along the surface to build up a computer-generated composite image. However, any analysis of the polished surface of the calcium carbonate filler in a polypropylene matrix proved impossible, Figure 3.2.13, because the magnification of the instrument was too low and the resolution poor in comparison to optical microscopy.

This method offers the potential for non-destructive visual analysis when high frequency sound is focussed below the surface of a solid. The resulting image would provide an accurate representation of the filler agglomerates *in situ* allowing not only individual size determination but also shape analysis. However, this refinement requires significant development before a reliable experimental technique emerges.

3.2.3 Image Analysis

3.2.3.1 Introduction

As discussed previously, the author considers that quantitative assessment of mixing is best achieved by direct measurement of filler agglomeration within the polymer matrix. It was concluded from the above review of sample preparation and examination procedures that the study of polished composite surfaces using reflected light microscopy had most potential as part of a quantitative characterization technique. However, the next step involves the determination of agglomerate size and frequency - known as quantitative microscopy or stereology - which is in itself a daunting task. This task, if it was undertaken manually using a graduated eyepiece fitted to a reflected light microscope would be extremely tedious, and measurement errors due to mental fatigue of the investigator would be potentially large and unquantifiable. Accordingly, the need for automatic particle sizing equipment arises because of the necessity that agglomerates be quantified with definably low statistical errors.

In the sections below details are given of how the image analyser can effectively measure the areas of particles on a polished specimen surface. However, the image analyser only relates these as totals for the field under examination in arbitrary machine-defined units, i.e. pixels. An interfaced computer uses its software to calibrate the measurements in operator-defined units and allows the determination of area size distributions. These distributions are expressed as equivalent area spherical diameters, and after statistical analyses to correct for sectioning errors at the surface, an average figure - number, mean volume diameter (MVD) - together with maximum detected particle diameter (D*max*), area fraction occupied by detected features (AF) and the standard deviation of area fraction (SD*af*) are derived which together describe mixture quality.

3.2.3.2 Assumptions

The image seen under a microscope is a two-dimensional representation of a three-dimensional object. This image may be that projected when a random test section of the object is examined by transmitted radiation or a random test surface at a given plane under reflected radiation. Thus, any measurements made from this image are approximations of the actual parameters assessed. For particle size measurement the most widely utilized parameter is 'particle diameter'. The particle diameters most frequently measured are [161]:

(*a*) Martin's diameter - a randomly positioned straight line intersects the particle and the length covering the particle is taken as Martin's diameter.

(*b*) Feret's diameter - is the maximum diameter between parallel planes maintained at a given angle for all measurements.

(*c*) Longest dimension - the maximum Feret's diameter regardless of plane orientation.

(*d*) Maximum chord - the maximum Martin's diameter.

(*e*) Perimeter diameter - an equivalent spherical diameter producing a circle of the same circumference as the measured particle.

(*f*) Equivalent area spherical diameter - the diameter of a circle covering the same area as that of the measured particle.

All these diameters are dependent on particle orientation when determined from a polished surface by reflected radiation; in this case statistical corrections have to be employed to allow for the possibility of not sectioning a particle at its maximum area, more of which follows later. However, of the above diameters, the equivalent area spherical diameter is by far the most accurate as it is easily measured and takes account of irregularly shaped particles. Also, more importantly, the measurement of equivalent area spherical diameters allows the use of statistical size distribution analyses which would otherwise be inapplicable to irregular shaped particles.

3.2.3.3 Data acquisition

The basic principle which lies behind Image Analysis involves translating an image into digital code so that data processing can be performed, Figure 3.2.14. The image may be entered into an Image Analyser system from a variety of sources. For semi-automatic analysis, a graphics tablet can be used which requires the operator to manually enter data points determined from previously produced micrographs. This method of entry makes the accurate determination of area data virtually impossible. Automatic analysis utilizes a high-resolution television camera which can either view a micrograph or be mounted on a microscope to directly view the image of the specimen. For this study, an Optomax IV Image Analyser (Micromeasurements Ltd) with a Chalnicon high-resolution camera was connected, via an image

splitter, to a Zeiss light microscope in reflected mode, Figure 3.2.15. In addition, the image splitter allowed the attachment of a 35mm camera to record interesting features.

The image analyser equipment consists of the above mentioned camera at the sharp end attached to a hardwired image processor which forms the main part of the equipment. This image processor displays the view seen by the camera on a VDU monitor onto which is superimposed a circular frame depicting the area from which data will be collected. The operator can determine the size of this circle to suit specific specimen fields.

Examination of highly polished composite surfaces by the image analyser camera requires very careful alignment of the specimen in order that the reflected light is as even as possible across the field of view. This is important as the whole concept of image analysis relies on the detection of variations in grey-levels (contrast) displayed by the specimen. If large variations in lighting contrast across the light polymer matrix surface are present then the detection of dark particles on the surface becomes unacceptably inaccurate. Small variations can be compensated for by utilizing a 'shade correction' feature built into the hardware which changes the contrast detection from linear to curved to allow for the usual situation when illumination is greater at the centre of a field than at the edges. A further control on the image analyser console allows the operator to set a limit either above or below which grey-levels of contrast will be detected within the circular frame, and features which are in this category are highlighted in white on the display VDU. This control is carefully manipulated so that the detected areas exactly match the agglomerates (which appear dark under unpolarised light) present on the almost white background of the highly polished specimen surface.

Once the detection area and grey-level have been set the operator

can manually initiate a scan of the field of view during which 'firmware' - dedicated microprocessors within the image analyser - measure three parameters of the image field. These parameters are the total number of features, total area of the features and the number of intersections of the camera scanner lines by detected features. This data on its own is of little use for particle size analysis because it only applies to the whole field of view and not individual features. In order to produce size distributions of the detected features, a microcomputer is interfaced to the image analyser to enable incremental sizing by software control of the firmware. Details of the software and data processing employed are found in the next section.

3.2.3.4 Data assimilation

The original software supplied with the interfaced Apple computer was found to be of a very generalized nature, so a prerequisite task involved the development of an entire suite of programs to measure section size distributions, make statistical analyses and to output data in a suitable form (See Appendix A for the software listings).

In order that the image analyser may measure size distributions, it is necessary for software to initiate a set number of scans across the circular field over a range of size classes. The software allows calibration of the image analyser so that measurements are expressed in a preferred dimension, other than digital picture points or 'pixels'. A standard number of size classes (15) is established by the software so that during a size distribution analysis the number of particles and their areas disappearing from the totals at each increase in size class limit are placed in the preceding size class. In this manner, a particle area distribution of raw data is collected over a number of fields for each specimen surface. The software simultaneously transforms the area data into an equivalent area spherical diameter

distribution and stores this raw data to floppy disk for subsequent statistical analysis. Additionally, measurements are made of total area of examination (At), area fraction of detected particles (AF), standard deviation of area fraction (SDaf) and the total number of intersections per unit length of the scan line (NI).

3.2.3.5 Statistical analysis

The most immediate statistical problem to be tackled during subsequent analysis is to consider how to transform a two-dimensional image at a random plane through the composite into a three-dimensional statistical representation. It will be recognized that particles, in this case agglomerates, could have been sectioned at any level of their diameter and that different agglomerates will probably be sectioned at different levels to produce a range of section diameters. Many different approaches have been propounded as mechanisms to correct for this situation and these are very effectively reviewed by Underwood.[194,195] The basic correction which allows for the statistical probabilities of sectioning at given fractions of the particle diameter is well established but the refinements which distinguish between area, diameter and chord distributions and the number of size classes supported are numerous, see Table 3.2.1.

3.2.3.5.1 Sectioning of a single sphere

As stated above, agglomerates have been measured not by observed diameter but rather by observed area which are then transformed into equivalent spherical diameters so that theory may be developed along the lines applicable to spheres. This approximation of particle shape to a sphere is considered insignificant compared to the increased accuracy of measurement and vastly increased availability of applicable theory. The basic theory that enables analysis of polydispersed

systems first involves the consideration of the probabilities of sectioning a single theoretical sphere with random planes. The probability P(*i*,*j*) of the plane crossing the sphere through a given slice of height, h, is:

$$P(i,j) = h/rmax = (h(i-1) - h(i))/rmax \qquad (3.1)$$

where *i*'s refer to section diameters and *j*'s refer to particle diameters. This probability can be expressed more usefully by substituting values of radii instead of height, h:

$$P(i,j) = 1/rmax \left[\sqrt{rmax^2 - r(i-1)^2} - \sqrt{rmax^2 - r(i)^2}\right] \qquad (3.2)$$

3.2.3.5.2 Sectioning of polydispersed spheres

When a polydispersed system is considered, *rmax* relates to radius of each size class of particles which produce a range of radii below *rmax* at the random plane so characterization involves the additional problem of unscrambling the sectioned surface features and relating them back to the original system of three-dimensional particles. One will readily appreciate that although two sectioned particles may present the same area at the surface, it is uncertain whether these sections originated from particles of the same size or different sized particles sectioned at different levels.

If the average diameter of all the particles is $\underline{D}$, then statistically the particles will only be cut by the test surface if they lie within a distance $\underline{D}/2$ above or below the test surface, viz. within a volume defined by the area of test surface and average diameter, $\underline{D}$. The number of particles, N*v*, contained within this volume must therefore equal the number of observed particle sections on the test surface, Na:

$$Nv = Na \,/\, \underline{D} \qquad (3.3)$$

Eqn.3.3 is considered by DeHoff [196] as representing "one of the fundamental relationships of quantitative metallography" and it is from

the assumption of this equation that all the following analyses are derived.

For a system of particles which have been divided into a number of size classes, Eqn.3.3 becomes:

$$Nv(j) = \sum_{i} Na(i,j,) \; / \; D(j) \qquad (3.4)$$

where the particles in each size class are taken as being the same diameter, viz. the mid-point diameter $D(j)$, $Nv(j)$ is the number of particles of diameter $D(j)$ per unit volume and $Na(i,j,)$ is the number of sections of diameter $D(i)$ per unit area produced by particles of $D(j)$. The equation means that the total number of sections of all diameters per unit of surface area, $\sum_{i} Na(i,j)$, produced by particles of single diameter $D(j)$ are required. Unfortunately, as mentioned above, these quantities cannot be measured directly from the section surface. Nevertheless, a quantity that can be determined is $\sum_{j} Na(i,j)$ which depicts the total number of sections of single size, $D(i)$ produced from particles of all diameters.

The probability $P(i,j)$ of sectioning a particle of diameter $D(j)$ to produce a section of diameter $D(i)$ has been defined in Eqn.3.2 above and the same equation can be expressed in terms of $Na(i,j)$:

$$P(i,j) = \sum_{j} Na(i,j,) \; / \; \sum_{i} Na(i,j,) \qquad (3.5)$$

This equation represents the ratio of the number of sections per unit area of one diameter, $D(i)$, to the total number of sections per unit area.

Rearranging Eqn's 3.4.and 3.5 we may write:

$$Nv(j) = \sum_{j} Na(i,j,) \; / \; [P(i,j).\; D(j)] \qquad (3.6)$$

Eqn.3.6 gives a basis on which to progress further towards determining the number of particles per unit volume for each size class, $Nv(j)$, so enabling the formulation of a three-dimensional size distribution. The first term $\sum_{j} Na(i,j)$ can be measured from the test surface or calculated, $P(i,j)$ can be calculated using Eqn.3.2 for a given number

of size classes and D(*j*) is either D*max* or an incremental fraction determined by the number of size classes.

At this point, it would be useful to reiterate that the sections observed on the polished surface are possibly derived from any size class particles. The maximum measured section, D*max*, must be equal to the diameter of the largest particle but the next largest section diameter could be derived from either the same sized particle or the largest particle. Accordingly, the calculation of the number of particles per unit volume in this next largest size class takes the number of observed sections of this diameter and subtracts the number of sections derived from the largest size class determined by the probability calculated in Eqn.3.2.

3.2.3.5.3 Schwartz-Saltykov (diameter) analysis

Of the analysis techniques for determining size distributions by diameter and area, detailed in Table 3.2.1, only two allow independent calculation of each size class interval and variable number of size classes.

The independent calculation of each size class interval eliminates the possibility of errors in the measurement of section diameters compounding with each sequential calculation proceeding from the largest diameter to the smallest. A variable number of size classes is desirable because it allows the analysis to be either very accurate using a large number of classes albeit at a time-penalty or a smaller number of classes can be specified for faster, less precise applications. Additionally, the usual situation is one where the value of D*max* is not known before analysis and if the largest size class is over-estimated a number of the size classes will be empty. When this occurs, as is the normal circumstance, the analysis must enable independent calculation of a smaller number of size classes. The area

analysis technique exhibiting these features is that developed by Saltykov which unfortunately relates all measurements to the maximum section area on a logarithmic scale, so giving extra weight to sections as they become progressively smaller which is exactly opposite to that required of analyses for agglomeration measurement. The only diameter analysis with the above-mentioned features is that named after its joint originators, Schwartz-Saltykov.

The Schwartz-Saltykov (diameter) analysis enables up to 15 size classes to be specified, but for reasonable accuracy a minimum of 7 are required. The analysis defines a term, which I shall call '#', as the ratio of D*max* to the total number of size classes, *k*. Thus, the first size class contains particles of diameter #, the second 2# and so on up to the largest diameter, D*max*, which equals *k*#. Table 3.2.2 details the notation used in the Schwartz-Saltykov (diameter) analysis. It should be noted that the bottom limit of the first size class, diameter #, should be equal to zero because of the manner in which the probabilities P(*i*,*j*) are calculated (described above and shown in detail below) but alternatively it can be set at a small defined particle size if account is taken of the error thus generated, see Section 3.2.3.6.

Using the notation from Table 3.2.2, it is possible to write an equation giving the total number of sections of the first size class per unit area:

$$Na(1) = \sum_{j} Na(1,j)$$
$$= Na(1,1) + Na(1,2) + /// + Na(1,j) + /// + Na(1,k) \qquad (3.7)$$

and for second size class:

$$Na(2) = \sum_{j} Na(2,j)$$
$$= Na(2,2) + Na(2,3) + /// + Na(2,j) + /// + Na(2,k) \qquad (3.8)$$

and so on for all the other size classes.

The probabilities, P(*i*,*j*), that the test surface will intersect

particles of various diameters D(*j*) to produce given section diameters D(*j*) can be calculated using Eqn.3.2 above. It is then possible to establish equations of Nv(*j*) in terms of Na(*i*,*j*) which are substituted into Eqn's 3.7, 3.8, etc leaving Nv(*j*) expressed as values of Na(*i*), the observed section diameters.

The Schwartz-Saltykov (diameter) analysis defines a generalized equation to describe Nv(*j*) in terms of Na(*i*):

$$Nv(j) = 1/\# \sum_{i=j}^{k} @(i,j).Na(i) \qquad (3.9)$$

where the coefficients, @(*i*,*j*), that appear in Table 3.2.3 have already been calculated by Schwartz-Saltykov and are used in the expanded working equation Eqn.3.10 below:

$$Nv(j) = 1/\# \; [@(i,j).Na(i) - @(i+1,j).Na(i+1) \; -//- \; @(k,j).Na(k) \qquad (3.10)$$

where *i* and *j* are equal to values between 1 and *k* (total number of size classes). The total number of particles per unit volume then can be calculated:

$$Nv = Nv(1) + Nv(2) + Nv(3) \; +//+ \; Nv(j) \; +//+ \; Nv(k) \qquad (3.11)$$

The coefficient @(*i*,*j*) is calculated by first finding P(*i*,*j*) from Eqn.3.2. In the case when there are 15 size classes ($k = 15$), the probability of a random test surface cutting particles of radius r(*15*) to produce sections with radii between r(*14*) *and* r(*15*) is:

$$P(15,15) = 1/r(15) \cdot \sqrt{r(15)^2 - r(14)^2}$$

$$= \sqrt{1 - 0.933^2} = 0.359$$

when substituted into Eqn.3.6 gives:

$$Nv(15) = Na(15,15) \; / \; 0.359 \; D(15)$$

$$= 2.785 \; Na(15,15) \; / \; D(15) \qquad (3.12)$$

from which Nv(*15*) can be calculated because Na(*15*,*15*) and D(*15*) are known. Na(*15*,*15*) can have only originated from particles of D(*15*) so it is equal to Na(*15*) from an equation similar to Eqn's 3.7 and 3.8.

It will be noted that if Eqn.3.12 is rearranged:

$$Nv(15) = 1/D(15) \; [2.785 \; Na(15)] \qquad (3.13)$$

it closely resembles Eqn.3.10. The only difference between Eqn's 3.13 and 3.10 is that the denominator in the former is the actual diameter, D_{max}, of the maximum sized particle while in the latter it is 1, which is D_{max}/k (k is the number of size classes). Therefore, $\theta(15,15) = 2.785/15 = 0.1857$

The values of $\theta(14,14)$ and $\theta(14,15)$ are calculated by again using Eqn.3.2. $P(14,15)$, the probability of the random test surface cutting particles of radius $r(15)$ to produce sections with radii between $r(13)$ and $r(14)$ is:

$$P(14,15) = 1/r(15) \cdot \sqrt{r(15)^2 - r(13)^2} - \sqrt{r(15)^2 - r(14)^2}$$

$$= \sqrt{1 - 0.867^2} - \sqrt{1 - 0.933^2} = 0.140$$

and by rearranging Eqn.3.6:

$$Na(14,15) = P(14,15).D(15).Nv(15)$$

$$= [0.140\ D(15)] \times [2.785\ Na(15)] / D(15)$$

$$= 0.390\ Na(15) \qquad (3.14)$$

Since Eqn.3.14 tells us that 39% of the section diameters $D(14)$ are derived from particles of diameter $D(15)$ we can state that:

$$Na(14,14) = Na(14) - 0.390\ Na(15)$$

$P(14,14)$, the probability of the random test surface cutting particles of radius $r(14)$ to produce sections with radii between $r(13)$ and $r(14)$ is:

$$P(14,14) = 1/r(14) \cdot \sqrt{r(14)^2 - r(13)^2} = \sqrt{1 - 0.929^2} = 0.371$$

From Eqn.3.6:

$$Nv(14) = [Na(14) - 0.390\ Na(15)] / 0.371\ D(14)$$

$$= 1/D(15)\ [2.888\ Na(14) - 1.125\ Na(15)]$$

Thus, $\theta(14,14) = 2.888/15 = 0.1925$ and $\theta(14,15) = -1.125/15 = -0.0750$

These calculations of $\theta(i,j)$ were only to illustrate how Schwartz-Saltykov derived the coefficients; for analysis of particle distributions the coefficients can be taken from Table 3.2.3 to calculate all values of $Nv(j)$.

From Eqn.3.11 it is now possible to derive a number frequency of particle diameters per unit volume, $Nv(\%)$, and hence the mean number diameter of the three-dimensional particles. A further refinement, particularly applicable in the detection of agglomerates, is to derive a volume frequency of particle diameters per unit volume, $Vv(\%)$, and obtain the mean volume diameter (MVD); this is the term I shall use for directly quantifying filler agglomeration within the polymer matrix. Mean volume diameter can be defined as:

$$MVD = \sqrt[3]{\Sigma Nv(j) \cdot D(j)^3 / \Sigma Nv(j)} \qquad (3.15)$$

which means that MVD is the diameter whose volume represents the total volume of particles per unit volume divided by the total number of particles per unit volume. Figure 3.2.16 shows, in the two graphs, the effect on the raw data when it is analyzed using the above technique and the value of MVD calculated from the Vv frequencies.

3.2.3.6 Estimation of errors

Error is defined as "mistake; wrong opinion; transgression; deviation from accurate result, observation, etc".[197] In statistical terms, the deviation from an accurate result is the quantity which must be defined to enable meaningful comparisons of data. Of course, when performing experiments it is unlikely that one would know if the result was truly accurate because, if it was the case, the experiment would have no originality. Bevington [198] has defined three sources of potential error that can arise during experiments:-

(*I*) Systematic errors - are reproducible inaccuracies arising from flawed technique or equipment for which statistical analysis is not generally useful.

(*II*) Random errors - result from indefinable quantities within the equipment, experimental materials or measurement. These can be estimated, if necessary, but require enormous effort for

any errors other than the most obvious.

(*iii*) Probable errors - these are the errors judged to have been made during measurement of the results and can usually be quantified to a high degree.

The probable experimental measurement error involved in image analysis consists of:- (*a*) the field area visualization error, (*b*) the section sizing error and (*c*) the error introduced by the Schwartz-Saltykov (diameter) analysis. The calculations below are made using data from one single experiment which resulted in some of the lowest agglomeration levels; these small particles will exhibit the largest potential measurement errors.

The image analyser system digitizes the detected surface features into square-shaped 'pixels' which are arbitrary machine units with sides of approximately 0.5mm. The square shape of the pixels eliminates another possible error due to space which would fall between circular pixels. The field area visualization error results from the possibility of the nominal circular detection field being determined either one pixel narrower or one pixel wider than the actual size. The nominal circular field area was equal to 112000sq-*um*. Therefore, as the linear magnification was calibrated as x310, at the screen the circular field had a diameter of 121.2mm. If the circular field is narrower it will have a diameter of 120.2mm. The difference in areas of the nominal and narrower fields as a ratio of the nominal area expresses the first half of the percentage field area visualization error, which is 1.644%. The error for oversizing is calculated in the same way and equals 1.657%. Therefore, the field area visualization error can be expressed as +/- 1.65%.

The section sizing error, a result of the machine being able to resolve highlighted sections only to +/- 1 pixel, relates to the possibility of the detector missing one pixel during measurement or

erroneously recording an extra pixel. The mean area of sections determined in this experiment was 314.2sq-um, an equivalent area spherical diameter of 20um, which at the VDU screen (linear magnification at x310) is 30.19sq-mm. A square pixel with sides of 0.5mm at the VDU screen will have an area of 0.25sq-mm and so that the error resulting if one pixel is missed equates as the ratio of the pixel area (0.25sq-mm) to the mean section area (30.19sq-mm) and equals 0.82%. The error resulting if a pixel is mistakenly recorded is the same so the section size error is expressed as +/- 0.82%.

The error introduced by the Schwartz-Saltykov (diameter) analysis results from the inability of the image analyser to assess section diameters below 5um when using reflected light. In our example the maximum size class, in which sections were detected, had a diameter of 84um. As measurements are determined by area, the error is the ratio of the 5um squared to 84um squared expressed as a percentage and is equal to +/- 0.17%

Therefore, the estimated experimental measurement error involved in determining sections areas, when utilizing this image analyser, is assessed as +/- 2.6%.

Table 3.2.1 List of a number of different transformation methods for deriving particle size distributions from measured sections

Method	Table of coefficients needed?	Independent calculation of each class interval?	Class interval scale required
DIAMETERS			
Wicksell (1925)	Yes	Yes	Dmax/15
Scheil (1931)	Yes	No	Dmax/15
Schwartz (1934)	Yes	Yes	Dmax/10
Schwartz-Saltykov (1958)	Yes	Yes	Dmax/k($k \leq 15$)
AREAS			
Johnson	Yes	No	ASTM grain size
Johnson-Saltykov	Yes	No	Absolute scale, not dependent on Dmax
Saltykov	No	Yes	Absolute scale, based on A/Amax ($k \leq 12$)
CHORDS			
Spektor	No	Yes	Continuous, or Dmax/k
Lord and Willis	No	Yes	Dmax/k
Cahn and Fullman	No	Yes	Continuous, or Dmax/k
Bockstiegel	No	Yes	Dmax/k

Table 3.2.2 Nomenclature used in Schwartz-Saltykov analysis

Number of group	Particle diameter	Number per unit volume	Section diameter	Number per unit area
1	#	Nv_1	0 to #	Na_1
2	2#	Nv_2	# to 2#	Na_2
3	3#	Nv_3	2# to 3#	Na_3
.	.	.	.	.
.	.	.	.	.
.	.	.	.	.
j	j#	Nv_j	(i - 1)# to i#	Na_i
.	.	.	.	.
.	.	.	.	.
.	.	.	.	.
k	k#	Nv_k	(k - 1)# to k#	Na_k

Table 3.2.3 Probability coefficients for Schwartz-Saltykov (diameter) analysis

	Coefficients, $@_{i,j}$														
	Na_1	Na_2	Na_3	Na_4	Na_5	Na_6	Na_7	Na_8	Na_9	Na_{10}	Na_{11}	Na_{12}	Na_{13}	Na_{14}	Na_{15}
Nv_1	+1.0000	0.1547	0.0360	0.0130	0.0061	0.0033	0.0020	0.0013	0.0009	0.0006	0.0005	0.0004	0.0003	0.0002	0.0001
Nv_2		+0.5774	0.1529	0.0420	0.0171	0.0087	0.0051	0.0031	0.0021	0.0015	0.0010	0.0009	0.0006	0.0006	0.0004
Nv_3			+0.4472	0.1382	0.0408	0.0178	0.0093	0.0057	0.0037	0.0026	0.0018	0.0013	0.0010	0.0007	0.0007
Nv_4				+0.3779	0.1260	0.0386	0.0174	0.0095	0.0058	0.0038	0.0027	0.0020	0.0016	0.0012	0.0009
Nv_5					+0.3333	0.1161	0.0366	0.0168	0.0094	0.0059	0.0040	0.0028	0.0021	0.0016	0.0013
Nv_6						+0.3015	0.1081	0.0346	0.0163	0.0091	0.0058	0.0041	0.0028	0.0022	0.0016
Nv_7							+0.2773	0.1016	0.0329	0.0155	0.0090	0.0057	0.0040	0.0029	0.0022
Nv_8								+0.2582	0.0961	0.0319	0.0151	0.0088	0.0056	0.0039	0.0028
Nv_9									+0.2425	0.0913	0.0301	0.0146	0.0085	0.0055	0.0039
Nv_{10}										+0.2294	0.0872	0.0290	0.0140	0.0083	0.0054
Nv_{11}											+0.2182	0.0836	0.0280	0.0136	0.0080
Nv_{12}												+0.2085	0.0804	0.0270	0.0132
Nv_{13}													+0.2000	0.0776	0.0261
Nv_{14}														+0.1925	0.0750
Nv_{15}															+0.1857
Nv	+1.0000	+0.4227	+0.2583	+0.1847	+0.1433	+0.1170	+0.0988	+0.0856	+0.0753	+0.0672	+0.0610	+0.0553	+0.0511	+0.0472	+0.0441

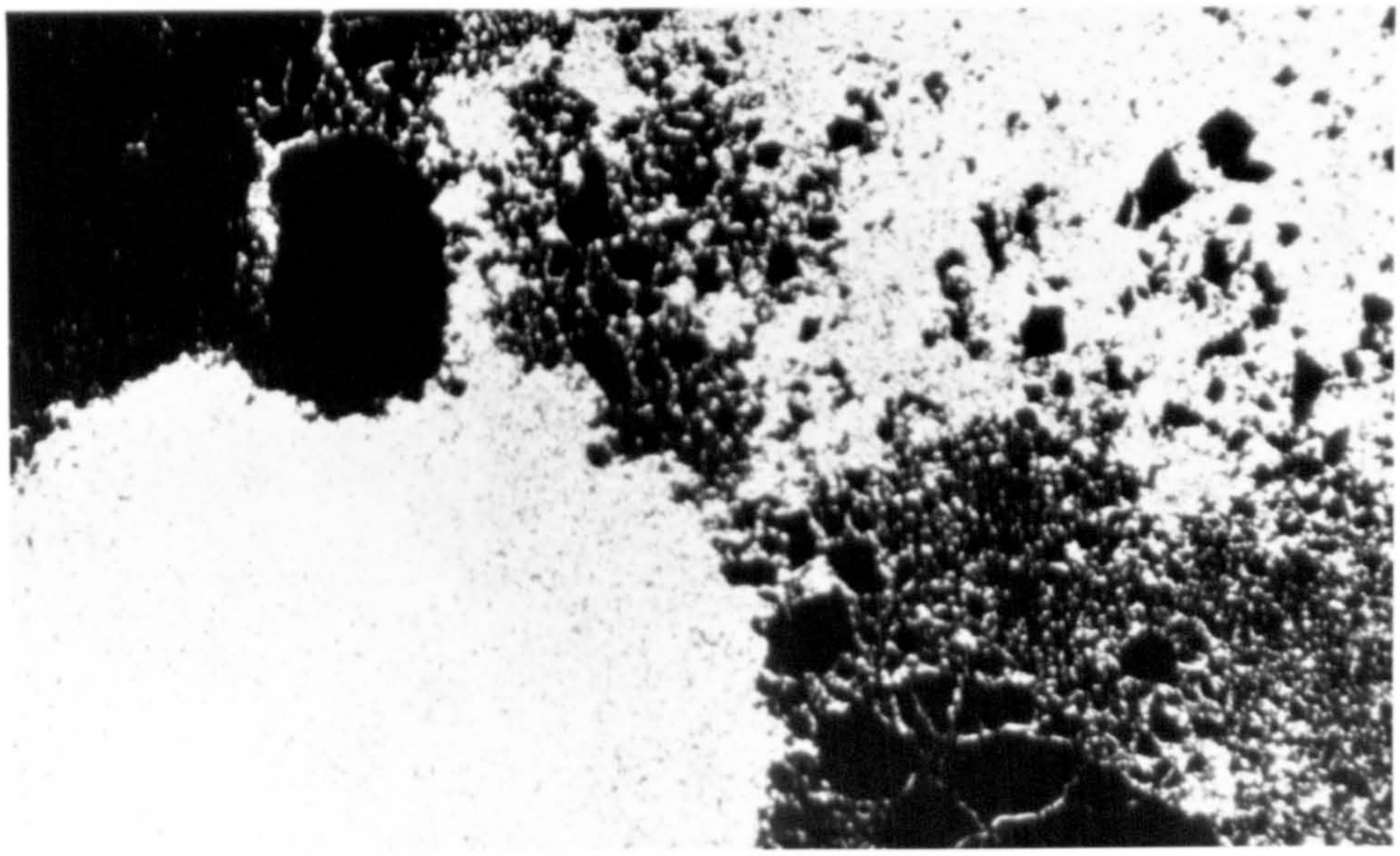

Fig.3.2.1 Transmitted light micrograph of material remaining after ashing of film (x33)

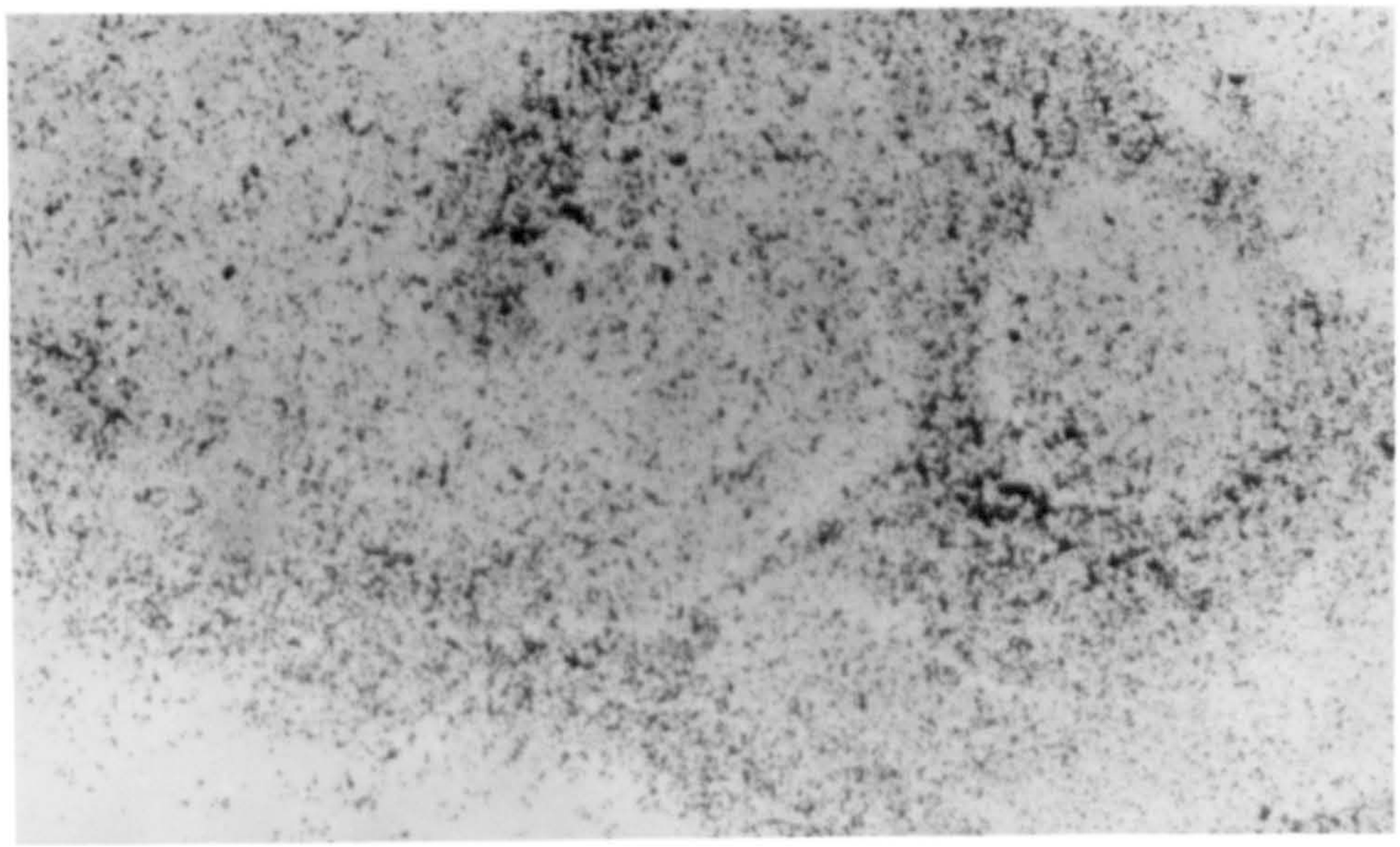

Fig.3.2.2 Transmitted light micrograph of material remaining after ashing of microtomed section (x66)

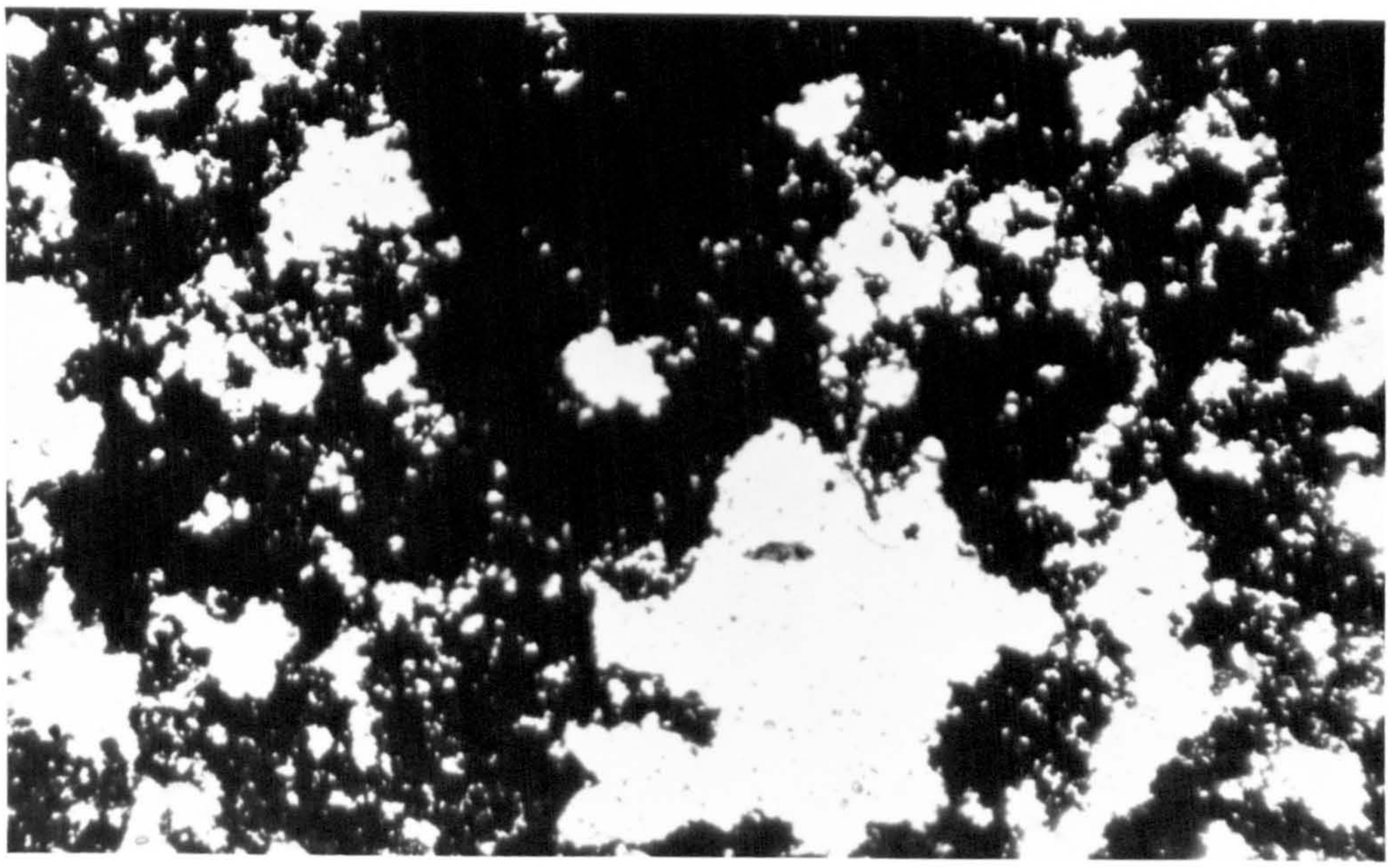

Fig.3.2.3 Transmitted light micrograph of material remaining after solvent extraction (x33)

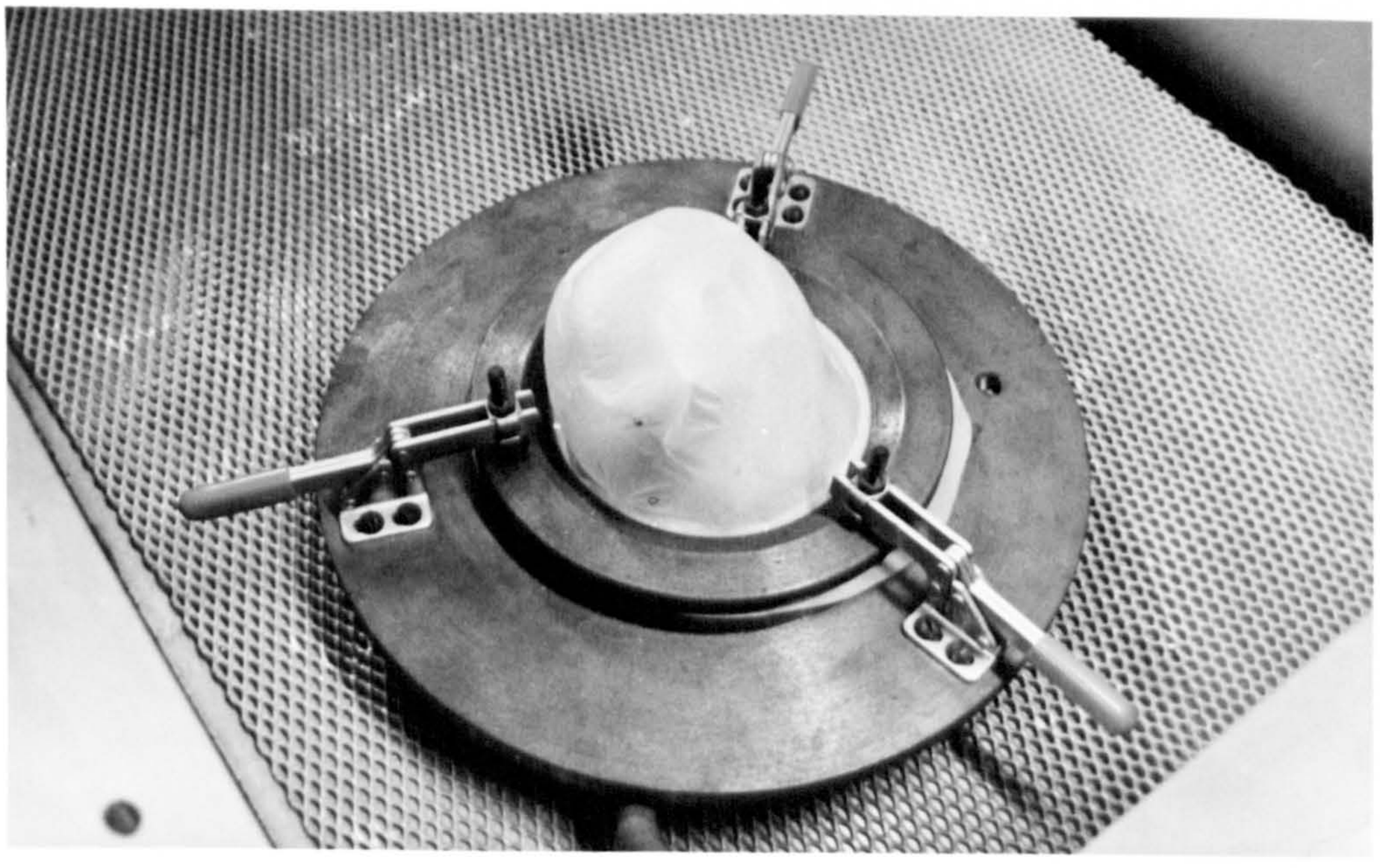

Fig.3.2.4 Bubble blowing apparatus

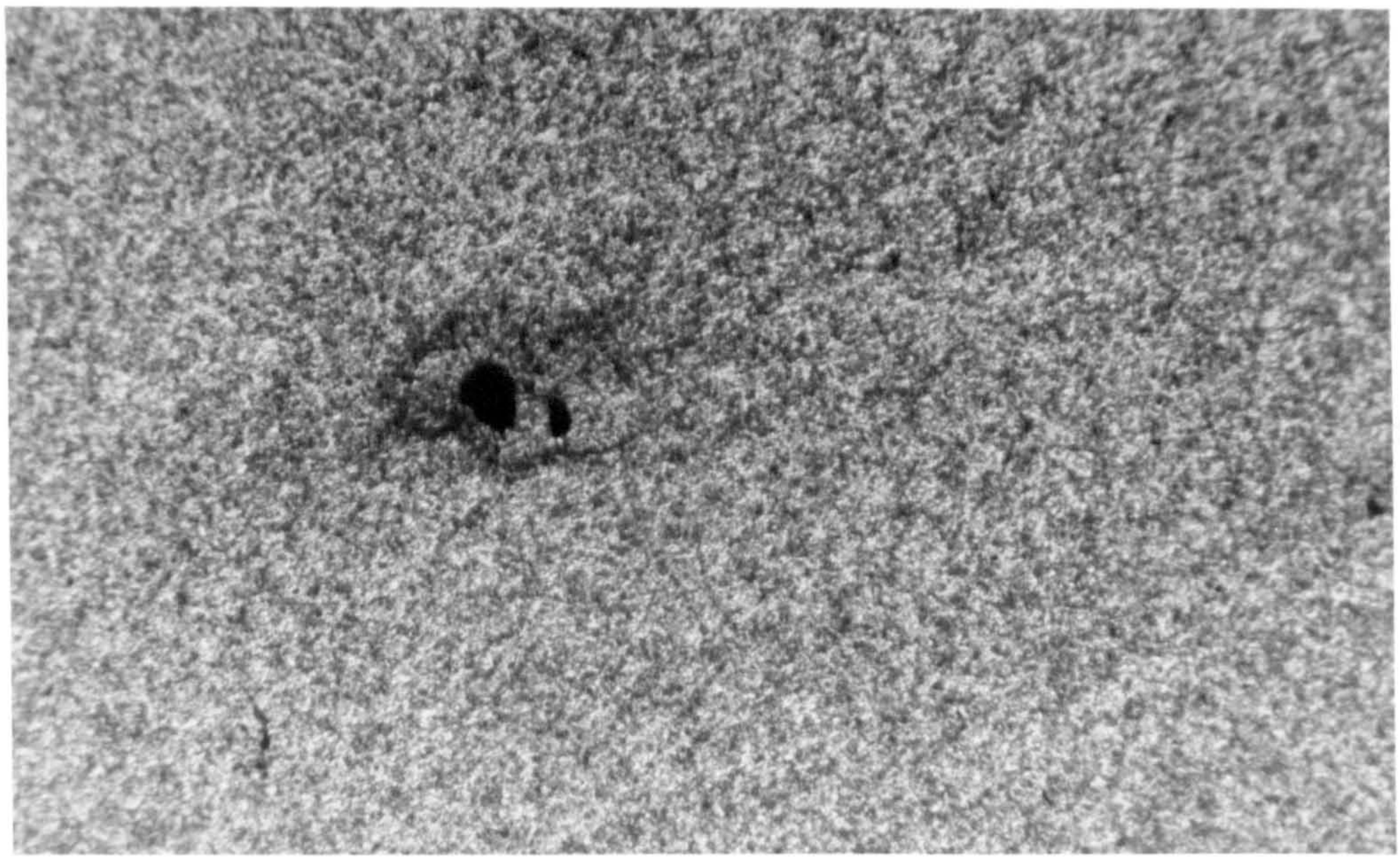

Fig.3.2.5 Transmitted light micrograph of part of blown bubble (x33)

Fig.3.2.6 Extruder of a laboratory film casting line

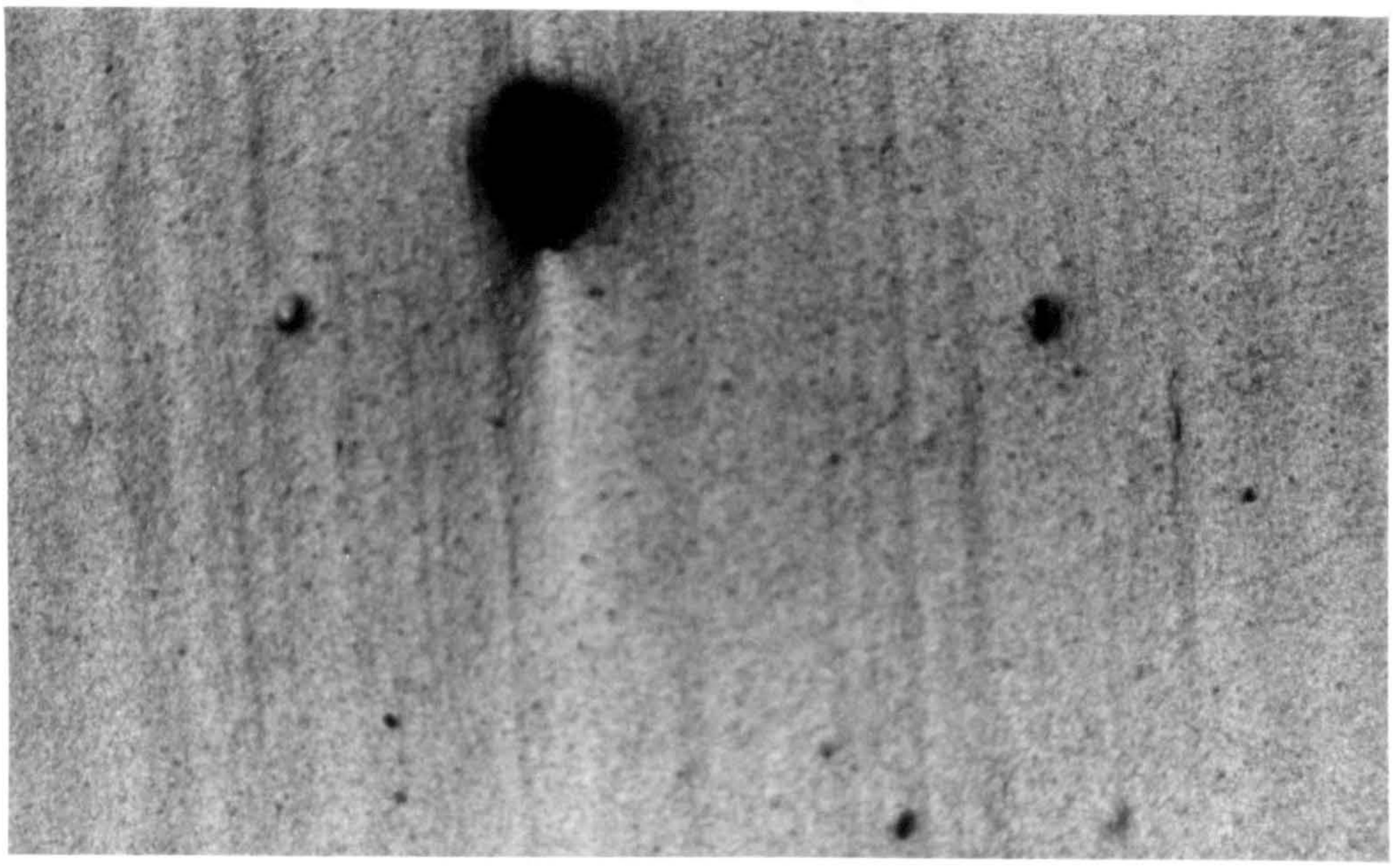

Fig.3.2.7 Reflected light micrograph of extruded tape (x33)

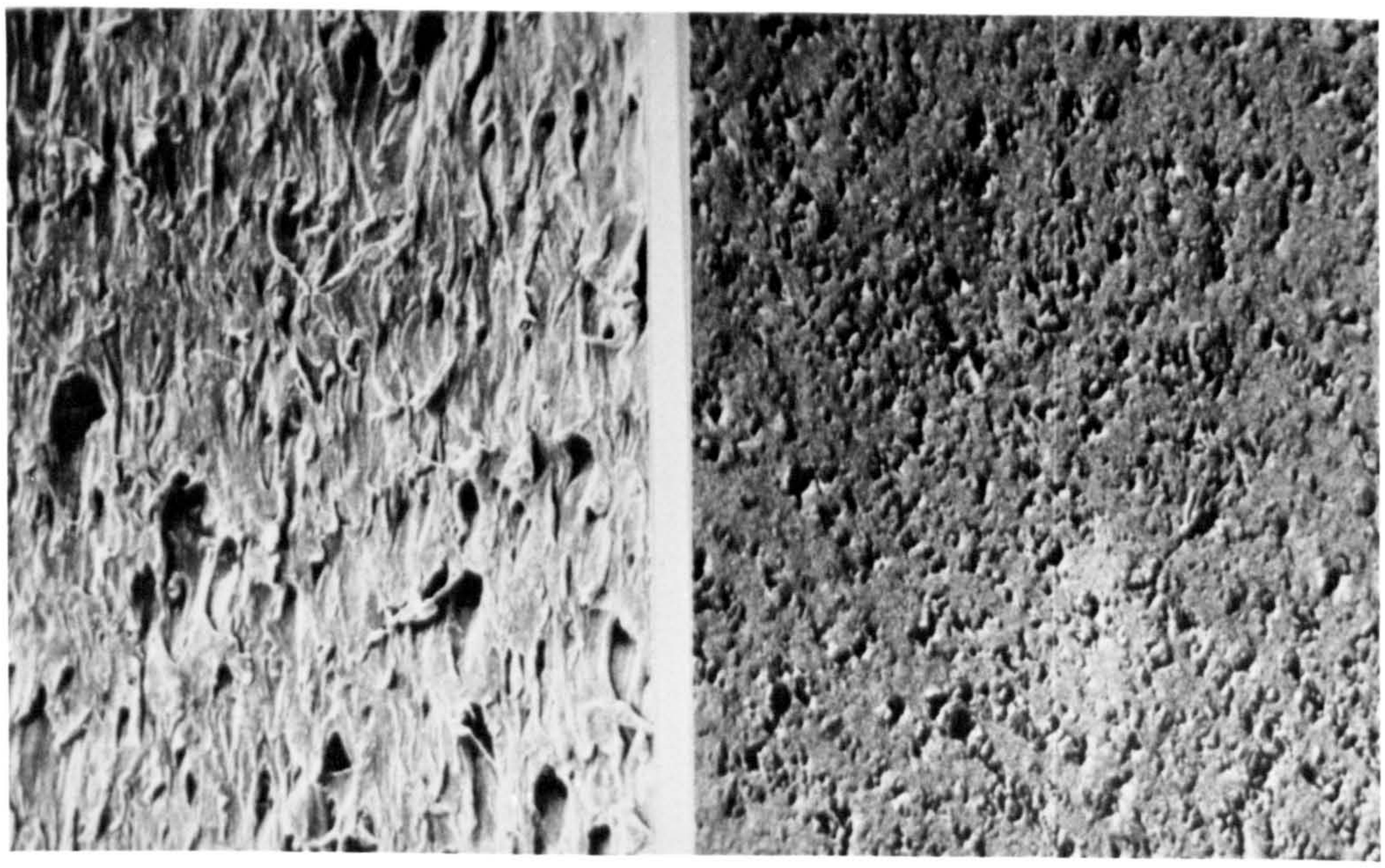

Fig.3.2.8 Scanning electron micrographs showing damage to microtomed surfaces (x875)

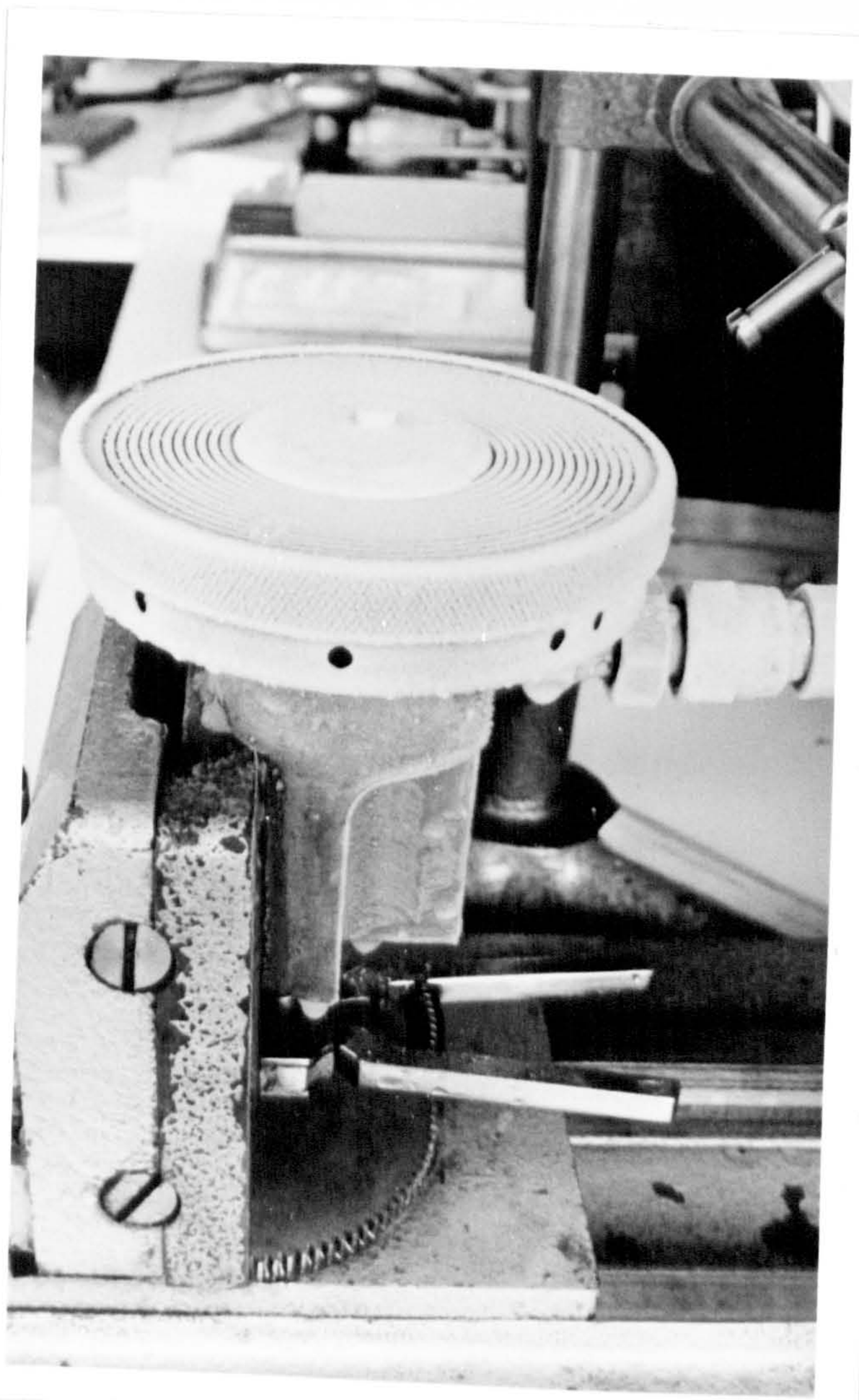

Fig.3.2.9 Steel bladed RAPRA-designed cryomicrotome

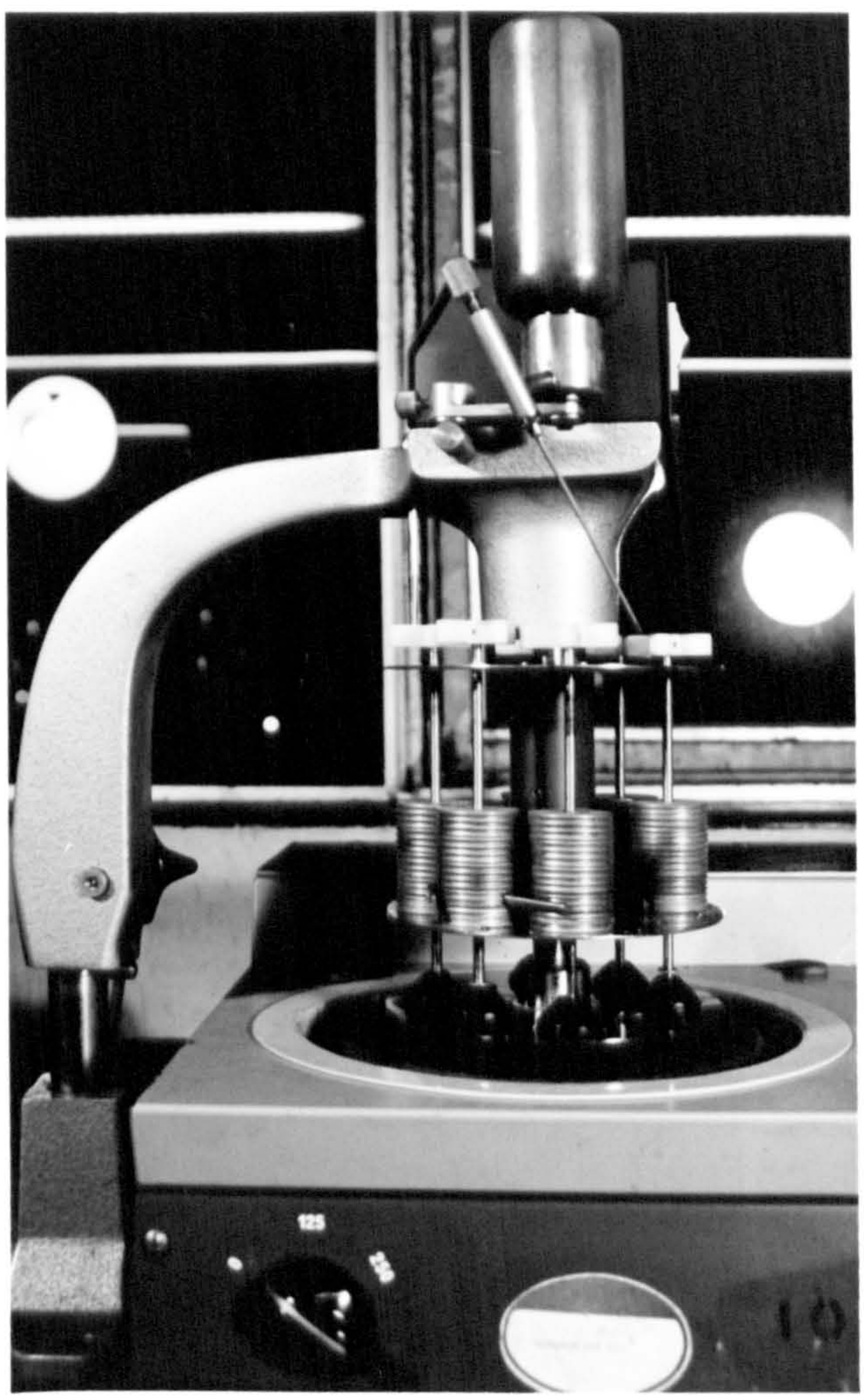

Fig.3.2.10 Mechanical block rotator

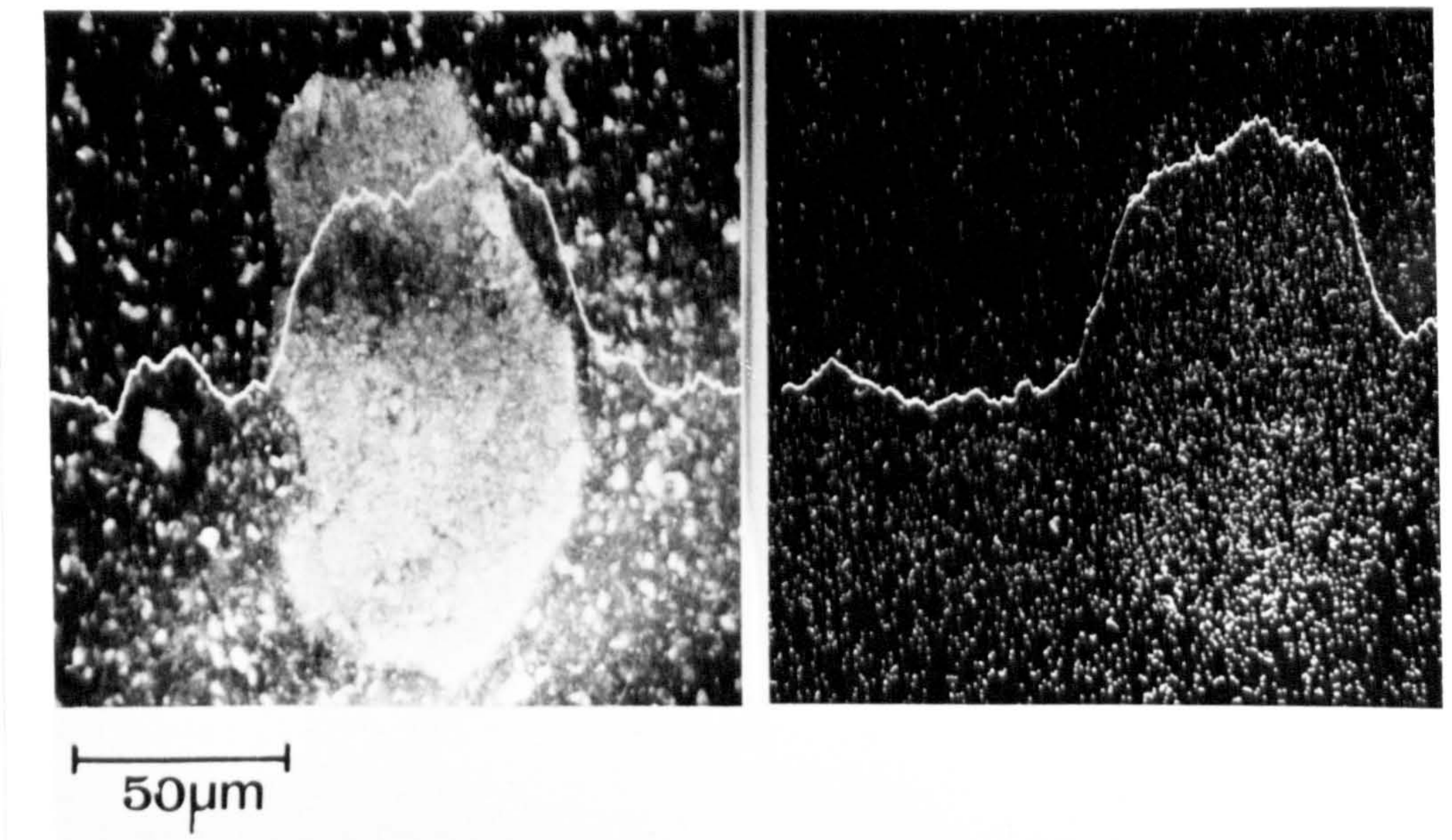

Fig.3.2.11 SEM (left) and X-ray dot-image of calcium ions detected on the sample surface

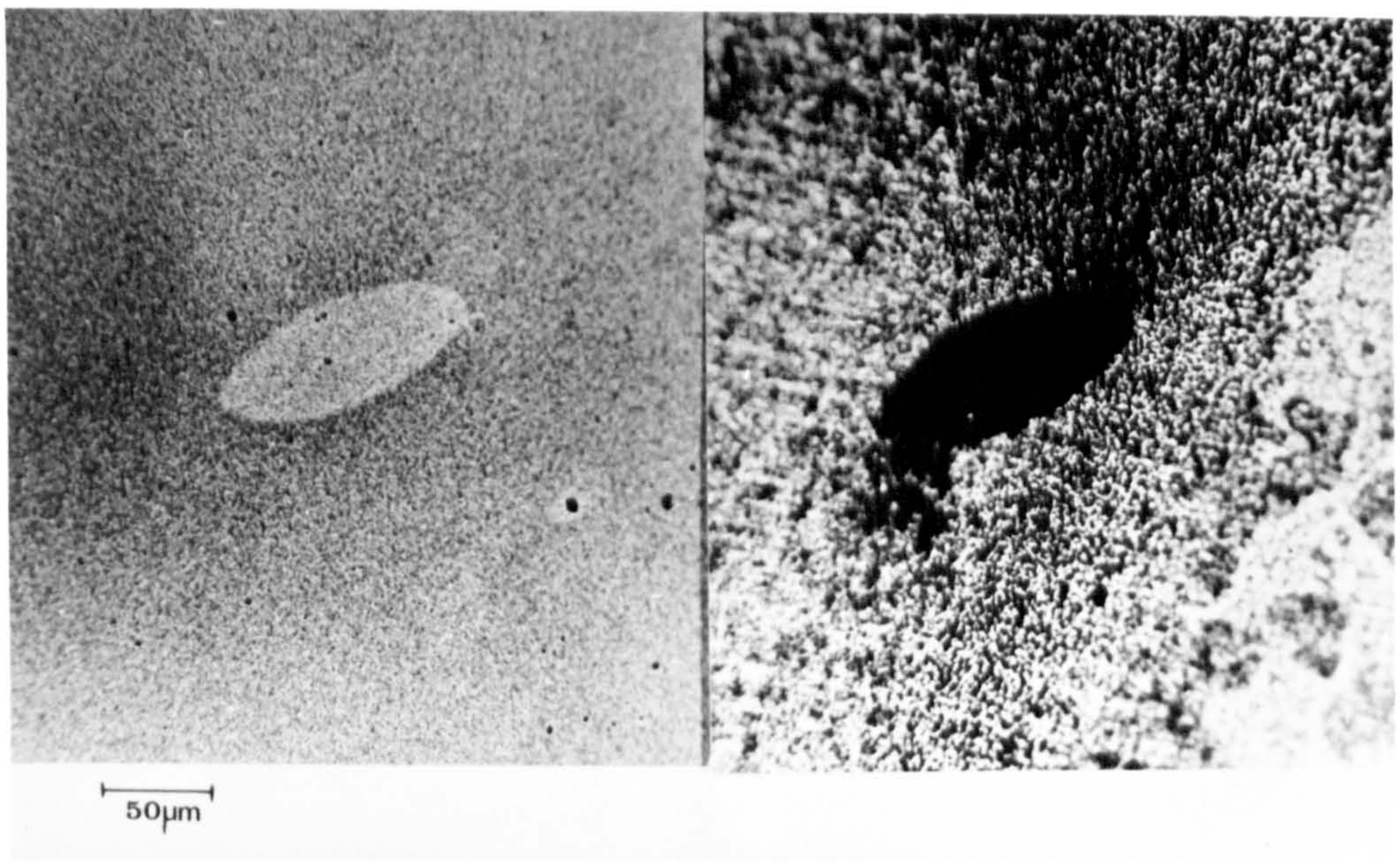

Fig.3.2.12 X-ray micronegative (left) viewed through a transmitted light microscope compared to microtomed section

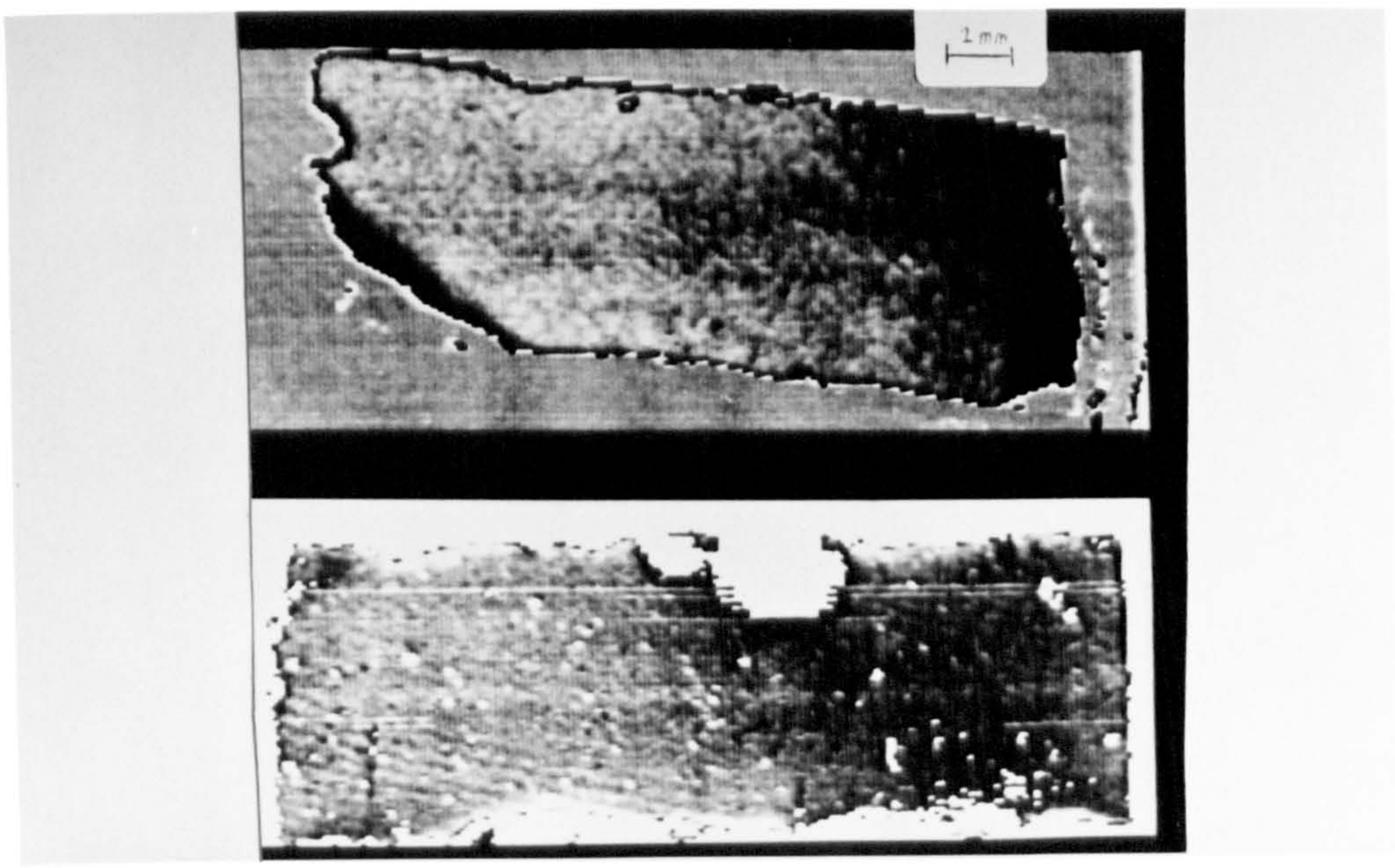

Fig.3.2.13 Specimens viewed by acoustic microscope in reflected mode

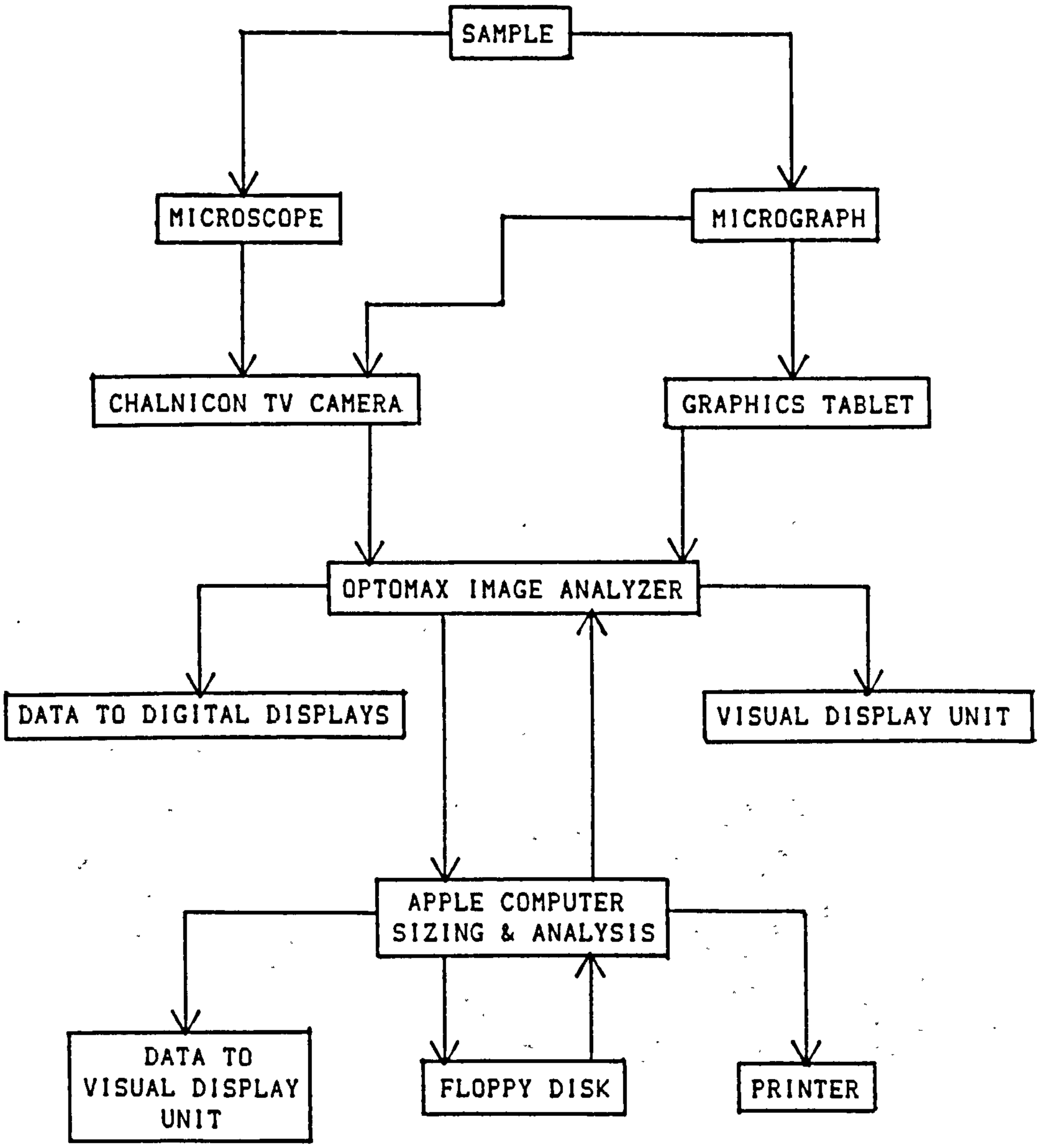

Fig.3.2.14 Principle components of image analysis

Fig.3.2.15 Optomax image analyser, Apple Computer and Zeiss microscope

Graph A

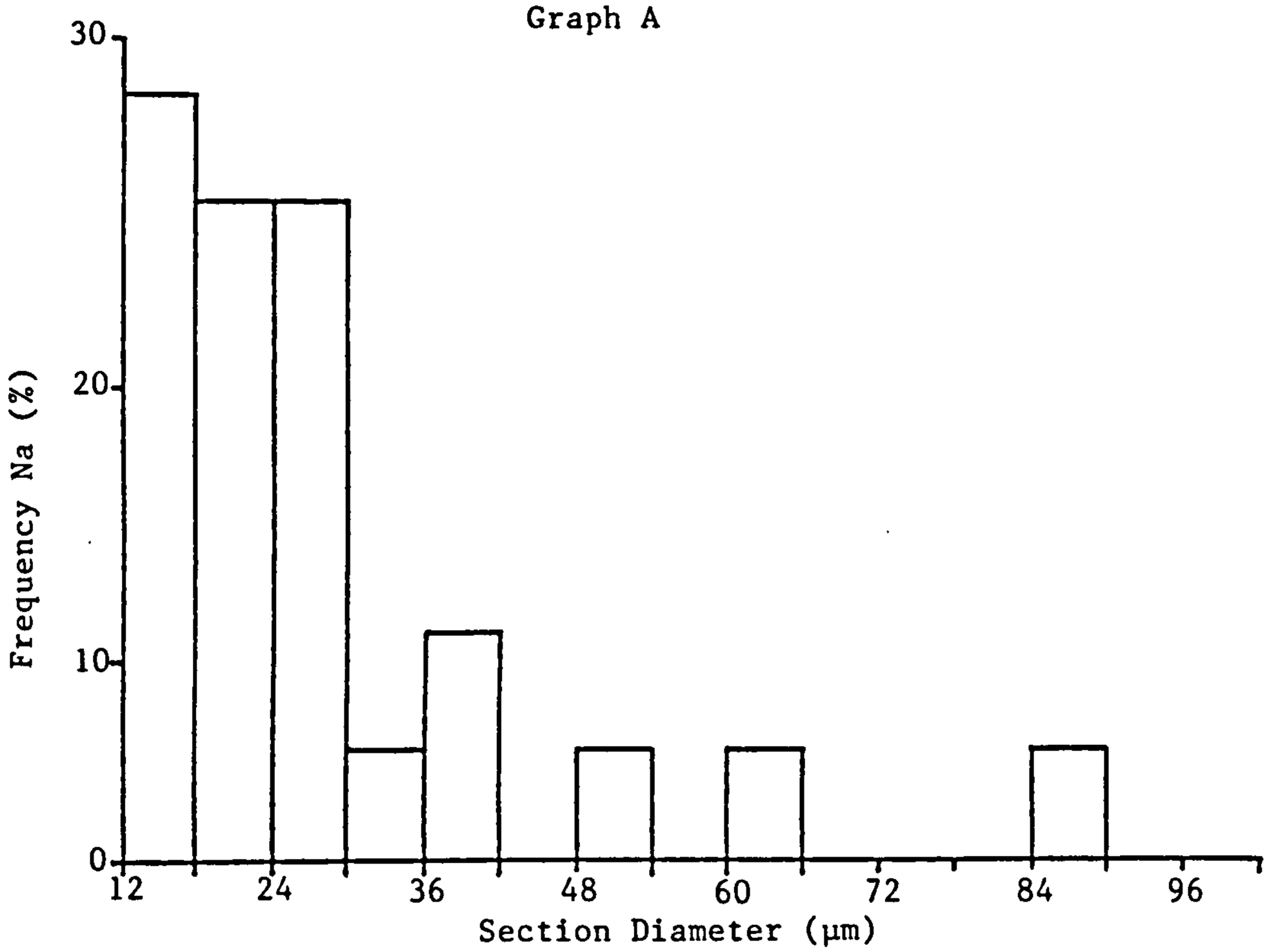

Graph B

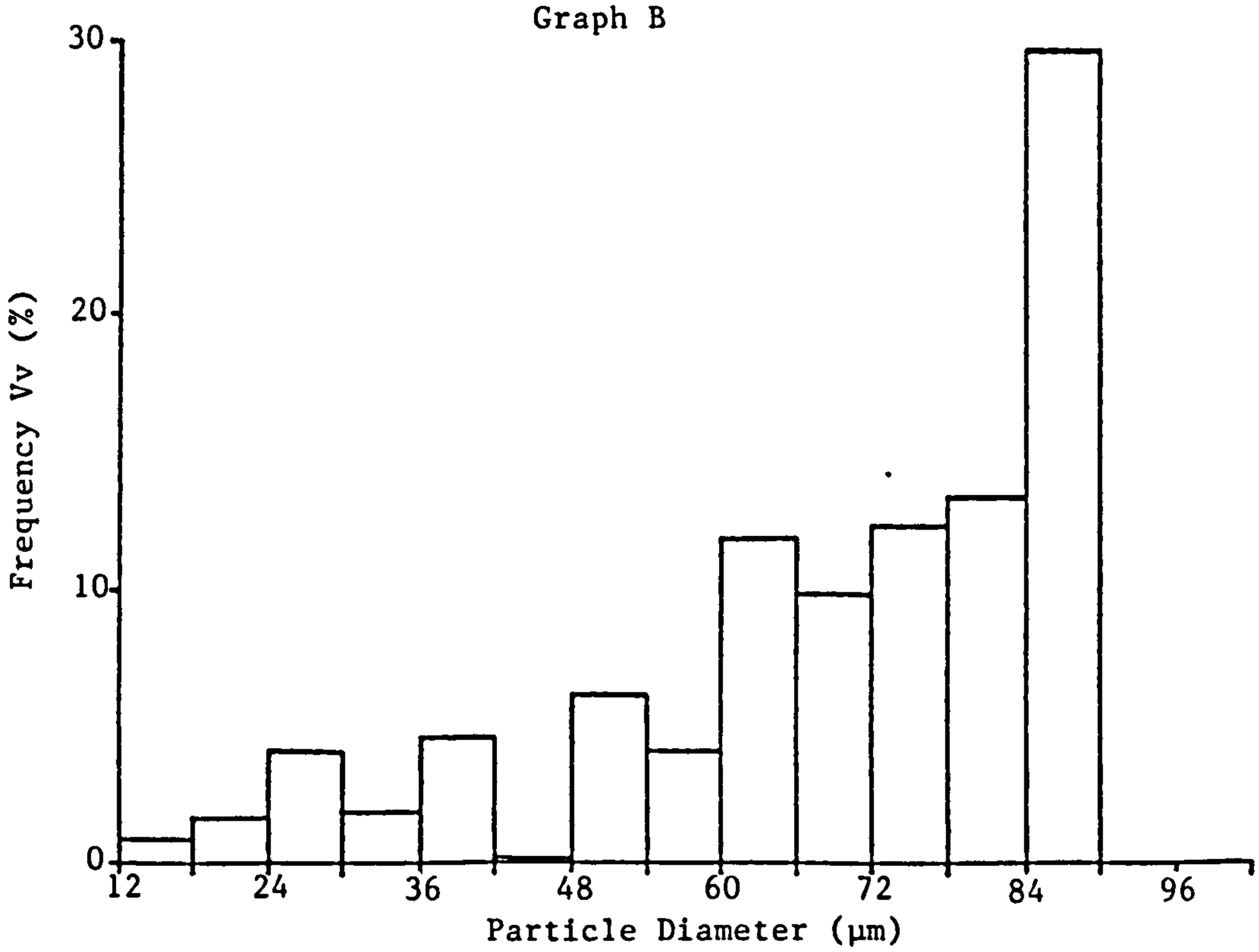

Fig.3.2.16 The effect of processing raw data measured from specimen surface (Graph A) using Schwartz-Saltykov (diameter) analysis expressed as a particle volume distribution (Graph B). Mean volume diameter (MVD) obtained from data in Graph B is 31.3 μm

3.3 DISPERSIVE AND DISTRIBUTIVE MIXING

3.3.1 Dispersive Mixing

The dispersive mixing characteristics of the TS40 co-rotating twin-screw compounding extruder are examined in the following series of experiments. These experiments employ 7 different calcium carbonate fillers, 2 different polymer matrices and various processing variables whose effects are analyzed by considering samples taken from the extrudate and, after removing the barrel, from along the screws.

3.3.1.1 Characterization of dispersive mixing

The technique employed for characterization of dispersion in calcium carbonate compounds is shown systematically in Figure 3.3.1.

Solid specimens taken from the extrudate and from the second stage of the screws were consolidated in a flash mould by heating at 225°C for 2min and pressing for 1min at a pressure of 4.3MPa. Semi-solid specimens taken from the first stage of the screws were placed in a 25mm diameter positive mould, heated at 250°C for 2min and pressed at 4.3MPa for 1min resulting in a disc approximately 6mm thick. Calcium carbonate raw powder specimens were tumble mixed with PP powder at 40wt% calcium carbonate, the mixture placed in an alumina crucible and heated in a furnace at 250°C. After 10min, the crucible was removed from the furnace and positioned on a hot plate while the specimen was stirred with a glass rod for 1min. The specimen was then pressed in the same way as a semi-solid specimen.

The time necessary to prepare as above, hand-grind on a range of 4 grades of emery paper, manually polish at 6 and 3um and remotely polish at 1um averaged 2hours/specimen. Many specimens required complete repolishing due to damage caused by surface contaminants or regrinding in addition to repolishing if surface section counts were of a low

order. Image analysis by direct reflected light microscopy took approximately 45min for a average total count of 30 fields of view.

3.3.1.2 Premixing conditions

It is normal practice to blend or intensively mix loose powder additives with powdered polymers before delivering them to the extrusion line. The calcium carbonate fillers utilized for these experiments came from the commercial range of Croxton & Garry Ltd and exhibit different geological origins, applied surface treatments and particle size ranges, as shown in Table 3.3.1. For most of the experiments, a powdered polypropylene (ICI - GW522M) was selected to form the polymer matrix except for a comparative experiment using as the matrix a more polar polymer, nylon 6,6 (ICI - Maranyl A100).

For the following experiments, the majority involve the use of premixes containing 40wt% of calcium carbonate filler in the polypropylene powder and these have been prepared using a Henschel high-speed dry mixer; batches of 2kg were mixed at 3000rpm for 5min. Prior to premixing samples of each of the 7 raw calcium carbonate powders were taken from the as-delivered bags, as well as samples from each calcium carbonate/ polypropylene premix. The compacted material remaining on the mixer blades was analyzed for Durcal 2. Each sample was prepared as detailed in Section 3.3.1.1 above and characterized by image analysis; results are shown in Table 3.3.2.

3.3.1.3 Material variables

3.3.1.3.1 Calcium carbonate characteristics

Each of the 7 calcium carbonate premixes were then processed using the TS40 co-rotating twin-screw extruder set up to operate at standard processing values, which are shown in Table 3.3.3. The premixes were starve-fed from the twin-screw volumetric dosing unit into the hopper

of the extruder at the maximum throughput possible in relation to machine power capacity and processing stability. On leaving the machine the melt was extruded through a 75mm wide by 3mm thick slit die into a water bath and this extrudate collected as an unsized strip.

For Durcal 2, an additional experiment was undertaken whereby the machine was stopped after achieving steady-state running conditions and the barrel shock-cooled by passing water through the heater elements piping. After approximately 30min of cooling, the hydraulic barrel withdrawal apparatus was used to carefully remove the barrel and expose the screws surrounded by solidified material, Figure 3.1.6. Samples of the material were taken from specified positions along the screws for subsequent image analysis.

The samples were prepared as detailed in Section 3.3.1.1 above and characterized by image analysis; results are shown in Table 3.3.4 and graphically in Figures 3.3.2 & 3.3.3.

3.3.1.3.2 Polymer polarity

Calcium carbonate filler (Durcal 2) was processed in two different polymer matrices; polypropylene (ICI - GW522M) and a more polar polymer, nylon 6,6 (ICI - Maranyl A100). Compounds of the nylon 6,6 matrix were extruded at screw speeds of 120 & 180rpm and compared to the polypropylene matrix at the same speeds. Nylon 6,6 granules, dried at 100°C in a vacuum oven overnight, were fed from the Simon Varifeeder. The calcium carbonate was separately fed from the K-Tron Soder feeder at a rate equivalent to 40wt% with the nylon 6,6 fed from the Simon Varifeeder.

The nylon 6,6 compounds were processed at the extruder settings in Table 3.3.5 and the polypropylene compounds as above. Samples were collected from the extrudate for each variant and analyzed. Dispersion results are detailed in Table 3.3.6 and are included in Figure 3.3.2.

3.3.1.4 Processing variables

3.3.1.4.1 Extruder screw speed

The 40wt% Durcal 2/ polypropylene premix was processed at screw speeds of 60, 120 and 180rpm but otherwise extruder settings were the same as those described in Table 3.3.3. At each screw speed, the extruder was shock-cooled after stable-running had been established and, after the barrel was withdrawn, samples were taken from the same positions along the screws as detailed in Table 3.3.4

Dispersion results are shown in Table 3.3.7 and Figures 3.3.3-3.3.5 which show the MVD and D*max* along the screws for each speed while Figure 3.3.6 compares the MVD of the 3 screw speeds.

3.3.1.4.2 Temperature profile

Barrel temperature profile was varied over 5 ranges; low, normal, high, flat and decreasing which are detailed at the foot of Table 3.3.8. The 40wt% Durcal 2/ polypropylene premix was otherwise processed at settings in Table 3.3.3. Table 3.3.8 details the dispersion results which are individually related to position of sampling along the screw for normal, low and high temperature profiles in Figures 3.3.3, 3.3.7 and 3.3.8; Figure 3.3.9 compares these 3 temperature profiles.

3.3.1.4.3 Position of filler entry

The twin ports half way along the barrel in its standard configuration present the possibility of feeding the filler at this point independently of the polymer powder. Two experiments were undertaken to investigate this feature; firstly, polymer and calcium carbonate were feed separately at the hopper and, after shock-cooling, samples taken from along the screws and analyzed, Figure 3.3.10.

Secondly, in order to evaluate the effects of the two halves of the extruder Durcal 2 calcium carbonate was fed, at a rate equivalent to 40wt%, into the molten polypropylene at the downstream entry port; the machine was shock-cooled and samples taken along the screws for image analysis, Figure 3.3.11. These two variables are plotted together with the dispersion along the screws for premix fed at the hopper in Figure 3.3.12 and details are given in Table 3.3.9.

3.3.1.4.4 Material output

As stated in Table 3.3.3, the output was maximized in the standard extrusion settings of Durcal 2/ polypropylene (at 18.3kg/hr). In these experiments, the extruder was operated at 80% and 60% of this output value, and samples collected from the extrudate; Table 3.3.10 details the image analysis dispersion results.

3.3.1.4.5 Screw/ barrel configurations

3.3.1.4.5.1 Configuration of metering screw section

The segmented nature of the extruder screws allows the alteration of the profile without resorting to changing the entire screw. This set of experiments was intended as an investigation of the influence of second-stage metering screw profile on calcium carbonate filler dispersion. In addition to the standard 8mm pitch metering screws, a set of 12mm and 16mm pitch metering screws were utilized for processing 40wt% Durcal 2 in polypropylene. Further, two of the melting elements were removed from midway along the screws, the second-stage screws moved along to fill the gap and these two elements placed at the extreme end of the metering section; see lower screw configuration in Figure 3.1.5.

For each configuration, the machine was operated to steady state conditions, the screws halted and the barrel shock-cooled before

withdrawal of the barrel to obtain samples from the metering screws. These samples were assessed by image analysis and the dispersion results are detailed in Table 3.3.11 and compared in Figure 3.3.13

3.3.1.4.5.2 Configuration of barrel sections

As mentioned previously, the TS40 extruder has the facility to operate with more than four barrel sections and so a series of experiments were undertaken using the five barrel configuration, see lower barrel configuration in Figure 3.1.2. The 40wt% Durcal 2/ polypropylene premix was fed at the hopper at low, normal and high screw speeds as defined in Table 3.3.7. Additionally, the filler was dosed separately into the molten polypropylene at either the first or second downstream entry ports. Samples were taken from the extrudate for each experiment and dispersion assessed by image analysis, Table 3.3.12.

3.3.2 Distributive Mixing

The distributive mixing characteristics of the TS40 co-rotating twin-screw compounding extruder are examined in the following series of experiments. These experiments involve first determining the optimum pigment loading which compromises between showing significant flow lines and allowing sufficient light to pass through the thin section. Samples were taken from the extrudate for all experiments and from the metering section of the screws, after shock-cooling and barrel withdrawal, for a number of the experiments; see Table 3.3.13 for detailed sampling locations.

3.3.2.1 Characterization procedure

The technique utilized for characterization of distributive mixing

of carbon black in a polypropylene matrix is shown systematically in Figure 3.3.14.

Initially, attempts were made to cut thin sections of polypropylene extrudate using a conventional steel-bladed sledge microtome. It proved extremely difficult to eliminate cutting lines while at the same time achieving sections thin enough for examination by light microscopy.

An alternative strategy for cutting thin slices of polymeric material is the use of 'glass-knife microtomy'. Glass-knife microtomy is a hybrid technique which emulates the ultramicrotome utilized for the preparation of electron microscope specimens. It differs mainly in that incremental movement of the cutting knife occurs mechanically rather that by electrical heating and in its ability to cut sections up to several microns thick. The main advantage of glass microtomy over the conventional metal-knife technique is that, when cutting marks appear, the glass knife can easily be replaced. Thin sections of the prepared specimen were mounted on a microscope slide in Canada Balsam beneath a cover slip ready for transmitted light microscopy.

The microscope slide specimens were viewed under the Zeiss microscope, in transmitted light mode, which was directly attached to the Optomax image analyser described in detail in Section 3.2.3 above. After adjustment of microscope functions, such as light source level, diaphragm openings and polarizing filters, contrast appeared acceptable to the image processor since it was then able to distinguish dark flow patterns from the background. The computer software necessary to control the image analyser via an IEEE interface was further refined so that it operated faster when only measuring 'area fraction of detected features' (AF) and 'standard deviation of AF' (SD*af*); the terms used to quantify distributive mixing. (See Appendix B for image analyser program for measurement of distributive mixing) For each specimen an

average of 60 fields of view were examined.

3.3.2.2 Pigment loading

A problem immediately encountered when initially examining carbon black pigmented polypropylene was that no light could pass through glass microtomed sections of extruded material. For these initial experiments, carbon black masterbatch (Cabot - PP1359 30% by weight carbon black) was tumble blended with polypropylene granules (ICI - GWM22) in such quantities to produce a final carbon black concentration of 2wt%. However, after a range (0.25% to 1.5%) of carbon black concentrations were considered, it was concluded that 0.5wt% resulted in a suitable compromise and this level of carbon black was utilized for subsequent experiments.

3.3.2.3 Processing variables

3.3.2.3.1 Extruder screw speed

The 0.5wt% carbon black/ polypropylene mixture was processed using the TS40 co-rotating twin-screw extruder set to operate at standardized processing values, which are shown in Table 3.3.14. The preblend was starve-fed from the single-screw Simon Varifeeder unit into the hopper of the extruder at the maximum throughput possible in relation to machine power capacity and processing stability. On leaving the machine the melt was extruded through a 6mm diameter rod die, drawn down to a 4mm diameter strand and cooled in a water bath. It was necessary to reduce the diameter of the strand because the glass knives utilized for the microtomy were also 6mm wide and needed to be larger than the specimen in order to cut sections satisfactorily.

The extruder was operated at a range of screw speeds between 30 and 180rpm both with and without the breaker plate present in the barrel head adaptor. Specimens were prepared directly from the

extruded 4mm strand using the technique described in Section 3.3.2.1 above and characterized by image analysis; results are shown in Table 3.3.15 and Figure 3.3.15.

3.3.2.3.2 Temperature profile

Barrel temperature profile was varied over three of the ranges utilized for calcium carbonate - low, normal and high - details of which are shown at the foot of Table 3.3.16. The materials were otherwise processed at settings in Table 3.3.14 and samples taken from each resulting extrudate for analysis.

3.3.2.3.3 Material output

Material was processed as previously using 80% and 60% of the maximum output value (13.0kg/hr). The extrudate was analyzed in each case and results are shown in Table 3.3.17.

3.3.2.3.4 Configuration of metering screw section

The same range of extruder metering screw configurations as those employed for calcium carbonate, Section 3.3.1.4.5.1 above, were utilized to process the 0.5wt% carbon black compound. The area fraction image analysis results for material extracted from the metering screws are shown in Table 3.3.18, individually plotted (AF and DDI) in Figures 3.3.16 to 3.3.19 and compared in Figure 3.3.20.

3.3.2.3.5 Position of pigment entry

In addition to processing the compound by adding the carbon black masterbatch with the polypropylene granules at the feed hopper, experiments were undertaken whereby the carbon black was separately metered into the downstream vent port. Analysis of material extended to the fully filled flights of the metering section; samples being

accessed by removal of the metering barrel section after halting the machine and shock-cooling the barrel jacket, Table 3.3.19 and Figure 3.3.21, comparison (with Figure 3.3.19) in Figure 3.3.22.

Table 3.3.1 Features of the selected calcium carbonate fillers

Trade Name	Geological Origin	Mean particle size (um)	Top cut (um)	Finer than 2um(%)	Surface treatment
Hakuenka CCR	Precipitated	0.08	-	-	Yes(CS)
Setacarb 13	Calcite (Urgonian)	0.70	3	96	No
Hydrocarb	Crystalline calcite (Urgonian)	1.50	7	70	No
Hydrocarb 95T	Crystalline calcite (Urgonian)	1.50	7	70	Yes(PT)
Millicarb	Crystalline calcite (Urgonian)	3.00	10	35	No
Durcal 2	Marble (Metamorphic)	3.00	10	40	No
Omyalene SL	Marble (Metamorphic)	3.00	10	40	Yes(PT)

CS = calcium stearate; PT = proprietary treatment.

Table 3.3.2 Image analysis results for specimens taken from the raw powders and premixes for the 7 different calcium carbonates in polypropylene powder.

		Image Analysis	
	Sample	Mean volume diameter [MVD] (um)	Maximum particle diameter [D*max*] (um)
Hakuenka CCR	Raw powder	178.0	900
	Premix	194.0	1000
Setacarb 13	Raw powder	241.0	570
	Premix	253.1	700
Hydrocarb	Raw powder	236.0	975
	Premix	247.8	1000
Hydrocarb 95T	Raw powder	126.1	450
	Premix	138.7	370
Millicarb	Raw powder	214.0	570
	Premix	231.1	600
Durcal 2	Raw powder	159.1	370
	Mixer blades	205.8	450
	Premix	168.7	530
Omyalene SL	Raw powder	171.0	700
	Premix	186.4	835

Table 3.3.3 Standard extruder settings for processing 40wt% calcium carbonate filler in polypropylene powder

Die Type	Strip (3mm x 75mm)
Screw speed	120rpm
Barrel	4 sections with venting in zone 3
Screws	17:1 L/D with 4 melting elements between zones 2 & 3 and 8mm pitch metering screws
Feed	Premix fed at the hopper from K-Tron Soder T20
Output	Maximum possible for stable processing and limited by motor current maximum of 20A
Temperature profile (°C)	Zone 1 = 185 Zone 2 = 195 Zone 3 = 205 Zone 4 = 215 Die = 220

Table 3.3.4 The effect of varying calcium carbonate characteristics on the level of dispersion

PP-	Sampling position	MVD (um)	D*max* (um)	AF (%)	SD*af* (%)	D*f* (%)	DDI
HCCR	1	26.7	96	5.50	2.78	13.8	0.049
S13	1	31.4	116	6.28	3.92	12.4	0.110
HY	1	26.7	63	1.47	0.85	10.8	0.004
H95T	1	22.5	48	3.26	1.72	16.2	0.018
M	1	19.1	56	5.68	4.59	8.3	0.084
OSL	1	21.2	64	2.91	2.02	11.4	0.019
D2	1	24.3	80	4.65	1.63	14.4	0.024
	2	23.7	72	3.16	2.14	14.0	0.022
	3	39.3	238	6.18	1.93	23.3	0.053
	4	93.4	270	9.07	4.07	55.4	0.284
	5	190.0	530	28.69	10.70	112.6	2.361
	6	135.1	490	8.20	6.74	80.1	0.425
	7	153.6	330	7.10	2.83	91.0	0.156
	8	168.7	530	11.26	5.56	100.0	0.482

See **Nomenclature** for explanation of symbols and codes: Materials processed at standard settings, see Table 3.3.3: Sampling position - 1 = extrudate; 2 = end of metering (zone 4); 3 = beginning of metering (zone 4); 4 = beginning of zone 3 (after melting elements); 5 = end of zone 2 (before melting elements); 6 = between zones 1 & 2; 7 = beginning of zone 1; 8 = initial feed.

Table 3.3.5 Extruder settings utilized during nylon 6,6 processing

Die Type	Rod (6mm diameter)
Screw speed	120 and 180rpm
Barrel	4 sections with venting in zone 3
Screws	17:1 L/D with 4 melting elements between zones 2 & 3 and 8mm pitch metering screws
Feed	Polymer and filler (40wt%) separately fed at the hopper
Output	Maximum possible for stable processing and limited by motor current maximum of 20A
Temperature profile (°C)	Zone 1 = 260 Zone 2 = 265 Zone 3 = 265 Zone 4 = 270 Die = 280

Table 3.3.6 The effect of matrix polarity on the level of dispersive mixing in the extrudate

D2-	Sampling position	MVD (um)	D*max* (um)	AF (%)	SD*af* (%)	D*f* (%)	DDI
PA-NS	1	9.9	38	10.29	1.64	6.2	0.021
PA-HS	1	9.4	20	1.33	0.93	5.9	0.002
PP-NS	1	24.3	80	4.65	1.63	14.4	0.024
PP-HS	1	22.4	64	3.44	1.19	13.3	0.013

See **Nomenclature** for explanation of symbols and codes: Materials processed at standard settings, see Tables 3.3.3 and 3.3.5: PA = nylon 6,6: PP = polypropylene powder: NS = normal screw speed (120rpm): HS = high screw speed (180rpm)

Table 3.3.7 The effect of varying extruder screw speed on the level of calcium carbonate dispersion

PP-D2-	Sampling position	MVD (um)	D*max* (um)	AF (%)	SD*af* (%)	D*f* (%)	DDI
SS	1	29.0	104	6.03	4.20	17.2	0.082
	2	30.2	120	4.77	3.93	17.9	0.060
	3	41.7	180	8.09	4.27	24.7	0.154
	4	64.5	206	14.79	5.47	38.2	0.622
	5	113.8	490	16.56	6.06	67.5	0.772
	6	149.8	800	23.46	6.21	88.7	1.520
	7	184.9	530	13.14	10.28	109.6	1.039
	8	168.7	530	11.26	5.56	100.0	0.482
NS	1	24.3	80	4.65	1.63	14.4	0.024
	2	23.7	72	3.16	2.14	14.0	0.022
	3	39.3	196	6.18	1.93	23.3	0.053
	4	93.4	270	9.07	4.07	55.4	0.284
	5	190.0	530	28.69	10.70	112.6	2.361
	6	135.1	490	8.20	6.74	80.1	0.425
	7	153.6	330	7.10	2.83	91.0	0.156
	8	168.7	530	11.26	5.56	100.0	0.482
HS	1	22.4	64	3.44	1.19	13.3	0.013
	2	23.8	64	3.87	2.04	14.1	0.025
	3	37.5	180	6.94	5.02	22.2	0.156
	4	80.7	206	9.31	6.42	47.8	0.460
	5	139.1	570	11.36	7.13	82.5	0.623
	6	175.4	450	14.06	8.51	104.0	0.920
	7	128.4	450	11.48	6.08	76.1	0.537
	8	168.7	530	11.26	5.56	100.0	0.482

See **Nomenclature** for explanation of symbols and codes: See foot of Table 3.3.4 for sampling positions: Materials processed at standard settings, see Table 3.3.3, except: SS = slow screw speed (60rpm): NS = normal screw speed (120rpm): HS = high screw speed (180rpm).

Table 3.3.8 The effect of varying extruder temperature profile on the level of calcium carbonate dispersion

PP-D2-	Sampling position	MVD (um)	D*max* (um)	AF (%)	SD*af* (%)	D*f* (%)	DDI
LT	1	26.8	64	2.63	0.92	15.9	0.008
	2	27.2	66	2.22	2.27	16.1	0.016
	3	45.6	180	4.63	3.20	27.0	0.066
	4	75.1	270	20.09	4.60	44.5	0.711
	5	121.7	530	24.58	5.15	72.4	0.974
	6	137.9	450	15.42	8.60	81.7	1.020
	7	217.0	1000	21.40	10.58	128.6	3.484
	8	168.7	530	11.26	5.56	100.0	0.482
NT	1	24.3	80	4.65	1.63	14.4	0.024
	2	23.7	72	3.16	2.14	14.0	0.022
	3	39.3	196	6.18	1.93	23.3	0.053
	4	93.4	270	9.07	4.07	55.4	0.284
	5	190.0	530	28.69	10.70	112.6	2.361
	6	135.1	490	8.20	6.74	80.1	0.425
	7	153.6	330	7.10	2.83	91.0	0.156
	8	168.7	530	11.26	5.56	100.0	0.482
HT	1	26.0	88	4.06	3.03	15.4	0.040
	2	30.2	96	5.06	4.14	17.9	0.068
	3	31.3	132	4.57	3.20	18.6	0.065
	4	82.0	206	4.91	2.53	48.6	0.096
	5	118.1	410	12.56	7.00	70.0	0.676
	6	162.8	600	15.02	6.45	96.5	0.745
	7	301.0	1500	18.36	7.20	178.4	3.051
	8	168.7	530	11.26	5.56	100.0	0.482
FT	1	39.2	96	6.20	5.16	23.2	0.103
DC	1	35.5	120	4.26	4.38	21.0	0.060

See **Nomenclature** for explanation of symbols and codes: See foot of Table 3.3.4 for sampling positions: Materials processed at standard settings, see Table 3.3.3, except: LT = low temperature profile (165/175/185/195/200): NT = normal temperature profile (185/195/205/215/220): HT = high temperature profile (205/215/225/235/240): FT = flat temperature profile (205): DC = decreasing temperature profile (220/215/205/195/185).

Table 3.3.9 The effect of position and mode of filler addition on the level of calcium carbonate dispersion

PP-D2-	Sampling position	MVD (um)	Dmax (um)	AF (%)	SDaf (%)	Df (%)	DDI
PH	1	24.3	80	4.65	1.63	14.4	0.024
	2	23.7	72	3.16	2.14	14.0	0.022
	3	39.3	196	6.18	1.93	23.3	0.053
	4	93.4	270	9.07	4.07	55.4	0.284
	5	190.0	530	28.69	10.70	112.6	2.361
	6	135.1	490	8.20	6.74	80.1	0.425
	7	153.6	330	7.10	2.83	91.0	0.156
	8	168.7	530	11.26	5.56	100.0	0.482
SH	1	20.6	48	3.28	2.38	12.9	0.025
	2	21.7	56	3.81	3.07	13.6	0.038
	3	42.9	228	6.38	3.31	27.0	0.094
	4	95.0	398	23.61	6.62	59.7	1.202
	5	267.0	1500	16.06	7.33	167.8	2.717
	6	265.5	1000	16.15	11.22	166.9	2.788
	7	261.0	1000	11.00	4.60	164.0	0.778
	8	159.1	370	9.48	5.54	100.0	0.404
SV1	1	100.2	302	6.86	2.52	63.0	0.133
	2	100.8	430	8.55	3.27	63.4	0.215
	3	521.4	2000	23.17	8.98	327.7	6.402
	4	159.1	370	9.48	5.54	100.0	0.404

See **Nomenclature** for explanation of symbols and codes: See foot of Table 3.3.4 for sampling positions: Materials processed at standard settings, see Table 3.3.3, except: PH = premix fed at hopper: SH = filler fed separately at hopper: SV1 = filler fed separately at vent

Table 3.3.10 The effect of extruder output rate on the level of dispersive mixing in the extrudate

PP-D2-	Sampling position	MVD (um)	D*max* (um)	AF (%)	SD*af* (%)	D*f* (%)	DDI
100%0	1	24.3	80	4.65	1.63	14.4	0.024
80%0	1	27.1	88	3.36	2.47	16.1	0.027
60%0	1	28.8	96	6.90	5.05	17.1	0.112

See **Nomenclature** for explanation of symbols and codes: Materials processed at standard settings, see Table 3.3.3, except: 100%0 = maximum output: 80%0 = 80% of maximum output: 60%0 = 60% of maximum output

Table 3.3.11 The effect of second-stage metering screw profile on the level of calcium carbonate dispersion

PP-D2-	Sampling position	MVD (um)	D*max* (um)	AF (%)	SD*af* (%)	D*f* (%)	DDI
8P	1	24.3	80	4.65	1.63	14.4	0.024
	2	23.7	72	3.16	2.14	14.0	0.022
	3	39.3	196	6.18	1.93	23.3	0.053
12P	1	23.3	56	4.46	2.19	13.8	0.032
	2	23.3	64	5.01	2.38	13.8	0.038
	3	31.9	132	9.57	5.06	18.9	0.212
16P	1	19.0	48	3.05	0.58	11.3	0.006
	2	20.3	56	2.53	1.49	12.0	0.012
	3	29.4	132	5.90	2.68	17.4	0.071
8P2D	1	24.5	64	3.16	2.25	14.5	0.023
	2	26.9	56	3.09	1.82	15.9	0.025
	3	28.6	132	6.51	2.09	17.0	0.061

See **Nomenclature** for explanation of symbols and codes: See foot of Table 3.3.4 for sampling positions: Materials processed at standard settings, see Table 3.3.3, except: 8P = 8mm pitch screw: 12P = 12mm pitch screw: 16P = 16mm pitch screw: 8P2D = 8mm pitch plus 2 mixing elements

Table 3.3.12 The effect of extruder barrel configuration on the level of dispersive mixing in the extrudate

PP-D2-	Sampling position	MVD (um)	Dmax (um)	AF (%)	SDaf (%)	Df (%)	DDI
4B-SS-PH	1	29.0	104	6.03	4.20	17.2	0.082
4B-NS-PH	1	24.3	80	4.65	1.63	14.4	0.024
4B-HS-PH	1	22.4	64	3.44	1.19	13.3	0.013
5B-SS-PH	1	25.6	64	4.79	4.60	15.2	0.071
5B-NS-PH	1	23.6	72	5.49	4.52	14.0	0.080
5B-HS-PH	1	21.6	48	3.21	1.81	12.8	0.019
5B-NS-SV1	1	64.9	196	4.07	2.76	40.8	0.050
5B-NS-SV2	1	113.3	330	5.69	5.99	71.2	0.262

See **Nomenclature** for explanation of symbols and codes: Materials processed at standard settings, see Table 3.3.3, except: 4B = 4 barrel section configuration: 5B = 5 barrel section configuration: SS = slow screw speed (60rpm): NS = normal screw speed (120rpm): HS = high screw speed (180rpm): PH = premix fed at hopper: SV1 = separate feed of filler into first vent port: SV2 = separate feed of filler into second vent port.

Table 3.3.13 Position of sampling from the metering screws after barrel withdrawal for carbon black compounds

Position No:	Dist from screw tips (mm)	Position along screws for different pitch			
		8mm	12mm	16mm	8mm+2D
1			EXTRUDATE		
2	16mm	F.2	F.1	F.1	Betw D.1-2
3	48	6	4	3	F.3
4	88	11	7	5	8
5	128	16	10	8	13
6	160	20	13	10	17

F = flight number

Table 3.3.14 Standard extruder settings for processing 0.5wt% carbon black pigment with polypropylene granules

Die Type	Rod (6mm diameter)
Screw speed	120rpm
Barrel	4 sections with venting in zone 3
Screws	17:1 L/D with 4 melting elements between zones 2 & 3 and 8mm pitch metering screws
Feed	Preblend fed at the hopper from Simon Varifeeder
Output	Maximum possible for stable processing and limited by motor current maximum of 20A
Temperature profile (°C)	Zone 1 = 175 Zone 2 = 185 Zone 3 = 195 Zone 4 = 205 Die = 210

Table 3.3.15 The effect of varying extruder screw speed, with and without a breaker plate present in the barrel head adaptor, on the level of carbon black distributive mixing in the polypropylene extrudate

PPG-CB-	Screw Speed (rpm)	AF (%)	SD*af* (%)	DDI
BP	30	1.15	0.68	0.002
	60	2.60	1.44	0.011
	90	3.24	1.84	0.018
	120	3.40	2.23	0.023
	150	5.05	3.77	0.057
	180	5.58	3.63	0.061
WBP	30	1.76	0.85	0.005
	60	3.37	3.54	0.011
	90	4.78	3.60	0.052
	120	4.28	2.08	0.027
	150	5.75	4.08	0.071
	180	5.93	2.42	0.044

See **Nomenclature** for explanation of symbols and codes: Materials processed at standard settings, see Table 3.3.14: BP = breaker plate present: WBP = without breaker plate present

Table 3.3.16 The effect of varying extruder temperature profile on the level of carbon black distributive mixing in the polypropylene extrudate

PPG-CB-	AF (%)	SD*af* (%)	DDI
LT	5.51	2.28	0.038
NT	3.40	2.23	0.023
HT	3.99	2.52	0.030

See **Nomenclature** for explanation of symbols and codes: Materials processed at standard settings, see Table 3.3.14, except: LT = low temperature profile (165/175/185/195/200): NT = normal temperature profile (185/195/205/ 215/220): HT = high temperature profile (205/215/225/235/240)

Table 3.3.17 The effect of extruder output rate on the level of carbon black distributive mixing in the polypropylene extrudate

PPG-CB-	AF (%)	SD*af* (%)	DDI
100%0	3.40	2.23	0.023
80%0	2.52	1.09	0.008
60%0	4.45	3.41	0.046

See **Nomenclature** for explanation of symbols and codes: Materials processed at standard settings, see Table 3.3.14, except: 100%0 = maximum output: 80%0 = 80% of maximum output: 60%0 = 60% of maximum output

Table 3.3.18 The effect of second-stage metering screw profile on the level of carbon black distributive mixing

PPG-CB-	Sampling position	AF (%)	SD*af* (%)	DDI
8P	1	3.40	2.23	0.023
	2	4.19	2.43	0.031
	3	4.81	2.65	0.039
	4	5.84	3.18	0.056
	5	6.29	3.15	0.060
	6	8.35	2.94	0.074
12P	1	2.82	2.92	0.025
	2	6.15	1.78	0.033
	3	6.63	3.25	0.065
	4	8.01	5.06	0.123
	5	7.98	2.94	0.071
	6	9.01	3.15	0.086
16P	1	2.98	1.06	0.009
	2	4.46	2.85	0.038
	3	5.88	2.58	0.046
	4	6.38	3.28	0.063
	5	9.48	4.23	0.122
	6	10.17	4.53	0.140
8P2D	1	0.46	0.34	0.001
	2	1.94	0.76	0.004
	3	3.58	1.76	0.019
	4	6.19	1.68	0.032
	5	7.15	1.72	0.037
	6	8.87	3.30	0.089

See **Nomenclature** for explanation of symbols and codes: See Table 3.3.13 for explanation of sampling position: Materials processed at standard settings, see Table 3.3.14, except: 8P = 8mm pitch screw: 12P = 12mm pitch screw: 16P = 16mm pitch screw: 8P2D = 8mm pitch plus 2 mixing elements

Table 3.3.19 The effect of position of pigment addition on the level of carbon black distributive mixing

PPG-CB-	Sampling position	AF (%)	SD*af* (%)	DDI
Hopper				
8P2D	1	0.46	0.34	0.001
	2	1.94	0.76	0.004
	3	3.58	1.76	0.019
	4	6.19	1.68	0.032
	5	7.15	1.72	0.037
	6	8.87	3.30	0.089
Vent				
8P2D	1	4.38	5.14	0.068
	2	5.83	4.84	0.086
	3	9.22	3.32	0.092
	4	10.53	6.43	0.205
	5	11.58	4.53	0.159
	6	14.14	5.29	0.227

See **Nomenclature** for explanation of symbols and codes: See Table 3.3.13 for explanation of sampling position: Materials processed at standard settings, see Table 3.3.14, except: 8P2D = 8mm pitch plus 2 mixing elements

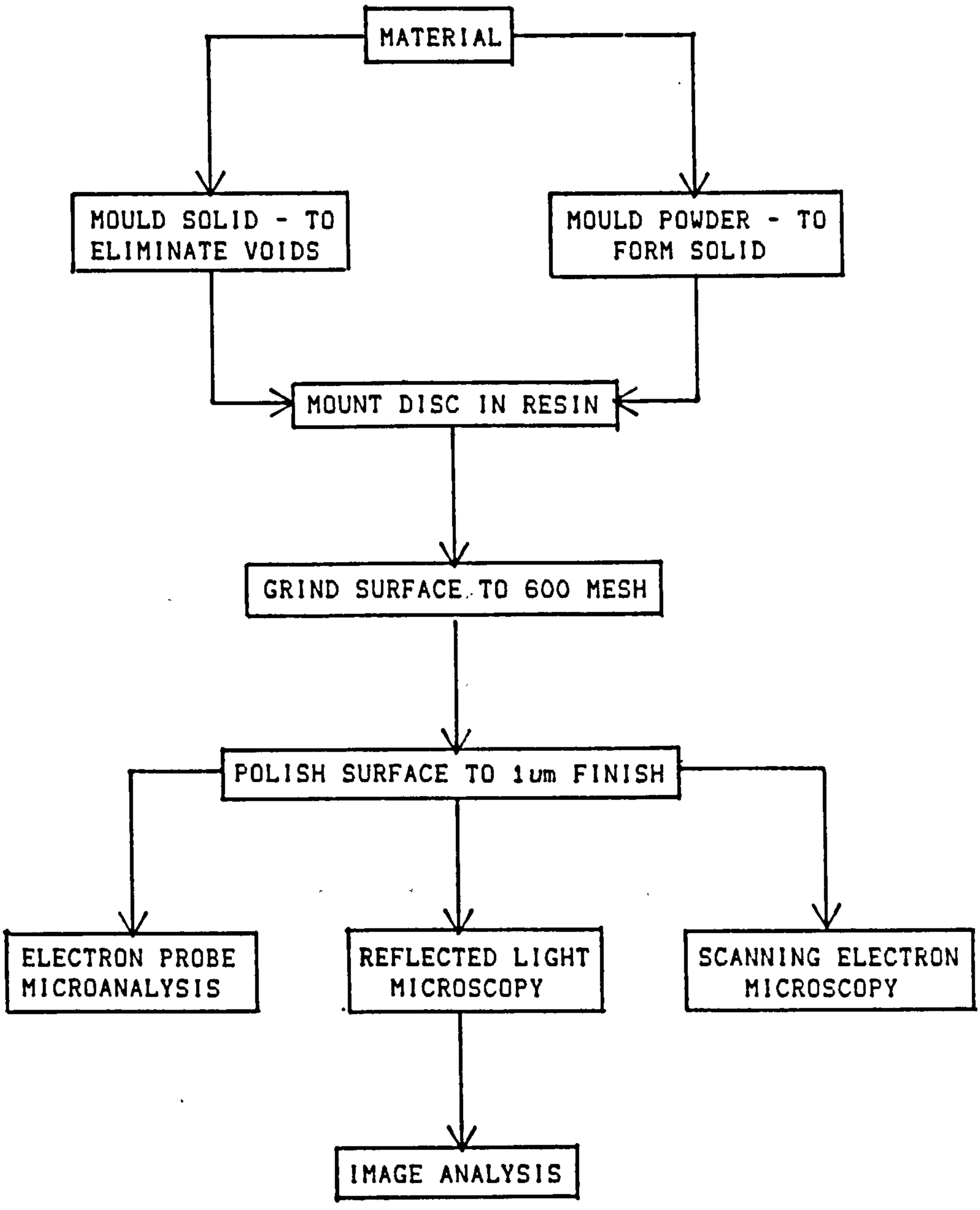

Fig.3.3.1 Outline of characterization of mixing technique for calcium carbonate filled specimens

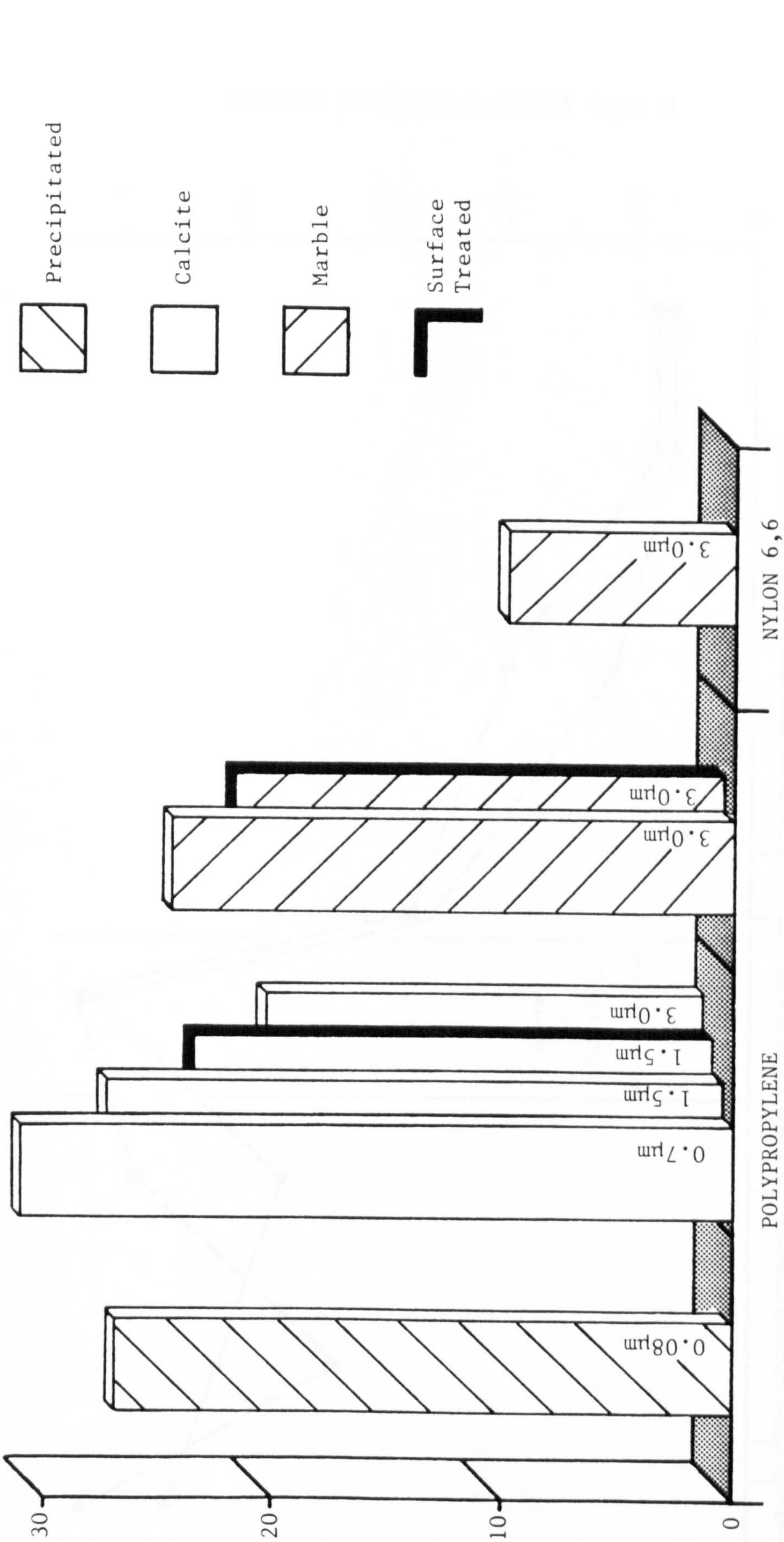

Fig. 3.3.2 The effect of varying calcium carbonate characteristics and polymer matrix

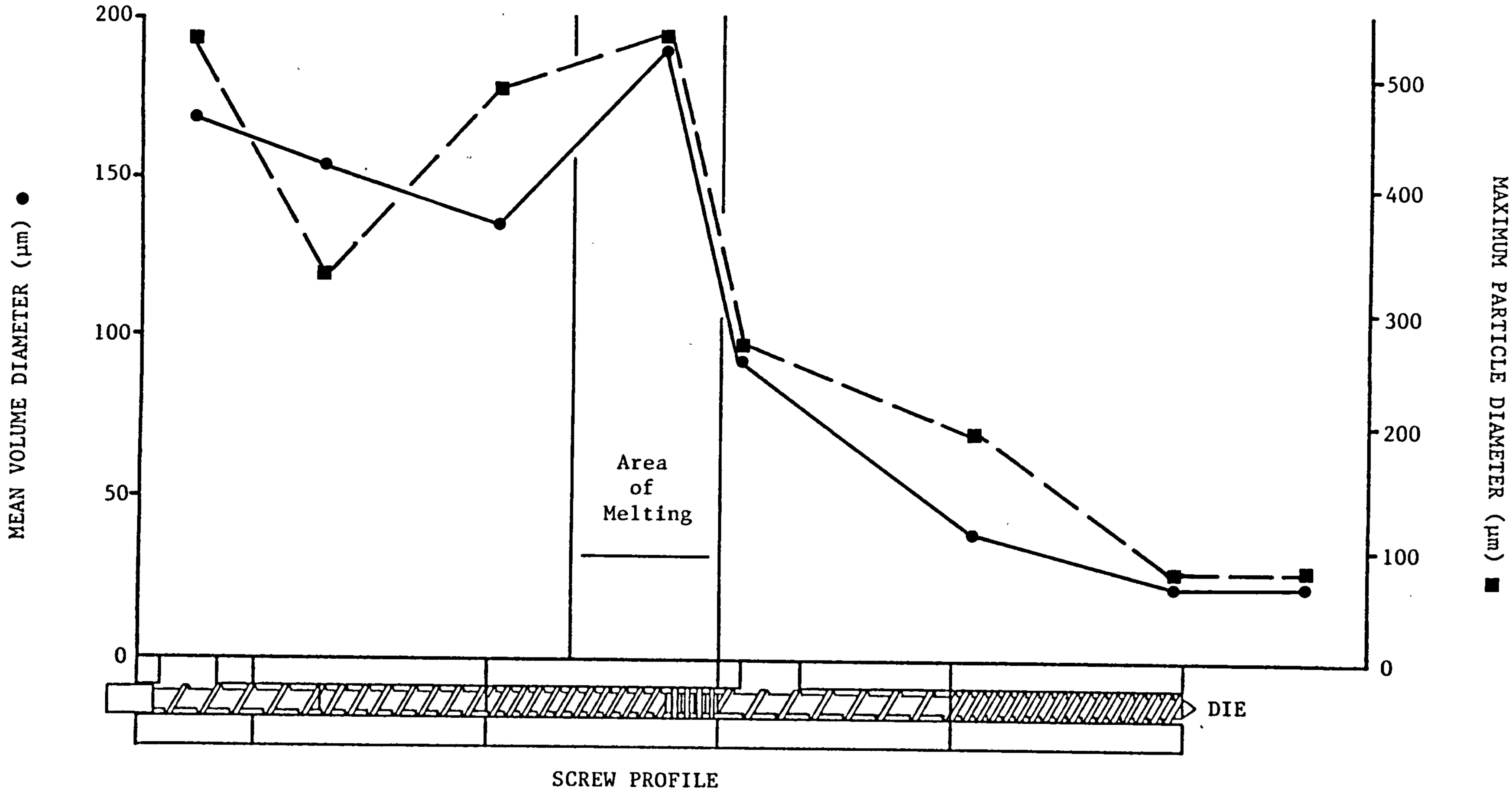

Fig. 3.3.3 Dispersion of Durcal 2 along the length of the screws at standard extruder settings

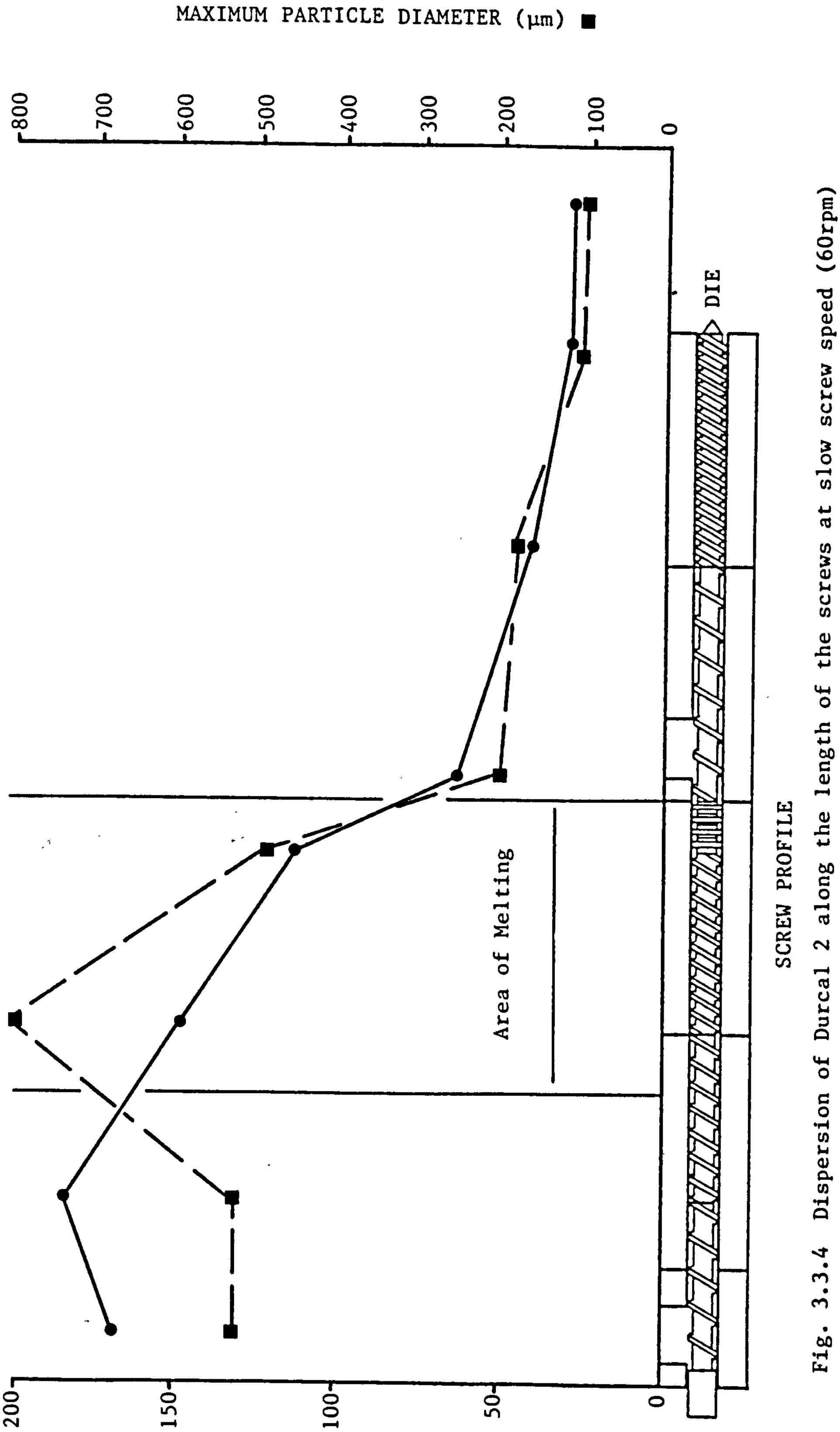

Fig. 3.3.4 Dispersion of Durcal 2 along the length of the screws at slow screw speed (60rpm)

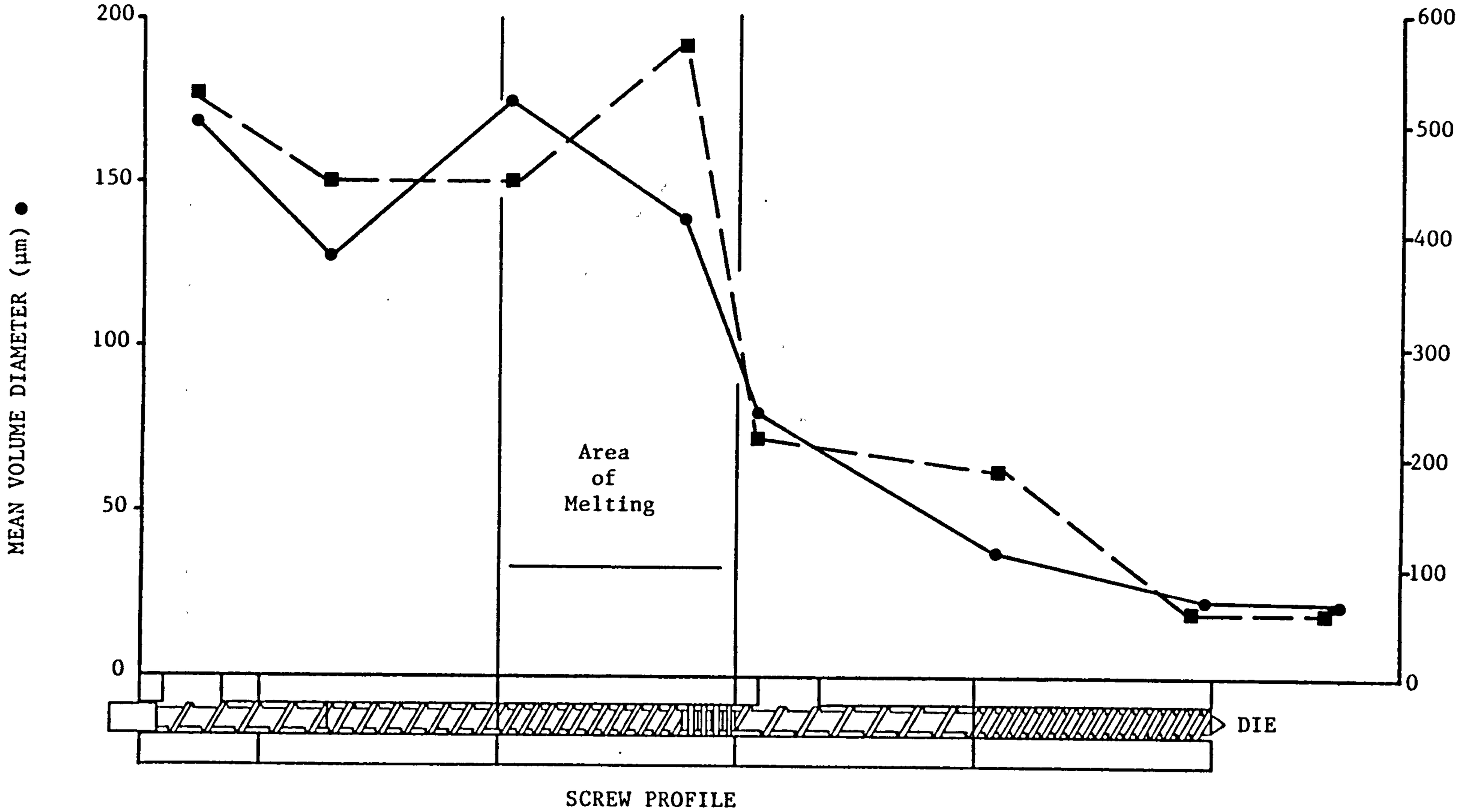

Fig. 3.3.5 Dispersion of Durcal 2 along the length of the screws at high screw speed (180rpm)

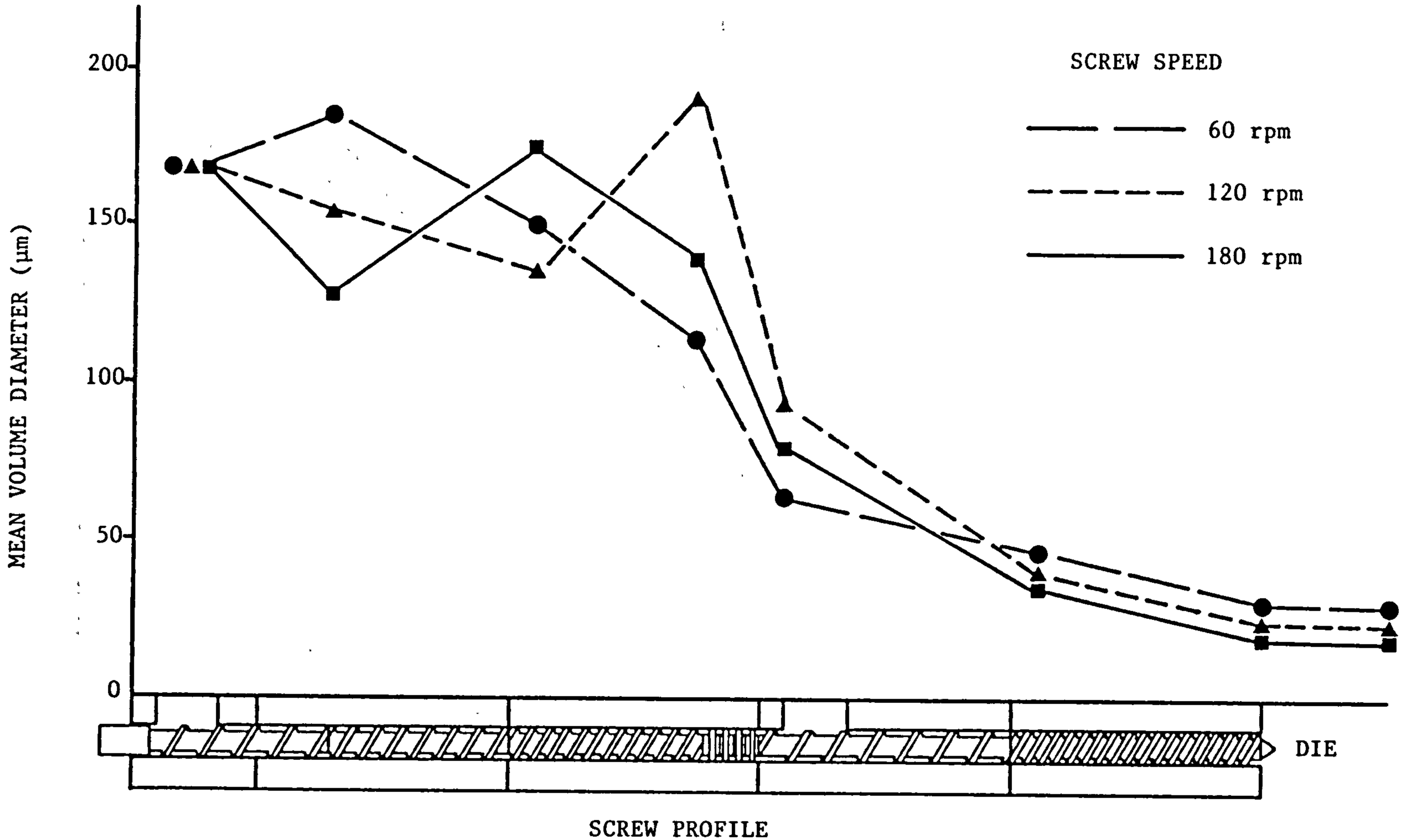

Fig. 3.3.6 Comparison of dispersion of Durcal 2 along the length of the screws at 60, 120 and 180rpm

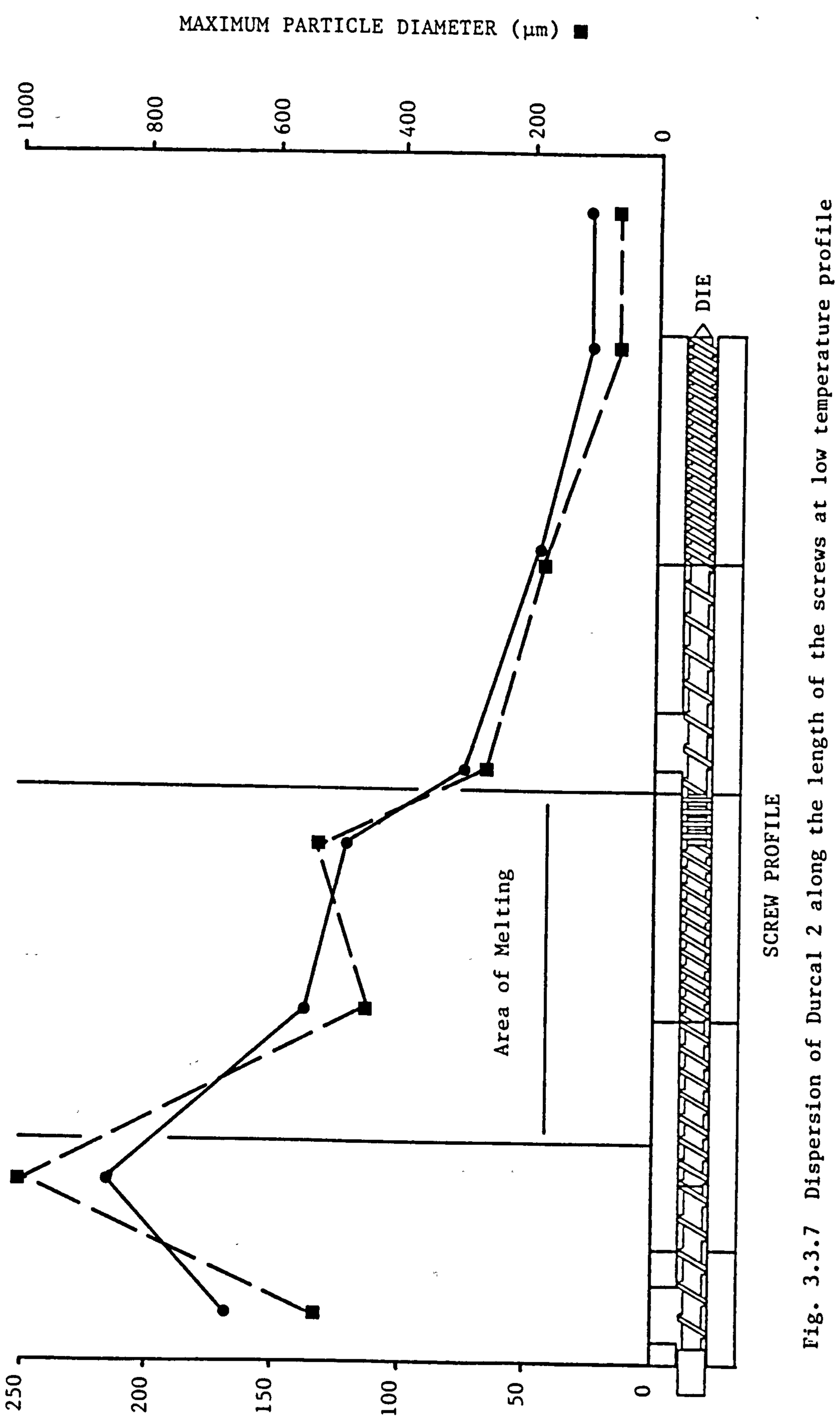

Fig. 3.3.7 Dispersion of Durcal 2 along the length of the screws at low temperature profile

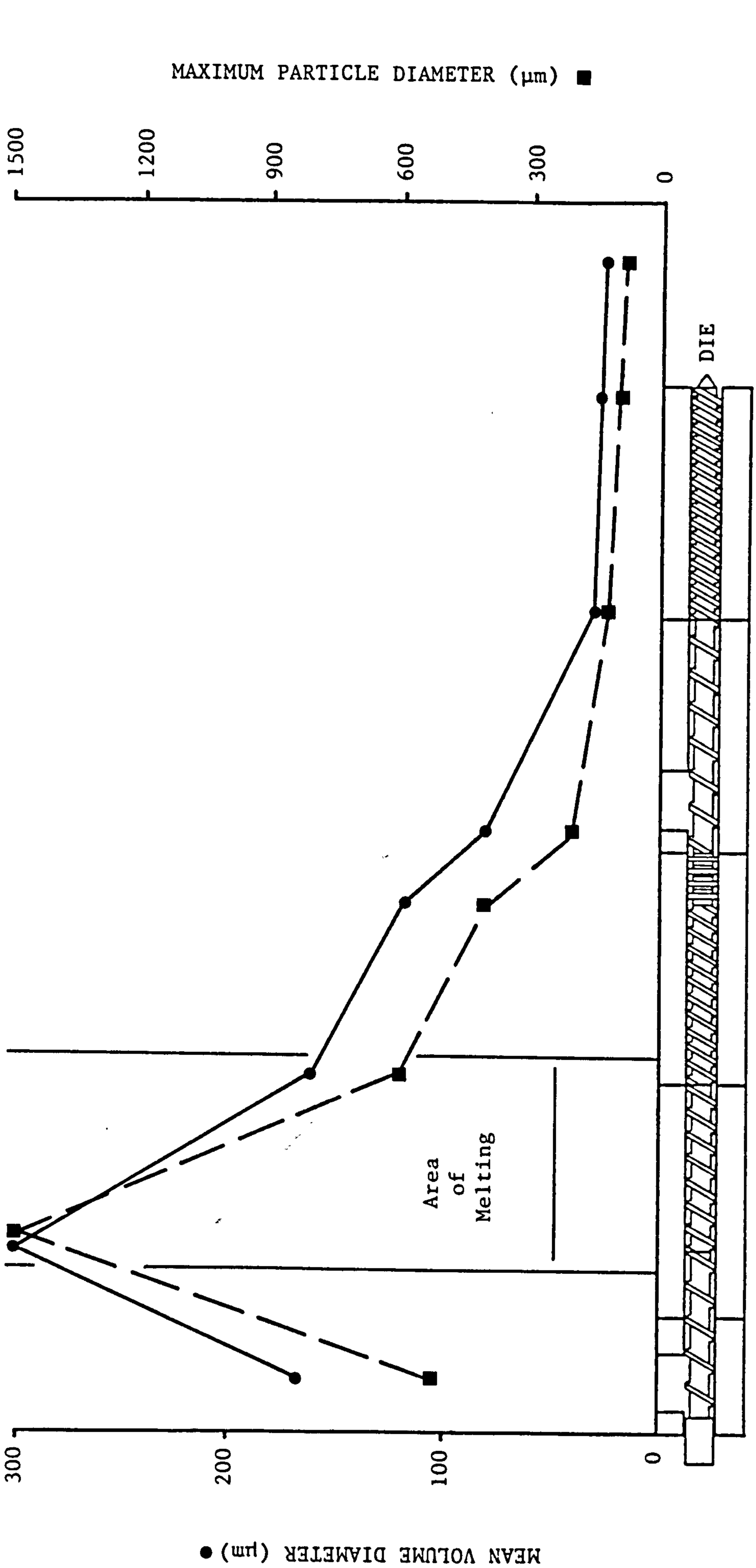

Fig. 3.3.8 Dispersion of Durcal 2 along the length of the screws at high temperature profile

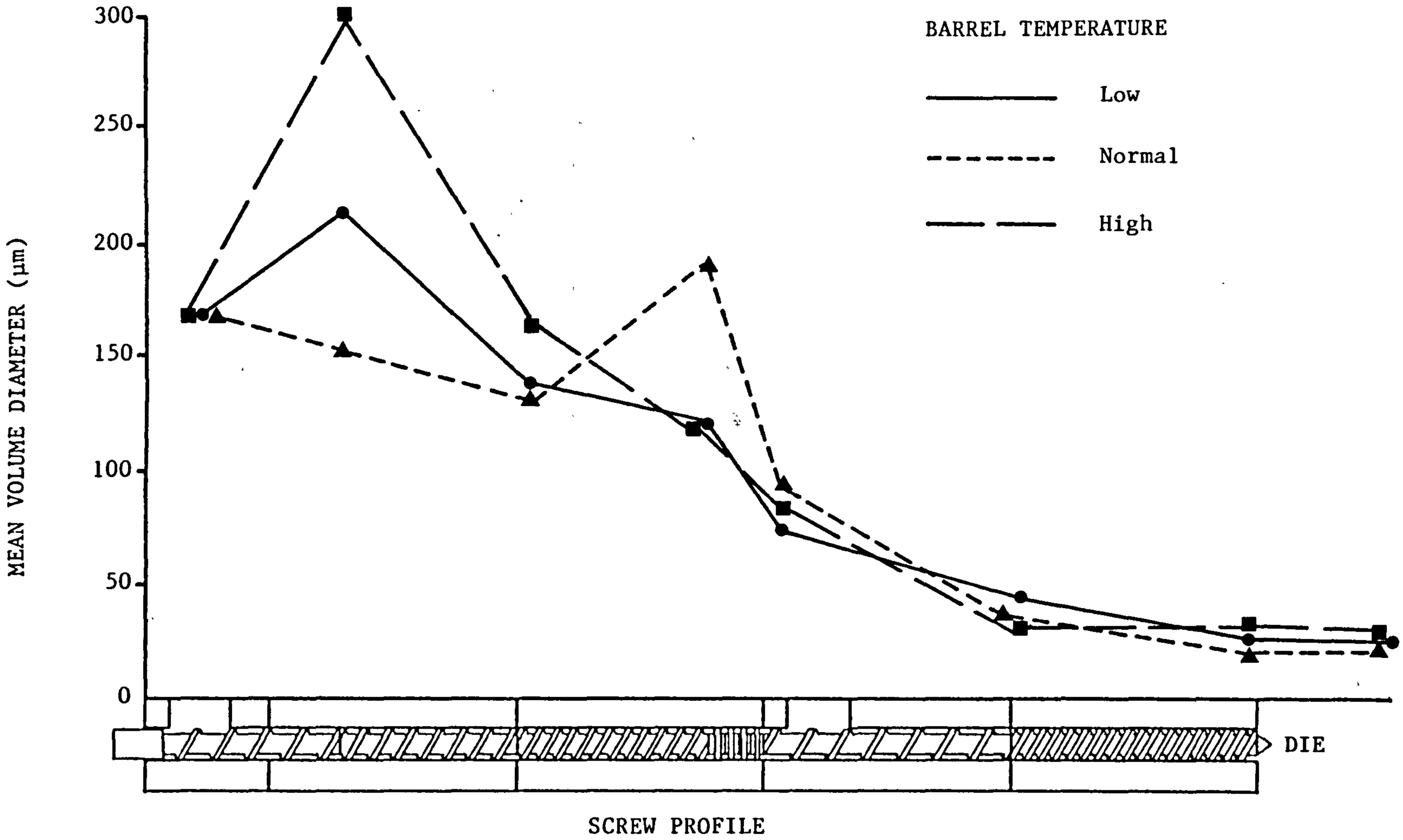

Fig. 3.3.9 Comparison of dispersion of Durcal 2 along the length of the screw at low, normal and high temperature profiles

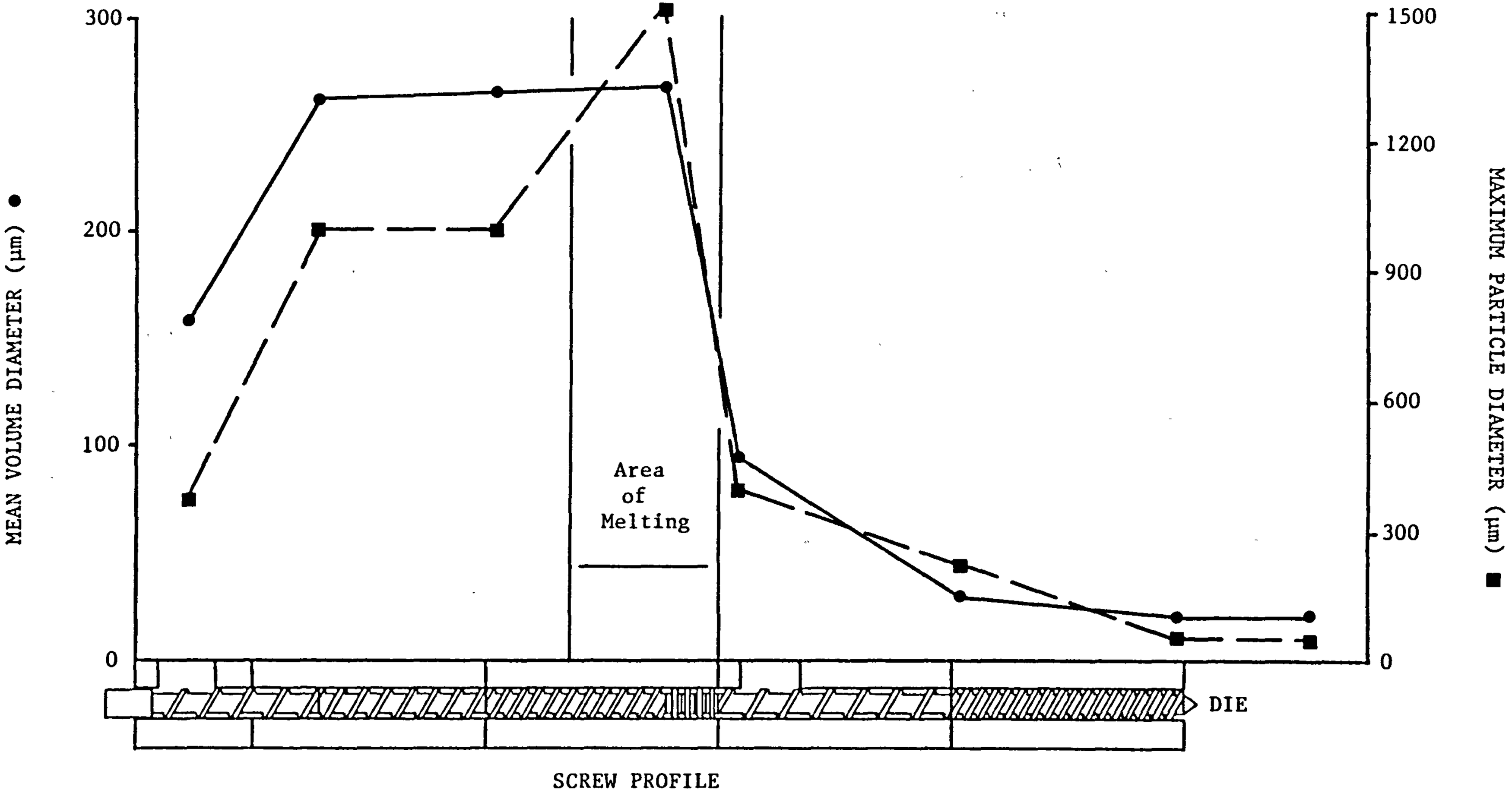

Fig. 3.3.10 Dispersion of Durcal 2 along the length of the screws when the calcium carbonate and polypropylene were separately fed at the hopper

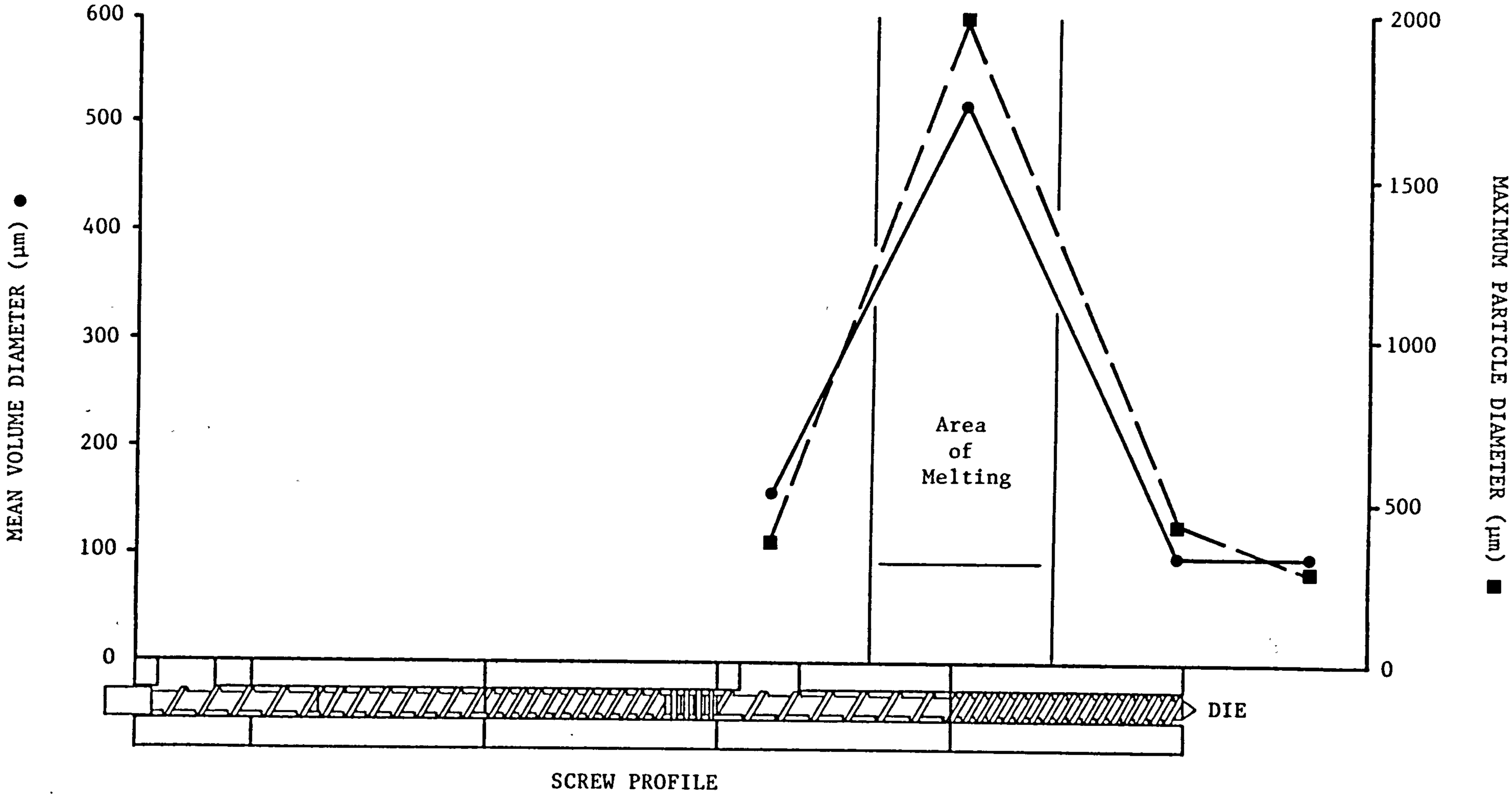

Fig. 3.3.11 Dispersion of Durcal 2 along the second stage of the screws when the calcium carbonate and polypropylene were separately fed at the downstream entry port

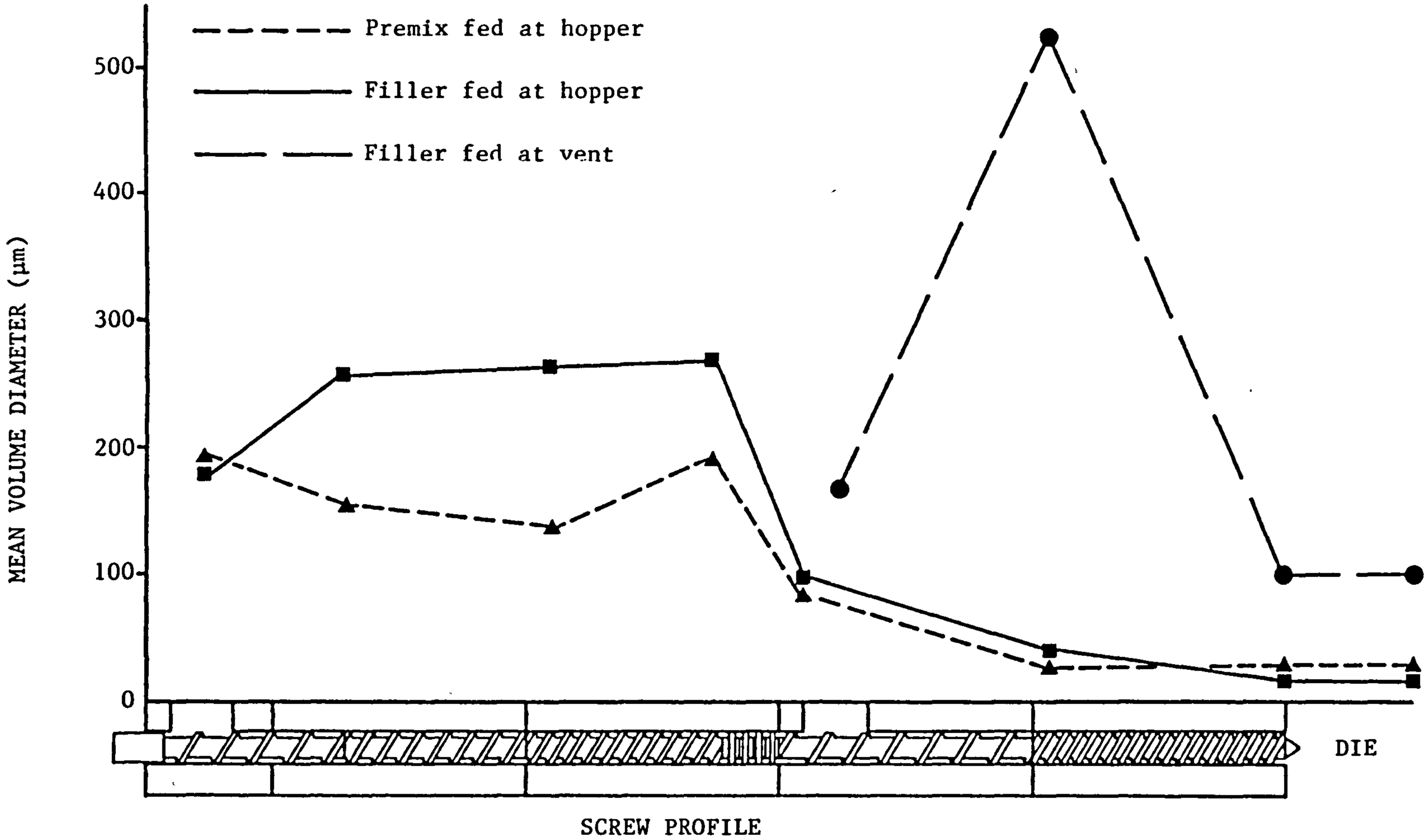

Fig. 3.3.12 Comparison of dispersion of Durcal 2 along the length of the screws as a function of position and mode of filler addition

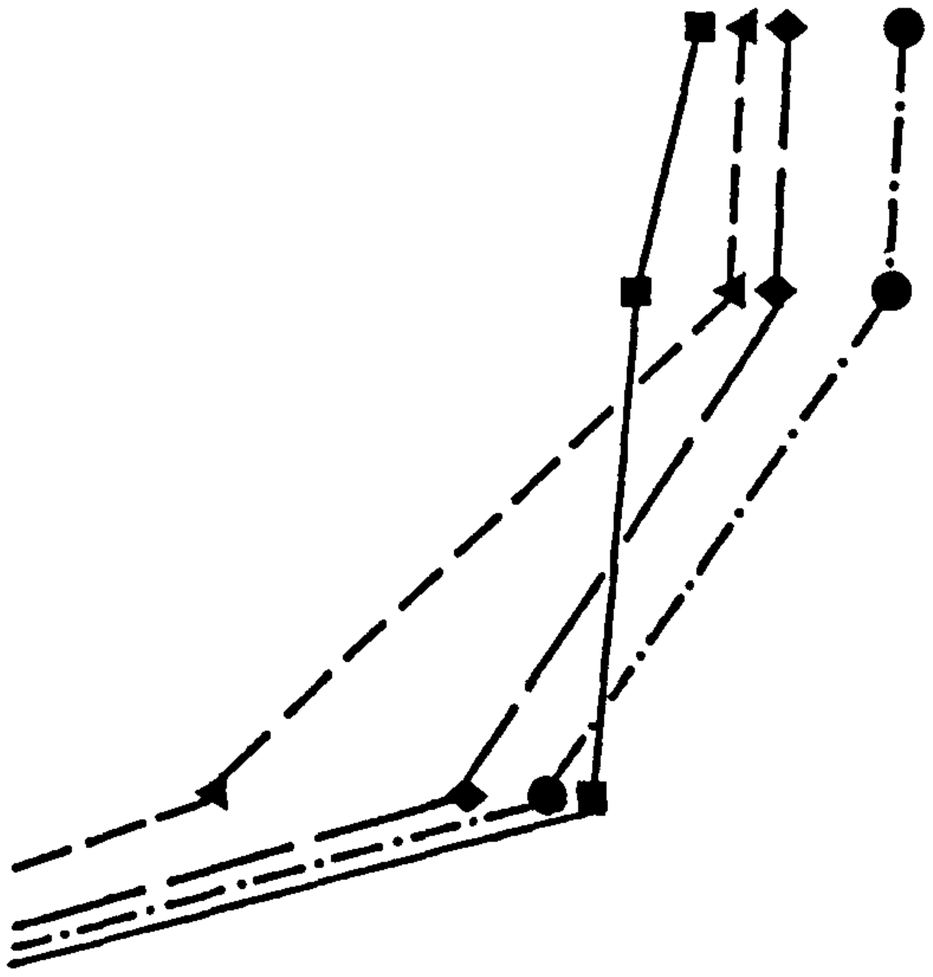

Fig. 3.3.13 Comparison of dispersion of Durcal 2 along the length of the second-stage metering screws for different metering screw profiles

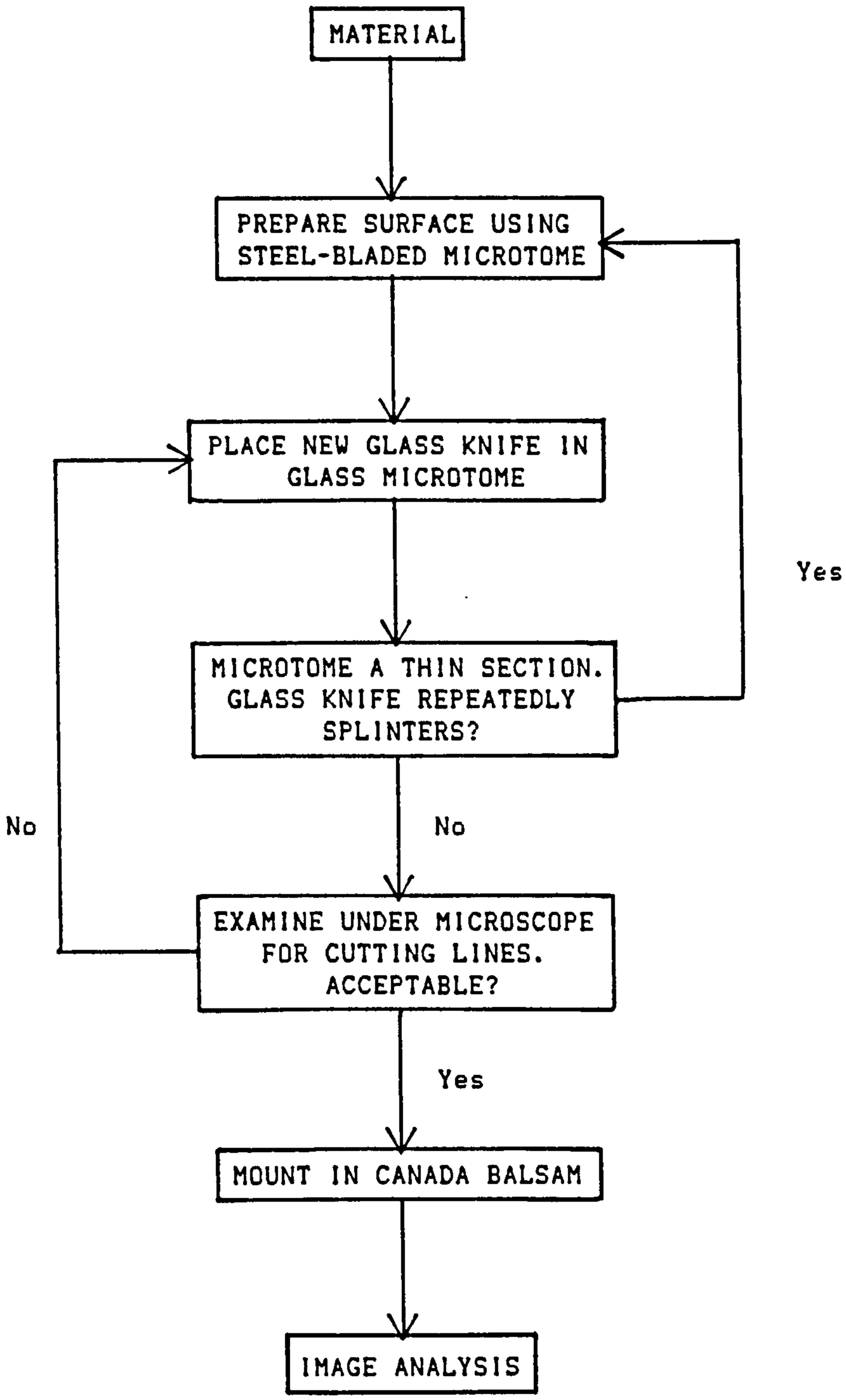

Fig.3.3.14 Outline of characterization of mixing technique for carbon black pigmented specimens

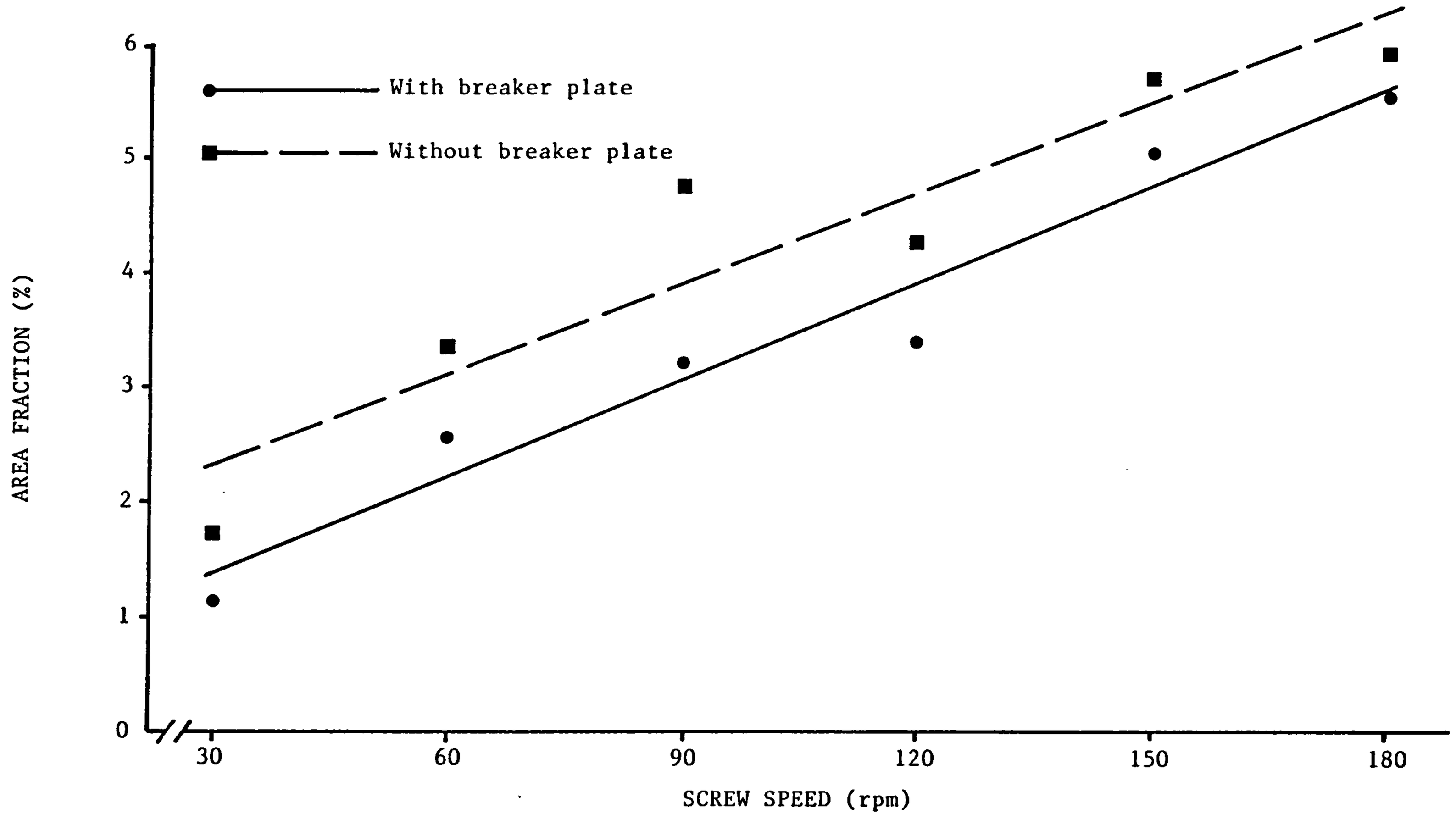

Fig. 3.3.15 Regression lines of area fraction on screw speed showing the effect of presence of the breaker plate on the level of carbon black distributive mixing

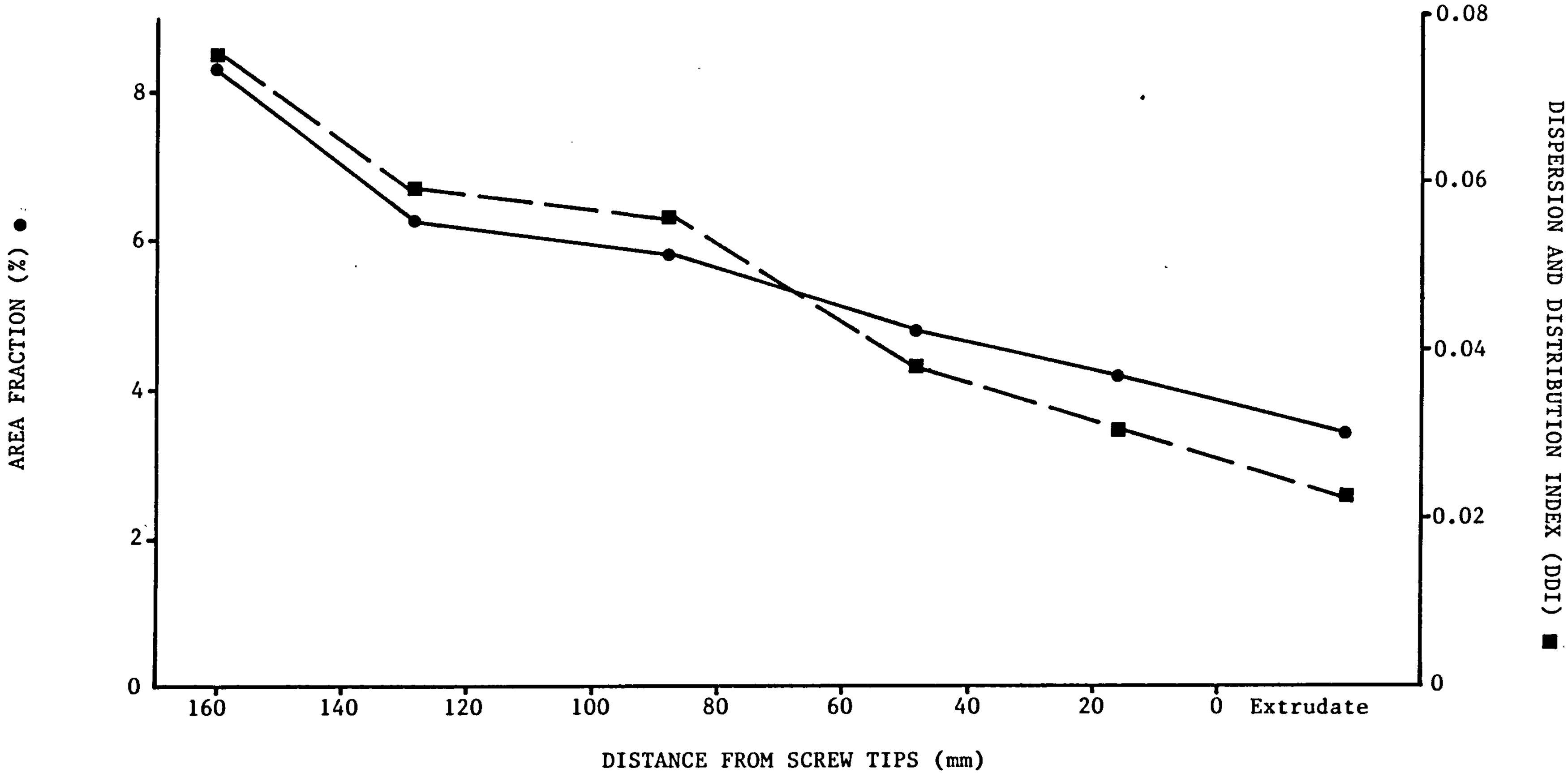

Fig. 3.3.16 Distributive mixing of carbon black along the length of the '8mm pitch' second-stage metering screws

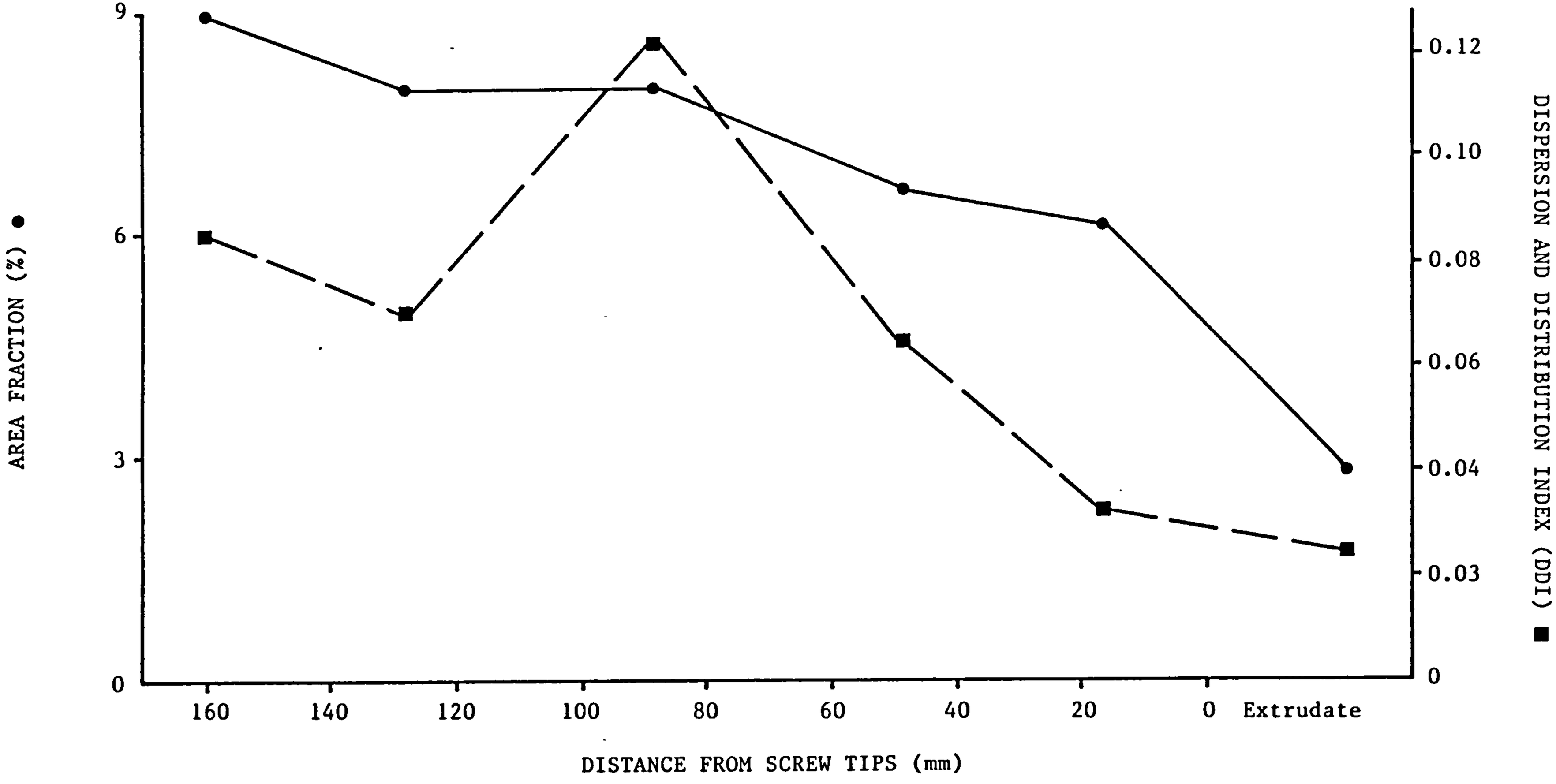

Fig. 3.3.17 Distributive mixing of carbon black along the length of the '12mm pitch' second-stage metering screws

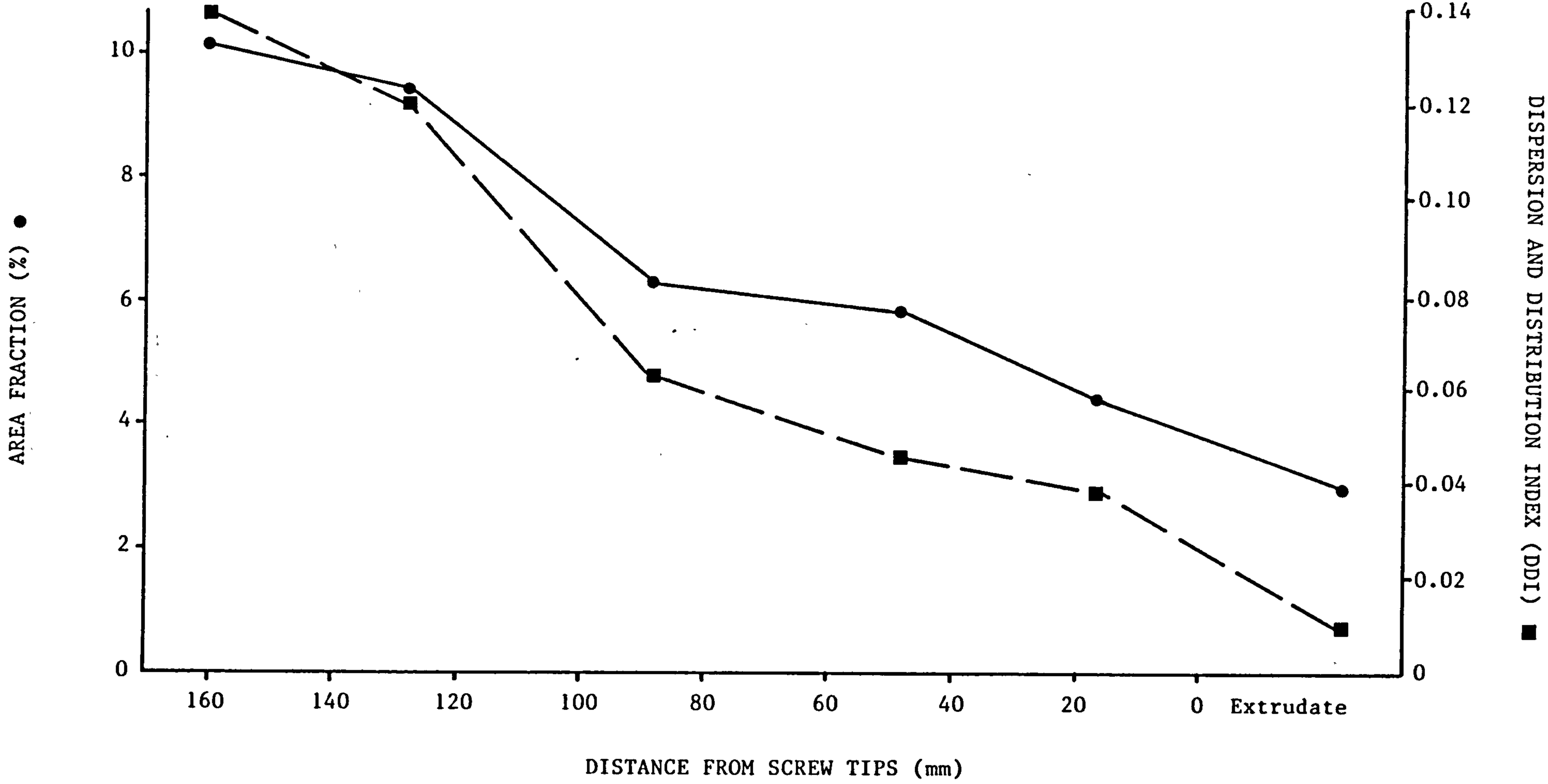

Fig. 3.3.18 Distributive mixing of carbon black along the length of the '16mm pitch' second-stage metering screws

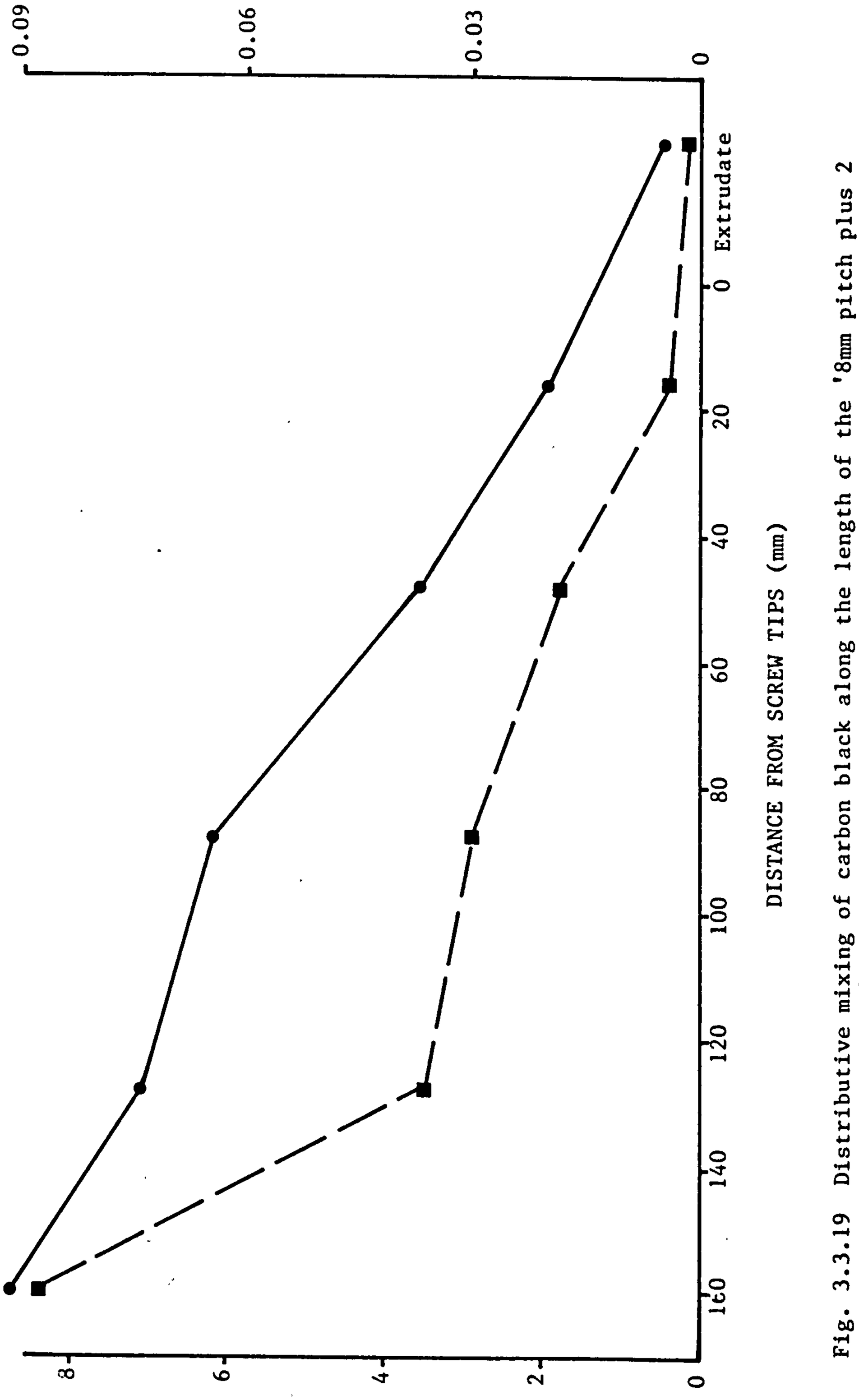

Distributive mixing of carbon black along the length of the '8mm pitch plus 2 mixing elements' second-stage metering screws

Fig. 3.3.19

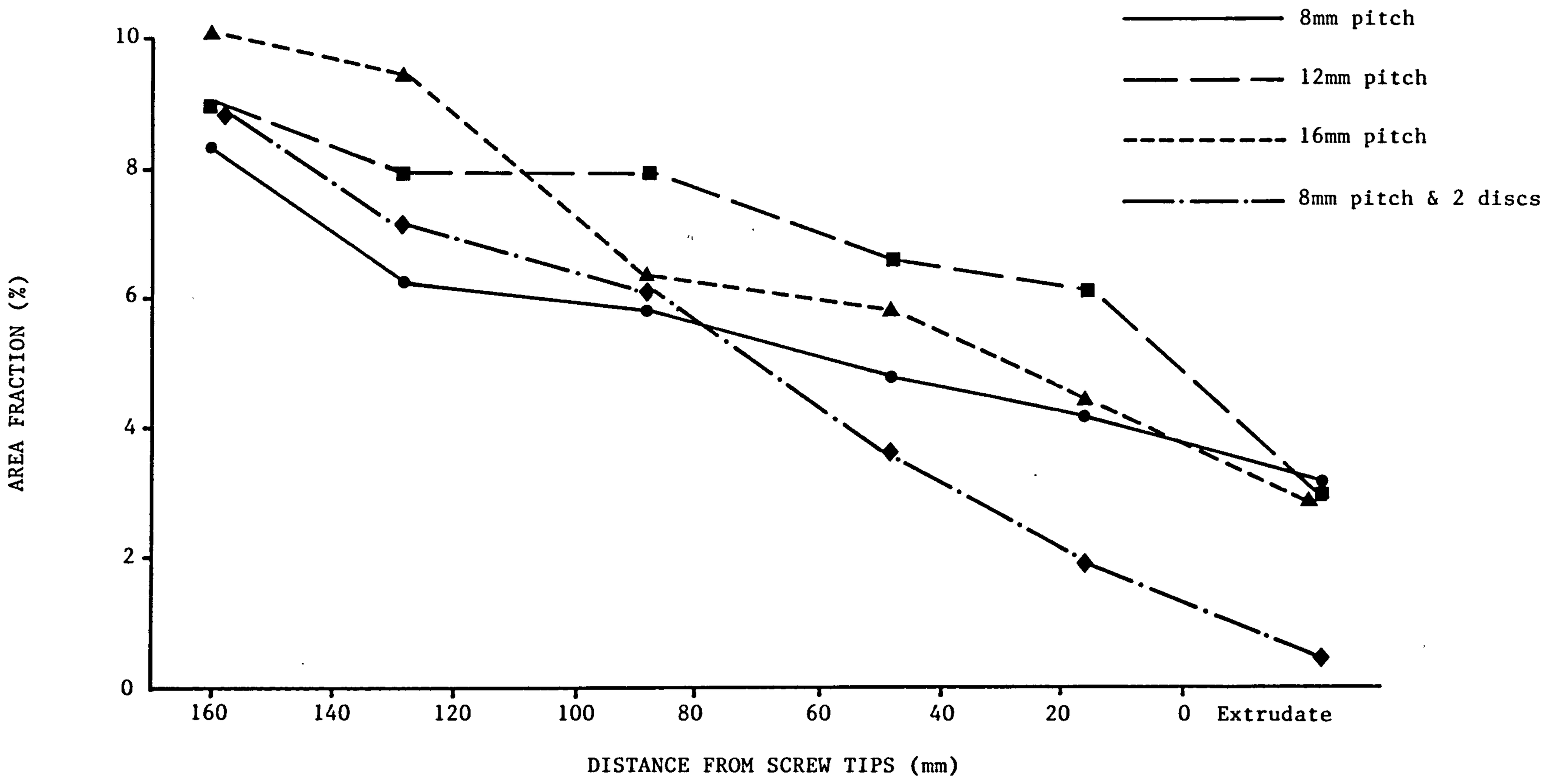

Fig. 3.3.20 Comparison of distributive mixing of carbon black along the length of the second-stage metering screws for different metering screw profiles

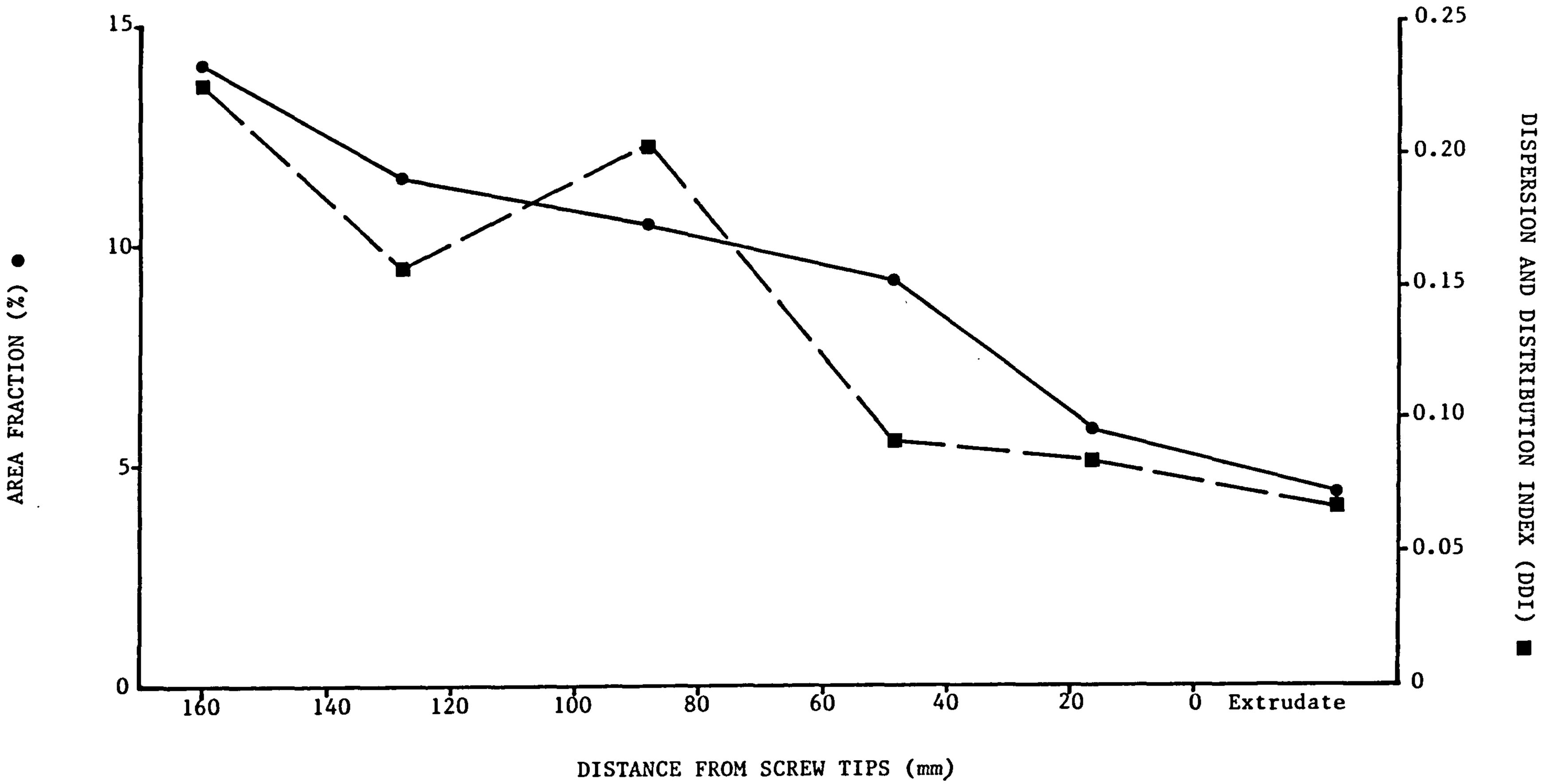

Fig. 3.3.21 Distributive mixing of carbon black along the length of the '8mm pitch plus 2 mixing elements' second-stage metering screws when carbon black masterbatch dosed separately into the downstream entry port

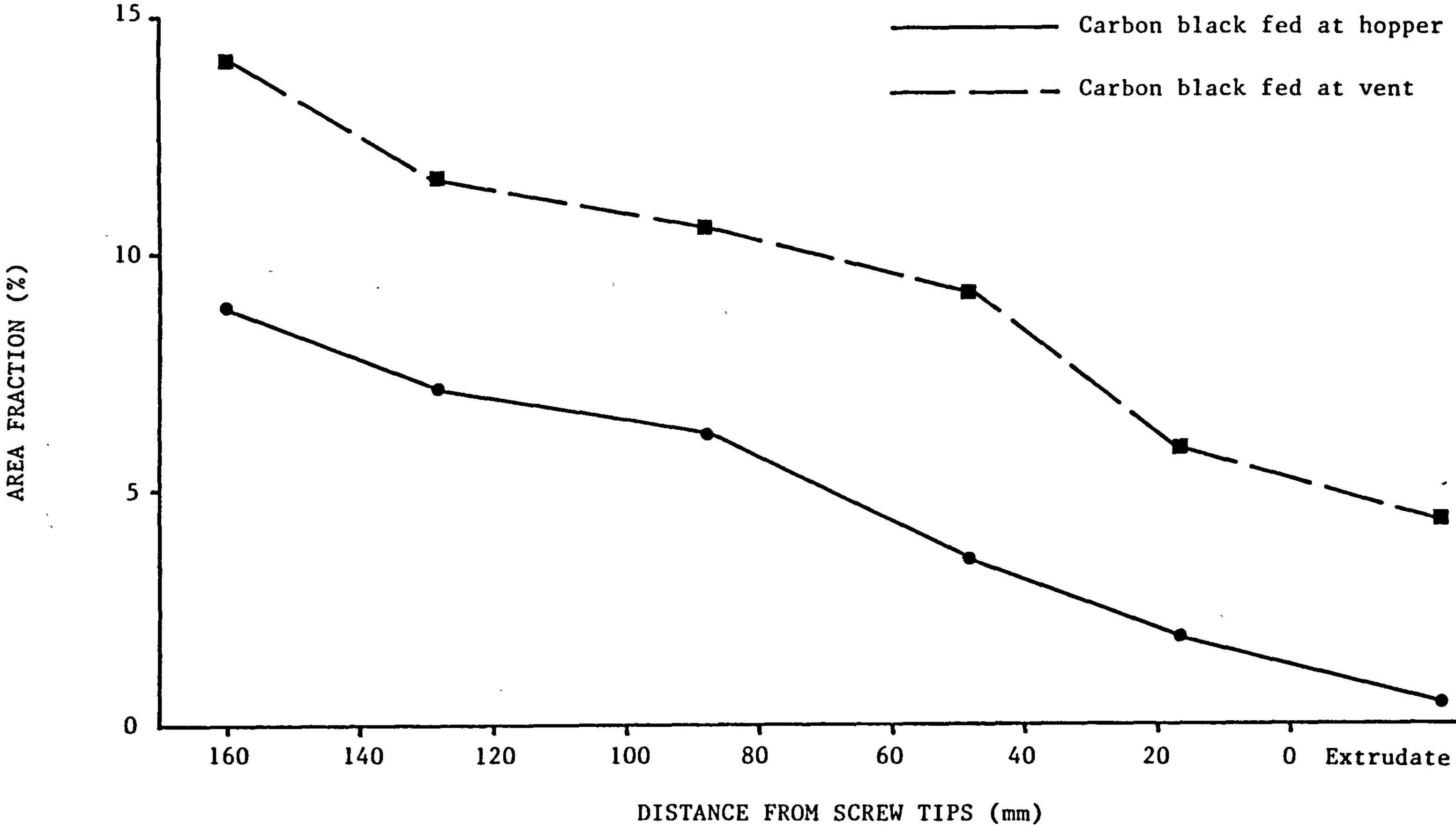

Fig. 3.3.22 Comparison of distributive mixing of carbon black along the length of the second-stage metering screws for different positions of carbon black masterbatch addition

3.4 MODEL EXPERIMENTS WITH PRECONDITIONED FILLER

As a consequence of observed variations in dispersion found in extrudate, with and without premixing of filler and polymer (discussed in Section 4.4), a series of experiments were designed to assess the importance of filler preconditioning on extrudate mixture quality. Parameters identified as being pertinent to the agglomeration of filler particles during preprocessing operations were moisture content, particle size and surface treatment, coupled with the level of temperature and pressure experienced.

3.4.1 Preconditioning Pressure

Calcium carbonate (Durcal 2) was dried in a vacuum oven at 100°C overnight to ensure no moisture remained. The dried powder was placed in the 25mm diameter cylindrical mould of a small hydraulic press and thin discs of material were prepared at room temperature using a range of consolidating pressures between 31.5 and 157.5MPa. Polypropylene powder was run through the extruder using standard conditions (Table 3.4.1) and compressed filler powder 'pellets' introduced with the polymer feed at the hopper. Separate experiments were also undertaken where the filler 'pellets' were added downstream, directly into the melt. In both cases, samples were taken from the resulting extrudate for subsequent analysis of filler dispersion (Table 3.4.2 and Figure 3.4.1).

3.4.2 Calcium Carbonate Moisture Content

The moisture contents of the calcium carbonate powders, taken directly from the bags as supplied, are shown in Table 3.4.3; these results were obtained by drying the powders overnight at 100°C. Undried Durcal 2 was compacted at a range of pressures between 31.5 and

157.5MPa and processed by addition at the hopper and vent ports (Figure 3.4.1).

Additionally, excess quantities of moisture were added to Durcal 2 powder and the moisture content verified as above. This moist material was compressed at 157.5MPa utilizing a mould temperature of 100°C in order that coherent pellets were formed; these pellets were processed both by addition at the hopper and vent ports. Image analysis results for all these experiments are given in Table 3.4.4.

3.4.3 Calcium Carbonate Characteristics

The range of calcites exhibiting different mean particle sizes (Setacarb 13, Hydrocarb and Millicarb) together with the marble calcium carbonates, one without and the other with surface coating (Durcal 2 and Omyalene SL) were prepared and processed as in Section 3.4.1 above. Results are shown in Table 3.4.5 and graph A of Figure 3.4.2.

3.4.4 Preconditioning Temperature

A range of moulding temperatures between 50 and 250°C were used to compress predried Durcal 2 at a pressure of 157.5MPa, and the pellets were added to the extruder at the hopper and vent ports. Image analysis results are found in Table 3.4.6 and graph B of Figure 3.4.2.

Table 3.4.1 Standard extruder settings for processing preconditioned calcium carbonate filler in polypropylene powder

Die Type	Strip (3mm x 75mm)
Screw speed	120rpm
Barrel	4 sections with venting in zone 3
Screws	17:1 L/D with 4 melting elements between zones 2 & 3 and 8mm pitch metering screws
Feed	Polymer fed at hopper from K-Tron Soder T20
Output	12.8kg/hr
Temperature profile (°C)	Zone 1 = 185 Zone 2 = 195 Zone 3 = 205 Zone 4 = 215 Die = 220

Table 3.4.2 The effects of preconditioning pressure and position of filler entry on the dispersion of Durcal 2 pellets in polypropylene extrudate

PP-PD2-	Entry position	MVD (um)	D*max* (um)	AF (%)	SD*af* (%)	DDI
31.5MPa	Hopper	22.0	52	2.32	1.76	0.006
63.0		68.0	250	3.57	2.13	0.065
94.5		97.8	250	2.63	1.51	0.031
126.0		173.9	410	8.67	4.05	0.270
157.5		187.9	370	10.47	6.98	0.562
31.5MPa	Vent	115.1	370	5.16	4.13	0.164
63.0		116.1	410	7.45	12.80	0.734
94.5		130.5	570	14.68	6.62	0.748
126.0		446.9	1500	17.44	8.32	3.348
157.5		422.1	2000	11.10	5.17	1.766

See **Nomenclature** for explanation of symbols and codes: Materials processed at standard settings, see Table 3.4.1: PP = polypropylene powder: PD2 = preconditioned Durcal 2: Filler dried overnight at 100°C and pellets formed at RT (23°C)

Table 3.4.3 Raw powder moisture contents for the 7 different calcium carbonates

Trade Name	Geological Origin	Mean particle size (um)	Surface treatment	Raw Powder Moisture Content (wt%)
Hakuenka CCR	Precipitated	0.08	Yes(CS)	1.926
Setacarb 13	Calcite (Urgonian)	0.70	No	0.347
Hydrocarb	Crystalline calcite (Urgonian)	1.50	No	0.159
Hydrocarb 95T	Crystalline calcite (Urgonian)	1.50	Yes(PT)	0.686
Millicarb	Crystalline calcite (Urgonian)	3.00	No	0.137
Durcal 2	Marble (Metamorphic)	3.00	No	0.105
Omyalene SL	Marble (Metamorphic)	3.00	Yes(PT)	0.547

CS = calcium stearate; PT = proprietary treatment.

Table 3.4.4 The effect of calcium carbonate moisture content and position of filler entry on the dispersion of Durcal 2 pellets in polypropylene extrudate

PP-PD2-	Moisture (%)	MVD (um)	D*max* (um)	AF (%)	SD*af* (%)	DDI
Hopper						
31.5MPa	0.11	28.7	90	3.03	1.64	0.016
63.0		98.6	210	4.29	4.00	0.077
94.5		101.7	250	3.49	2.25	0.060
126.0		230.2	570	6.55	7.24	0.365
157.5		387.5	835	8.06	11.14	1.381
157.5	22.8	567.2	1750	15.55	13.35	6.387
Vent						
31.5MPa	0.11	132.6	250	6.59	3.01	0.153
63.0		234.6	450	10.66	9.33	0.765
94.5		312.1	1250	14.24	6.11	2.008
126.0		402.7	1250	16.07	6.64	2.462
157.5		509.6	1500	19.46	11.14	5.003
157.5	22.8	901.8	2000	22.41	6.98	4.813

See **Nomenclature** for explanation of symbols and codes: Materials processed at standard settings, see Table 3.4.1: PP = polypropylene powder: PD2 = preconditioned Durcal 2: Filler pellets formed at 100°C to dispel residual moisture

Table 3.4.5 The effect of calcium carbonate characteristics and position of filler entry on the dispersion of pellets in polypropylene extrudate

PP-	MPS (um)	MVD (um)	D*max* (um)	AF (%)	SD*af* (%)	DDI
Hopper						
S13	0.7	226.3	570	12.30	10.13	0.958
HY	1.5	100.9	212	2.72	2.34	0.049
M	3.0	147.7	290	4.11	3.38	0.107
D2	3.0	187.9	370	10.47	6.78	0.562
OSL	3.0	40.1	114	2.85	2.02	0.019
Vent						
S13	0.7	461.4	1500	33.62	14.25	11.056
HY	1.5	151.4	530	12.50	7.23	0.695
M	3.0	331.8	570	18.15	14.93	2.084
D2	3.0	422.1	2000	11.17	5.17	1.766
OSL	3.0	122.8	450	6.32	3.27	0.181

See **Nomenclature** for explanation of symbols and codes: Materials processed at standard settings, see Table 3.4.1: PP = polypropylene powder: MPS = nominal mean particle size : Filler dried overnight at 100°C and pellets formed at 157.5MPa/ RT

Table 3.4.6 The effects of preconditioning temperature and position of filler entry on the dispersion of Durcal 2 pellets in polypropylene extrudate

PP-PD2-	Entry position	MVD (um)	D*max* (um)	AF (%)	SD*af* (%)	DDI
50°C	Hopper	90.0	210	1.52	1.20	0.014
100		232.2	490	6.06	10.31	0.481
150		253.3	570	4.04	4.06	0.126
200		291.5	835	15.51	11.84	2.825
250		559.4	1500	15.10	8.38	3.856
50°C	Vent	235.7	695	13.52	12.50	2.600
100		406.3	975	23.77	10.77	3.939
150		529.4	1500	21.06	10.17	4.943
200		672.3	1750	26.09	13.75	11.038
250		529.0	2000	22.97	13.22	9.343

See **Nomenclature** for explanation of symbols and codes: Materials processed at standard settings, see Table 3.4.1: PP = polypropylene powder: PD2 = preconditioned Durcal 2: Filler dried overnight at 100°C and pellets formed at 157.5MPa

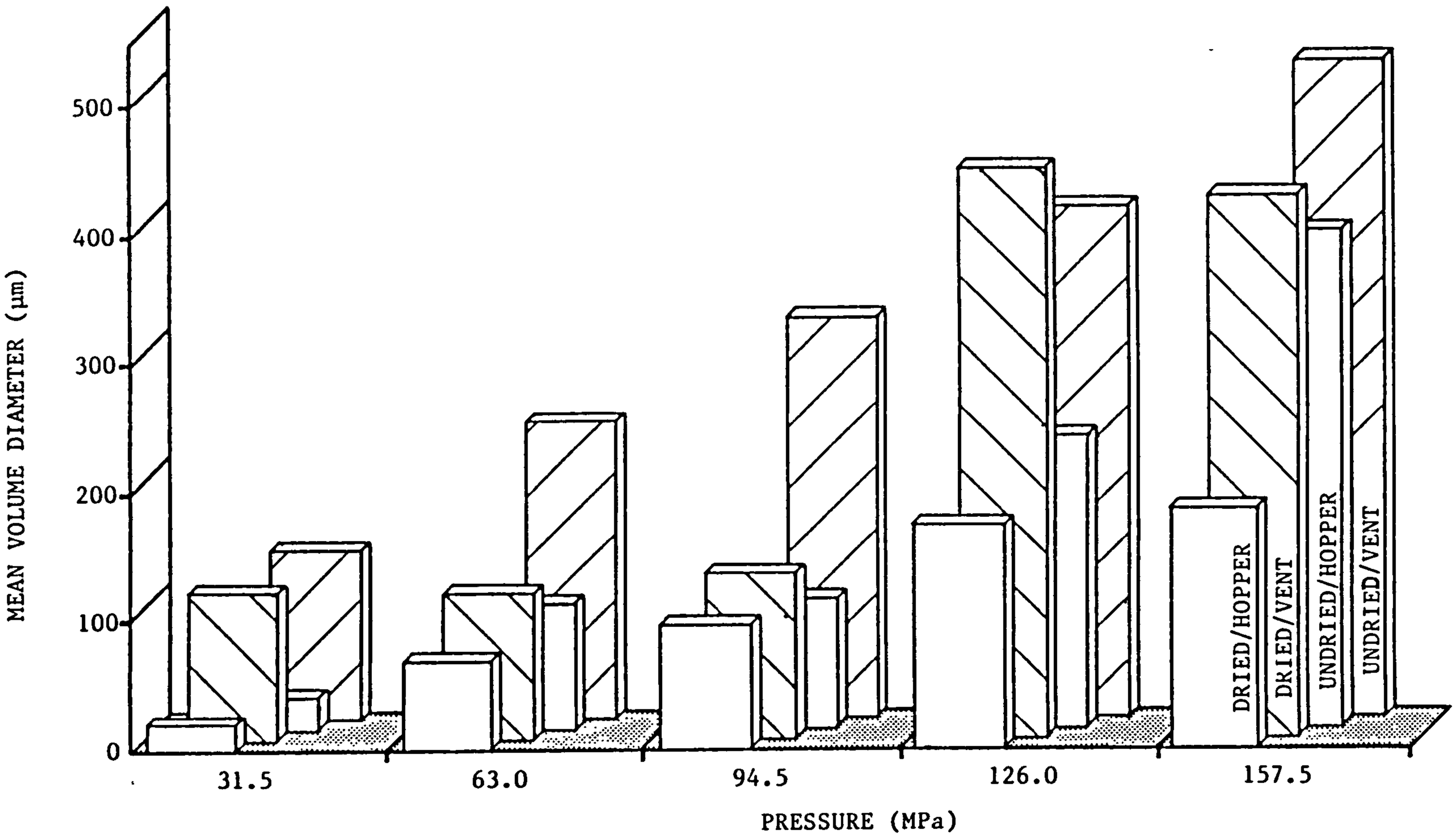

Fig. 3.4.1 The effects of preconditioning pressure, moisture content and position of filler entry on the dispersion of Durcal 2 pellets in polypropylene extrudate after processing at standard extruder settings (See Table 3.3.3)

Graph A

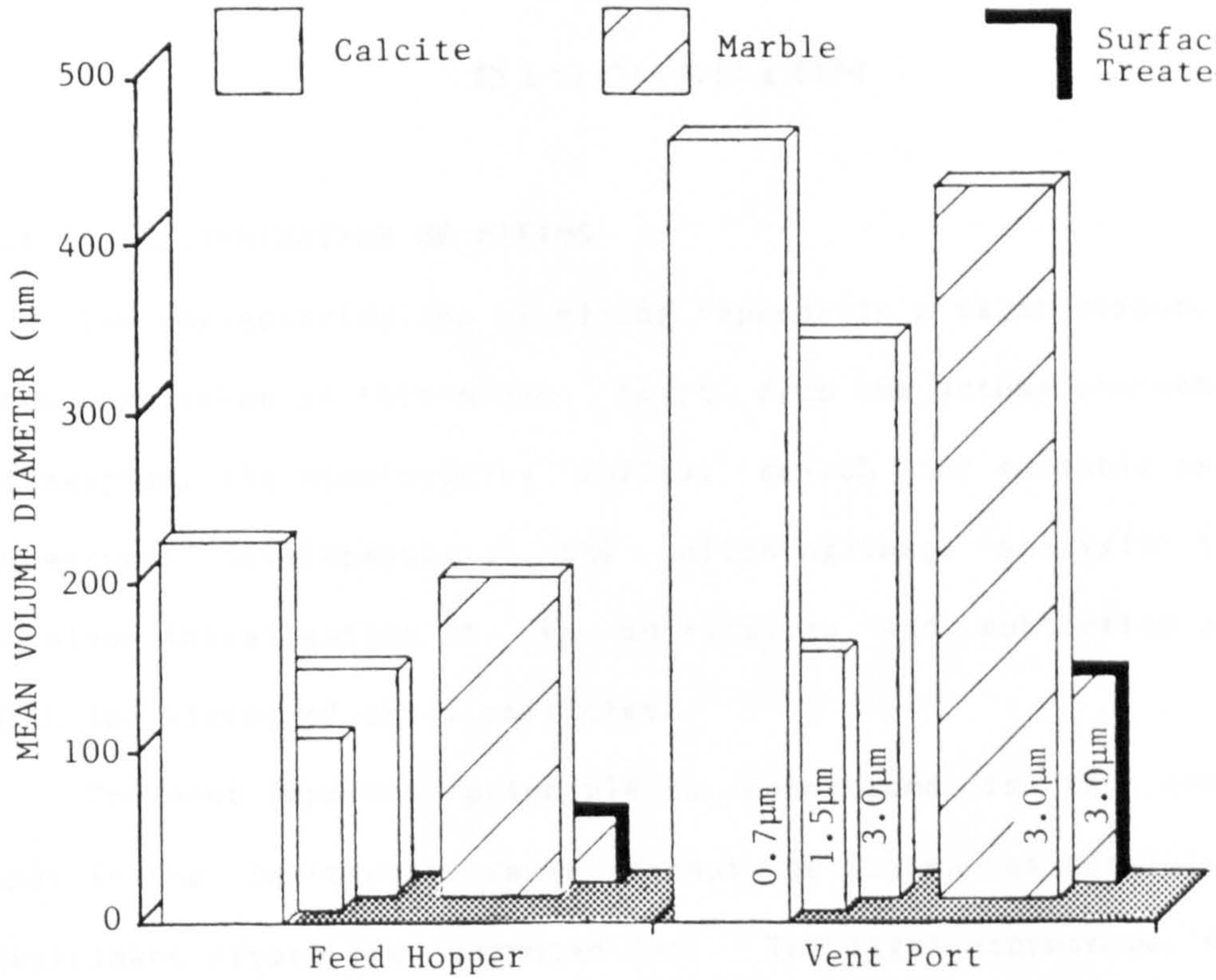

Graph B

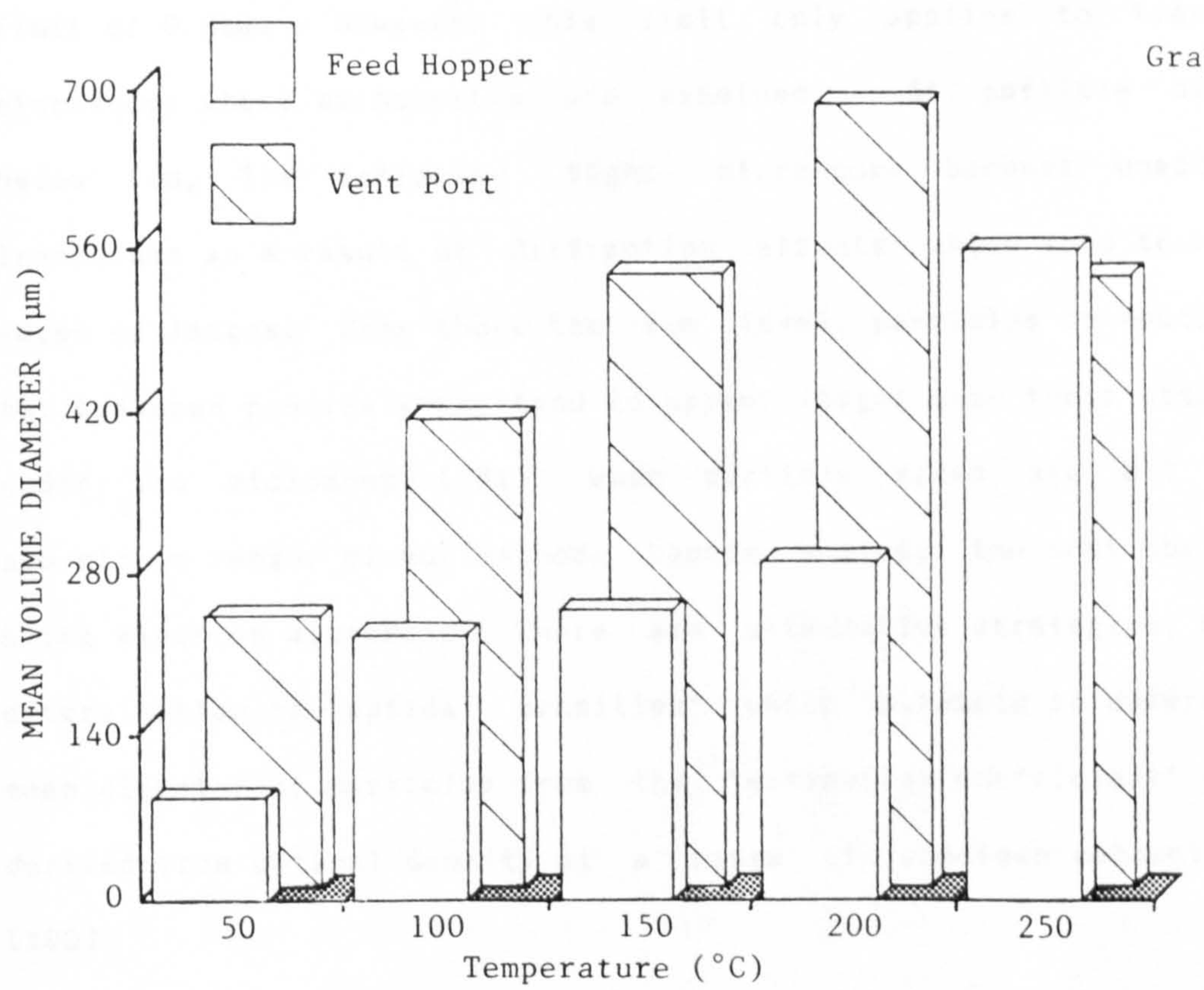

Fig. 3.4.2 The effects of calcium carbonate characteristics and position of filler entry (Graph A) and preconditioning temperature (Graph B) on the dispersion of Durcal 2 pellets in polypropylene extrudate after processing at standard extruder settings (Table 3.3.3)

CHAPTER 4

DISCUSSION

4.1 CHARACTERIZATION OF MIXING

The characterization of mixing represents a major component of the work undertaken in this study. Apart from the actual characterization of samples, the wide-ranging initial search for suitable methods and subsequent development of the polishing/image analysis techniques involved investigation of the intricacies and subtleties associated with the sizing of small particles.

The most important principle to understand is that measurements made in the low-micron range cannot be taken as absolute, even if experiment errors are accounted for. The light microscope, when using white light (0.6um), has a theoretical minimum quantifiable diameter limit of 0.8um. However, this limit only applies to transmitted microscopy where silhouettes are examined. At particle diameters below 5um, the reflected light microscope becomes unacceptably inaccurate as a result of diffraction effects which tend to blur the edges of images. Even above the 5um level, particles or sections are not measured precisely and tend to appear larger than their actual size under the microscope.[161] When particle sizes are all in the sub-micron range, direct methods become scarce; the most obvious one being electron microscopy. There are alternative strategies, viz. the determination of 'optical densities' which attempts to determine the mean diameter of particles from the 'extinction coefficient' which is derived from optical density at a range of specimen concentrations. [160]

This difficulty in directly measuring sub-5um sections using light

made the determination of section sizes for the nylon 6,6 specimens extremely laborious because a magnification of x810 had to be utilized. The resulting area of the circular detection field was of the order of 0.02sq-mm compared to the next lower magnification of x310 which had a detection field of 0.14sq-mm. Additionally, due to the diffraction effects the results will be subject to a wide margin of error. For these nylon 6,6 specimens it would have been more appropriate to examine them by scanning electron microscopy with the image analyzer camera directly attached. However, this set-up was not feasible for a limited study although it would be justified in situations where section diameters of this order were commonplace.

Alternatively, micrographs of the specimen surface could be produced from the scanning electron microscope VDU and these examined using the image analyzer camera with a light board illuminating the micrograph from below. Drawbacks of this technique are that it still requires significant differentials in contrast between matrix and particles for accurate image analysis, and the extra preparation procedures necessary to produce scanning electron micrographs represent a further increase in the total analysis time for each specimen. Figure 4.1.1 shows some scanning electron micrographs and their corresponding X-ray spectrum analysis images for Durcal 2, processed at standard extruder settings, of specimens taken from positions 1 to 5 along the extruder screws.

The image analyzer, as calibrated for the polypropylene matrix experiments, was arranged so that particles below 7.5um were not involved directly in particle size distribution calculations. Nonetheless, sections between 5 and 7.5um were counted to enable estimates to be made of the statistical inaccuracies which are related to the inverse of the square root of the number of sections measured. An average 4000 to 5000 particle sections were taken as a reasonable

compromise between statistical accuracy and the time involved in gathering this quantity of data from the specimen surface. Bearing in mind that the measure of dispersive mixing adopted was 'mean volume diameter' (MVD), which is suited to agglomeration measurements because it tends to emphasize the influence of large features, the effect of particles below 5um on volume statistics for the Schwartz-Saltykov analysis is considered negligible.

Fortunately, the usual method of determining size distributions of particles is to fit them in one of a range of size classes. As each particle need only be measured sufficiently accurately to fit it into one of these classes, it will be appreciated that measurement resolution is related to the number of size classes adopted. The higher the number of classes the more accurate will be their representation of the actual size distribution. However, as the number of size classes increases, the size of each incremental class becomes smaller and so the accuracy of measurement of the particles being studied must increase proportionately. It will be seen that these two requirements are contradictory and that another compromise must be made in order to balance these two opposing elements. For measurements made using the image analyzer in this study a fixed number of size classes was adopted so that as particle size distributions became larger the size of classes increased, offsetting additional errors of lower resolution for large particle sections at high magnifications found by Smith.[190]

The estimated experimental error calculated in Section 3.2.3.6 above relates to absolute determination of size by the image analyzer without considering the resolution of the microscope or the statistical error due to the number of particles counted, as discussed above. However, when size classes are used for distributions the error involved can be estimated with more confidence. For the 15 size

classes, a particle section will invariably be placed in either the correct size class or the one above or below this class and the error therefore is +/-3.33%

It will have been noted in a previous section that for semi-solid and powder specimens it was found necessary to press the material in a closed compression mould in order to facilitate subsequent polishing and analysis procedures. The pressure used in pressing was maintained at as low a setting as possible, while a high moulding temperature encouraged easy flow within the mould, so as not to influence filler dispersion. After pressing of the material into discs, the size of any voids still present fell below the sizing limit of the microscope/ image analyzer equipment.

On examining the specimen surfaces, after subsequent grinding and polishing of the specimen, it was often discovered that some aggregates within the agglomerates had been dislodged from the surface of agglomerates during the diamond polishing stage causing serious damage to the highly polished polymer surface on their departure. The resulting scratch lines made repolishing of specimen surfaces a regular occurrence. However, this phenomena resulted in the agglomerates on the polymer surface appearing under the microscope as very shallow pits similar to having been etched, which enhanced edge definition of the agglomerates.

When high levels of agglomeration were encountered during image analysis, it was established that the measurement of surface sections in excess of 590um, with the camera attached to the reflected light microscope, became problematic because these sections started to fill more than 25% of the circular detection area. Consequently, the number of sections decreased markedly so requiring a significant increase in the number of fields analyzed. In order to offset this phenomena, when sections of this magnitude were discovered on a specimen surface,

an additional analysis was undertaken which did not require the reflected light microscope. The camera of the image analyzer was fitted with a high aperture zoom lens which was able to satisfactorily resolve surface sections above 500*um*. Raw data results from the two sources were then merged into one raw section size distribution for statistical analysis to allow for the possibility of sectioning particles at a plane other than their largest area (Schwartz-Saltykov diameter analysis). Examples of some of the worst case views encountered for Durcal 2, processed at standard conditions, are shown in Figure 4.1.2 which also indicates the location along the extruder screws where each specimen was taken.

A complementary series of experiments were concerned with distributive mixing characterization as this is usually the final stage in any mixing process. The assessment of distributive mixing in polymer compositions has presented great difficulty, due largely to the lack of appropriate and reproducible experimental techniques.[199] Direct manual analysis of local mixture quality by microscopy demands considerable time and patience from the operator, and interpretation of the results is often highly subjective. This latter point is clearly illustrated in BS2782: Part 8 (Methods 823A and 823B) 1978 and BS2782: Part 11 (Method 1106A) 1983, concerned with methods for assessing pigment dispersion in polyethylene, and polyolefin pipes and fittings, respectively. These techniques require that thin sections of the specimen be examined by transmitted light at 100x magnification. The resulting image is then compared with a number of standardized micrographs, so that it may be graded for mixture quality. In the first-mentioned standard, the worst field of view for each specimen is also examined for streaks or smears and rated as better or worse that one standard photomicrograph, thus giving a very approximate measure of distributive mixing. Comparisons of mixture quality determined by the

BS2782 ratings with area fraction (AF) measurements, assigned using the Optomax image analyzer, were found to be generally consistent [200] so indicating that AF varies in a linear manner with mixing progression.

In the distributive mixing of two similar viscous liquids which undergo laminar flow, the degree of mixing can be assessed from either the total interfacial area between the components or, more commonly, from their striation thickness.[201] This approach has been adopted by many workers in order to quantify distributive mixture quality, often from direct measurement of the striation thickness of material streaks or flow patterns, using a graduated eyepiece fitted to a microscope. Ideally, an average value for striation thickness would be measured from a large number of fields of view of the specimen. However, the technical difficulties in obtaining meaningful results can be formidable, particularly in identifying the positions for striation thickness measurement in complex flow fields, and also when attempting to distinguish between mixtures of relatively equal uniformity at a specified sample magnification.

A semi-automatic approach, which has been applied to the measurement of striation thickness in pigmented polymers, involves the use of an optical microdensitometer.[163,199] A specimen prepared in the form of a thin film is mounted on a microdensitometer so that a finely focused light beam passes through it. By scanning the specimen in a direction normal to the light path, the intensity of the transmitted beam varies according to changes in optical density, determined by the position and thickness of the streaks across the width of the specimen. The resulting light transmission traces from the microdensitometer can then be analyzed to provide some average measure for striation thickness and hence a quantitative measure of mixture quality. A principal difficulty of this technique is that as mixing progresses, and the striation thickness decreases, the streak

width will approach a dimension of the same order as the beam size, so that the instrument is eventually unable to distinguish between pigmented and unpigmented regions. This limitation in resolving power can be partly overcome by using a finer scale of examination, i.e. by analyzing photographic negatives of the specimen which have been produced using a transmitted light microscope. An example of a microdensitometer trace determined from a specimen analyzed in this way is shown in Figure 4.1.3. Nevertheless, in spite of the magnification used (100x), problems arising from instrument resolution may still be apparent, adding to complications resulting from variations in microscope lighting across the specimen and density fluctuations originating from changes in the negative grain size.

Carbon black masterbatch was used, for these experiments, at a low concentration (0.5wt%) to allow easy visualization of glass-knife microtomed sections by transmitted light microscopy. This level of carbon black content has also been established as the most useful by Smith [190] who studied a range of concentrations from 0.25% to 3% and determined that samples containing 1% or more carbon black were difficult or impossible to evaluate using an image analyzer.

The image analysis of these carbon black specimens was again conducted directly via the camera without resort to micrographs; area and intercept parameters were selected as the most useful basis for calculation of mixing indices. Three indices were selected for subsequent feasibility studies: (a) area fraction; (b) standard deviation of area fraction; and (c) mean free path.

Mean free path is calculated from the following equation [194]:

$$MFP = (1 - AF) / N_L$$

where N_L = number of intercepts (N) per unit length

= N / circular frame area.

MFP is a quantity which represents the distance, in three dimensions,

which can be travelled through the specimen before encountering another feature of interest. However, MFP is a term intended to quantify particulate systems in three dimensions, whilst flow patterns (striations) tend to exhibit continuous lines in the plane of examination. Furthermore, as can be seen from the equation above, the calculation of MFP relies on N_l, which is a term dependent on orientation in non-particulate systems, and thus subject to unacceptable errors.

Therefore, flow lines (striations) were characterized by measuring their detected area as a fraction of the area of circular detection frame, 'area fraction' (AF) and the standard deviation of AF (SDaf). For these quantities to provide a measure of distributive mixing they must vary in direct relation to the progress of mixing. It is possible to utilize AF measurements of features in cross section to quantify distributive mixing of carbon black without recourse to allowances for sectioning errors because, unlike agglomerate particles, the flow lines (striations) will tend to be mostly two-dimensional. Thus, if flow lines are observed within the specimen section it is probable that this image is approximately similar, in terms of area fraction, at a plane slightly removed above or the below the original. Figure 4.1.4 shows typical fields of 0.5wt% carbon black in polypropylene for experiment PPG-CB-8P2D at sampling positions 1 to 6 along the extruder screws.

Theoretically, as particle sizes and flow lines get smaller their total surface area will remain similar or even increase [171] because laminar mixing is specifically intended as a means of increasing the magnitude of the polymer/filler interfacial area. However, this effect is not shown under the light microscope because as the level of laminar mixing progresses the sizes of these features drop below the resolution limit and effectively disappear from the area fraction value. This

phenomenon relates specifically to the concept of 'scale of scrutiny' [92,202] which Danckwerts [202] originally defined as 'the minimum size of the regions of segregation that would cause the mixture to be imperfect for the intended purpose' and expressed as either a length, an area, or a volume. In the case of measurement of agglomerate sizes and carbon black flow lines, this quantity will be expressed in terms of the 'image magnification' (IM) used during examination of the specimens by the light microscope. Necessarily, the magnitude of IM must be sufficient to identify imperfections in the mixture which will be of interest.

For calcium carbonate dispersions, the term 'agglomerate' will not apply to a particle until its diameter exceeds the 'top cut' value of the material specification because image analysis cannot distinguish between a large primary aggregate and an agglomerate composed of smaller aggregates. Therefore, the value of IM needs to be large enough to enable measurement of particles down to the top-cut value; in the case of Durcal 2 this is 10μm and IM values used were x310, x224 and x130. For carbon black distributions, the size of the flow lines of interest, for either aesthetic or UV protection, is more than adequately assessed at the IM value used for all the experiments (x330).

Area fraction can be said therefore to act as an effective measure of the mean level of distributive mixing and is equivalent to the 'scale of segregation' term introduced by Danckwerts [202] in that it is a measure of the magnitude of unmixed components in an imperfect mixture. Linear scale of segregation (S) is defined as the integral of the coefficient of correlation (R(r)) between concentrations at two points separated by a distance r:

$$S = \int_{\bullet}^{\infty} R(r)\, dr \qquad (4.1)$$

where $R(r) = \overline{(a_1 - \bar{a}).(a_2 - \bar{a})} \;/\; \overline{(a - \bar{a})^2}$ (4.2)

and a_1, a_2 & $\bar{a}$ are the actual concentrations of the component of interest at points *1* & *2* distance r apart and the mean concentration respectively.

As a measure of distributive mixing, the value of AF is high when striations are prominent and decreases in relation to flow line size. A specimen exhibiting ideal mixing, in which striations are all below the microscope resolution limit, would give an AF value of zero, assuming no pigment agglomerates existed. The last point is worth expanding upon because it will be appreciated that AF measures high contrast features which include agglomerates. However, analyzes which attempt to quantify only distributive mixing in the presence of agglomerates ignore the fact that deagglomeration must precede distribution. Where agglomerates are present, the value of AF represents a measure of the mean level of overall mixing (dispersive and distributive).

It will be noted that area fraction, AF, only measures the mean level of mixing; it does not indicate the variation in mixing between different areas of the composite material. The standard deviation of area fraction (SD*af*) does quantify the variation about a mean value of AF, measured from all the areas examined. The value of SD*af* is equivalent to the 'intensity of segregation' term conceived by Danckwerts [202] which can be defined simply as [203]:

$$I = S^2 / \sigma_o^2 \qquad (4.3)$$

where the intensity of segregation (I) is the ratio of the measured variance (S^2) divided by the variance of a completely segregated system (σ_o^2). The intensity of segregation therefore reflects the departure of the concentration in the various regions from the mean, but not the size of the regions [203], and will tend towards zero as the distribution of mixing becomes more uniform from field to field whilst

remaining a function of 'scale of scrutiny' (IM in these experiments).

Nevertheless, the value of SD*af* when postulated as an independent measure of distributive mixing, fails in one critical respect, i.e. distributive mixing may be consistently bad throughout a specimen and give rise to a relatively low value of SD*af*, but a similar value could result from better overall distributive mixing exhibiting the same area-to-area variation. In other words, SD*af* is a function of both AF and IM, so if SD*af* is related to these two parameters in a single mathematical index the above scenario is negated.

The product of AF and SD*af* combines the mean value of mixing and the distribution about the mean to provide a measure of both the dispersive and distributive mixing. In order that specimens examined at different magnifications can be compared, the product of AF and SD*af* is divided by image magnification (IM) and can be expressed as:

$$DDI = [AF(\%) \times SDaf(\%)] / IM \qquad (4.4)$$

where DDI stands for 'Dispersion and Distribution Index'. This index remains a function of concentration of filler present in any specimen because AF will definitely increase with increasing concentration but not necessarily in a linear manner. Therefore, the author considers that the DDI quantity should only be utilized to compare specimens of the same filler concentration as opposed to others who have defined an 'Agglomeration Index' [204]:

$$AI(\%) = AF(\%) / \text{Pigment Volume Concentration} \qquad (4.5)$$

with the implied intention of allowing comparisons of mixture quality at different pigment concentrations.

Values of DDI have also been calculated for the calcium carbonate filled compounds and are shown in each results table. In these cases, AF is measuring the level of agglomeration from the sections of agglomerates visible at a random plane through the sample; SD*af* is measuring the distribution of section areas from field to field. Of

course, these sections do not represent the true particle size distribution because of sectioning errors and the AF values are not corrected. However, if all that is required is a approximate comparison between different samples, say for quality control purposes, then this method is of use, especially as cumulative values can be displayed on the computer VDU in real-time. For measurements made on images that are projected from the actual particle diameters there will be no sectioning errors and DDI would be as relevant as it is in the measurement of distributive mixing.

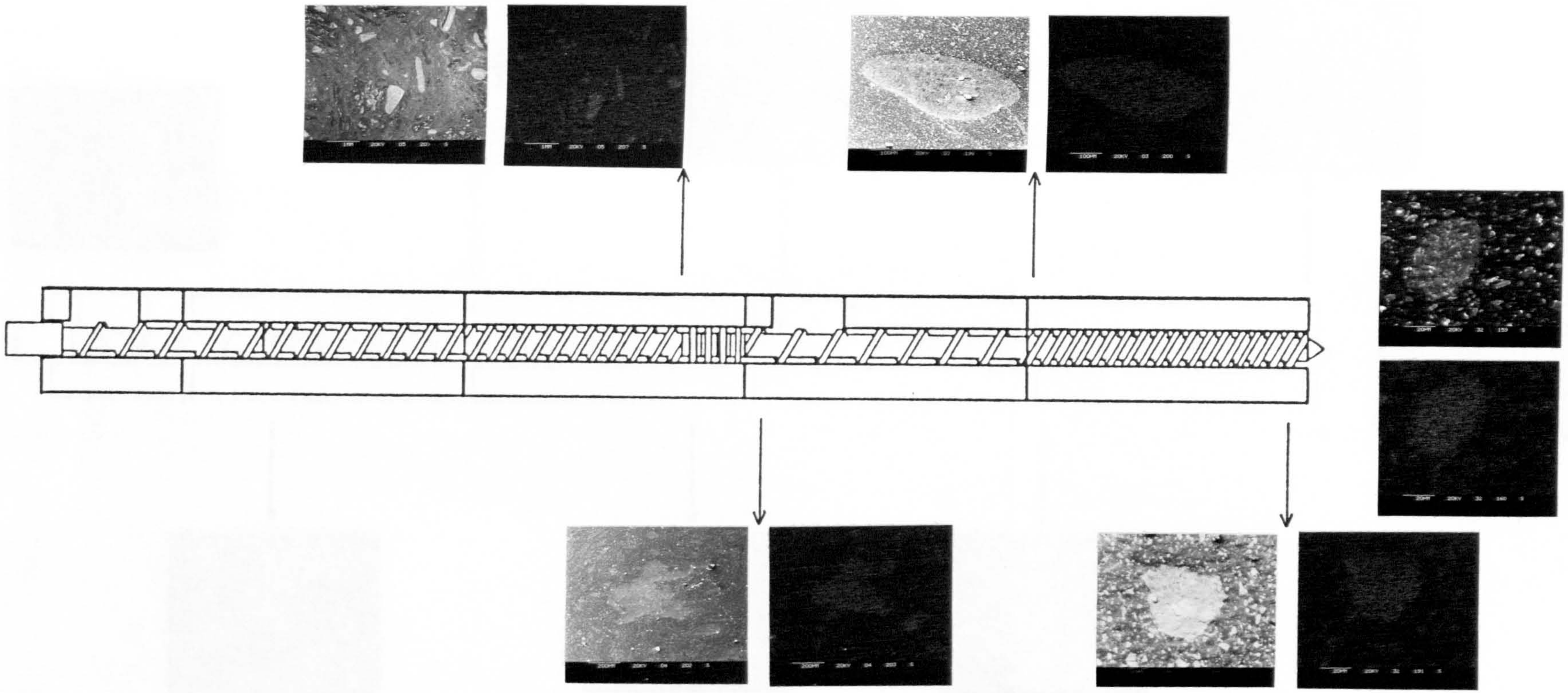

Fig.4.1.1 SEM and X-ray micrographs of PP/Durcal 2 samples, processed at standard extruder settings, taken from positions 1 to 5 (See Table 3.3.4 PP-D2)

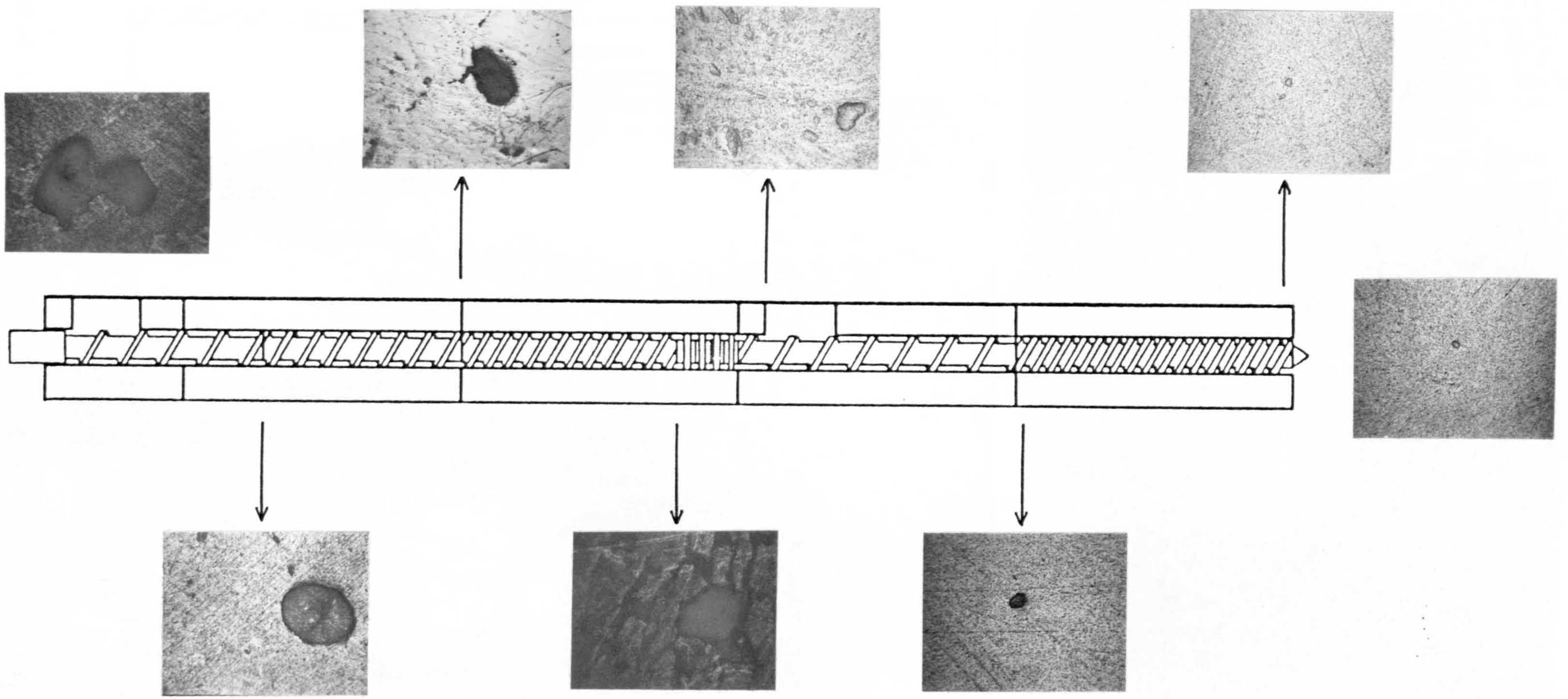

Fig.4.1.2 Reflected light micrographs showing some of the worst case views encountered for PP/Durcal 2 samples, processed at standard settings, taken from positions 1 to 8 (See Table 3.3.4 and Fig.3.3.3)

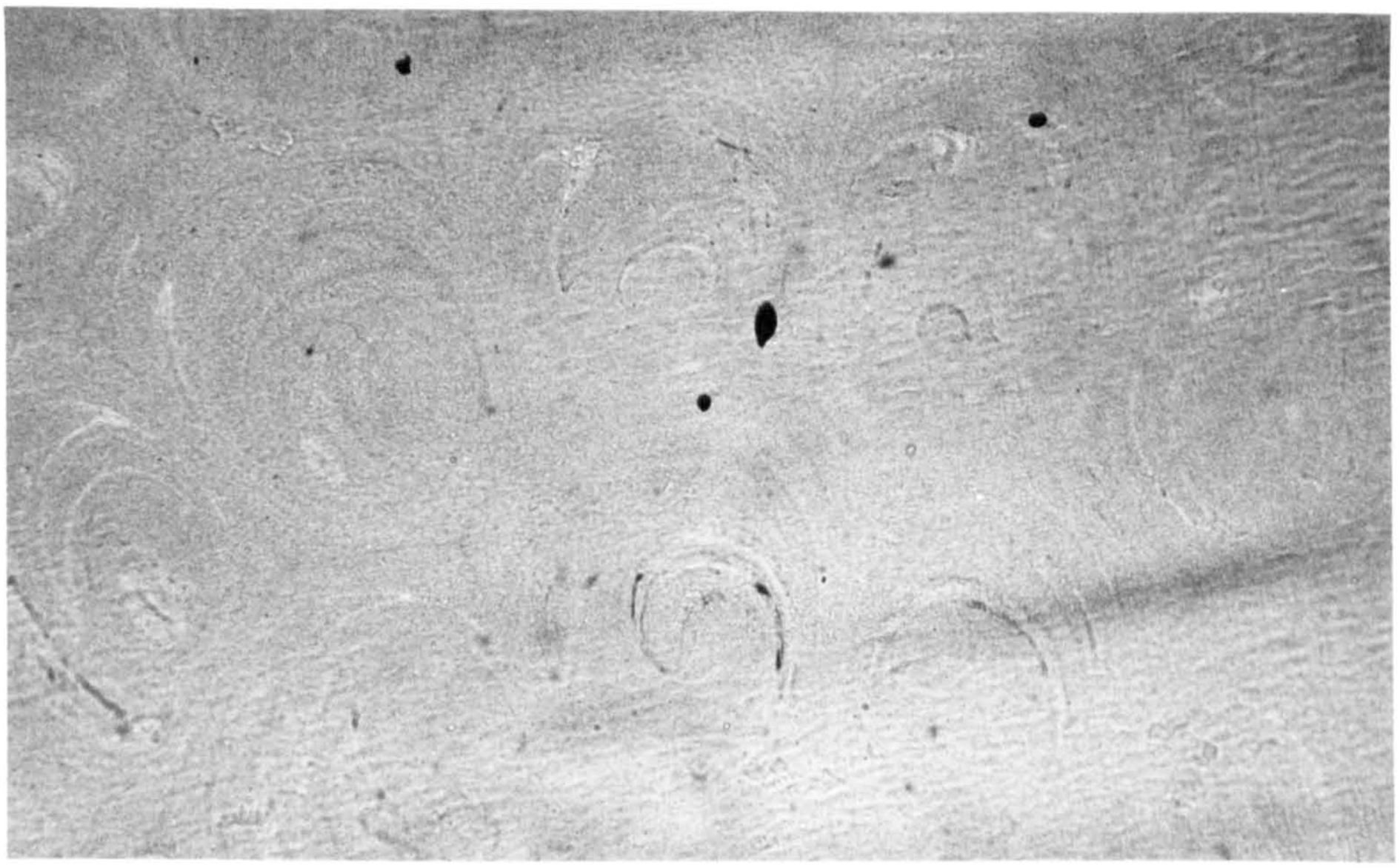

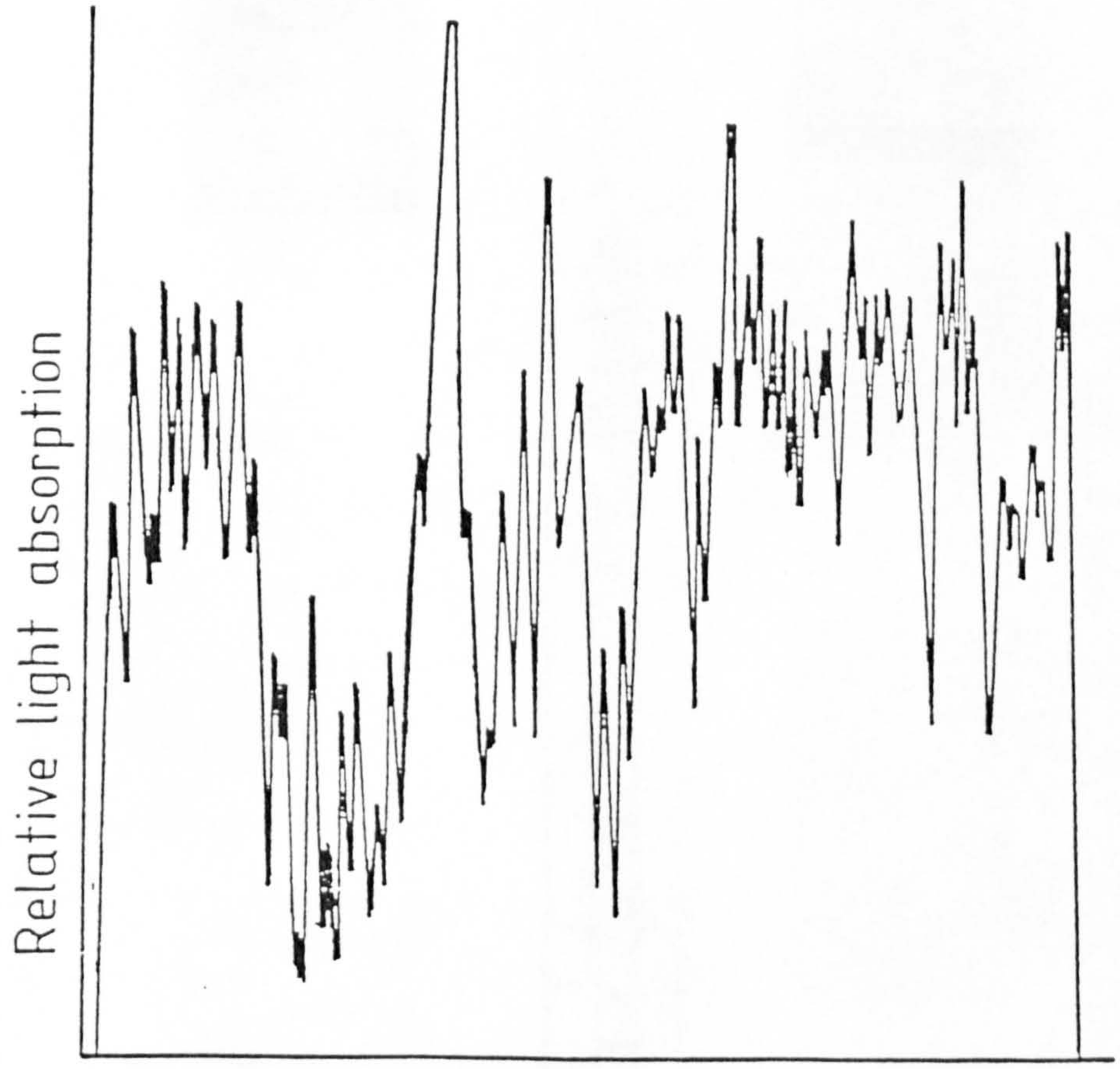

Fig.4.1.3 Optical microdensitometer trace from negative of micrograph shown above (PPG-CB-BP-120 in Table 3.3.15)

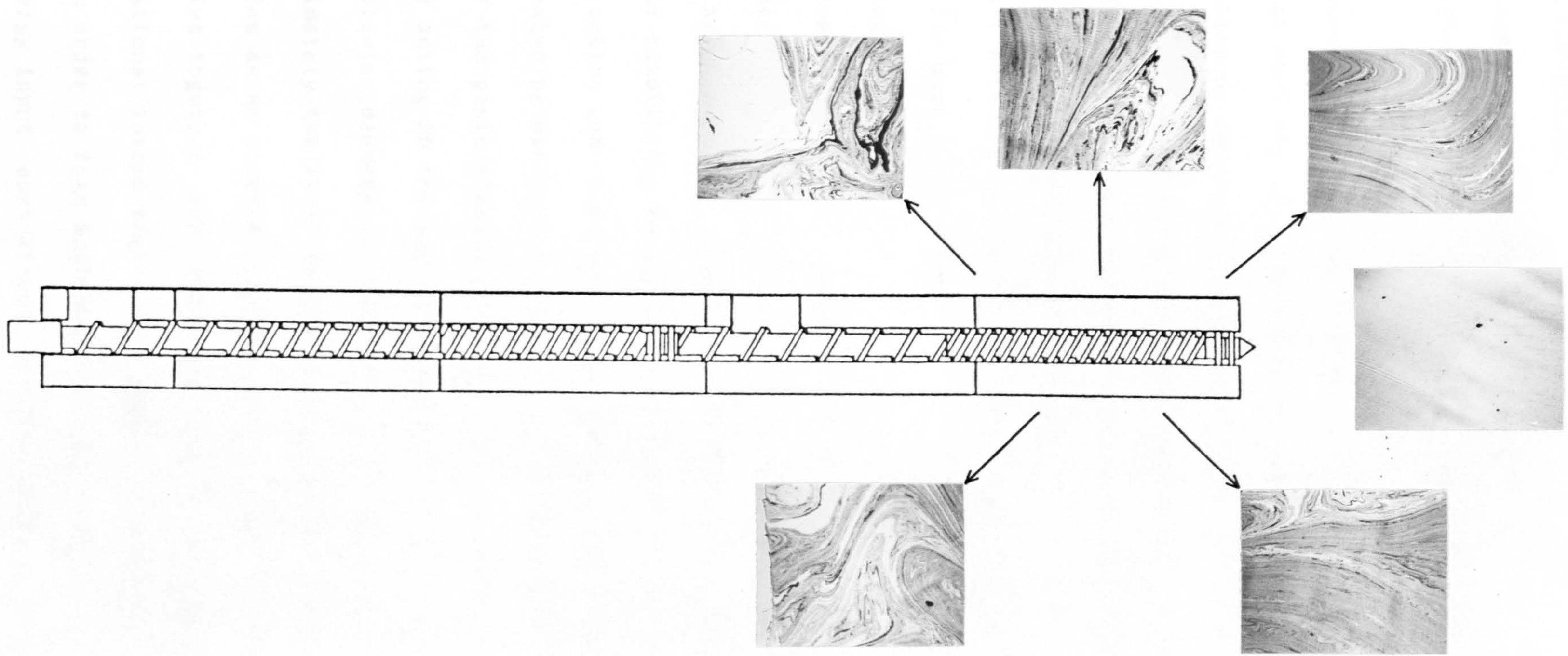

Fig.4.1.4 Transmitted light micrographs showing typical fields for 0.5wt% carbon black in polypropylene, processed using 8mm + 2D metering section, taken from sampling positions 1 to 6 (See Table 3.3.18 and Fig.3.3.19)

4.2 AGGLOMERATION

4.2.1 Agglomerate Formation and Strength

Agglomeration is said to occur when aggregates become associated because of binding forces within relatively loosely-bonded agglomerates. In the case of pigments, primary-particle aggregates are formed at much higher compaction stress levels during the course of preparation or subsequent processing due to surface forces, particle growth, or even sintering and these aggregates are relatively immune to regular polymer processing machinery. The so-called ultimate primary particle size, defined as the smallest particulate piece of the minor component existing in the system, may range from a few hundredths of a micron for most organic pigments up to 1um or more for some inorganic variants.[205]

Fine particulate powders have a tendency to agglomerate spontaneously in order to reduce both surface area and surface energy, whilst also settling under the influence of gravity. Without a physical stabilizing force, the particles will converge until a balance of attraction and repulsion is reached, but agglomeration will be accelerated by exterior forces such as vibration or compaction. [206]

As inorganic powders decrease in particle size, the force of gravity acting on the particles declines rapidly (by the third power of the particle diameter), while natural adhesion forces increase by approximately the first or second power of diameter. When taking 1um particles as an example, van der Waals' adhesion forces attracting the particles together are some six orders of magnitude larger than gravitational forces trying to separate them.[207]

In order to form aggregates or agglomerates of inorganic powders, the energy input must exceed a value which will result in one of a

number of localized bonding phenomena:

(*i*) Mechanical bonding

(*ii*) Electrostatic

(*iii*) Van Der Waals

(*iv*) Liquid bridges

(*v*) Solid bridges

These mechanisms of bonding are categorized in terms of increasing resultant bonding strength although the initial bonding energy input may not be related proportionately. For example, chemical reactions on the pigment surface which form solid bridges may require little, if any, mechanical energy input apart from surface moisture or contaminants. However, the bonds formed will be the most difficult to dissociate during polymer processing.

4.2.1.1 Mechanical bonding

Mechanical bonding or interlocking of the calcium carbonate particles, which are very approximately spherical, is unlikely to be of significance as these forces will be very weak. Bonding of this type is more effective when dealing with particles that have surface roughness, or those which are fibrous or plate-like.

4.2.1.2 Electrostatic bonding

Electrostatic forces originate from accumulated charges generated, for example, by repeated impact between adjacent surfaces and these forces tend to be greater in conducting rather than non-conducting materials. The adhesion force (F) between two conducting spheres of radius (R) is given by

$$F = \varepsilon \cdot \varepsilon_{\circ} \cdot U^{2} \cdot R / 2a_{\circ} \qquad (4.6)$$

where ε = dielectric constant of the gas

$\varepsilon_{\circ}$ = absolute dielectric constant of vacuum

a_o = distance between the two surfaces in contact (e.g. 0.5nm)

U = contact potential difference (0 to 0.5V depending on materials)

In non-conductors, ,the charge may extend into the particle surface to a depth of up to 1um; conductors only retain this charge in several layers of surface molecules.[207]

4.2.1.3 Van der Waals' forces

The van der Waals' forces which originate from fluctuating dipoles existing in materials are one order of magnitude greater than electrostatic adhesion forces between conductors arising from contact potential.

For spherical bodies of radii (R), the van der Waals' adhesion force (F) is inversely proportional to the square of the distance (a) between their surfaces:

$$F = (h\bar{w} \cdot R) / (16\pi \cdot a^2) \qquad (4.7)$$

where $h\bar{w}$ is the Lifshitz-van der Waals' constant, which varies between 1eV and 10eV depending on the materials in contact and where distance (a) is of the order of 0.5nm.

4.2.1.4 Liquid-bridge forces

Liquid-bridge forces are generally about four times larger than the van der Waals' forces and will occur in moist agglomerates at a level dependent on the degree of liquid saturation in the total pore volume of the agglomerate. These forces are discussed in connection with the preconditioning of filler experiments in Section 4.2.4 below.

4.2.1.5 Solid bridges

Solid bridges can be formed between particles on crystallizing from solution or by sintering, resulting in extremely strong

interactive forces. For particles bonded by crystallized salt, the strength of the agglomerate is dependent on the conditions present when drying occurred. For solid bridges, the first stage of sintering is of interest because these will serve to strengthen adhesion forces between particles. Welding of point contacts results from localized heating during compaction.[208] An example of this phenomena is the case where a low melting point material is stored in quantity for a period of time after which it is found that particle adhesion has occurred at the lower levels of the container.[207] Again, a more detailed appraisal of these forces is undertaken in Section 4.2.4 below.

4.2.2 Influence of Premixing on Filler Agglomeration

Premixing of a particulate filler with solid particles of polymer is a common precursor to the processing of polymer compounds, as previously mentioned. However, it has been found that this stage of processing can create agglomerates rather than disrupting them and that these highly-impacted agglomerates are transferred to the melt processing stage.[170,206]

Examination of the mixing chamber of the Henschel high-speed mixer after the prescribed mixing period had elapsed revealed that premix material had compacted onto the mixer blades and, to a lesser extent, onto the inner casing. This compacted material was sampled for each of the seven different calcium carbonates considered and ashed in a furnace as detailed in Section 3.2.1.1.1 above. The levels of calcium carbonate found in these samples were surprisingly high, see Table 4.2.1.

The powders having the finer initial mean particle size, Table 3.3.1, exhibited the higher levels of compaction. Further, ashing of the premix before use for processing showed that the nominal 40wt% calcium carbonate content had been reduced by up to 4% in one case,

Setacarb 13; the missing material presumably having remained adhered to the inside of the mixer. Image analysis of the material from the mixer blades (Durcal 2) revealed a level of agglomeration higher than both the initial raw powder samples and the premix as supplied to the extruder, Table 3.3.2.

4.2.3 Effect of Solid 'Dry' Processing

During the initial period when the calcium carbonate/polymer materials have just entered the extruder, the possibility of further agglomeration is present. It would occur before the polymer has softened, as a result of the material being compressed between a number of combinations of hard surfaces, viz. polymer/polymer, polymer/mixer or metal/metal.[206] This solid 'dry' processing stage will vary in extent according to the machine variables being employed. The length of the screws covered by this phase is related to factors controlling speed of melting; these factors include levels of shear and, particularly for twin-screw extruders, the extent of barrel jacket heating.

When the filler/polymer powder enters the extruder through the hopper it encounters a hot stationary barrel wall and two cooler rotating screw surfaces. In these first few moments, the coefficient of friction will be equivalent to that predicted by conventional solid friction theory which depends on normal pressure and the relative speed of two slipping surfaces; at the surface velocities encountered in twin-screw extruders the effect of screw speed is negligible.[31,49] During this short period it is very probable that filler agglomeration will occur and that this compaction may extend into the initial stages of melting with the polymer film acting as a highly viscous liquid binder. Figure 3.3.12 indicates that this prediction actually correlates to dispersion levels within the extruder when the filler is

fed separately from the polymer (i.e. there is no premixing stage). The area of melting when utilizing both hopper and vent port sourced filler, Figures 3.3.10 and 3.3.11, acts as the delineator between agglomeration and dispersion characteristics. The vent port feeding of filler naturally results in a much higher agglomeration level in the final extrudate but it exhibits a dispersion profile which follows those incorporating segmented discs. This initial agglomeration trend is much less apparent when the machine is fed with premixed material particularly when operated at medium to high screw speeds, Figures 3.3.3 and 3.3.5. The possibility arises that the premixing of filler with polymer does serve to intermingle the particles to good effect, in the initial stages of extrusion, even if the price is a higher agglomeration value in the extrudate.

4.2.4 Filler Preconditioning Parameters

Agglomerate formation by powder compaction has been well studied and comprises two related mechanisms: rearrangement of particles by sliding over one another to produce a close-packed structure, and development of enhanced interparticle adhesion forces.[208] As confirmed in connection with the premixing experiments above, densification through particle rearrangement depends to a large degree on initial particle size. The more finely divided the powder, the lower its bulk density and the greater the opportunity for rearrangement. On deformation, the particles are pushed closer together providing a stronger, more coherent structure. Voids between surrounding particles can be filled by deformation (elastic or plastic) or by fragmentation mechanisms; contingent upon the physical characteristics of the material under compaction, in addition to the magnitude and speed of application of the compressing forces. If plastic deformation occurs at the point of contact between two

particles, both the surface area of contact and van der Waals' adhesion force may increase creating substantially greater interparticle attraction. [207]

Tadmor and Gogos [203] state that in polymer processing, particulate solids are compacted prior to melting inside most processing machinery and the performance of these machines is greatly influenced by the compaction behaviour of the solids. Compaction of the filler powder in an idealized cylindrical mould utilizing a normal force (F_o) at the top ram will generate a certain normal stress as well as a radial stress. Therefore, a portion of the applied force is transferred into a residual radial stress which will lessen the force (F_1) transmitted to the bottom of the mould. Assuming that the wall friction is fully mobilized, the ratio of axial/radial stresses and the coefficient of friction at the wall are constant; the ratio of applied to transmitted force is:

$$F_o / F_1 = \exp (4f'_w . K . L) / D) \qquad (4.8)$$

where f'_w = coefficient of friction of the wall

K = ratio of radial to axial stresses; independent of location

L = initial length of mould

D = diameter of mould

During controlled experiments, when irregularly shaped limestone particles were subjected to an increasing centrifugal compression force, the interparticle adhesion was shown to increase due to particle rearrangement and greater surface contact.[207]

The role played by water in agglomerate formation has received considerable attention.[207,209] The tensile strength of moist agglomerates formed into pellets can be determined from the amount of liquid saturation (S) which is defined as the ratio of pore volume occupied by the liquid to the total pore volume of the pellet. In studies with moist limestone particles, measured and calculated values

of agglomerate tensile strength have been related to liquid saturation. In the capillary state, when liquid saturation is greater than 0.8 (i.e. more than 80% of the void space between the particles is filled with water), the agglomerate is held together by outer pressure because a capillary suction pressure (P*k*) is formed in the liquid space. The theoretical tensile strength of the agglomerate (σ_t) is then given by:

$$\sigma_t = Pk \,.\, S \qquad (4.9)$$

Of greater relevance to the present discussion is the situation for moist agglomerates having less than 30% of the void spaces filled with water (0 > S > 0.3). In this liquid-bridge (pendular) state, a theoretical tensile strength can be calculated from the mean value of the number of contact points multiplied by the adhesion force component in the tensile strength direction:

$$\sigma_t = (1 - \varepsilon / c) \,.\, (F^* / x^2) \qquad (4.10)$$

where ε = porosity

x = mean particle diameter

F^* = mean adhesion force transmitted at a contact point, given by:

$$F^* = Fh \,.\, \gamma \,.\, x \qquad (4.11)$$

where γ = surface tension of the liquid

Fh = a dimensionless adhesion number.

Results for calcium carbonate particles show that maximum agglomeration tensile strength in the liquid-bridge state is nearly three times less than that formed by a capillary liquid mechanism. However, compared to 'dry' limestone agglomerates (i.e. dried and then conditioned at 55% relative humidity (20°C)), liquid-bridge forces (S=0.25) increased the maximum agglomerate tensile strength threefold. [209]

Table 4.2.1 Ashing results for specimens taken from the mixer blades for the 7 different calcium carbonates

Trade Name	Geological Origin	Mean particle size (um)	Surface treatment	Mixer Blades (wt% CC)
Hakuenka CCR	Precipitated	0.08	Yes(CS)	79.7
Setacarb 13	Calcite (Urgonian)	0.70	No	93.1
Hydrocarb	Crystalline calcite (Urgonian)	1.50	No	73.9
Hydrocarb 95T	Crystalline calcite (Urgonian)	1.50	Yes(PT)	66.8
Millicarb	Crystalline calcite (Urgonian)	3.00	No	65.5
Durcal 2	Marble (Metamorphic)	3.00	No	73.6
Omyalene SL	Marble (Metamorphic)	3.00	Yes(PT)	63.1

CC = calcium carbonate; CS = calcium stearate; PT = proprietary treatment

4.3 MELTING AND WETTING

It is significant that dispersion of filler does not occur in a uniform, progressive manner along the machine but increases markedly through the region just prior to and including the segmented elements, located midway along the extruder. Observations on material extracted from the screws, after shock cooling and subsequent removal of the barrel, indicates that this region coincides with the melting zone for the polymer. Hence, there is a strong correlation between fusion of the polymer and maximum rate of dispersion of the calcium carbonate filler (for example see Figures 3.3.3 to 3.3.5).

Melting in the compounder occurs over a relatively narrow region of the screws, undoubtedly influenced by the fact that for much of the first stage the screws are only partially filled with polymer. When the screws are filled, the shear rate developed is [82]:

$$\dot{\gamma} = (\pi . D_e . n) / h \qquad (4.12)$$

where n = screw speed

h = channel depth

D_e = equivalent diameter of screws and is given by:

$$2 / \pi . (\pi D - \sqrt{2 D h}) = 2D - 0.9003 \sqrt{D h} \qquad (4.13)$$

where D = external diameter of the screws.

Additionally, there is considerable mechanical energy input during passage of material through the segmented discs, which act as partial barriers to flow, as evidenced by the considerable overheating that occurred in zone 2 of the machine before barrel cooling was implemented. It is probable that the observed increase in dispersion rate results from the greater shear stresses imposed on filler at the interface between molten polymer and compacted feedstock combined with the substantial localized shearing that will occur through the segmented discs. Mechanical shear heating will be further enhanced at

the area of melting due to the coefficient of friction between the polymer and other surfaces increasing in magnitude as a function of the process temperature; reaching a peak at the polymer melting point.[31] Above the polymer melting point, the polymer/metal restraining behaviour will be governed by viscous drag, which will give rise to melt shearing, and diminishes as the process temperature rises.

A high barrel temperature profile (each zone increased by 20°C from the normal settings) resulted in the area of melting, observed after the barrel was withdrawn, having been displaced nearer to the hopper end of the machine. This phenomena would be predicted but of interest is the corresponding movement of the area of maximum rate of dispersion. In this example, the segmented discs have played only a minor role in the overall reduction of filler agglomeration; a reduction of the viscous shear developed in the lower viscosity melt is the probable cause.

Examination of samples extracted from the extruder after processing at a low barrel temperature (20°C below normal in each zone) revealed that the onset of melting had again been accelerated. The measured throughput, after achieving steady state extrusion, was found to be approximately 23% lower than that obtained for the normal temperature profile. The increased restriction to the flow presented by the segmented discs in this situation may explain the reduction, taking into account that the process material had received a lower thermal energy input. In order that material could pass the discs, the necessary melting energy would have to be provided mechanically by the screws; a situation necessitating a greater pressure build-up which, in turn, will only be achieved by back-up of compacted material along the machine.

Calcium carbonate filler added to the molten polymer, via the downstream entry port, bypasses this zone of high mechanical energy

input and consequently the ultimate filler agglomeration in the compound is greatly increased (Figure 3.3.11).

Evidence to support the important role of the melting process in polymer mixing has been reported in relation to flow through single-screw extruders.[199] It was shown that less laminar shear mixing is evident in the metering zone where the polymer is fully fused than in the melting zone where a combination of solid bed and melt pool exists. Shearing occurring within the melt film, which links the movement of polymer from the solid bed to the melt pool at the rear of the channel, was considered to be of particular importance.

Once the polymer has been thoroughly melted, the resulting melt must be able to wet the filler particles as completely as possible. The main driving force which causes spreading is defined as [210]:

$$F = \gamma_{SV} - \gamma_{SL} - \gamma_{LV} \cos\theta_d \qquad (4.14)$$

where γ_{SL} = surface tension of polymer on filler

γ_{SV} = surface tension of filler/ vapour interface

γ_{LV} = surface tension of polymer/ vapour interface

θ_d = the dynamic contact angle.

When spreading ceases, F = 0 and [210]:

$$\gamma_{SV} - \gamma_{SL} = \gamma_{LV} \cos\theta_s \qquad (4.15)$$

where θ_s = the static contact angle achieved after prolonged contact times. When θ_s is considered to be the contact angle at equilibrium on plane solid surfaces, Eqn.4.15 is known as Young's equation. Substituting eqn.4.15 into eqn.4.14 gives [210]:

$$F = \gamma_{LV} (\cos\theta_s - \cos\theta_d) \qquad (4.16)$$

where F = the effective surface driving force for spreading.

Initial wetting requires that the pigment and polymer be sufficiently well mixed so that no separation occurs when shearing takes place during mixing. This stage often controls the whole process of mixing and can affect the final mixture quality as a

consequence.[211] After dispersion of the filler agglomerates, the polymer should envelop all the new smaller particles and replace any air at their surfaces.

A plastics ability to wet-up pigments is partially dependent on the presence of polar groups on the surface of a polymer. Therefore, polar polymers, such as polyesters and polyamides, will produce better dispersions than non-polar polyolefins.[205] The levels of dispersion measured in the nylon extrudate experiments (Table 3.3.6/Figure 3.3.2) confirm this contention by exhibiting values nearly a third lower than corresponding polypropylene matrices.

Alternatively, the value of surface tension for the polymer/filler interface can be reduced by coating with a surfactant which has an affinity for the particular polymer. This lowers the filler surface energy and enables the polymer to displace the vapour (air) from the filler surface because the force balance will be altered in its favour. However, coating of the filler surface prior to polymer processing introduces another variable, viz. the coated versions of the calcium carbonates employed for this study (Table 3.4.3) exhibited sharply higher levels of surface moisture than uncoated equivalents.

4.4 DISPERSION

Dispersive mixing in polymer processing operations involves the breakdown of agglomerates or clumps of solid particles in a deforming viscous liquid; three principal stages generally being embodied within this mechanism.[205,212]

Firstly, wetting of the particulate component by the polymer melt is required and is clearly aided if the compatibility between the solid and liquid phases is high or if it is increased by modifications to the surface characteristics of the components.

Secondly, rupture of aggregates or agglomerates is accomplished by exposing the mixture to high stress zones in the processing apparatus. When the induced internal stresses that result from viscous drag on the particles exceed some critical value, agglomerate breakdown will ensue.

Finally, intimate wetting of the particles should occur by replacement of air at the filler-melt interface, but this may become increasingly difficult with solid particles of high surface area, which may also be porous. Overlap between these three stages of dispersion is probable.

In any compounding operation, such as twin-screw extrusion, an essential requirement for effective dispersive mixing is the generation of stresses sufficient to exceed the important critical threshold value. Additionally, in order to achieve uniformity, it is important that all fluid elements should repeatedly pass the high stress zone. It is possible to accomplish these requirements through judicious design of machinery. The rheological characteristics of the deforming liquid phase and degree of cohesion between particles also have an important influence on the extent of dispersion.

An analysis of forces required to break apart agglomerates can be made by considering a single agglomerate, in the form of a rigid

dumbbell, consisting of two beads of unequal radii (r_1 and r_2) connected together and placed in a homogeneous velocity field of an incompressible Newtonian fluid.[203] The force, developed in the connector, tending to separate the beads depends on the dumbbell orientation and the extent of viscous drag from the surrounding fluid.

If the two beads are in contact with one another, the maximum separating force (F*max*) is obtained when the dumbbell orientation is 45° to the direction of shear whilst being proportional to the shear stress ($\mu\dot{\gamma}$) and the product of $r_1 . r_2$:

$$Fmax = 3\pi . \mu . \dot{\gamma} . r_1 . r_2 \qquad (4.17)$$

where μ = melt velocity

$\dot{\gamma}$ = shear rate

The maximum separating force in an elongational flow field occurs when the dumbbell is aligned in the direction of flow according to:

$$Fmax = 6\pi . \mu . \dot{\varepsilon} . r_1 . r_2 \qquad (4.18)$$

where $\dot{\varepsilon}$ = rate of elongation.

Equations 4.16 and 4.17 implicitly assume that the spheres will not affect the flow field and that the dumbbell interaction can be neglected.[50] Nevertheless, the inference from this analysis, is that less force is required to break apart combinations of larger beads than smaller ones and that dispersive mixing is enhanced under conditions of high shear stress or increasing rates of elongational flow. Although at equivalent deformation rates the separating force developed between the beads in elongation flow is double that obtained in shear flow, in reality it is generally easier to generate much larger shear rates; consequently, this form of flow is usually the predominating mechanism for dispersion.

4.4.1 Material and Processing Variables

Most experiments were undertaken using the two-stage screw

geometry shown at the top in Figure 3.1.5. Unless otherwise indicated, the screw pitch in the metering zone was 8mm, although in some experiments this was changed to 12 and 16mm. Alternatively, two pairs of the segmented mixing discs were introduced into the end of the metering zone (bottom screw in Figure 3.1.5).

Changes in screw geometry within the second stage metering zone appear to have little influence on mean volume diameter for the screw geometries (Figures 3.1.2 and 3.1.5) and material compositions under investigation. Observed differences are shown in Figure 3.3.13, with expanded ordinate axis, but these are small and not considered significant. Similarly, the adoption of a fifth barrel section and extended screws (Figure 3.1.2) did not result in any substantial improvement in final dispersion of the filler (Table 3.3.12). Size reduction will only occur during dispersive mixing operations when the shear stresses developed in the polymer exceed some critical value, this being higher than the interparticle agglomerate forces. Dispersion therefore becomes more difficult as particle size decreases and agglomerate strength increases. At some point, a limiting level of dispersion may be reached, dependent both on the conditions of maximum shear experienced in the machine and the interparticle adhesion characteristics of the filler system.

It seems likely that, for the 40wt% calcium carbonate/ polypropylene composite considered in this study, the highest levels of shear stress occur in the melting zone, as described earlier. The subsequent lower levels of shear experienced in the second-stage metering zone contribute less to overall dispersion. Although shear stress generated in the melt undoubtedly increases as the screw pitch is reduced from 16 to 8mm, these differences are not reflected by changes in mean volume diameter; presumably, since shear stress values are below the threshold level necessary to cause substantially more

dispersion. However, the dispersion index (defined by the mean volume diameter, MVD) is not only dependent on the maximum level of shear encountered in the machine, but also on the available time during which the agglomerates are exposed to the zone of maximum shear intensity. In an ideal mixing operation, sufficient time must be allowed to ensure that all agglomerates present pass through the region of greatest shear.

The continuing, but less sudden, increase in filler dispersion observed downstream from the melting zone observed for all the parameters investigated, suggests that not all agglomerates have been exposed to the conditions of high shear existing in this region and that these may subsequently break-down to yield a lower overall average value of dispersion. It is fortunate that the strength of any agglomerates are unlikely to approach that of the solid material; this is due to voids being present which will tend to undermine the strength, as will cracks.[98] Figure 4.4.1 shows the structure of a Durcal 2 agglomerate viewed by a scanning electron microscope at three different magnifications; the structure of the agglomerate in view is clearly defined.

The dispersion (MVD) of samples taken from the extrudate of the different calcium carbonate compounds, Figure 3.3.2, indicates that the level of agglomeration remains inversely proportional to the initial mean particle diameter, as detailed in Section 4.2.2 above. This maintenance of the differential between the filler dispersions from one end of the extruder to the other, although of a low magnitude, suggests that agglomeration of the calcium carbonate during premixing does indeed introduce additional compaction. These differences in dispersion appear more significant when comparisons of Df (the ratio of measured MVD to that of the initial feed) are made for one series of calcium carbonates (Setacarb 13, Hydrocarb and Millicarb) whose origins

are similar.

The trend is in marked contrast to one processing variable - conventional barrel temperature profile (LT, NT and HT in Table 3.3.8) - which exhibited no significant differences in extrudate dispersion. A variation of processing temperature could be expected to alter the shearing conditions within the extruder, Figure 3.3.9 which compares LT, NT and HT illustrates levels of dispersion along the extruder. Nevertheless, in spite of these fluctuations, the final dispersions are uniform. When the premixing stage was omitted by metering the filler and polymer into the extruder hopper separately, the ensuing extrudate agglomeration was found to have been lowered from MVD24.3um to MVD20.6um (Table 3.3.9 sample codes PP-D2-PH and PP-D2-SH). Thus, a series of additional experiments were devised whereby the calcium carbonate filler was preconditioned as detailed in Section 3.4 above and discussion of the dispersion analysis is in Section 4.4.2 below.

Preconditioning of the seven different calcium carbonate fillers resulted in a level of agglomeration in the extrudate up to 7 times higher than when the fillers were premixed and processed as normal. However, these results (Table 3.4.5/Figure 3.4.2 Graph A) do not exhibit the same trend as previously, i.e. the level of agglomeration for preconditioned filler does not appear related to initial mean particle diameter. The filler pellets introduced into the extruder during these particular preconditioning experiments had been compacted at the highest set pressure (157.5MPa). It is highly probable that sintered solid bridges have formed at aggregate interfaces and that it is the strength characteristics of these bridges which are now influencing dispersion behaviour.

Final dispersion in the extrudate showed a reduction for each of the coated versions (Table 3.3.4/Figure 3.3.2). For preconditioned filler pellets processed through the extruder the differences in

dispersion were very significant (Table 3.4.5/Figure 3.4.2). The large change in dispersion for coated versions indicates that they were much more able to resist agglomeration under the influence of compaction pressure and thus justify their additional cost factor.

4.4.2 Preconditioning of Filler

It will be apparent from the previous discussion that, except for the position of filler addition to the compounder, operating conditions were found to have little influence on overall dispersion at the extrudate for the calcium carbonate filler studied.

Results from the model experiments undertaken to establish the role of filler characteristics and extraneous conditions (moisture, temperature and pressure) on filler dispersion are shown in Figures 3.4.1 and 3.4.2.

Specimen discs of calcium carbonate (Durcal 2), prepared using increasing conditions of pressure and temperature, were introduced into the compounder either with the polymer feed or into the downstream entry port. The extrudate was analyzed, as previously described, to assess the breakdown of the filler particles. Figures 3.4.1 and 3.4.2 show that filler samples prepared using increasing conditions of temperature or pressure show less tendency to disperse. For the reasons given earlier, this condition is greatly enhanced when filler is introduced downstream in to the melt. The presence of moisture is also shown to be of great significance in influencing calcium carbonate dispersion (Figure 3.4.1). Predried material gave appreciably lower values of mean volume diameter when compared with filler containing residual quantities of absorbed moisture or when water was deliberately incorporated in excess amounts.

The agglomeration formed by various pressing temperatures is detailed in Table 3.4.6/Figure 3.4.2; the pellets which passed through

the entire machine (from the hopper) gave similar agglomeration levels in the extrudate for the middle temperatures. However, the highest pressing temperature produced a very significant jump in agglomeration which may be an indication of sintering effects at the interparticle contact points. This experiment (PP-PD2-250) represents the most severe preconditioning conditions of temperature and pressure applied to the filler. However, the experiment where excess moisture was added to the filler before compacting (PP-PD2-157.5-22.8 in Table 3.4.4) produced a higher agglomeration level in the extrudate. The presence of high moisture levels during compaction therefore appears to be at least as significant as the magnitude of physical factors acting on the filler.

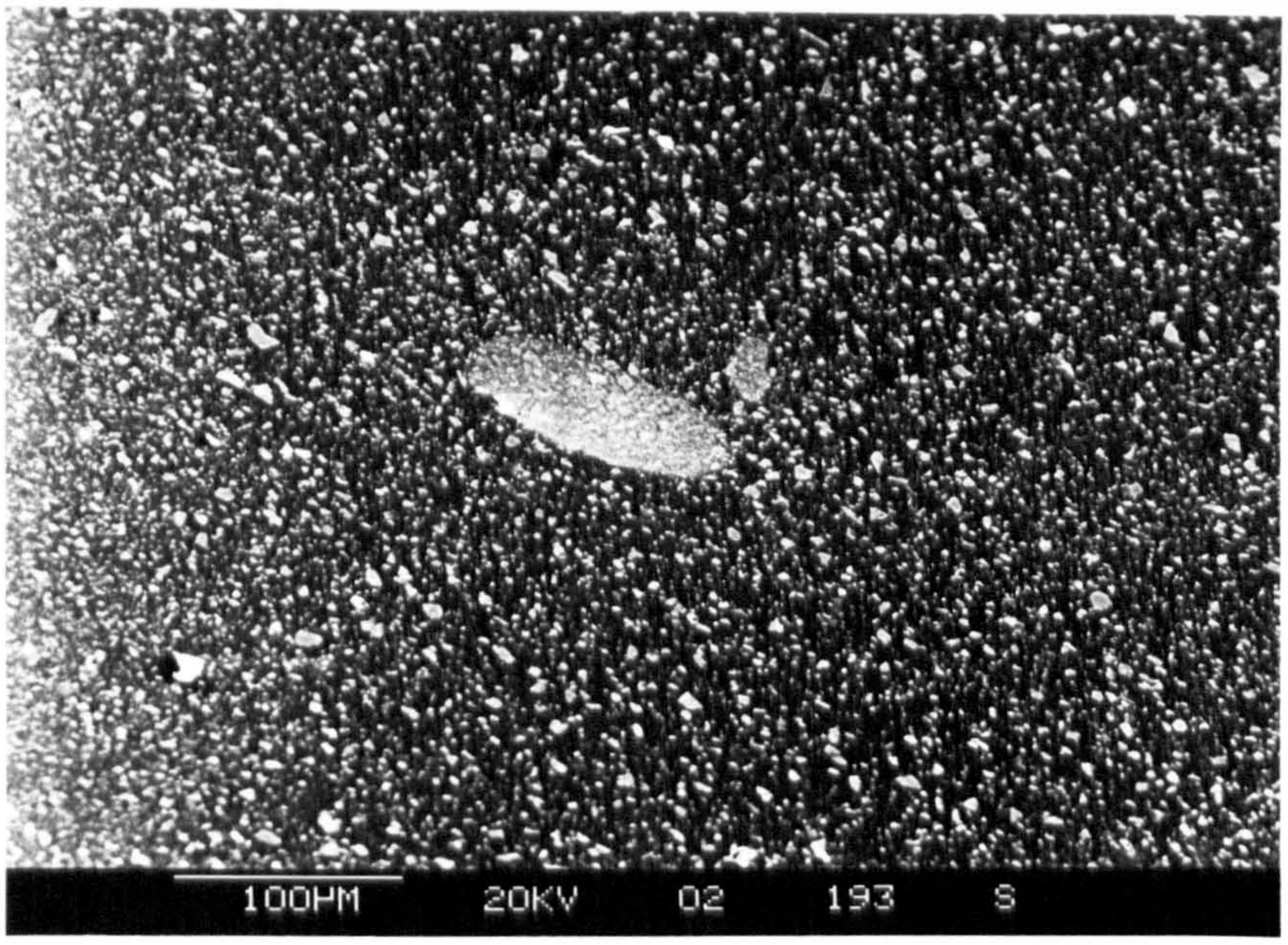

Fig.4.4.1 Scanning electron micrographs showing structure of a Durcal 2 agglomerate found at the end of the screws (position 2)

4.5 DISTRIBUTION

Laminar or distributive mixing will tend to increase the spatial randomization of particles within a fluid medium without any reduction in particle size. It could be suggested that distributive mixing is akin to increasing the entropy of the system and that the progress of mixing be followed by measurement of this term.[4] However, measurements of a directly quantifiable entity, rather than entropy, involves assessment of physical effects which result from or closely follow the progress of mixing. The most obvious physical attribute of a laminar mixture is the array of pigmented flow lines, of varying magnitude and frequency, which will be present within a given element of an overall specimen material.

One of the most widely accepted theoretical terms used to describe these features is that of 'interfacial surface area' [100,101,213-217] between the polymer matrix and the pigmented flow lines (striations). In practice, 'striation thickness' is the actual measurement that can be determined from the sample field of view. [89]

Taking a block of specimen material consisting length (L), width (W), and height (H) with a number (n) of equally spaced striations [4], the total interfacial area (A) will be:

$$A = 2 n L W \qquad (4.19)$$

Striation thickness (r) is defined as the average distance between the centres of adjacent flow lines in the sample and relates total interfacial surface area (A) to the total volume of the system (V):

$$V = (L W) (H) = (A / 2 n) . (n r) = 0.5 A r \qquad (4.20)$$

For constant volume, two different mixtures can be compared [102]:

$$\text{Volume} = 0.5 A' r' = 0.5 A'' r'' \qquad (4.21)$$

Rearranging Eqn.4.21, reveals that:

$$A'' / A' = r' / r'' \qquad (4.22)$$

Eqn.4.22 shows that as the interfacial surface area increases, the striation thickness decreases in a proportional manner.

Many investigators have utilized this relationship to study ordered distributive mixing [102,218-220]; this is relatively simple to characterize. The problems arising when measuring these values for random distributive mixing, e.g. after extrusion or compounding of powders and melts, will be formidable due to the random size and orientation of the flow lines. This results, in part, from the continuously reducing size and separation of the striations which require an increasing scale of scrutiny to detect any variations in composition. The measurement of striation thickness by light microscopy and eyepiece graticule or the use of a microdensitometer are two established methods available to visualize flow, as described in Section 4.1 above. The automatic image-analysis-based light microscopy technique is a possible solution to these problems of resolution and efficiency of data collection.

4.5.1 Processing Variables

A number of experiments were undertaken which again utilized the normal two-stage screw geometry, shown at the top of Figure 3.1.5. A series of extruder screw speeds between 30 and 180rpm were used to process the 0.5wt% carbon black/polypropylene mixture, and the distributive mixing values (Table 3.3.15/Figure 3.3.15) determined from the extrudate for each of six speeds. The breaker plate, normally located in the barrel head adaptor, was removed and a second series of experiments were carried out at the same screw speeds. Comparison of the regression lines reveals that the rate of change of area fraction with respect to screw speed remains similar whether or not the breaker plate is present. The area fraction value has merely been displaced to a higher level; this increase being nearly constant in absolute terms

regardless of screw speed. The breaker plate might therefore be said to contribute a fixed amount of laminar mixing to the melt as it passes through independent of screw speed employed. This scenario is highly probable as a given element of melt when travelling towards and through the breaker plate has no opportunity to do so more than once or in more than one manner regardless of the speed it is travelling. Therefore, the breaker plate increases the distributive mixing within the extrudate by an amount which would require an increase in screw speed of approximately 45rpm to compensate for its absence.

Further experiments were concerned with the effect of the screw pitch of the final metering zone of the extruder on distributive mixing. Four metering screw configurations; 8mm, 12mm, 16mm and 8mm plus 2 segmented discs (designated 8P, 12P, 16P and 8P2D respectively in Table 3.3.18) were utilized for processing and, after the machine had achieved steady state running conditions, it was crash-cooled and solid material removed from specified locations along the screws (Table 3.3.13). Results of image analysis from these specimens are shown individually in Figures 3.3.16 to 3.3.19 and compared in Figure 3.3.20. The most striking feature of the comparison between the screw configurations is the grouping around an AF value of 3% for the 8mm, 12mm and 16mm pitch screws whilst the 8mm pitch screw with two segmented discs at the extreme end exhibited a value more than 6 times less.

An additional experiment, whereby the carbon black masterbatch was dosed into the molten polymer at the vent entry port at a rate to achieve the same 0.5wt% carbon black concentration in the extrudate (Table 3.3.19/Figures 3.3.21 and 3.3.22), suggests that eliminating the first stage of the extruder from mixing shows a fixed quantifiable change in AF in the same way as the removal of the breaker plate. That is, the level of distributive mixing (AF) is displaced approximately 5%

higher along the length of the metering zone with the extrudate showing a similar increase. It will be noted that in bypassing the first stage of the extruder, the carbon black material has not only missed the melting region but has also not passed through the first two sets of discs (at the end of the first stage).

4.5.2 Distributive Mixing Contribution of Discs

Gale [18] considered that, for effective distributive mixing in a single-screw extruder, the incorporation of interrupted flights, barriers and pins were not completely satisfactory as a means of melt reorientation. He stated that the idealized mixing system will need the action of a die face cutter to enable reorientation and has developed this idea into the Cavity Transfer Mixer (CTM) which can be added to the die end of a single-screw extruder.[200,221] The segmented discs as utilized in the intermeshing co-rotating twin-screw extruder are considered to act in exactly the manner of a die face cutter as they sweep past one another, with the only route for the melt to follow being through the six narrow slits in each of the discs.

This type of segmented disc (Figures 3.1.3 and 3.1.4) has been studied by Kosel [12] for use in a single-screw extruder in comparison with other types of screw sections with pin inserts. Segmented discs of this sort are the only mixing elements (other than kneading cams for high shearing) that will function effectively on a twin-screw extruder. There are two related problems with barrier designs of mixing element [222,223] as invisaged for single-screw extruders: (a) they may not intermesh with one another unless slotted like the discs; and (*b*) as they will not have a very close fit between them, as would be needed to stop material leakage, the whole concept of a barrier screw element is lost.

4.5.3 Reorientation within the Twin-Screw Extruder

Martelli [82] in considering intermeshing co-rotating twin-screw extruders, has estimated the magnitude of melt reorientation for the same type of trapezoid-shaped screws as the TS40.[224] He found that the material moves around the 'figure of eight' of the two screws at about 0.65 of the machine screw speed (n). However, for simplicity in calculations of mixing, he approximated this value to 0.5n. As the division and merging of material occurs twice on each 'figure of eight', the material mixes once every turn of the actual screws per minute of residence time. This successive division and merging of the material accumulates so that at 20rpm there would be 2^{20} or 1,048,576 mixings per minute of residence time at a given screw flight location.

However, an analysis which calculates the mixing received by a single element of material is informative. If the single element is followed along the screws of the TS40 extruder, then the number of flights of the screws (ignoring the segmented discs and any conveying differences between solid and melt) will be 48 (for the standard screw with an 8mm pitch metering section - top of Figure 3.1.5). Therefore, 96 divisions of material will occur and the number of accumulated mixing events experienced by this element will be 2^{96} or 7.9×10^{28} which, together with the reorientating action of the 4 pairs of segmented discs, should ensure sufficient distributive mixing!

CHAPTER 5

CONCLUSIONS

A wide-ranging investigation of potential sample preparation and examination techniques for direct quantitative analysis of dispersion and distribution within a polymer matrix revealed that these are best allied with image analysis to enable greatly accelerated accumulation of data. Consequently, the preparation and examination techniques were assessed with this objective in mind. In the case of calcium carbonate filled polypropylene, the fine polishing of surfaces for examination by reflected light microscopy proved the most satisfactory method whilst for carbon black pigmented polypropylene, glass microtomy of sections and transmitted light microscopy were selected. Both types of specimen were examined using a microscope which was directly interfaced to an image analyzer.

The closely-intermeshing co-rotating twin-screw compounding extruder specially developed for use in this study and others at Brunel, proved extremely efficient for dispersion in the face of widely varied machine parameters, viz. screw speed, barrel temperature profile and throughput.

Dispersive mixing at the extrudate was significantly influenced only by adding the calcium carbonate filler at the vent entry port, which is not surprising as this eliminates half of the machine from compounding.

The premixing of calcium carbonate and polypropylene before processing appeared to create additional compaction in the filler. A series of experiments in which filler was pelletized revealed that the moisture level in the filler prior to compaction was a very significant

factor in the subsequent dispersion levels at the extrudate. Additionally, the compaction pressure and temperature, over the range studied, influenced dispersion to a considerable extent. When the premixing stage was omitted, the level of agglomeration was found to be slightly lower at the extrudate (MVD24.3um reduced to MVD20.6um).

Distributive mixing was discovered to be influenced more by machine parameters particularly the presence of the breaker plate in the adaptor head and the imposition of two pairs of segmented discs at the end of the metering screws. The presence of the breaker plate was calculated to be equivalent to an increase in screw speed of 45rpm. When two of the four pairs of segmented discs were transferred to the end of the screws, the level of distributive mixing was found to have increased by in excess of six times compared to the standard screw configuration.

SUGGESTIONS FOR FURTHER WORK

1. An investigation of kneading cam elements to introduce additional shear for improved dispersive mixing. These cams should be studied because the original slotted discs did not have any significant influence on dispersion of calcium carbonate fillers within the polymer matrix, after their utilization as melting elements. The kneading elements will be most effective when they restrict a significant proportion of flow to a high shear region at their periphery against the barrel wall; this could be achieved by adopting more than the now usual 3-faced elements. However, the benefits of restricted flow in terms of dispersion will be offset by a decrease in overall material throughput of the machine and increased localized wear of both the elements and barrel.

2. Flow visualization could be achieved by substituting a section of the steel barrel wall with a clear rigid polymer (such as PMMA). The use of hot polymer melts is obviously impossible so alternative ambient-temperature flow materials, which closely emulate the original polymer rheological characteristics, must be substituted; wall paper adhesive has been suggested. This exercise would be an extension of the studies of melt flow already undertaken for the TS40 twin-screw extruder.[224] This study involved shock-cooling and careful removal of solidified process material for examination from specific locations around and between the screws, after the machine had been dosed with small quantities of carbon black masterbatch.

3. As mentioned in Section 3.2.2.4 above, acoustic microscopy failed to resolve calcium carbonate surface agglomerates at the magnifications then available. However, this method of examination is potentially very powerful as a means of non-destructive three-dimensional analysis because it presents the possibility of imaging structures within a solid matrix. This technique deserves a significant effort to try and eliminate the outstanding problems, viz. the generation of an acoustic beam of sufficient intensity and coherence to penetrate the solid whilst not being scattered and absorbed to such an extent as to undermine the resolution. This examination technique, if realized, in combination with computer-controlled image analysis would form an extremely efficient quantitative sizing and mixture quality assessment method.

REFERENCES

1. ESS J.W., HORNSBY P.R., LIN S.Y. and BEVIS M.J.: *Plast. Rubb. Proc. Appl.* 4(1) (1984) 7.
2. ESS J.W. and HORNSBY P.R.: *Polymer Testing* 6(3) (1986) 205.
3. ESS J.W. and HORNSBY P.R.: *Plast. Rubb. Proc. Appl.* 8(3) (1987) 147.
4. McKELVEY J.M.: Polymer Processing (Wiley, 1962).
5. SCHENKEL G.: Plastics Extrusion Technology and Theory (Iliffe, 1966)
6. PEARSON J.R.A.: Mechanics of Polymer Processing (Elsevier, 1985)
7. STREET L.F.: *Plast. Engng.* 1(6) (1961) 289.
8. JANSSEN L.P.B.M.: Twin Screw Extrusion (Elsevier, 1978)
9. KRUDER G.A., NICHOLS R.J. and RIDENOUR R.E.: *SPE 34th ANTEC* (1976) 450.
10. BRAUN K.J. and HELMY H.A.: *Polymer Extrusion Conf, London* (Jun 1979) 7.1.
11. INGEN HOUSZ J.F. and MEIJER H.E.H.: *Plast. Rubb. Proc.* (Sep/Oct 1980) 123.
12. KOSEL U.M.: *Plast. Polym.* 39(143) (1971) 319.
13. KRUEGER W.L.: *SPE 39th ANTEC* (1981) 676.
14. MAILLEFER C.: *Mod. Plast.* (Jan 1963) 132.
15. KRUDER G.A. and RIDENOUR R.E.: *Plast. Engng.* 33(11) (1977) 33.
16. MADDOCK B.H.: *SPE J.* 23(7) (1967) 23.
17. RAUWENDAAL C.J.: *Polym. Engng. Sci.* 26(18) (1986) 1245.
18. GALE G.M.: *Polymer Extrusion II Conf, London* (May 1982) 18.1.
19. MURAKAMI K.: *SPE 32nd ANTEC* (1974) 562.
20. KRUEGER W.L.: *SPE 39th ANTEC* (1981) 679.

21. PITTMAN J.F.T. and PITMAN G.L.: *Polymer Extrusion II Conf, London* (May 1982) 19.1.

22. WOOD R.: *Plast. Rubb. Intl.* 4(5) (1979) 207.

23. PENN W.S.: PVC Technology (Maclaren, 1966) Ch.16.

24. GRIFF A.L.: "Extrusion Equipment" *Encyclopaedia of Plastics Equipment* 201.

25. MUZZY J.D. and JACKSON K.W.: *SPE 34th ANTEC* (1976) 58.

26. RAUWENDAAL C.J.: *Polym. Engng. Sci.* 21(16) (1981) 1092.

27. HERRMANN H. and BURKHARDT U.: *Plast. Rubb. Proc.* (Sep 1980) 101.

28. SCHOENGOOD A.A.: *SPE J.* 29 (1973) 21.

29. MARTELLI F.: *SPE J.* 27(1) (1971) 25.

30. SQUIRES P.H.: *SPE J.* 14 (1958) 24.

31. CHUNG C.I.: *SPE J.* 26 (May 1970) 32.

32. JANSSEN L.P.B.M. and SMITH J.M.: *Plast. Rubb. Proc.* (Sep/Oct 1980) 115.

33. MACK W.A.: *Plast. Technol.* 17 (1971) 35.

34. JANSSEN L.P.B.M. and SMITH J.M.: *Plast. Rubb. Proc.* (Jun 1976) 90.

35. WERNER H. and EISE K.: *SPE 37th ANTEC* (1979) 181.

36. SMITH J.M., JANSSEN L.P.B.M., DE KONING W.L. and ABELN P.P.J.: *Polym. Engng. Sci.* 18(8) (1978) 660.

37. PRAUSE J.J.: *Plast. Technol.* 14(3) (1968) 52.

38. BAUER B.E.: *Krauss-Maffei News* 3 (1977) 9.

39. MACK W.A.: *SPE 29th ANTEC* (1971) 278.

40. HERRMANN H. and ELSE K.: *SPE 39th ANTEC* (1981) 614.

41. TODD D.B.: *Polym. Engng. Sci.* 15(6) (1975) 437.

42. MACK W.A. and HERTER R.: *Chem. Engng. Prog.* 72 (Jan 1976) 64.

43. WERNER H. and CURRY J.: *SPE 39th ANTEC* (1981) 623.

44. GRAS D.: *Plast. Technol.* 18 (Feb 1972) 40.

45. JANSSEN L.P.B.M., MULDERS L.P.H.R.M. and SMITH J.M.: *Plast. Polym.* 43(165) (1975) 93.

46. GALE G.M.: *RAPRA Members J.* (Mar 1974) 68.

47. GALE G.M.: *RAPRA Members J.* (Apr 1974) 105.

48. SCHENKEL G.: Plastics Extrusion Technology and Theory (Iliffe, 1966)

49. TADMOR Z. and KLEIN I.: Engineering Principles of Plasticating Extrusion (Krieger, 1978)

50. RAUWENDAAL C.: Polymer Extrusion (Hanser, 1986).

51. PATON J.B., SQUIRES P.H., DARNELL W.H., CASH F.M. and CARLEY J.F.: Processing of Thermoplastic Materials (Edited by: E.C. Bernhardt, Van Nostrand Reinhold, 1959) Ch.4.

52. MADDOCK B.H.: *SPE J.* 17(4) (1961) 368.

53. FENNER R.T. and WILLIAMS J.G.: *Polym. Engng. Sci.* 11(6) (1971) 474.

54. FENNER R.T., COX A.P.D. and ISHERWOOD D.P.: *SPE 36th ANTEC* (1978) 494.

55. McKELVEY J.M.: *SPE 36th ANTEC* (1978) 507.

56. CHOO K.P., NEELAKANTAN N.R. and PITTMAN J.F.T.: *Polym. Engng. Sci.* 20(5) (1980) 349.

57. RAUWENDAAL C.J.: *SPE 38th ANTEC* (1980) 110.

58. BYAM J.D. and COLBERT G.P.: *Plast. Rubb. Proc.* (Sep/Oct 1980) 95.

59. AGUR E.E. and VLACHOPOULOS J.: *SPE 40th ANTEC* (1982) 465.

60. KLEIN I.: *SPE 34th ANTEC* (1976) 444.

61. KLEIN I. and KLEIN R.: *SPE 36th ANTEC* (1978) 519.

62. KRUDER G.A. and NUNN R.E.: *SPE 38th ANTEC* (1980) 62.

63. MADDOCK B.H.: *SPE J.* 15(5) (1959) 383.

64. TADMOR Z.: *Polym. Engng. Sci.* 6 (Jul 1966) 185.

65. VERMEULEN J.R., SCARGO P.G. and BEEK W.J.: *Chem. Engng. Sci.* 46 (1971) 1457.

66. EDMONDSON I. and FENNER R.T.: *Polymer* 16(1) (1975) 49.

67. LINDT J.T.: *SPE 34th ANTEC* (1976) 429.

68. McCLELLAND D.E. and CHUNG C.I.: *SPE 39th ANTEC* (1981) 653.

69. ELBIRLI B., LINDT J.T., GOTTGETREU S.R. and BABA S.M.: *SPE 40th ANTEC* (1982) 469.

70. ELBIRLI B., LINDT J.T., GOTTGETREU S.R. and BABA S.M.: *SPE 40th ANTEC* (1982) 472.

71. ELBIRLI B., LINDT J.T., GOTTGETREU S.R. and BABA S.M.: *Polym. Engng. Sci.* 24(12) (1984) 988.

72. MADDOCK B.H.: *SPE J.* 16(4) (1960) 373.

73. JANSSEN L.P.B.M., NOOMEN G.H. and SMITH J.M.: *Plast. Polym.* 43 (Aug 1975) 135.

74. CARLEY J.F. and STRUB R.A.: *Ind. Engng. Chem.* 45(5) (1953) 970.

75. CARLEY J.F., MALLOUK R.S. and McKELVEY J.M.: *Ind. Engng. Chem.* 45(5) (1953) 974.

76. CARLEY J.F. and STRUB R.A.: *Ind. Engng. Chem.* 45(5) (1953) 978.

77. McKELVEY J.M.: *Ind. Engng. Chem.* 45(5) (1953) 982.

78. MALLOUK R.S. and McKELVEY J.M.: *Ind. Engng. Chem.* 45(5) (1953) 987.

79. CARLEY J.F. and McKELVEY J.M.: *Ind. Engng. Chem.* 45(5) (1953) 989.

80. KRUDER G.A. and NUNN R.E.: *SPE 39th ANTEC* (1981) 648.

81. STEWARD E.L.: *Plast. Engng.* 41(1) (1985) 53.

82. MARTELLI F.G.: Twin-Screw Extrusion: A Basic Understanding (Van Nostrand Reinhold, 1983)

83. JANSSEN L.P.B.M. and SMITH J.M.: *Polymer Rheology & Plastics Processing Conf, Loughborough* (Sep 1975) 160.

84. MAHESHRI J.C. and WYMAN C.E.: *Polym. Engng. Sci.* 20(9) (1980) 601.

85. BURKHARDT K., HERRMANN H. and JAKOPIN S.: *SPE 36th ANTEC* (1978) 498.

86. KAO S.V. and ALLISON G.R.: *Polym. Engng. Sci.* 24(9) (1984) 645.

87. SECOR R.M.: *Polym. Engng. Sci.* 26(14) (1986) 969.

88. MEIJER H.E.H. and ELEMANS P.H.M.: *Polym. Engng. Sci.* 28(5) (1988) 275.

89. MOHR W.D.: Processing of Thermoplastic Materials (Edited by: E.C. Bernhardt, Van Nostrand Reinhold, 1959) Ch.3.

90. CLUMP C.W.: Mixing Theory and Practice Vol.2 (Edited by: V.W. Uhl and J.B. Gray, Academic Press, 1967) Ch.10

91. MOHR W.D., SAXTON R.L. and JEPSON C.H.: *Ind. Engng. Chem.* 49(11) (1957) 1857.

92. MOORE W.R.: *P. I. Trans. J.* 32 (1964) 247.

93. BRODKEY R.S.: Mixing: Theory and Practice - Vol.1 (Edited by: V.W. Uhl and J.B. Gray, Academic Press, 1966) Ch.2.

94. LEWIS T.B. and NIELSON L.E.: *Trans. Soc. Rheol.* 12(3) (1968) 421.

95. GREGORY R.B.: *Plast. Polym.* 38 (Apr 1970) 120.

96. PINTO G. and TADMOR Z.: *Polym. Engng. Sci.* 10(5) (1970) 279.

97. MATTHEWS G.: Vinyl and Allied Polymers Vol.2 (Butterworth, 1972) Ch.10

98. SMITH M.J.: *J. Oil Col. Chem. Assoc.* 56 (1973) 165.

99. JAKOPIN S.: *Amer. Chem. Soc. - Div. of Organic Coatings & Plastics Chem.* (Aug 1973) 144.

100. SHERIDAN L.A.: *78th National Meeting - Amer. Inst. Chem Engrs.* (Aug 1974).

101. ERWIN L.: *Polym. Engng. Sci.* 18(7) (1978) 572.

102. NG K.Y. and ERWIN L.: *Polym. Engng. Sci.* 21(4) (1981) 212.

103. PEACH N.: *Plast. Engng.* 39(11) (1983) 19.

104. BERGEN J.T.: Processing of Thermoplastics Materials (Edited by: E.C. Bernhardt, Van Nostrand Reinhold, 1959) Ch.7.

105. GASKELL R.E.: *J. Appl. Mech.* 17 (Sep 1950) 334.

106. NICHOLS R.J., KRUDER G.A. and RIDENOUR R.E.: *SPE 34th ANTEC* (1976) 361.

107. ROSATO D.V.: *Plastics World* (Jul 1976) 38.

108. MOTOYOSHI M.: *Japan Plast. Age* 20(185) (1982) 35.

109. ELBIRLI B., LINDT J.T., GOTTGETREU S.R. and BABA S.M.: *SPE 41th ANTEC* (1983) 104.

110. CHENG C.Y.: *SPE 34th ANTEC* (1976) 358.

111. YI B. and FENNER R.T.: *Plast. Polym.* 43 (1975) 224.

112. SKOBLAR S.M.: *Plast. Technol.* 20(10) (1974) 37.

113. BIKALES N.M.: "Compounding" *Ency. Polym. Sci. Technol.* 4 118.

114. COLLINS S.H.: *Plast. Comp.* 5(4) (1982) 29.

115. GALE G.M.: *SPE 41st ANTEC* (1983) 109.

116. HAN C.D., KIM Y.W. and CHEN S.J.: *J. Appl. Polym. Sci.* 19 (1975) 2831.

117. EISE K., CURRY J. and NANGERONI J.F.: *Polym. Engng. Sci.* 23(11) (1983) 642.

118. SCHULE E.C.: "Compounding" *Ency. of Plast. Equip.* 106.

119. WHITE D.H. and WOLF D.: *SPE 38th ANTEC* (1980) 53.

120. WHITE D.H., WOLF D. and SCHOTT N.R.: *SPE 40th ANTEC* (1982) 427.

121. JANSSEN L.P.B.M., BOETES R, and SMITH J.M.: *Polymer Extrusion II Conf, London* (May 1982) 25.1.

122. ALLEN G.B.: *Polymer Extrusion II Conf, London* (May 1982) 14.1.

123. PREDOHL I.W.: *Polymer Extrusion II Conf, London* (May 1982) 11.1.

124. YANG B. and LEE L.J.: *Polym. Engng. Sci.* 26(3) (1986) 197

125. YANG B. and LEE L.J.: *Polym. Engng. Sci.* 26(3) (1986) 205.

126. JOHNSON A.E. and LUNT J.M.: *Mod. Plast.* (Jul 1976) 58.

127. LUNT J.M. and SHORTALL J.B.: *Plast. Rubb. Proc.* 5(2) (Jun 1980) 37.

128. KUBAT J. and STROMVALL H.E.: *Plast. Rubb. Proc.* (Jun 1980) 45.

129. JAKOPIN S.: *SPE 37th ANTEC* (1979) 987.

130. WOOD A.S.: *Mod. Plast. Intl.* (Feb 1980) 36.

131. DEANIN R.D.: *Amer. Chem. Soc. - Div. of Organic Coatings & Plastics Chem.* 37(2) (1977) 440.

132. WALTER S.: *Plast. Engng.* 37(6) (1981) 24.

133. FORGER G.: *Plastics World* 36(8) (1978) 44.

134. STADE K.: *Polym. Engng. Sci.* 17(1) (1977) 50.

135. MOSKAL E.A.: *Plast. Design Proc.* (Jan 1977) 10.

136. KUPFER A.D. and ROZETT R.: *SPE 42nd ANTEC* (1984) 191.

137. KATZ H.S. and MILEWSKI J.V.: Handbook of Fillers and Reinforcements for Plastics (Van Nostrand Reinhold, 1978)

138. CROWE G.C. and KUMMER P.E.: *Plast. Comp.* 1(3) (1978) 14.

139. WATERMAN N.A., TRUBSHAW R. and PYE A.M.: *Mats. Engng. Appl.* 1 (1978) 74.

140. DE SOUZA A.S., AUGUSTYN E.J., LEWIS H.T. and NAUGHTON F.C.: *SPE 37th ANTEC* (1979) 492.

141. McFARREN G.A., SANDERSON T.F. and SCHAPPELL F.G.: *SPE 34th ANTEC* (1976) 19.

142. HAN C.D., SANDFORD C. and YOO H.J.: *SPE 36th ANTEC* (1978) 257.

143. HAN C.D., VAN DEN WEGHE T., SHETE P. and HAW J.R.: *SPE 38th ANTEC* (1980) 241.

144. MONTE S.J. and SUGERMAN G.: *SPE 38th ANTEC* (1980) 486.

145. HAN C.D., LUO H.L. and MIJOVIC J.: *SPE 40th ANTEC* (1982) 82.

146. MITSUISHI K., KODAMA S. and KAWASAKI H.: *Polym. Engng. Sci.* 25(17) (1985) 1069.

147. CHOW T.S.: *J. Polym. Sci. Polym. Phys.* 20 (1982) 2103.

148. NEILSEN L.E.: *J. Comp. Mats.* 1 (1967) 100.

149. FRIEDRICH K. and KARSCH U.A.: *J. Mats. Sci.* 16 (1981) 2167.

150. RADOSTA J.A.: *SPE 42nd ANTEC* (1984) 145.

151. ERWIN L. and DOHNER J.: *SPE 42nd ANTEC* (1984) 116.

152. HORNSBY P.R. and SOTHERN G.R.: *Plast. Rubb. Proc. Appl.* 4(2) (1984) 165.

153. BELL S.H. and CROWL V.T.: Dispersion of Powders in Liquids (Edited by: G.D. Parfitt, Applied Science, 1973) Ch.7.

154. WOLF D. and WHITE D.H.: *AIChE J.* 22(1) (1976) 122.

155. ZUILICHEM V.D.J. et al: *Lebensm - Wiss. u. Technol.* 6(5) (1973)

156. NAUMAN E.B.: *Chem. Engng. Sci.* 32 (1977) 359.

157. KROMER H.M.: "Introduction to torque rheometry" Haake Inc, 1978.

158. BYERS J.T.: *Rubber World* 189(3) (1983) 26.

159. COTTEN G.R.: *Amer. Chem. Soc - Rubb. Div. Conf, Houston, Texas* (Oct 1983) Paper No:38.

160. CARR W.: Particle Size Analysis (Edited by: M.J. Groves, Heyden, 1978) 3.

161. ALLEN T.: Particle Size Measurement (Chapman & Hall, 1981).

162. HENNEKA T.A. and ROTZ C.A.: *SPE 39th ANTEC* (1981) 223.

163. BEST W.G. and TOMFOHRDE H.F.: *SPE J.* 15 (1959) 139.

164. HOWARD J.B.: *Polym. Engng. Sci.* 6 (Jul 1966) 217.

165. EBELL P.C. and HEMSLEY D.A.: *Rubb. Chem. Technol.* 54(4) (1981) 698.

166. MUTAGAHYWA B.H. and HEMSLEY D.A.: *Plast. Rubb. Proc. Appl.* 5(3) (1985) 219.

167. SAWYER L.C.: *Polym. Engng. Sci.* 19(5) (1979) 377.

168. SHORTALL J.B. and PENNINGTON D.: *Plast. Rubb. Proc. Appl.* 2(1) (1982) 33.

169. GOLDSMITH P.L.: *Brit. J. Appl. Phys.* 18 (1967) 813.

170. SMITH M.J.: *Powd. Technol.* 5 (1971/72) 229.

171. SMITH M.J.: *Microscope* 19 (1971) 337.

172. MEDALIA A.I.: *Rubber Age* 97(1) (1965) 82.

173. DWYER J.L., MANALAN D.A. and MORTON R.R.A.: Particle Size Analysis (Edited by: M.J. Groves and J.L. Wyatt-Sargent, 1970) 114.

174. BARTOSIEWICZ L. and EICHEN E.: Microstructural Analysis: Tools & Techniques (Edited by: J. L. McCall and W. M. Mueller, Plenum Press, 1973) p.67.

175. SEBASTIAN D.H. and BIESENBERGER J.A.: *SPE 41st ANTEC* (1983) 121.

176. DAVIDSON J.A.: *J. Appl. Polym. Sci.* 27(9) (1982) 3219.

177. FELTY D.C. and MURAYAMA T.: *J. Appl. Polym. Sci.* 26(3) (1981) 987.

178. SCHWEIZER R.A.: *Plast. Comp.* 4(4) (1981) 58.

179. JENKINSON G.W.: *Intl. Lab.* (Jan/Feb 1984) 37.

180. HESS W.M. and McDONALD G.C.: *Rubb. Chem. Technol.* 56(5) (1983) 892.

181. VON TURKOVICH R. and ERWIN L.: *SPE 40th ANTEC* (1982) 439.

182. DOBROTH T., DRUHAK G. and ERWIN L.: *SPE 41st ANTEC* (1983) 124.

183. HORNSBY P.R.: *Plast. Comp.* 6(3) (1983) 65.

184. HORNSBY P.R. and WATSON C.L.: *Plast. Rubb. Proc. Appl.* 6(2) (1986) 169.

185. ABRAM J., BOWMAN J., BEHIRI J.C. and BONFIELD W.: *Plast. Rubb. Proc. Appl.* 4(3) (1984) 261.

186. ALLAN P.S., BEVIS M.J. and HORNSBY P.R.: *Mod. Plast. Intl.* 17(4) (1987) 38.

187. GROSS S.: *Israel J. Chem.* 9 (1971) 601.

188. GRIFFIN G.J.L.G.: *Unpublished work*, Brunel University, Uxbridge, England.

189. TIOXIDE LTD.: "Dispersion and dispersibility/ Pigmentation and processing of melt plastics" *Tioxide Technical Information Sheet.*

190. SMITH M.J.: *Microscope* 16 (1968) 123.

191. RICHARDSON J.H.: Microstructural Analysis: Tools and Techniques (Edited by: J.L. McCall and W.M. Mueller, Plenum Press, 1973) 23.

192. DARLINGTON M.W. and McGINLEY P.L.: *J. Mats. Sci. (Letters)* 10 (1975) 906.

193. GIBLIN R.: *Shell Polymers* 4(2) (1980) 54.

194. UNDERWOOD E.E.: Quantitative Stereology (Addison-Wesley, 1970).

195. UNDERWOOD E.E.: Quantitative Microscopy (Edited by: R.T. De Hoff and F.N. Rhines, McGraw-Hill, 1968) Ch.6.

196. DE HOFF R.T.: Quantitative Microscopy (Edited by: R.T. De Hoff and F.N. Rhines, McGraw-Hill, 1968) Ch.5.

197. DICTIONARY: Oxford University Press,1977

198. BEVINGTON P.R.: Data Reduction and Error Analysis for the Physical Sciences (McGraw-Hill, 1969).

199. EDWARDS M.F., GOKBORA M.N. and ZAYADINE K.Y.: *Polymer Extrusion II Conf, London* (May 1982) 17.1

200. LIN S.Y. and BEVIS M.J.: *Plast. Rubb. Proc. Appl.* 7(1) (1987) 29.

201. SPENCER R.S. and WILEY R.H.: *J. Colloid Sci.* 6 (1951) 133.

202. DANCKWERTS P.V.: *Appl. Sci. Res.* A3 (1952) 279.

203. TADMOR Z. and GOGOS C.G.: Principles of Polymer Processing (Wiley, 1979)

204. HESS W.M. and GARRET M.D.: *J. Oil Col. Chem. Assoc.* 54 (1971) 24.

205. AHMED M.: Colouring of Plastics (Van Nostrand Reinhold) Ch.6.

206. SMITH M.J.: *J. Oil Col. Chem. Assoc.* 57 (1974) 36.

207. RUMPF H. and SCHUBERT H.: Ceramic Processing Before Firing (Edited by: G.J. Onoda Jr. and L.L. Hench, Wiley Interscience, 1978) Ch.27.

208. SMITH M.J.: *J. Oil Col. Chem. Assoc.* 56 (1973) 155.

209. SCHUBERT H., HERRMANN W. and RUMPF H.: *Powder Technol.* 11 (1975) 121.

210. LAU W.W.Y. and BURNS C.M.: *J. Coll. Interf. Sci.* 45(2) (1973) 295.

211. REEVE T.B. and DILLIS W.L.: *J. Col. App.* 1(1) (1971) 25.

212. PARFITT G.D.: Dispersion of Powders in Liquids (Applied Science, 1973)

213. MOHR W.D., SAXTON R.L. and JEPSON C.H.: *Ind. Engng. Chem.* 49(11) (1957) 1855.

214. GALE G.M. and PENNY M.T.: *SPE 38th ANTEC* (1980) 69.

215. MATTHEWS G.: Polymer Mixing Technology (Applied Science, 1982)

216. MOKHTARIAN F. and ERWIN L.: *SPE 40th ANTEC* (1982) 476.

217. BIGIO D. and STRY W.: *SPE 45th ANTEC* (1987) 170.

218. BIGG D.M.: *Polym. Engng. Sci.* 15(9) (1975) 684.

219. GAILUS D.W. and ERWIN L.: *SPE 39th ANTEC* (1981) 639.

220. BIGIO D.I., BOYD J.D., ERWIN L. and GAILUS D.W.: *Polym. Engng. Sci.* 25(5) (1985) 305.

221. LIN S.Y.: *Plast. Rubb. Proc. Appl.* 8(3) (1987) 133.

222. GALE G.M.: "Masterbatch flow patterns in polyethylene extrusion" *RAPRA Members Report* No:16.

223. AMELLAL K. and ELBIRLI B.: *Polym. Engng. Sci.* 28(5) (1988) 311.

224. HORNSBY P.R.: *Plast. Rubb. Proc. Appl.* 7(4) (1987) 237.

APPENDIX A

IMAGE ANALYSER COMPUTER PROGRAMS FOR DISPERSIVE MIXING

A.1 Measurement Program

```
10  REM ...MASTER DISKETTE        CREATED ON 48K SYSTEM BY      J.H.ESS

20  REM ...NON-METALLIC MATERIALSIMAGE ANALYSIS PROGRAM FOR  OPTOMAX SYSTE
    M IV
30 D$ =  CHR$ (4): REM  CTRL-D
35  PRINT D$"PR#1": PRINT : POKE  - 12528,7: PRINT D$"PR#0": REM ...SETS P
    RINTER INTENSITY TO MAXIMUM
40  TEXT : HOME : HTAB 11: PRINT "*** SYSTEM IV ***"
50  VTAB 8: HTAB 2:.PRINT "(I)       IMAGE MEASUREMENT PROGRAM"
60  VTAB 11: HTAB 2: PRINT "(D)       DATA & STATS PROGRAM"
65  VTAB 14: HTAB 2: PRINT "(S)       SURF.AREA OF AGGLOMERATES"
67  VTAB 17: HTAB 2: PRINT "(F)       FIBRE LENGTH (GRAPHICS TABLET)"
70  VTAB 23: HTAB 2: PRINT "YOUR CHOICE ";: POKE 49168,0
80  GET A$: IF A$ = "I" THEN  PRINT "LOADING-I": PRINT D$"RUN MEASUREMENT,
    D1": END
82  IF A$ = "X" THEN  HOME : PRINT : PRINT D$"RUN D,D1": END
85  IF A$ = "S" THEN  PRINT "LOADING-S": PRINT D$"RUN M/2,D1": END
87  IF A$ = "F" THEN  PRINT "LOADING-F": PRINT D$"RUN F,D1": END
90  PRINT "LOADING-D": PRINT D$"RUN DATA/STATS,D1": END

]LOAD MEASUREMENT
]LIST

10  REM  ...MEASUREMENT/J.H.E.

20  CLEAR
30  DIM TF(17),DT(17)
40  TEXT : HOME : HTAB 11: PRINT "*** SYSTEM IV ***"
50  VTAB 3: HTAB 7: PRINT "IMAGE MEASUREMENT PROGRAM"
60  VTAB 14: INPUT "INPUT SAMPLE NAME    ";SNE$
70  VTAB 16: INPUT "INPUT OPERATOR NAME ";OPR$
80 A =  LEN (SNE$) +  LEN (OPR$): IF A > 26 THEN  GOTO 40
90  VTAB 18: INPUT "INPUT DATE           ";DTE$
100 D$ =  CHR$ (4):I1$ = "@?(:'":I2$ = "@?H:":I3$ = "@H" +  CHR$ (95) + ":
    ":I4$ = "'": REM ...COMMAND STRINGS FOR IEEE INTERFACE

110 D1 = 50:D2 = 250: REM  ...TIME DELAYS FOR SYSTEM IV

120  PRINT : GOSUB 520: GOSUB 1390: GOSUB 1670
130  HOME : PRINT " SYSTEM IV IMAGE MEASUREMENT PROGRAM"
140  VTAB 6: HTAB 4: PRINT "(SPC) TO READ"
150  VTAB 8: HTAB 4: PRINT "'W' TO CLEAR SCREEN"
160  VTAB 10: HTAB 4: PRINT "'P' FOR PRINT-OUT"
170  VTAB 12: HTAB 4: PRINT "'R' TO RECALIBRATE"
180  VTAB 14: HTAB 4: PRINT "'F' TO FILE"
190  VTAB 16: HTAB 4: PRINT "'S' FOR NEW SAMPLE"
200  VTAB 18: HTAB 4: PRINT "'Q' TO QUIT"
210 FC = 0:TF = 0:TA = 0:TI = 0:Z = 0:TC = 0:S0 = 0:S1 = 0: FOR J = 1 TO 1
    7:DT(J) = 0: NEXT J
220  VTAB 24: HTAB 1: POKE 49168,0
230  GOSUB 1170: VTAB 23: HTAB 1: CALL  - 868:FH = F * CAL:FH$ =  STR$ (FH
    ):FH$ =  LEFT$ (FH$,5): PRINT "     FRAME = ";FH$" "UN$" DIAM.";
240 KB =  PEEK (49152): IF KB < 128 THEN 230
250 KB$ =  CHR$ (KB - 128): IF KB$ = "Q" THEN  VTAB 23: HTAB 1: CALL  - 86
    8: PRINT "QUIT - ARE YOU SURE? (Y/N)";: POKE 49168,0
260  IF KB$ = "Q" THEN  GET KA$: IF KA$ <  > "Y" AND KA$ <  > "N" THEN  GOTO
    260: IF KA$ = "N" THEN  GOTO 220
270  IF KA$ = "Y" THEN  TEXT : HOME : PRINT : PRINT D$"EXEC RESET,D1": END

280  IF KB$ = "W" THEN  GOTO 130
290  IF KB$ = "S" THEN  POKE  - 16368,0: RUN
300  IF KB$ = "R" THEN  POKE  - 16368,0: HOME : GOTO 120
310  IF KB$ = "F" THEN  GOTO 1220
320  IF KB$ = "P" THEN  PRINT : PRINT D$"PR#1":PF% = 1: PRINT : PRINT : PRINT
    ; PRINT : PRINT : GOTO 340
330  GOSUB 1010:FA = .7855 * (F ^ 2) * (CAL ^ 2):TF = TF + FA:AR = A * CAL
     ^ 2:TA = TA + AR:TI = TI + 1:TC = TC + C:FC = FC + 1:S0 = S0 + AR /
    FA:S1 = S1 + AR ^ 2 / FA ^ 2
335 PA = 1E2 * AR / FA:PA$ =  STR$ (PA):PA$ =  LEFT$ (PA$,4):TP = 1E2 * TA
     / TF:TP$ =  STR$ (TP):TP$ =  LEFT$ (TP$,4): GOSUB 1800
340 DS$ =  STR$ (DS): HOME : PRINT OPR$,: PRINT DTE$;: HTAB 35: PRINT "(";
    DS$;"%)"
```

```
350  PRINT SNE$;: HTAB 25: PRINT "MAG.="M1$: PRINT
360  PRINT "SYSTEM IV IMAGE MEASUREMENT PROGRAM"
370  PRINT : PRINT "     NUMBER OF FIELDS: "FC: PRINT : PRINT "PARAMETER
      THIS FIELD  CUMULATIVE"
380 FA =  INT (FA):TF =  INT (TF)
390  VTAB 10: HTAB 1: PRINT "FIELD AREA  "FA;: HTAB 26: PRINT TF;: IF PF% THEN
      POKE 36,40: PRINT "SQUARE "UN$
400 AR =  INT (AR * 1E1 + .5) / 1E1:TA =  INT (TA)
410  VTAB 11: HTAB 1: PRINT "DETECTED    "AR;: HTAB 26: PRINT TA;: IF PF% THEN
      POKE 36,40: PRINT "SQUARE "UN$
430  VTAB 13: HTAB 1: PRINT "AREA FRACT.  "PA$;: HTAB 26: PRINT TP$;: IF P
     F% THEN  POKE 36,40: PRINT "%"
440  IF FC >  = 2 THEN M1 = TA / TF:Z1 = 1E2 *  SQR (M1 * M1 + (S1 - 2 * M
     1 * S0) / FC):Z1$ =  STR$ (Z1):Z1$ =  LEFT$ (Z1$,4)
450  IF FC >  = 2 THEN  VTAB 14: HTAB 7: PRINT "+-";: HTAB 26: PRINT Z1$
460  VTAB 16: HTAB 1: PRINT "# I'CPT     "I;: HTAB 26: PRINT TI
470 IL = I / FA:IL =  INT (IL * 1E6 + .5) / 1E6:NL = TI / TF:NL =  INT (NL
      * 1E5 + .5) / 1E5
480  VTAB 17: HTAB 1: PRINT "N(L)        ";IL;: HTAB 26: PRINT NL;: IF PF%
      THEN  POKE 36,40: PRINT "PER "UN$
490  VTAB 19: HTAB 1: PRINT "# FEATURES  "C;: HTAB 26: PRINT TC
500  IF PF% THEN  PRINT : PRINT D$"PR#0":PF% = 0: GOTO 340
510  GOTO 220
520  REM ...SET CALIBRATIONS
530 CA% = 0
540  PRINT D$"OPEN CAL DATA,D1": PRINT D$"READ CAL DATA": INPUT M1$,M2$,M3
     $,M4$,M5$,M6$,C1,C2,C3,C4,C5,C6,U1$,U2$,U3$,U4$,U5$,U6$,BL,TL,NG: PRINT
     D$"CLOSE CAL DATA"
550  HOME : PRINT "CALIBRATION TABLE": PRINT
560  INVERSE : HTAB 10: PRINT "MAG.";: HTAB 20: PRINT "CAL.FACTOR";: HTAB
     35: PRINT "UNITS": NORMAL
570  VTAB 5: PRINT "(1)";: HTAB 10: PRINT M1$;: HTAB 23: PRINT C1;: HTAB 3
     5: PRINT U1$;"/PP"
580  VTAB 7: PRINT "(2)";: HTAB 10: PRINT M2$;: HTAB 23: PRINT C2;: HTAB 3
     5: PRINT U2$;"/PP"
590  VTAB 9: PRINT "(3)";: HTAB 10: PRINT M3$;: HTAB 23: PRINT C3;: HTAB 3
     5: PRINT U3$;"/PP"
600  VTAB 11: PRINT "(4)";: HTAB 10: PRINT M4$;: HTAB 23: PRINT C4;: HTAB
     35: PRINT U4$;"/PP"
610  VTAB 13: PRINT "(5)";: HTAB 10: PRINT M5$;: HTAB 23: PRINT C5;: HTAB
     35: PRINT U5$;"/PP"
620  VTAB 15: PRINT "(6)";: HTAB 10: PRINT M6$;: HTAB 23: PRINT C6;: HTAB
     35: PRINT U6$;"/PP"
630  VTAB 19: INVERSE : PRINT "NB";: NORMAL : PRINT " MAKE SURE FRAME IS I
     N 'CIRCULAR' MODE"
640  VTAB 21: PRINT "TYPE NUMBER FROM 1 TO 6 OR 'CAL'": PRINT
650  PRINT "YOUR CHOICE? ";: GET KB$
660  IF KB$ = "1" THEN CAL = C1:UN$ = U1$:M$ = M1$: RETURN
670  IF KB$ = "2" THEN CAL = C2:UN$ = U2$:M$ = M2$: RETURN
680  IF KB$ = "3" THEN CAL = C3:UN$ = U3$:M$ = M3$: RETURN
690  IF KB$ = "4" THEN CAL = C4:UN$ = U4$:M$ = M4$: RETURN
700  IF KB$ = "5" THEN CAL = C5:UN$ = U5$:M$ = M5$: RETURN
710  IF KB$ = "6" THEN CAL = C6:UN$ = U6$:M$ = M6$: RETURN
720  IF KB$ <  > "C" THEN  GOTO 550
730  HOME : VTAB 2: HTAB 4: PRINT "RECALIBRATION ROUTINE"
740 CA% = 1
750  VTAB 6: HTAB 4: INPUT "INPUT POSITION NO:";P
760  IF P = 1 THEN  VTAB 8: HTAB 4: INPUT "INPUT UNITS ";U1$: VTAB 10: HTAB
     4: INPUT "INPUT MAG. ";M1$
770  IF P = 2 THEN  VTAB 8: HTAB 4: INPUT "INPUT UNITS ";U2$: VTAB 10: HTAB
     4: INPUT "INPUT MAG. ";M2$
780  IF P = 3 THEN  VTAB 8: HTAB 4: INPUT "INPUT UNITS ";U3$: VTAB 10: HTAB
     4: INPUT "INPUT MAG. ";M3$
790  IF P = 4 THEN  VTAB 8: HTAB 4: INPUT "INPUT UNITS ";U4$: VTAB 10: HTAB
     4: INPUT "INPUT MAG. ";M4$
800  IF P = 5 THEN  VTAB 8: HTAB 4: INPUT "INPUT UNITS ";U5$: VTAB 10: HTAB
     4: INPUT "INPUT MAG. ";M5$
810  IF P = 6 THEN  VTAB 8: HTAB 4: INPUT "INPUT UNITS ";U6$: VTAB 10: HTAB
     4: INPUT "INPUT MAG. ";M6$
820  VTAB 12: HTAB 4: PRINT "INPUT FRAME HT IN ";
830  IF P = 1 THEN  PRINT U1$;
840  IF P = 2 THEN  PRINT U2$;
850  IF P = 3 THEN  PRINT U3$;
860  IF P = 4 THEN  PRINT U4$;
870  IF P = 5 THEN  PRINT U5$;
880  IF P = 6 THEN  PRINT U6$;
890  INPUT " ";H
```

```
900  VTAB 24: POKE 34,23: PRINT : PRINT D$"PR#3": PRINT I1$ + "00000" + I4
     $: FOR J = 1 TO D1: NEXT J
910  PRINT I1$ + "I" + I4$;: FOR J = 1 TO D2: NEXT J
920  PRINT I2$;: PRINT D$"PR#0": INPUT X,X,X,F: PRINT D$"PR#3": PRINT I3$:
      PRINT D$"PR#0": PRINT D$"IN#0"
930  POKE 34,0:CAL = H / F:CAL =  INT (CAL * 1E3 + .5) / 1E3
940  IF P = 1 THEN C1 = CAL
950  IF P = 2 THEN C2 = CAL
960  IF P = 3 THEN C3 = CAL
970  IF P = 4 THEN C4 = CAL
980  IF P = 5 THEN C5 = CAL
990  IF P = 6 THEN C6 = CAL
1000  GOTO 550
1010  REM ...READ SYSTEM IV OUTPUT

1020  VTAB 23: HTAB 1: CALL  - 868: PRINT "WORKING...."
1030  FOR J = 1 TO (NG + 2)
1040  IF J = 1 THEN CL = 0: GOTO 1060
1050 CL = (BL + GS * (J - 2)) * SC
1060 AL = (CL ^ 2) * .7853982:AL =  INT (AL):AL = AL + 100000
1070  VTAB 24: POKE 34,23: PRINT : PRINT D$"PR#3": PRINT I1$ +  STR$ (AL) +
     I4$: FOR TX = 1 TO D1: NEXT TX
1080  PRINT I1$ + "I" + I4$;: FOR TX = 1 TO D2: NEXT TX
1090  PRINT I2$: PRINT D$"PR#0": INPUT AR,CT,IN,FR,DS: PRINT D$"PR#3": PRINT
     I3$: PRINT D$"PR#0": PRINT D$"IN#0"
1100 TP(J) = CT
1110  IF J = 2 THEN A = AR:C = CT:I = IN:F = FR
1120  NEXT J
1130  FOR J = 1 TO (NG + 2)
1140  IF J < (NG + 2) THEN TP(J) = TP(J) - TP(J + 1)
1150 DT(J) = TP(J) + DT(J)
1160  NEXT J: POKE 34,0: RETURN
1170  REM ...JUST READ FRAME SIZE - IGNORE OTHER OUTPUTS

1180  VTAB 24: POKE 34,23: PRINT : PRINT D$"PR#3": PRINT I1$ + "00000" + I
     4$: FOR J = 1 TO D1: NEXT J
1190  PRINT I1$ + "I" + I4$;: FOR J = 1 TO D2: NEXT J
1200  PRINT I2$: PRINT D$"PR#0": INPUT X,X,X,F: PRINT D$"PR#3": PRINT I3$:
      PRINT D$"PR#0": PRINT D$"IN#0"
1210  POKE 34,0: RETURN
1220  REM ...FILE DATA

1230  HOME : VTAB 3: HTAB 1: PRINT "**PLACE DATA DISK IN DRIVE '2' AND PRE
     SS <RETURN>";: POKE  - 16368,0: WAIT  - 16384,128
1240  VTAB 6: HTAB 1: PRINT "YOUR DATA WILL BE FILED UNDER THE DESCRIPTOR:
     _ "
1250  PRINT D$"PR#1": PRINT "YOUR DATA WILL BE FILED UNDER THE DESCRIPTOR:
     _ ": PRINT D$"PR#0"
1260 F = 1:F$ =  STR$ (F)
1270 FL$ = OPR$ + "/" + SNE$ + "/" + F$
1280  ONERR  GOTO 1300
1290  PRINT  CHR$ (4)"VERIFY M:"FL$",D2":F = F + 1:F$ =  STR$ (F): GOTO 12
     70
1300  POKE 216,0: IF  PEEK (222) <  > 6 THEN 1290
1310  PRINT D$"OPEN M:"FL$: PRINT D$"WRITE M:"FL$: PRINT BL: PRINT TL: PRINT
     UN$: PRINT SNE$: PRINT FC: PRINT TP: PRINT NL: PRINT TF: PRINT NG: PRINT
     SD: FOR J = 1 TO (NG + 2): PRINT DT(J): NEXT J: PRINT D$"CLOSE M:"FL$
     : PRINT D$"LOCK M:"FL$
1320  VTAB 9: HTAB 8: PRINT FL$: PRINT D$"PR#1": PRINT : HTAB 8: PRINT FL$
     : PRINT D$"PR#0"
1330  FOR J = 1 TO 1000: NEXT J
1380  GOTO 340
1390  REM ...SET SIZING CALIBRATIONS

1400 SC = 1 / CAL
1410  HOME : HTAB 5: PRINT "EXISTING SIZING CALIBRATIONS"
1420  VTAB 4: HTAB 1: PRINT "NUMBER OF SIZE CLASSES = ";NG
1430  VTAB 6: HTAB 1: PRINT "BOTTOM LIMIT = ";BL;UN$
1440  VTAB 8: HTAB 1: PRINT "TOP LIMIT    = ";TL;UN$
1450 GS = (TL - BL) / NG
1460  VTAB 10: HTAB 1: PRINT "THUS GROUP SIZE = "; INT (GS * 1E2 + .5) / 1
     E2;UN$
1470  VTAB 14: HTAB 1: PRINT "USE EXISTING CALIB.   (E)"
1480  VTAB 16: HTAB 1: PRINT "CHANGE CALIB.         (C)"
1490 D$ =  CHR$ (4)
1500  VTAB 18: HTAB 1: PRINT "YOUR CHOICE? ";
1510  GET A$: IF A$ = "E" AND CA% THEN  PRINT "E": GOTO 1610
```

```
1520  IF A$ = "E" THEN  PRINT "E": GOTO 1660
1530  HOME : HTAB 5: PRINT "CHANGE SIZING CALIBRATIONS"
1540  VTAB 4: HTAB 1: PRINT "INPUT BOTTOM LIMIT(MIN="; INT (7.5 * CAL * 1E
      1) / 1E1;UN$;")";: HTAB 30: INPUT " ";BL
1550  VTAB 6: HTAB 1: PRINT "INPUT TOP LIMIT (MAX="; INT (150 * CAL);UN$;"
      )";: HTAB 30: INPUT " ";TL
1560  VTAB 8: HTAB 1: INPUT "INPUT NUMBER OF SIZE CLASSES ";NG
1570  IF NG > 14 THEN  GOTO 1560
1580  VTAB 20: HTAB 1: PRINT "IS THIS OK? (Y/N)";: POKE 49168,0
1590  GET A$: PRINT : IF A$ = "Y" THEN  GOTO 1610
1600  GOTO 1530
1610 D$ =  CHR$ (4): PRINT D$"OPEN CAL DATA": PRINT D$"DELETE CAL DATA": PRINT
      D$"OPEN CAL DATA": PRINT D$"WRITE CAL DATA"
1620  PRINT M1$: PRINT M2$: PRINT M3$: PRINT M4$: PRINT M5$: PRINT M6$
1630  PRINT C1: PRINT C2: PRINT C3: PRINT C4: PRINT C5: PRINT C6
1640  PRINT U1$: PRINT U2$: PRINT U3$: PRINT U4$: PRINT U5$: PRINT U6$
1650  PRINT BL: PRINT TL: PRINT NG: PRINT D$"CLOSE CAL DATA"
1660  POKE  - 16368,0: RETURN
1670  HOME : VTAB 2: PRINT "PLEASE MAKE SURE THE SIZER IS ON 'AUTO'"
1680  VTAB 4: PRINT "AND THAT YOU ARE IN 'FULL COUNT' MODE"
1690  VTAB 23: HTAB 1: PRINT "PRESS (SPC) TO CONTINUE";
1700  GET KB$: RETURN
1800  REM ...STANDARD DEVIATION  OF S.A.

1810  IF FC = 1 THEN  RETURN
1820 D = (PA - TP) ^ 2
1830 Z = Z + D
1840 SD = (Z / FC) ^ .5:SD =  INT (SD * 1E3 + .5) / 1E3
1850 RETURN
```

A.2 Statistics Program

```
10  REM ...MASTER DISKETTE      CREATED ON 48K SYSTEM BY      J.W.ESS

20  REM ...NON-METALLIC MATERIALSIMAGE ANALYSIS PROGRAM FOR  OPTOMAX SYSTE
    M IV
30 D$ =  CHR$ (4): REM  CTRL-D
35  PRINT D$"PR#1": PRINT : POKE  - 12528,7: PRINT D$"PR#0": REM ...SETS P
    RINTER INTENSITY TO MAXIMUM
40  TEXT : HOME : HTAB 11: PRINT "*** SYSTEM IV ***"
50  VTAB 8: HTAB 2: PRINT "(I)      IMAGE MEASUREMENT PROGRAM"
60  VTAB 11: HTAB 2: PRINT "(O)      DATA & STATS PROGRAM"
65  VTAB 14: HTAB 2: PRINT "(S)      SURF.AREA OF AGGLOMERATES"
67  VTAB 17: HTAB 2: PRINT "(F)      FIBRE LENGTH (GRAPHICS TABLET)"
70  VTAB 23: HTAB 2: PRINT "YOUR CHOICE ";: POKE 49168,0
80  GET A$: IF A$ = "I" THEN  PRINT "LOADING-I": PRINT D$"RUN MEASUREMENT,
    D1": END
82  IF A$ = "X" THEN  HOME : PRINT : PRINT D$"RUN D,D1": END
85  IF A$ = "S" THEN  PRINT "LOADING-S": PRINT D$"RUN M/2,D1": END
87  IF A$ = "F" THEN  PRINT "LOADING-F": PRINT D$"RUN F,D1": END
90  PRINT "LOADING-O": PRINT D$"RUN DATA/STATS,D1": END

]LOAD O
]LIST

10  REM ...DATA AND STATS PROGRAM/J.W.E.

20  CLEAR :D% = 0:D$ =  CHR$ (4)
25  POKE  - 12528,7
30  TEXT : HOME : HTAB 5: PRINT "*** DATA AND STATS PROGRAM ***"
40  VTAB 5: HTAB 5: PRINT "(O)     DATA RETRIEVAL"
50  VTAB 7: HTAB 5: PRINT "(S)     STEREOMETRY/STATS"
60  VTAB 9: HTAB 5: PRINT "(C)     COMPARE/COMBINE DATA"
70  VTAB 11: HTAB 5: PRINT "(T)     TRANSFORM SCALES"
80  VTAB 15: HTAB 5: PRINT "(Q)     QUIT"
90  VTAB 22: HTAB 1: PRINT "YOUR CHOICE? ";: POKE 49168,0: GET KB$
100  IF KB$ = "O" THEN  CLEAR : GOTO 170
110  IF KB$ = "S" AND D% THEN  GOTO 570
120  IF KB$ = "S" THEN  VTAB 22: HTAB 1: PRINT "**YOU MUST RETRIEVE YOUR D
     ATA FROM DISK   IN DRIVE '2' FIRST**": FOR A = 1 TO 5000: NEXT A: GOTO
     30
130  IF KB$ = "C" THEN  PRINT "LOADING-C": PRINT D$"EXEC RESET,D1": END
140  IF KB$ = "T" THEN  PRINT "LOADING-T": PRINT D$"EXEC RESET,D1": END
150  IF KB$ = "Q" THEN  PRINT "QUIT": PRINT D$"EXEC RESET,D1": END
160  GOTO 90
170  REM ...DATA RETRIEVAL

180 D% = 1: TEXT : HOME : HTAB 8: PRINT "*** DATA RETRIEVAL ***"
190  ONERR  GOTO 260
200  VTAB 6: HTAB 1: PRINT "PLACE DATA DISK IN DRIVE '2'"
210  VTAB 9: HTAB 1: INPUT "INPUT FILE DESCRIPTOR ";FL$
215  VTAB 12: HTAB 1: INPUT "INPUT SAMPLE NAME ";SNE$
220 D$ =  CHR$ (4)
230  PRINT : PRINT D$"VERIFY M:"FL$",D2": POKE 216,0
240  PRINT D$"OPEN M:"FL$: PRINT D$"READ M:"FL$: INPUT BL,TL,UN$,FC,TP,NL,
     TF: PRINT D$"CLOSE M:"FL$
250  DIM N(17): GOTO 270
260  HOME : VTAB 11: PRINT "SORRY-NO SUCH NAME": FOR I = 1 TO 2000: NEXT I
     : GOTO 180
270  PRINT D$"OPEN M:"FL$: PRINT D$"READ M:"FL$: INPUT X,X,X$,X,X,X,X: FOR
     J = 1 TO 17: INPUT N(J): NEXT J: PRINT D$"CLOSE M:"FL$
280  DIM S(16),S$(17),SM(16),NV(17),NA(16),D(16),DT(16),VT(16),F(15,15)
290 SI = 0:NP = 0
300  HOME : PRINT FL$" HOLDS RAW SIZE DATA AS FOLLOWS:": PRINT  CHR$ (7)
310  PRINT : PRINT "SIZE CLASS     MID SIZE        NUMBER": PRINT :GS = (TL
      - BL) / 15
320  FOR J = 1 TO 16
330  IF J = 1 THEN S(1) = BL:SI = BL: GOTO 380
340  IF J = 16 THEN S(16) = TL: GOTO 380
350 SI = SI + GS
360 S(J) = SI
370 S$(J) =  STR$ (S(J)):S$(J) =  LEFT$ (S$(J),5):S(J) =  VAL (S$(J))
380  NEXT J
```

```
390  FOR J = 2 TO 16
400 NP = NP + N(J)
410  NEXT J
420  FOR J = 1 TO 17
430 Q$ = "-"
440  IF J = 1 THEN S$(1) = "(" +  STR$ (S(1)): GOTO 480
450  IF J = 17 THEN S$(17) = ")" +  STR$ (S(J - 1)): GOTO 480
460 S$(J) =  STR$ (S(J - 1)) + Q$ +  STR$ (S(J))
470 SM(J) = S(J - 1) + (.5 * GS):SM(J) =  INT (SM(J) * 100) / 100
480  IF J = 1 THEN  PRINT S$(1),,N(1): GOTO 510
490  IF J = 17 THEN  PRINT S$(17),,N(17): GOTO 510
500  PRINT S$(J),SM(J),N(J)
510  NEXT J
520  PRINT "ALL SIZE DATA IN "UN$"          "NP" TOTAL"
530  IF PF% THEN  PRINT : PRINT : PRINT : PRINT : PRINT D$"PR#0":PF% = 0
540  PRINT "'P' FOR PRINT-OUT,(SPC)FOR MENU ";: POKE 49168,0: GET KB$
550  IF KB$ = "P" THEN  PRINT : PRINT D$"PR#1":PF% = 1: PRINT : PRINT : PRINT
     "       SYSTEM IV DATA AND STATS PROGRAM": PRINT : GOTO 290
560  IF KB$ = " " THEN  GOTO 30
570  REM ...STEREOMETRY/STATS

580 D% = 0:PF% = 0
590  HOME : VTAB 3: HTAB 1: PRINT "**DO YOU REQUIRE SCHWARTZ-SALTYKOV
      (DIAMETER) ANALYSIS**"
600  VTAB 10: HTAB 1: PRINT "THIS ANALYSIS IS OF USE WHEN CROSS-     SECTI
     ONS ARE BEING EXAMINED. IT TAKES   ACCOUNT OF THE FACT THAT PARTICLE
           DIAMETERS SEEN IN CROSS-SECTION MAY NOT BE THE TRUE DIAMETERS B
     ECAUSE EACH"
610  PRINT "PARTICLE COULD HAVE BEEN CUT AT ANY     LEVEL OVER ITS HEIGHT
     IN THE THIRD      DIMENSION"
620  VTAB 22: HTAB 1: PRINT "YOUR CHOICE-YES(Y) OR NO(N)?";: POKE 49168,0:
      GET KB$
630  IF KB$ = "N" THEN  HOME : PRINT "WORKING....": GOTO 860
640  VTAB 22: HTAB 1: CALL - 868: PRINT "WORKING...."
650  REM ...SCHWARTZ-SALTYKOV (DIAMETER) ANALYSIS / GROUP SIZE = GS: TOTAL
      FIELD AREA = TF
660  FOR J = 1 TO 16
670 NA(J) = N(J) / TF: REM ...NA(J)=NO./UNIT AREA
680  NEXT J
682 J = 0
684 J = J + 1
686  IF NA(J) > 0 THEN HP = J
688  IF J < 15 THEN  GOTO 684
700  REM ...CALCULATION OF CORRECTED VALUES
710  DATA  1,.1547,.036,.013,.0061,.0033,.002,.0013,.0009,.0006,.0005,.000
     4,.0003,.0002,.0001,.5774,.1529,.042,.0171,.0087
720  DATA  .0051,.0031,.0021,.0015,.001,.0009,.0006,.0006,.0004,.4472,.138
     2,.0408,.0178,.0093,.0057,.0037,.0026,.0018,.0013
730  DATA  001,.0007,.0007,.3779,.126,.0386,.0174,.0095,.0058,.0038,.0027,
     .002,.0016,.0012,.0009,.3333,.1161,.0366,.0168,.0094
740  DATA  .0059,.004,.0028,.0021,.0016,.0013,.3015,.1081,.0346,.0163,.009
     1,.0058,.0041,.0028,.0022,.0016,.2773,.1016,.0329,.0155
750  DATA  .009,.0057,.004,.0029,.0022,.2582,.0961,.0319,.0151,.0088,.0056
     ,.0039,.0028,.2425,.0913,.0301,.0146,.0085,.0055,.0039
760  DATA  .2294,.0872,.029,.014,.0083,.0054,.2182,.0836,.028,.0136,.003,.
     2085,.0804,.027,.0132,.2,.0776,.0261,.1925,.075,.1857
770  FOR B = 1 TO 15
772  FOR J = B TO 15
774  READ A
776 F(B,J) = A
778  NEXT J
780  NEXT B
785  FOR B = 1 TO HP
790  FOR J = B TO HP
800  IF J = B THEN D(J) = NA(J) * F(B,J): GOTO 820
810 D(J) = D(J - 1) - (NA(J) * F(B,J))
820  NEXT J
830 NV(B) = D(HP) / GS
840  NEXT B
842  FOR J = (HP + 1) TO 16
844 NV(J) = 0
846 NEXT J
850  GOTO 890
860  FOR J = 2 TO 16
870 NV(J) = N(J)
880  NEXT J
890  REM ...DATA ACCUMULATION
```

```
900  FOR J = 2 TO 16
910 ZN = ZN + NV(J): REM ...ZN=NV TOTAL
920 Z1 = Z1 + (NV(J) * SM(J))
930 Z2 = Z2 + (NV(J) * (SM(J) ^ 2))
940 Z3 = Z3 + (NV(J) * (SM(J) ^ 3))
950 Z4 = Z4 + (NV(J) * (SM(J) ^ 4))
960  NEXT J
970 DN = Z1 / ZN
980 DV = (Z3 / ZN) ^ .3333
990 DOV = Z3 / Z2
1000 DW = Z4 / Z3
1010 UR = DW / DN
1020 SAVR = 4 * NL
1030 TP = TP / 100
1040 MFP = (1 - TP) / NL
1050 DN$ =  STR$ (DN):DN$ =  LEFT$ (DN$,5)
1060 DV$ =  STR$ (DV):DV$ =  LEFT$ (DV$,5)
1070 DOV$ =  STR$ (DOV):DOV$ =  LEFT$ (DOV$,5)
1080 DW$ =  STR$ (DW):DW$ =  LEFT$ (DW$,5)
1090 UR$ =  STR$ (UR):UR$ =  LEFT$ (UR$,5)
1100 SAVR =  INT (SAVR * 1E6 + .5) / 1E6:SAVR$ =  STR$ (SAVR)
1110 MFP$ =  STR$ (MFP):MFP$ =  LEFT$ (MFP$,5)
1160  FOR J = 2 TO 16
1170 DT(J) =  INT ((NV(J) / ZN) * 1E5 + .5) / 1E3: REM ...DT(J) = %(NUMBER
     ) IN EACH GROUP
1180  NEXT J
1190 J = 1
1200 J = J + 1
1210  IF DT(J) > 0 THEN LP = SM(J)
1220  IF J < 15 THEN  GOTO 1200
1230  IF KB$ = "Y" THEN  GOTO 1242
1242  FOR J = 2 TO 16
1243 VT(J) = (SM(J) ^ 3) * NV(J):VT(J) =  INT ((VT(J) / Z3) * 1E5 + .5) /
     1E3: NEXT J: REM ...VT(J) = %(VOLUME) IN EACH GROUP
1250  HOME : PRINT "THE RESULTS FOR "SNE$" ARE AS FOLLOWS:-": PRINT  CHR$
     (7)
1260  PRINT : PRINT "MID SIZE("UN$")","% (NO.FREQ.)";: IF PF% THEN  POKE 3
     6,30: PRINT "%(VOL.FREQ.)"
1265  PRINT
1270  FOR J = 2 TO 16
1280  PRINT SM(J),DT(J);: IF PF% THEN  POKE 36,30: PRINT VT(J)
1285  IF PF% = 0 THEN  PRINT
1290  NEXT J
1300  IF PF% THEN  PRINT : PRINT : PRINT : PRINT D$"PR#0":PF% = 0
1310  PRINT : PRINT "'P' FOR PRINT-OUT"
1320  PRINT "(SPC) FOR STEREOMETRIC RESULTS ";: POKE 49168,0: GET KB$
1330  IF KB$ = "P" THEN  PRINT : PRINT D$"PR#1":PF% = 1: PRINT : PRINT : GOTO
     1250
1340  IF KB$ = " " THEN  GOTO 1360
1350  GOTO 1310
1360  HOME : PRINT "STEREOMETRIC RESULTS FOR "SNE$" ARE:- ": PRINT : PRINT
     : PRINT  CHR$ (7)
1370  PRINT "MEAN NO.PTCL.DIAM.";: HTAB 27: PRINT DN$" "UN$: PRINT
1380  PRINT "MEAN VOL.DIAM.";: HTAB 27: PRINT DV$" "UN$: PRINT
1390  PRINT "MEAN VOL./SURF.DIAM.";: HTAB 27: PRINT DOV$" "UN$: PRINT
1400  PRINT "MEAN WEIGHT DIAM.";: HTAB 27: PRINT DW$" "UN$: PRINT
1410  PRINT "UNIFORMITY RATIO";: HTAB 27: PRINT UR$: PRINT
1420  PRINT "SURF.AREA/VOL.RATIO";: HTAB 27: PRINT SAVR$" "UN$"-1": PRINT
1430  PRINT "MEAN FREE PATH";: HTAB 27: PRINT MFP$" "UN$: PRINT
1440  PRINT "LARGEST PTCL.DIAM.";: HTAB 27: PRINT LP" "UN$
1450  IF PF% THEN  PRINT : PRINT : PRINT : PRINT D$"PR#0":PF% = 0
1460  VTAB 22: PRINT "'P' FOR PRINT-OUT, 'Q' FOR MENU,"
1470  PRINT "'N' FOR NO. OR 'V' FOR VOL.BAR GRAPH ";: POKE 49168,0: GET KB
     $
1480  IF KB$ = "P" THEN  PRINT : PRINT D$"PR#1":PF% = 1: PRINT : GOTO 1360

1490  IF KB$ = "N" THEN  GOTO 1520
1495  IF KB$ = "V" THEN  GOTO 1570
1500  IF KB$ = "Q" THEN  GOTO 10
1510 GOTO 1460
1520  REM ...TRANSFER DATA TO DISK FOR BAR GRAPH PROGRAM

1530 D$ =  CHR$ (4):V$ = "NUMBER"
1540  PRINT
```

```
1550  PRINT D$"OPEN GRAPH DATA,D1": PRINT D$"WRITE GRAPH DATA": FOR J = 2 TO
      16: PRINT DT(J): NEXT J: PRINT BL: PRINT TL: PRINT UN$: PRINT SNE$: PRINT
      V$: PRINT D$"CLOSE GRAPH DATA"
1560  PRINT D$"RUN GRAPH PLOT,D1": END
1570 D$ =  CHR$ (4):V$ = "VOLUME"
1580  PRINT
1590  PRINT D$"OPEN GRAPH DATA,D1": PRINT D$"WRITE GRAPH DATA": FOR J = 2 TO
      16: PRINT VT(J): NEXT J: PRINT BL: PRINT TL: PRINT UN$: PRINT SNE$: PRINT
      V$: PRINT D$"CLOSE GRAPH DATA"
1600  PRINT D$"RUN G/P,D1": END

]LOAD G/P
]LIST

10  REM ...GRAPH PLOT

20 D$ =  CHR$ (4)
30  DIM DT(15)
40  PRINT D$"OPEN GRAPH DATA,D1": PRINT D$"READ GRAPH DATA": FOR J = 1 TO
     15: INPUT DT(J): NEXT J: INPUT BL,TL,UN$,SNE$,V$: PRINT D$"CLOSE GRAP
     H DATA"
60  FOR J = 1 TO 15
70  IF J = 1 THEN VS = DT(J)
80  IF DT(J) > VS THEN VS = DT(J)
90  NEXT J
100 J = 0
110 J = J + 10: IF VS > J THEN 110
120  IF J > 100 THEN J = 100
130 VS = J:VA = VS / 10:K = 150 / VA:L =  INT (K * VA)
140  HGR : HCOLOR= 3: HPLOT 9,0 TO 9,150 TO 279,150
150  FOR J = 9 TO 279 STEP 18: HPLOT J,150 TO J,154: NEXT J
160  FOR J = 150 TO 0 STEP  - K: HPLOT 5,J TO 9,J: NEXT J
170 J = 1:XL = 10:ST = 17
180 YY = L * (1 - DT(J) / VS)
190  IF YY <  = L - .1 THEN 210
200  GOTO 220
210  HPLOT XL,150 TO XL,YY TO XL + ST - 1,YY TO XL + ST - 1,150
220 XL = XL + ST + 1
230 J = J + 1: IF J <  = 15 THEN 180
240  HOME : VTAB 21: HTAB 1: PRINT "HOR: "BL" TO "TL" "UN$"  VERT: 0 TO "V
     S"%": PRINT  CHR$ (7)
250  VTAB 22: HTAB 1: PRINT "'P' FOR PRINT-OUT, 'Q' FOR MENU ";: POKE 4916
     8,0: GET KB$
260  IF KB$ = "Q" THEN  PRINT : PRINT  CHR$ (4)"EXEC RESET,D1": END
265  POKE  - 12528,7
270  VTAB 1: HTAB 1: PRINT : PRINT D$"PR#1": PRINT : PRINT : PRINT "OPTOMA
     X IV PARTICLE SIZE CLASSIFICATION FOR "SNE$: PRINT : PRINT "HORIZONTA
     L SCALE: "BL" TO "TL" "UN$: PRINT "VERTICAL SCALE: 0 TO "VS"%("V$")":
      PRINT : PRINT
275  PRINT D$"PR#0": POKE  - 12528,1
280  POKE  - 12529,255: POKE  - 12524,0: PRINT D$"PR#1": PRINT : PRINT  CHR$
     (17): PRINT D$"PR#0": POKE  - 12506,0
290  PRINT D$"EXEC RESET,D1": END
```

APPENDIX B

IMAGE ANALYSER COMPUTER PROGRAM FOR DISTRIBUTIVE MIXING

```
10  REM ....MEASUREMENT OF SURFACE AREA OF AGGLOMERATES - J.H.E.

20  CLEAR
30  DIM TP(17),DT(17)
40  TEXT : HOME : HTAB 11: PRINT "*** SYSTEM IV ***"
50  VTAB 3: HTAB 5: PRINT "SURFACE AREA OF AGGLOMERATES"
60  VTAB 14: INPUT "INPUT SAMPLE NAME    ";SNE$
70  VTAB 16: INPUT "INPUT OPERATOR NAME ";OPR$
80 A =  LEN (SNE$) +  LEN (OPR$): IF A > 26 THEN  GOTO 40
90  VTAB 18: INPUT "INPUT DATE           ";DTE$
100 D$ =  CHR$ (4):I1$ = "@?(:'":I2$ = "@?4:":I3$ = "@H" +  CHR$ (95) + ":
     ":I4$ = "'": REM ...COMMAND STRINGS FOR IEEE INTERFACE
110 D1 = 50:D2 = 250: REM  ...TIME DELAYS FOR SYSTEM IV

120  PRINT : GOSUB 450: GOSUB 1130: GOSUB 1180
130  HOME : PRINT " SYSTEM IV IMAGE MEASUREMENT PROGRAM"
140  VTAB 6: HTAB 4: PRINT "(SPC) TO READ"
150  VTAB 8: HTAB 4: PRINT "'W' TO CLEAR SCREEN"
160  VTAB 10: HTAB 4: PRINT "'P' FOR PRINT-OUT"
170  VTAB 12: HTAB 4: PRINT "'R' TO RECALIBRATE"
180  VTAB 16: HTAB 4: PRINT "'S' FOR NEW SAMPLE"
190  VTAB 18: HTAB 4: PRINT "'Q' FOR MENU"
200 FC = 0:TF = 0:TA = 0:TI = 0:Z = 0:FP = 0:MFP = 0:TC = 0:S0 = 0:S1 = 0:
     FOR J = 1 TO 15:DT(J) = 0: NEXT J
210  VTAB 24: HTAB 1: POKE 49168,0
220  GOSUB 1080: VTAB 23: HTAB 1: CALL  - 868:FH = F * CAL:FH$ =  STR$ (FH
     ):FH$ =  LEFT$ (FH$,5): PRINT "     FRAME = ";FH$" "UN$" DIAM.";
230 KB =  PEEK (49152): IF KB < 123 THEN 220
240 KB$ =  CHR$ (KB - 128): IF KB$ = "Q" THEN  VTAB 23: HTAB 1: CALL  - 86
     8: PRINT "QUIT - ARE YOU SURE? (Y/N)";: POKE 49168,0
250  IF KB$ = "Q" THEN  GET KA$: IF KA$ <  > "Y" AND KA$ <  > "N" THEN  GOTO
     250: IF KA$ = "N" THEN  GOTO 210
260  IF KA$ = "Y" THEN  TEXT : HOME : PRINT : PRINT D$"EXEC RESET,D1": END

270  IF KB$ = "W" THEN  GOTO 130
280  IF KB$ = "R" THEN  GET KB$: HOME : GOTO 120
290  IF KB$ = "S" THEN  POKE  - 16368,0: RUN
300  IF KB$ = "P" THEN  PRINT : PRINT D$"PR#1":PF% = 1: PRINT : PRINT : PRINT
     : PRINT : PRINT : GOTO 320
310  GOTO 940
320 DS$ =  STR$ (DS): HOME : PRINT OPR$,: PRINT DTE$;: HTAB 35: PRINT "(";
     DS$;"%)"
330  PRINT SNE$;: HTAB 25: PRINT "MAG.="M$: PRINT
340  PRINT "SYSTEM IV SURFACE AREA MEASUREMENT"
350  PRINT : PRINT "     NUMBER OF FIELDS: "FC: PRINT : PRINT "PARAMETER
      THIS FIELD  CUMULATIVE"
360  VTAB 10: HTAB 1: PRINT "FIELD AREA  "FA;: HTAB 26: PRINT TF;: IF PF% THEN
      POKE 36,40: PRINT "SQUARE "UN$
370  VTAB 11: HTAB 1: PRINT "DETECTED    "AR;: HTAB 26: PRINT TA;: IF PF% THEN
      POKE 36,40: PRINT "SQUARE "UN$: PRINT
380  VTAB 12: HTAB 1: PRINT "N.F.P.      "FP;: HTAB 26: PRINT MFP;: IF PF%
      THEN  POKE 36,40: PRINT UN$
390  VTAB 13: HTAB 1: PRINT "AREA FRACT. "PA;: HTAB 26: PRINT TP;: IF PF% THEN
     POKE 36,40: PRINT "%": PRINT : PRINT
400  IF PF% THEN 420
410  IF FC = 1 THEN 430
420  VTAB 16: HTAB 1: PRINT "S.D.OF AREA FRACTION = "SD
430  IF PF% THEN  PRINT : PRINT D$"PR#0":PF% = 0: GOTO 320
440  GOTO 210
450  REM ...SET CALIBRATIONS
460 CA% = 0
470  PRINT D$"OPEN C-D/2,D1": PRINT D$"READ C-D/2": INPUT M1$,M2$,M3$,M4$,
     M5$,M6$,C1,C2,C3,C4,C5,C6,U1$,U2$,U3$,U4$,U5$,U6$: PRINT D$"CLOSE  C-
     D/2"
480  HOME : PRINT "CALIBRATION TABLE": PRINT
490  INVERSE : HTAB 10: PRINT "MAG.";: HTAB 20: PRINT "CAL.FACTOR";: HTAB
     35: PRINT "UNITS": NORMAL
500  VTAB 5: PRINT "(1)";: HTAB 10: PRINT M1$;: HTAB 23: PRINT C1;: HTAB 3
     5: PRINT U1$;"/PP"
510  VTAB 7: PRINT "(2)";: HTAB 10: PRINT M2$;: HTAB 23: PRINT C2;: HTAB 3
     5: PRINT U2$;"/PP"
```

```
520  VTAB 9: PRINT "(3)";: HTAB 10: PRINT M3$;: HTAB 23: PRINT C3;: HTAB 3
     5: PRINT U3$;"/PP"
530  VTAB 11: PRINT "(4)";: HTAB 10: PRINT M4$;: HTAB 23: PRINT C4;: HTAB
     35: PRINT U4$;"/PP"
540  VTAB 13: PRINT "(5)";: HTAB 10: PRINT M5$;: HTAB 23: PRINT C5;: HTAB
     35: PRINT U5$;"/PP"
550  VTAB 15: PRINT "(6)";: HTAB 10: PRINT M6$;: HTAB 23: PRINT C6;: HTAB
     35: PRINT U6$;"/PP"
560  VTAB 19: INVERSE : PRINT "NB";: NORMAL : PRINT " MAKE SURE FRAME IS I
     N 'CIRCULAR' MODE"
570  VTAB 21: PRINT "TYPE NUMBER FROM 1 TO 6 OR 'CAL'": PRINT
580  PRINT "YOUR CHOICE? ";: GET KB$
590  IF KB$ = "1" THEN CAL = C1:UN$ = U1$:M$ = M1$: RETURN
600  IF KB$ = "2" THEN CAL = C2:UN$ = U2$:M$ = M2$: RETURN
610  IF KB$ = "3" THEN CAL = C3:UN$ = U3$:M$ = M3$: RETURN
620  IF KB$ = "4" THEN CAL = C4:UN$ = U4$:M$ = M4$: RETURN
630  IF KB$ = "5" THEN CAL = C5:UN$ = U5$:M$ = M5$: RETURN
640  IF KB$ = "6" THEN CAL = C6:UN$ = U6$:M$ = M6$: RETURN
650  IF KB$ <  > "C" THEN  GOTO 480
660  HOME : VTAB 2: HTAB 4: PRINT "RECALIBRATION ROUTINE"
670 CA% = 1
680  VTAB 6: HTAB 4: INPUT "INPUT POSITION NO:";P
690  IF P = 1 THEN  VTAB 8: HTAB 4: INPUT "INPUT UNITS ";U1$: VTAB 10: HTAB
     4: INPUT "INPUT MAG. ";M1$
700  IF P = 2 THEN  VTAB 8: HTAB 4: INPUT "INPUT UNITS ";U2$: VTAB 10: HTAB
     4: INPUT "INPUT MAG. ";M2$
710  IF P = 3 THEN  VTAB 8: HTAB 4: INPUT "INPUT UNITS ";U3$: VTAB 10: HTAB
     4: INPUT "INPUT MAG. ";M3$
720  IF P = 4 THEN  VTAB 8: HTAB 4: INPUT "INPUT UNITS ";U4$: VTAB 10: HTAB
     4: INPUT "INPUT MAG. ";M4$
730  IF P = 5 THEN  VTAB 8: HTAB 4: INPUT "INPUT UNITS ";U5$: VTAB 10: HTAB
     4: INPUT "INPUT MAG. ";M5$
740  IF P = 6 THEN  VTAB 8: HTAB 4: INPUT "INPUT UNITS ";U6$: VTAB 10: HTAB
     4: INPUT "INPUT MAG. ";M6$
750  VTAB 12: HTAB 4: PRINT "INPUT FRAME HT IN ";
760  IF P = 1 THEN  PRINT U1$;
770  IF P = 2 THEN  PRINT U2$;
780  IF P = 3 THEN  PRINT U3$;
790  IF P = 4 THEN  PRINT U4$;
800  IF P = 5 THEN  PRINT U5$;
810  IF P = 6 THEN  PRINT U6$;
820  INPUT " ";H
830  VTAB 24: POKE 34,23: PRINT : PRINT D$"PR#3": PRINT I1$ + "00000" + I4
     $: FOR J = 1 TO D1: NEXT J
840  PRINT I1$ + "I" + I4$;: FOR J = 1 TO D2: NEXT J
850  PRINT I2$;: PRINT D$"PR#0": INPUT X,X,X,F: PRINT D$"PR#3": PRINT 13$:
      PRINT D$"PR#0": PRINT D$"IN#0"
860  POKE 34,0:CAL = H / F:CAL =  INT (CAL * 1E6 + .5) / 1E6:CAL$ =  STR$
     (CAL)
870  IF P = 1 THEN C1 =  VAL (CAL$)
880  IF P = 2 THEN C2 =  VAL (CAL$)
890  IF P = 3 THEN C3 =  VAL (CAL$)
900  IF P = 4 THEN C4 =  VAL (CAL$)
310  IF P = 5 THEN C5 =  VAL (CAL$)
920  IF P = 6 THEN C6 =  VAL (CAL$)
930  GOTO 480
940  REM ...READ SYSTEM IV OUTPUT

950 AL = 100000
960  VTAB 24: POKE 34,23: PRINT : PRINT D$"PR#3": PRINT I1$ +  STR$ (AL) +
     I4$: FOR TX = 1 TO D1: NEXT TX
970  PRINT I1$ + "I" + I4$;: FOR TX = 1 TO D2: NEXT TX
980  PRINT I2$: PRINT D$"PR#0": INPUT AR,CT,IN,FR,DS: PRINT D$"PR#3": PRINT
     I3$: PRINT D$"PR#0": PRINT D$"IN#0"
990 FA = .7855 * (FR ^ 2) * (CAL ^ 2):TF = TF + FA:AR = AR * CAL ^ 2:TA =
     TA + AR:FC = FC + 1
1000 FA =  INT (FA):TF =  INT (TF)
1010 AR =  INT (AR * 1E1 + .5) / 1E1:TA =  INT (TA)
1020 PA = 1E2 * AR / FA:PA =  INT (PA * 1E3 + .5) / 1E3:TP = 1E2 * TA / TF
     :TP =  INT (TP * 1E3 + .5) / 1E3
1030 I = IN / FA:TI = TI + IN:NL = TI / TF
1040 FP = (1 - (AR / FA)) / I:FP =  INT (FP * 1E2 + .5) / 1E2:MFP = (1 - (
     TA / TF)) / NL:MFP =  INT (MFP * 1E2 + .5) / 1E2
1050  IF FC = 1 THEN MFP = FP
1060  GOSUB 1220
1070  POKE 34,0: GOTO 320
```

```
1080  REM ...JUST READ FRAME SIZE - IGNORE OTHER OUTPUTS

1090  VTAB 24: POKE 34,23: PRINT : PRINT D$"PR#3": PRINT I1$ + "00000" + I
     4$: FOR J = 1 TO D1: NEXT J
1100  PRINT I1$ + "I" + I4$;: FOR J = 1 TO D2: NEXT J
1110  PRINT I2$: PRINT D$"PR#0": INPUT X,X,X,F: PRINT D$"PR#3": PRINT I3$:
      PRINT D$"PR#0": PRINT D$"IN#0"
1120  POKE 34,0: RETURN
1130  IF CA% <  > 1 THEN  RETURN
1140 D$ =  CHR$ (4): PRINT : PRINT D$"OPEN C-D/2": PRINT D$"DELETE C-D/2":
      PRINT D$"OPEN C-D/2": PRINT D$"WRITE C-D/2"
1150  PRINT M1$: PRINT M2$: PRINT M3$: PRINT M4$: PRINT M5$: PRINT M6$
1160  PRINT C1: PRINT C2: PRINT C3: PRINT C4: PRINT C5: PRINT C6
1170  PRINT U1$: PRINT U2$: PRINT U3$: PRINT U4$: PRINT U5$: PRINT U6$: PRINT
     D$"CLOSE C-D/2": RETURN
1180  HOME : VTAB 2: PRINT "PLEASE MAKE SURE THE SIZER IS ON 'AUTO'"
1190  VTAB 4: PRINT "AND THAT YOU ARE IN 'FULL COUNT' MODE"
1200  VTAB 23: HTAB 1: PRINT "PRESS (SPC) TO CONTINUE";
1210  GET KB$: RETURN
1220  IF FC = 1 THEN  RETURN
1230 D = (PA - TP) ^ 2
1240 Z = Z + D
1250 SD = (Z / FC) ^ .5:SD =  INT (SD * 1E3 + .5) / 1E3
1260  RETURN
```

APPENDIX C

NOMENCLATURE

At	Total area of examination
AF	Area fraction of detected features
BP	Breaker plate present in barrel head adaptor
CB	Cabot PP1359 carbon black masterbatch let-down to 0.5% (by weight)
CC	Calcium carbonate
D	Arithmetic mean diameter
D*f*	Ratio of measured MVD to that of the initial feed
D(*i*)	Section equivalent spherical diameter
D(*j*)	Particle equivalent spherical diameter
D*max*	Maximum particle diameter
D2	Durcal 2
DC	Decreasing temperature profile (220/215/205/195/185°C)
DDI	Dispersion and distribution index (= [AF x SD*af*]/image mag.)
FT	Flat temperature profile (205°C)
H95	Hydrocarb 95T
HCCR	Hakuenka CCR
HS	High screw speed (180rpm)
HT	High temperature profile (205/215/225/235/240°C)
HY	Hydrocarb
IM	Image magnification
LT	Low temperature profile (165/175/185/195/200°C)
M	Millicarb
MVD	Mean volume diameter
N*a*	Observed number of sectioned particles per unit area of field

N_l	Number of intersections of television scan line per unit length
N_v	Calculated number of particles per unit volume of specimen
NS	Normal screw speed (120rpm)
NT	Normal temperature profile (185/195/205/215/220°C)
OSL	Omyalene SL
$P(i,j)$	Probability of test surface intersecting particles of equivalent diameter j to yield sections of equivalent diameter i
PA	Nylon 6,6
PD2	Preconditioned Durcal 2
PH	Calcium carbonate/ polypropylene powder premix fed at hopper
PP	Polypropylene powder
PPG	Polypropylene granules
S13	Setacarb 13
SD_{af}	Standard deviation of area fraction
SH	Separate feed of filler and polymer at hopper
SS	Slow screw speed (60rpm)
SV1	Separate feed of filler at first vent into molten polymer
SV2	Separate feed of filler at second vent into molten polymer
WBP	Without breaker plate in barrel head adaptor
i	Refers to sectioned particle diameters
j	Refers to actual particle diameters
60%O	60% of maximum output
80%O	80% of maximum output
100%O	Maximum output
4B	4 barrel extruder configuration
5B	5 barrel extruder configuration

8P	8mm pitch metering section
12P	12mm pitch metering section
16P	16mm pitch metering section
8P2D	8mm pitch metering section plus 2 mixing elements at end of screw